XEROPHILIC FLIGHTLESS GRASSHOPPERS (ORTHOPTERA: ACRIDIDAE: MELANOPLINAE: *MELANOPLUS*: THE PUER GROUP) OF THE SOUTHEASTERN U.S.A.: AN EVOLUTIONARY HISTORY

A Dissertation

by

DEREK ALEXANDER WOLLER

Submitted to the Office of Graduate and Professional Studies of
Texas A&M University
in partial fulfillment of the requirements for the degree of

DOCTOR OF PHILOSOPHY

Chair of Committee,	Hojun Song
Committee Members,	Gregory Sword
	Spencer Behmer
	Jessica Light
Head of Department,	David Ragsdale

December 2017

Major Subject: Entomology

ABSTRACT

The 27 flightless grasshopper species of the Puer Group (Orthoptera: Acrididae: Melanoplinae: *Melanoplus*) comprise a biological system of fascinating complexity in the southeastern U.S.A. that was heavily influenced by sea level fluctuations during the Pliocene and Pleistocene, especially during the latter. These shifts resulted in an oceanic island system that can now be classified as a landlocked archipelago, one that still reflects the patterns of its ancestral roots in terms of speciation and dispersal. To better understand speciation patterns in this group, I used several synergistic methods: molecular-based phylogenetic reconstruction, divergence time estimation, correlative microscopy and 3D model reconstruction of copulation, and shape analysis of male genitalia in an evolutionary time-based phylogenetic framework.

As predicted, aside from general sea level changes, my evidence indicates that the biogeographical and speciation history of this system was shaped dominantly by allopatry in the form of oceanic islands in the past and, more recently, sympatry via sexual selection, especially for the species in peninsular Florida. My quantitative evidence also added strong support for the concept, especially in light of evolutionary time, that sexual selection can drive genital evolution divergently and rapidly. My investigation of the function of genital components (some new to science) during copulation was combined with shape analyses of five of those genital components to reveal that sexual selection's evolutionary tempo on these components is accelerating and/or decelerating. The relative speed was found to be dependent upon the component

and its associated function(s). I also discovered that one of the youngest Puer Group clades has speciated at a rapid rate that may possibly be the highest yet for insects.

The obvious complexity of this biological system requires additional investigation at finer scales to further dissect the intriguing patterns and processes of evolution herein revealed to be at work. Continued analyses of the Puer Group, both quantitative and descriptive, are encouraged, especially because the threat of destruction and fragmentation of the group's xeric habitats (especially scrub) looms large. Speciation is still largely a biological black box, but its inner workings will continue to be slowly revealed with further illuminating studies like this one.

DEDICATION

To Elizabeth for her eternal patience, support, encouragement, love, formatting skills, and the promise of many more adventures to come.

To all my family who have been nothing but supportive and encouraging during this journey (and many previous), especially my parents, Pam and Kevin Woller, and my mother-in-law, Michele Kerr.

To Theodore Huntington "Hub" Hubbell (1897-1989), from whom this project essentially originated in 1932 and who encouraged others to see the Puer Group for what it is: a deep well of evolutionary knowledge.

To Mark Deyrup of Archbold Biological Station in Florida, whose haunting final sentence from his 1989 work on arthropod endemics found in Florida's unique scrub habitat made an indelible mental mark and directly inspired me to pick up Hubbell's torch and re-light his shadowed path. Deyrup wrote (referring to the rapid loss of scrub): "It is sad to think of North American biogeographers and evolutionary biologists preparing large scale grant proposals to study the biotic patterns of distant island chains, while their opportunities in Florida slip away." Sad indeed as a veritable cornucopia of scientific discoveries awaits you in Florida. What are you waiting for?!

Finally, to the grasshoppers of Florida: I'll be back soon!

ACKNOWLEDGEMENTS

I'm definitely not the proverbial island, which means that an extraordinary amount of people contributed to this project. The majority will be thanked here by name and others will be thanked individually in future publications about this biological system. First and foremost, I thank my advisor, Hojun Song for his support (both academically and financially), encouragement, and for allowing me to find my own way much of the time, but also knowing when to provide the necessary bread crumbs to follow. I also thank my two sets of committees for their guidance during the long route I took to arrive at this moment: my original at the University of Central Florida (UCF) where I began my Ph.D. (David Jenkins, Eric Hoffman, I. Jack Stout, and Mark Deyrup (Archbold Biological Station in Florida)) and my current one: Greg Sword, Spencer Behmer, and Jessica Light. Furthermore, I thank all my fellow graduate students and many undergraduates (especially within Song Lab) who shared ideas and encouragement throughout this journey – they know who they are. Additionally, I thank my fellow employees at USDA: APHIS: PPQ: CPHST Phoenix Lab, especially the team to which I belong: the Rangeland Management Grasshopper and Mormon Cricket Management Team of Larry E. Jech, Lonnie R. Black, and K. Chris Reuter. Special thanks to Matthew Ciomperlik (Laboratory Director, CPHST Mission and Phoenix Labs) and Dustin Krompetz (M3 Consulting Group) for driving long hours while I wrote in the backseat.

Loans for the plethora of specimens used throughout all chapters were provided by 14 institutions/individuals (in acquisition order): **1)** Mark F. O'Brien, Collections

Manager of the University of Michigan's Museum of Zoology's (UMMZ) Insect Division; **2)** Mark Deyrup, Senior Research Biologist and Curator of the Archbold Biological Station arthropod collection (ABS); **3)** Paul Skelley, Entomology Section Administrator of the Florida State Collection of Arthropods (FSCA); **4)** E. Richard Hoebeke, Associate Curator and Collections Manager of the University of Georgia Collection of Arthropods (UGCA); **5)** Bob Blinn, Natural Science Curator I of the North Carolina State University Insect Museum; **6)** Trip Lamb's personal collection of ethanol-preserved specimens used for a 2005 study; **7)** Jason Weintraub, Collection Manager of the Academy of Natural Sciences of Drexel University (ANSP); **8)** JoVonn G. Hill, Assistant Research Professor of the Mississippi Entomological Museum of Mississippi State University (MEM) and current caretaker of the *Melanoplus* collection of the U.S. National Entomological Collection (USNM); **9)** Ed Riley, Assistant Curator (retired) of the Texas A&M University Insect Collection (TAMU); 1**0)** John Capinera's personal collection at the University of Florida; **11)** Jason J. Dombroskie, Collection Manager of the Cornell University Insect Collection (CUIC); **12)** Michael L. Ferro, Collection Manager of the Clemson University Arthropod Collection (CUAC); **13)** Alex B. Orfinger's personal collection; and **14)** Shawn L. Kelly, Collections Manager of the Stuart M. Fullerton Collection of Arthropods at the University of Central Florida (UCFC).

For Chapter II, I thank the following contributors: David Almquist of Florida Natural Areas Inventory for providing GIS files of physiographic features, Magdalena Sorger for advice on southeast U.S. GIS map files, Kevin L. Woller for advice on GIS

map files and manipulation, plus geological knowledge. Three geologists from the Florida Geological Survey gave me helpful geological advice: Thomas M. Scott, Guy "Harley" Means, and Christopher P. Williams. Bill Clark answered many questions about his web-based program Earthpoint while Alexei Drummond, Huw A. Ogilvie, and Remco Bouckaert assisted me with questions about multispecies coalescent analyses. Some of the specimens included in the molecular phylogeny were provided by J.G. Hill (who also joined me in field collecting) and T. Lamb. The field assistants (UCF students, friends, family, and colleagues) who collected specimens with me under Florida Park Service Research/Collecting Permits #10031210 and 05281410 from the Florida Department of Environmental Protection, Division of Recreation and Parks were: Cody Gale, Paolo Fontana, Shawn L. Kelly, Ely Kosnicki (we've come full-circle!), Ricardo Mariño-Pérez, Vince Morris, Ji Min Noh, A.B. Orfinger, Brian Silverman, Paola Tirello, Colleen Werner, and K.L. Woller.

For Chapter III, I thank the following contributors: Beny Wipfler (Jena Institut für Spezielle Zoologie und Evolutionsbiologie mit Phyletischem Museum, Friedrich-Schiller University, Germany) for facilitating micro-CT scanning, photographing the micro-CT sample, assisting with Amira comprehension, and suggesting manuscript improvements. Micro-CT scanning assistance was provided to Wipfler by Si-Qin Ge (Institute of Zoology, Chinese Academy of Sciences, Beijing), with critical point drying of the specimens by Stuart M. Fullerton (1940-2014) and S.L. Kelly (who also helped collect specimens), both at the Stuart M. Fullerton Collection of Arthropods, Department of Biology, UCF. SEM use, training, and scheduling were provided by Yongho Sohn,

Kirk Scammon, and Karen Glidewell at UCF's AMPAC Materials Characterization Facility. Field assistants (UCF undergraduate/graduate students, friends, family, and colleagues) who collected specimens with me under the same permits mentioned earlier were: C. Gale, Steven Gotham, Elizabeth C. Kerr-Woller, E. Kosnicki, A.B. Orfinger, I. J. Stout, and Pam H. and K.L. Woller, while Ben Gochnour and Hannah Stephens guided me to the population used for micro-CT. Teresa Porri, a Research Associate with the Cornell Biotechnology Resource Center Imaging Facility provided micro-CT data assistance and software training while Amira Customer Support Specialists, especially K. Tinoco, helped me learn Amira. PDF3D's technical support team and my 3D PDF beta tester, M.L. Ferro, helped the 3D PDF come to life. Manuscript improvements were suggested by David C. Eades (who also shared personal communications), J.G. Hill, M. Schmitt, Douglas Whitman, and one anonymous reviewer.

For Chapter IV, I thank the following contributors: Dean C. Adams, Emma Sherratt, and Michael Collyer of the *geomorph* (R package) team patiently answered many queries, and Elizabeth C. Kerr-Woller for her timely assistance with some figures and analyses, and field-collecting specimens. The other field assistants (UCF students, friends, family, and colleagues) who collected specimens under the same permits mentioned earlier were: G. Alava, M. Deyrup, Samantha Evans, Lauren Faucher, C. Gale, S. Gotham, Brighton Hall, S.L. Kelly, E.C. Kerr-Woller, Austin Kladke, E. Kosnicki, Ian Kutch, R. Mariño-Pérez, V. Morris, J.M. Noh, A.B. Orfinger, Aileen Perilla, Ryan Ridenbaugh, B. Silverman, H. Song, I.J. Stout, C. Werner, P.H. and K.L. Woller, and the Restoration Ecology Class.

CONTRIBUTORS AND FUNDING SOURCES

This work was supervised by a dissertation committee consisting of Professors Hojun Song [advisor], Gregory Sword, and Spencer Behmer of the Department of Entomology and Professor Jessica Light of the Department of Wildlife and Fisheries Sciences.

For Chapter II, the BioGeoBEARS analyses were provided by Dr. Nicholas J. Matzke, a Discovery Early Career Researcher Award fellow in the Division of Evolution, Ecology, and Genetics, Research School of Biology, at the Australian National University in Canberra, Australian Capital Territory.

Chapter III was authored by me and my advisor, and originally published in the Journal of Morphology, volume 278, pages 334 to 359 on January 23, 2017 (DOI 10.1002/jmor.20642) and is Copyright © 1999 - 2017 John Wiley & Sons, Inc. All Rights Reserved. The content of this journal article has been included here with permission from the publisher (as requested, a letter indicating such has been submitted separately).

General guidance and support for this dissertation were given by all my committee members, but I received the most interaction and assistance from my advisor. Beyond these, all other work conducted for the dissertation was completed independently by me.

Graduate study was supported by a number of sources: **1)** my advisor's start-up funds from both the University of Central Florida (UCF) and Texas A&M University

(TAMU), **2)** Graduate Teaching Assistantships at UCF and TAMU, **3)** 2012 Orthopterists' Society Research Grant for fieldwork, **4)** NSF Grant IOS-1253493 awarded to my advisor, and **5)** a 2017 TAMU Office of Graduate and Professional Studies Dissertation Fellowship.

NOMENCLATURE

PG	Puer Group
PGss	Puer Group *sensu stricto*
MYO	Millions of Years Old
MYA	Millions of Years Ago
micro-CT	micro-computed tomography
DSLR	digital single lens reflex
SEM	scanning electron microscopy

TABLE OF CONTENTS

Page

LIST OF FIGURES

Page

LIST OF TABLES

Page

CHAPTER I

INTRODUCTION

Biological diversity, or biodiversity, supports human civilization in that we look to nature, particularly plants and animals, to provide for our needs, wants, and, often, even our technological innovations. Therefore, it is in humanity's best interests to continue to maintain rich levels of biodiversity and yet the speciation process (in which one species is separated into two or more distinct organisms) by which biodiversity arises is still shrouded in mystery. To shed light on this intriguing process, the power of a geologically-young living laboratory was harnessed: unique physiographic features of the southeastern United States (primarily in peninsular Florida) known as ridges and hills *(*White, 1970; Hubbell, 1985; Webb, 1990; Deyrup, 1990, Myers, 1990; Turner et al., 2006) and their associated (and also-unique) xeric ecosystems that are populated with high numbers of endemic organisms (Deyrup, 1989, 1990; Myers, 1990; Webb 1990; Mushinsky and McCoy, 1995; Deyrup and Carrel, 2011), like the insect group that is the focus of this study: fascinating xerophilic flightless grasshoppers (Hubbell, 1932; Deyrup, 1996) whose evolutionary history is being explored on multiple levels.

One of the most well-known xeric habitats in Florida is scrub, which is quite dry and highly distinctive in terms of flora and fauna, but which is also vanishing at an alarming rate due to habitat destruction and fragmentation (Deyrup, 1990; Turner et al., 2006; Weekley et al., 2008). The ridges and hills that scrub and several of the other Florida-based xeric habitats are often associated with were formerly oceanic islands

during the sea level fluctuations that occurred during the Pleistocene era (0.0117 to 2.58 million years ago) *(*Deyrup, 1989; Hine, 2009; Swaby et al., 2016*)*. Today, these ridges and hills can still be considered to be a archipelago, albeit a landlocked one, similar to the modern-day Florida Keys because, for one, they are still slightly higher in elevation compared to their surroundings (Hubbell, 1932; Hubbell, 1961; White, 1970; Hubbell, 1985*;* Webb, 1990*;* Deyrup, 1990, Myers, 1990; Lane, 1994; Turner et al., 2006*)*. They are also generally isolated from each other by biological barriers formed by non-scrub ecosystems in-between (Webb 1990), similar to an ocean effect. Furthermore, these xeric habitats support numerous endemic organisms found nowhere else on Earth, probably due to their unique biotic characteristics (White, 1970; Deyrup, 1989, 1990; Myers 1990; Webb 1990; Mushinsky and McCoy, 1995; Deyrup and Carrel, 2011).

Charles Darwin (1809-1882) was an English naturalist and one of the most well-known fathers of evolutionary biology, specifically the theory of natural selection (Browne, 2010). One of his most famed discoveries that helped him formulate the theory was that of the many species of finches scattered across the Galápagos Islands off the west coast of Ecuador. Island biodiversity increased when new species arose as these birds evolved unique beak adaptations for eating corresponding unique foods (Darwin, 1872; Lamichhaney et al., 2015). Although the speciation system of this present study is focused on flightless grasshoppers, it is also extraordinarily similar (and far closer to home), but instead of beaks the genitalia of males have evolved in wildly-divergent directions. One of the primary biological pressures leading to these obvious genitalia

differences is not related to food competition as in the finches, but, rather, sexual competition, better known as sexual selection (Eberhard, 1985).

The Puer Group (PG) currently includes 27 species of flightless grasshoppers belonging to the genus *Melanoplus* Stål, 1873 (Orthoptera: Acrididae: Melanoplinae) and presents some of the clearest evidence of the isolation of their respective xeric habitats due to their wildly-divergent male genitalia, which are used to separate these insects into species (Rehn and Hebard, 1916; Hubbell, 1932; Strohecker, 1960; Deyrup, 1996; Squitier et al., 1998; Otte, 2012 ("2011")). Moreover, this relatively young group of small-bodied insects appears to have primarily speciated via the dual mechanisms of geographic isolation (allopatry) and genitalia evolution (sexual selection) (Hubbell, 1932; Hubbell, 1985; Deyrup, 1996; Lamb and Justice, 2005). The underlying purposes of this project are to **1)** better comprehend the speciation process, in general, which is a biological black box for most organisms, and **2)** to specifically elucidate the role and interplay of these dual mechanisms driving speciation in this system.

This study contains three chapters and objectives that synergistically build upon each other: **Chapter II: 1)** Reconstruct the evolutionary relationships (phylogeny) of the PG using mitochondrial genomes and three nuclear genes per species as the project's backbone; **2)** Estimate relative rates of PG species divergence using estimated ages of ridges/hills; **Chapter III:** A comprehensive look at the function of genitalia during copulation of an exemplar PG species via correlative microscopy (a combination of micro-computed tomography, digital single lens reflex camera photography with focal stacking, and scanning electron microscopy) and 3D model reconstruction in order to

better understand which components sexual selection might be acting on in an evolutionary sense; and **Chapter IV:** Examine the evolution of PG male genitalia in a phylogenetic framework based on evolutionary time using shape analysis. Overall, this project will shed new light on both the natural history of a distinctive and vulnerable ecosystem as well as a poorly-understood and captivating group of creatures, add resolution to the geological history of the southeast (especially Florida), make strides towards better comprehending the speciation process, bring forth a greater understanding of the evolution of male genitalia in insects, and explore new frontiers in biology and technology.

CHAPTER II

MAPPING THE EVOLUTION OF XEROPHILIC FLIGHTLESS GRASSHOPPERS IN THE LAND-LOCKED ARCHIPELAGO OF PENINSULAR FLORIDA

Introduction

The landmass that is currently recognized as the state of Florida in the United States is the exposed portion of a much larger geological feature known as the Florida Platform (Fig. 2-1A) (Lane, 1994; Scott et al., 2001; Allen and Main, 2005; Hine, 2009; Swaby et al., 2016), which is estimated to be 530 million years old (MYO) (Cambrian) (Allen and Main, 2005; Swaby et al., 2016), with the oldest section of the exposed portion estimated to only be 25 MYO (late Oligocene) (Webb, 1990; Swaby et al., 2016). For perspective, the other four states that compose what this study herein refers to as the southeast, Alabama, North and South Carolina, and Georgia, range greatly in age from present-day (primarily Florida's eastern half) to over a billion years old (Precambrian) (Swaby et al., 2016). Based on this and the extrapolation that for over 95% of its existence, Florida's landmass was below sea level, the exposed portion of Florida is geologically young relative to the majority of the southeastern U.S. (Swaby et al., 2016). Furthermore, only until relatively recently, beginning during the middle of the Miocene (around 11 million years ago (MYA)), does geological evidence suggest that a land mass of some size existed consistently to be colonized by non-marine organisms (Hubbell, 1961), findings primarily based on a rich fossil record, particularly from the

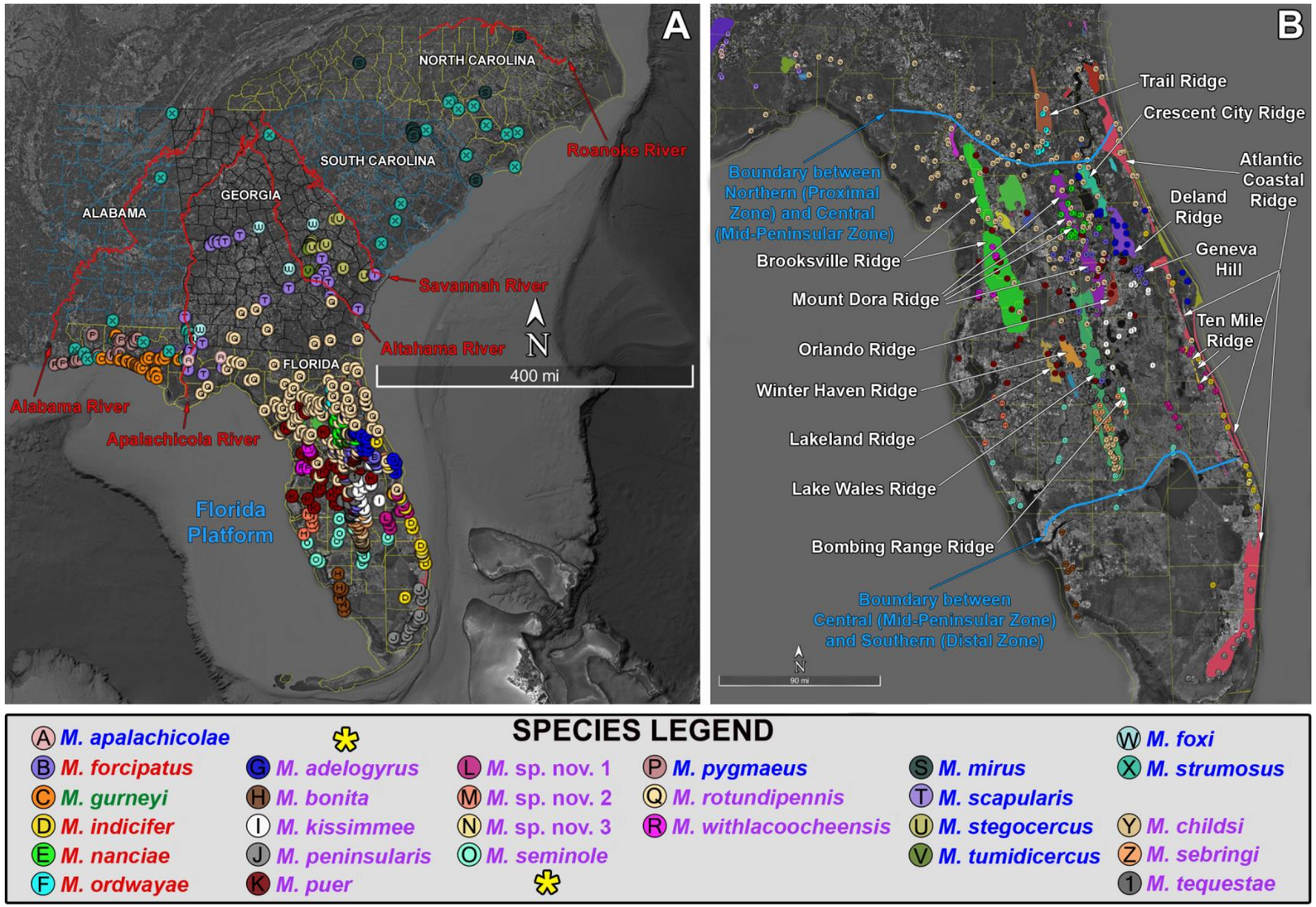

Figure 2-1. Modern-day geographical distributions of the Puer Group: A. The five states comprising the southeastern U.S.A. as defined in this study are identified along with the five major river boundaries dividing the species in the regions beyond peninsular Florida. The Florida Platform is labeled for increased understanding and is far beneath the ocean. B. Peninsular Florida, plus all of its major ridges and hills, with the 12 ridges and one hill labeled that are the focus of this study. Also included are the three major physiographic zones of this region (White, 1970). *The Species Legend is organized into columns according to historical subgroup in alpha order (see Fig. 2-4; Table 2-1): 1 = Forcipatus Group, 2/3 = Puer Group sensu stricto (PGss) – bookended by golden stars, 4 = Rotundipennis Group, 5 = Scapularis Group, 6 = Strumosus and Tequestae Groups. Within each subgroup, species are in alpha order by specific name and colored by major lineage (see Fig. 2-6).

last ice age, of unearthed terrestrial vertebrates, such as mastodons, rhinoceroses, bears, and ground sloths (Webb, 1990; Hine, 2009; Swaby et al., 2016).

During the Pleistocene (0.0117 -2.58 MYA), ice sheets did not reach into the southeast, so it may have been used as an area of biotic refugia, but it was also a time of great abiotic change for the region with sea level fluctuating hundreds of meters over numerous cycles (Deyrup, 1989; Hine, 2009; Swaby et al., 2016). At peak interglacial stages, the sea level around Florida was about 40 to 46 meters above its current height, most likely transforming peninsular Florida into an oceanic archipelago, similar to what the Florida Keys look like today (Hubbell, 1932; Hubbell, 1961; Webb, 1990; Lane, 1994). Additionally, during the peak of the last glacial advance (about 22,000 years ago), Florida was up to three times larger than it is presently, but as the last ice age drew to a close the amount of exposed land diminished, the climate became wetter, and habitats shifted and changed (Allen and Main, 2005; Swaby et al., 2016). What was once a true archipelago became a series of landlocked islands, physiographic features now referred to as ridges (21 recognized, but only 12 relevant to this study) and hills (15 recognized, but only 1 relevant to this study) (Fig. 2-1B) that are higher than the surrounding areas (which are almost entirely slightly above sea level) and which were formed at various points during the glacial cycles, probably as coastal dunes (White, 1970; Hubbell, 1985; Webb, 1990*;* Deyrup, 1990, Myers, 1990; Turner et al., 2006*).*

The most intriguing thing about this landlocked archipelago of uplands is that it mostly continued to function like an oceanic archipelago in terms of the flourishing of flora and fauna, with a relatively high proportion of plant and arthropod endemics (the

majority most likely autochthonous) with poor dispersal abilities (Deyrup 1990). At first glance, this seems especially curious given the fact that these islands are technically connected by a non-hostile matrix, one that even contains pockets of the various xeric ecosystems that dominate the islands, but, then again, perhaps not, given the relatively short geological time scale. For further perspective, the most dominant of the xeric ecosystems is known as Florida scrub (hereafter scrub), one of the southeast's most ancient ecosystems with an estimated age of 20 million years, which means that it has persisted for almost as long as a portion of Florida's landmass has been exposed (Webb 1990). Scrub is a highly pyrogenic ecosystem, characterized by low-growing, semi-sclerophyllous vegetation, especially oaks and ericaceous shrubs, sometimes with a sparse pine overstory (Deyrup, 1989; Myers, 1990). Scrub species are adapted to severe drought associated with sandy soil, extreme scarcity of soil nutrients, and periodic, high-intensity fires (White, 1970; Myers 1990), which might explain the high proportion of endemics (40-60% of all known species) found in this ecosystem and on the ridges/hills it frequently occupies (Deyrup, 1989). Endemics include the Florida scrub-jay (*Aphelocoma coerulescens* Bartram, 1791, a federally listed species), two lizards, over 24 species of plants, and numerous arthropods (Deyrup, 1989, 1990; Mushinsky and McCoy, 1995). As a testament to the high levels of endemism in these regions (but not high levels of overall species richness compared to non-xeric ecosystems and between the ridges/hills), 46 arthropod species (Deyrup, 1989, 1990) were known to be endemic across all of the state's scrub habitats until a 2012 study (Deyrup and Carrel) closely examined residents of one of the largest, most well-studied ridges, Lake Wales Ridge,

and found 91 more species endemic to that ridge alone, many of which were beetles. Unfortunately, many of scrub's endemics may be threatened or endangered by habitat destruction and fragmentation (Deyrup, 1990; Turner et al., 2006; Weekley et al., 2008).

One group of Florida arthropod endemics stands out from the rest because it presents some of the clearest evidence of the relative isolation of various xeric ecosystems, especially scrub, largely within peninsular Florida (Deyrup, 1996). This group of 27 species of tiny, flightless (brachypterous) grasshoppers is known as the Puer Group *sensu lato* (PG) (Table 1) and belongs to the genus *Melanoplus* Stål, 1873 (Orthoptera: Acrididae: Melanoplinae), the most specious grasshopper genus in the world with more than 300 species that are mainly distributed throughout North America (Cigliano et al., 2017). Based on similar morphology and geographic distribution, the PG (e.g., Fig. 2-2) was erected in 1916 (Rehn and Hebard) and has undergone several

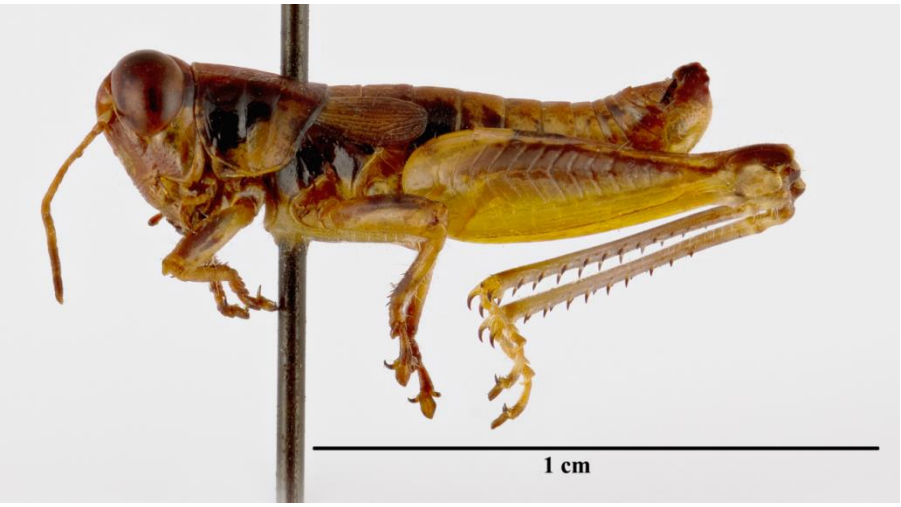

Figure 2-2: A typical morphological representation of the left habitus of an adult male member of the Puer Group. This species is *Melanoplus puer*, the eponymous member of the group.

taxonomic changes since. These include the further splitting of the group into six *sensu stricto* groups (Table 2-1), and hereafter referred to as historical subgroups, based largely on morphology with some emphasis on geography (Hubbell, 1932; Strohecker, 1960; Deyrup, 1996; Lamb and Justice, 2005; Otte, 2012 ("2011"); Hubbell, unpublished notes), and the description of new species as recently as 2012 ("2011") (Otte), with three new species (included here) awaiting description. The PG is restricted to the southeast, with the majority of species found in peninsular Florida, and, much like Darwin's famed finches and their unique beaks (Darwin, 1872; Lamichhaney et al., 2015), these grasshoppers are also predominantly separated into species by distinct morphological characters; in this case, male genitalia, especially the shape of the internal aedeagus (Fig. 2-3).

Deyrup (1996) listed four biological factors that make the PG an ideal group of biogeographic indicators. These grasshoppers demonstrate **(i)** relatively poor mobility and **(ii)** display high habitat specificity, which confine them to specific islands and xeric ecosystems; (**iii)** the main mechanism of speciation in the PG is likely to be driven by sexual selection on male genitalia, the evolution of which is often referred to as rapid and divergent (Eberhard, 1985), and **(iv)** the morphological divergence in the male genitalia are easily observable (Fig. 2-3), which can help make judgments about reproductive isolation and relationships among populations. Thus, investigating the evolutionary history of these grasshoppers combined with the Florida peninsula's unique landlocked island chain of ridges/hills make for a wonderful laboratory to deeply explore the complex biological process of speciation, starting with better understanding the

Table 2-1. **A-G**. Taxonomic information, DNA specimen information, and locality data for the 31 specimens of the 31 species used to reconstruct the molecular phylogenies. Species are organized in alpha order by specific name within historical groups.

A

Species (Sp.)	In/Outgroup	Historical s.s. Group	s.s. Group: # of Sp.	Modern Major Lineage	TAMUIC-IGC ID	Fresh DNA	Locality Data (GPS coordinates are in WGS84 format)
M. apalachicolae Hubbell, 1932	ingroup	Forcipatus Group	1	B	OR1326	yes	FL: Liberty Co., less than 1/4 mi. from SE edge of Torreya State Park, off W. side of NW Torreya Park Rd., [30.551949,-84.945577], 2-X-2014, Field #PG163-1-A, oak-pine forest w/scrubby oaks and gopher apple patches, coll. D.A. Woller & K. Woller
M. forcipatus Hubbell, 1932	ingroup	Forcipatus Group	2	C	OR1313	yes	FL: Seminole Co., Chuluota Wilderness Area, both sides of trail, [28.619361,-81.056057], 13-V-2014, Field #PG123-2-B, overgrown scrub along perimeter of very dense pine flatwoods, coll. D.A. Woller & H. Song
M. gurneyi Strohecker, 1960	ingroup	Forcipatus Group	3	A	OR1327	yes	FL: Bay Co., Econfina Creek Wildlife Management Area, at S end of property just N of Hwy 20 on E side of trail, [30.427695,-85.567802], 2-X-2014, Field #PG160-1-A, reminiscent of sandhills, coll. D.A. Woller & K. Woller
M. indicifer Hubbell, 1933	ingroup	Forcipatus Group	4	C	OR1311	yes	FL: Brevard Co., Malabar Scrub Sanctuary, along sides of various trails, but primarily at coordinates, [28.004746,-80.581205], 15-VIII-2014, Field #PG151-1-A, somewhat overgrown classic scrub, coll. D.A. Woller, B. Silverman, & S.L. Kelly

Table 2-1 Continued.

B

Species (Sp.)	In/Outgroup	Historical s.s. Group	s.s. Group: # of Sp.	Modern Major Lineage	TAMUIC-IGC ID	Fresh DNA	Locality Data (GPS coordinates are in WGS84 format)
M. nanciae Deyrup, 1997	ingroup	Forcipatus Group	5	C	OR1331	yes	FL: Marion Co., Ocala National Forest, Big Scrub, 500 meters South of Big Scrub Campground on Forest Road 588/SE 241st Ave., [29.045266,-81.754964], 26-V-2013, Field #PG127-1-B, roller-chopped classic scrub with dense pine forest near-by, coll. D.A. Woller & E. Kosnicki
M. ordwayae Deyrup, 1997	ingroup	Forcipatus Group	6	C	OR1322	yes	FL: Clay Co., Mike Roess Gold Head Branch State Park, mainly on E. side of the trail just NE of park entrance, [29.847725,-81.961243], 18-IX-2014, Field #PG155-1-A, somewhat overgrown sandhills, coll. D.A. Woller
M. adelogyrus Hubbell, 1932	ingroup	Puer Group	1	D	OR1308	yes	FL: Volusia Co., Lake George State Forest, just SE of intersection of State Forest Roads 7 & 19, just off both sides of road, [29.180483,-81.503633], 25-V-2103, Field #PG126-1-B, managed pine flatwoods, coll. D.A. Woller & E. Kosnicki
M. bonita Otte, 2012 ("2011")	ingroup	Puer Group	2	D	OR1332	yes	FL: Collier Co., just W. of perimeter of Railhead Scrub Preserve, W. of I-75 & E. of Old 41 Rd. off Sun Century Rd., mainly on E. side of railroad tracks, [26.305475,-81.791579], 24-IV-2014, Field #PG136-1-A, primarily gopher apple patches with scrub rosemary bald near-by, coll. D.A. Woller & S.L. Kelly

Table 2-1 Continued.

C

Species (Sp.)	In/Outgroup	Historical s.s. Group	s.s. Group: # of Sp.	Modern Major Lineage	TAMUIC-IGC ID	Fresh DNA	Locality Data (GPS coordinates are in WGS84 format)
M. kissimmee Otte, 2012 ("2011")	ingroup	Puer Group	3	D	OR1324	yes	FL: Orange Co., Split Oak Forest Wildlife and Environmental Area, entrance at the curve of Clapp Simms Duda Rd., on both sides of Trail #1, [28.351667,-81.206111], 14-V-2014, Field #PG138-1-A, overgrown scrub, coll. D.A. Woller, C. Gale, & J.M. Noh
M. peninsularis Hubbell, 1932	ingroup	Puer Group	4	D	OR1319	yes	FL: Miami-Dade Co., Everglades National Park, Long Pine Key area, off W. and E. sides of Pinelands Trail along E. track of looped trail, [25.423913,-80.679398], 24-V-2014, Field #PG145-1-A, unique, but resembles sandhills, coll. D.A. Woller
M. puer (Scudder, 1878)	ingroup	Puer Group	5	D	OR1526	yes	FL: Seminole Co., Lower Wekiva River Preserve State Park, not too far N. of split in "C" trail , [28.832770,-81.402874], 16-X-2014, Field #PG179-1-D, scrubby flatwoods, coll. D.A. Woller
M. seminole Hubbell, 1932	ingroup	Puer Group	6	D	OR1527	yes	FL: Glades Co., Palmdale, vacant lot bordered by 5th St., Main St., Pine Ave., & 3rd St., [26.941892,-81.306959], 18-X-2014, Field #PG180-1-A, scrub-like sandhills, coll. D.A. Woller & S.L. Kelly

Table 2-1 Continued.

D

Species (Sp.)	In/Outgroup	Historical s.s. Group	s.s. Group: # of Sp.	Modern Major Lineage	TAMUIC-IGC ID	Fresh DNA	Locality Data (GPS coordinates are in WGS84 format)
M. sp. nov. 1	ingroup	Puer Group	7	D	OR1528	yes	FL: Brevard Co., St. Sebastian River Preserve SP, along Scrub Jay Link Trail, trailhead just N. of Fellsmere Rd./CR 512, [27.770833,-80.565000], 16-V-2015, Field #PG200-1-A, overgrown scrub, coll. D.A. Woller, S.L. Kelly, & A. Orfinger
M. sp. nov. 2	ingroup	Puer Group	8	D	OR1276	yes	FL: Hillsborough Co., Little Manatee River State Park, 5 miles S. of Sun City, on both sides of trail slightly NE of park entrance off of Lightfoot Rd., [27.658500,-82.374083], 27-III-2013, Field #PG121-1-A, resembles pine flatwoods, coll. D.A. Woller & S.L. Kelly
M. sp. nov. 3	ingroup	Puer Group	9	D	OR1529	yes	FL: Martin Co., Jonathan Dickinson SP, not far from parking lot along Kitching Creek Nature Trail, [26.993056,-80.147222], 16-V-2015, Field #PG201-1-B, pine flatwoods, coll. D.A. Woller, S.L. Kelly, & A. Orfinger
M. pygmaeus Davis, 1915	ingroup	Rotundipennis Group	1	B	OR1309	yes	AL: Baldwin Co., Gulf State Park, [30.271389,-87.654722], 4-X-2013, edge of maritime forest, coll. J.G. Hill
M. rotundipennis (Scudder, 1878)	ingroup	Rotundipennis Group	2	D	OR1318	yes	FL: Lake Co., Rock Springs Run State Reserve, on both sides of Ethel Trail, mainly towards entrance along main park road (CR433), [28.804542,-81.453300], 18-IV-2014, Field #PG1013-B, overgrown, "classic" scrub w/near-by sandhills and pine flatwoods, coll. D.A. Woller

Table 2-1 Continued.

E

Species (Sp.)	In/Outgroup	Historical s.s. Group	s.s. Group: # of Sp.	Modern Major Lineage	TAMUIC-IGC ID	Fresh DNA	Locality Data (GPS coordinates are in WGS84 format)
M. withlacoocheensis Squitier, Deyrup, & Capinera, 1998	ingroup	Rotundipennis Group	3	D	OR1320	yes	FL: Citrus Co., Withlacoochee State Forest, Citrus Tract, about 1/4 of a mile S of Forest Road 10 and not too far E. of Holder Mine Campground, [28.796592,-82.393544], Field #PG148-1-B, 10-VII-2014, classic sandhills, coll. D.A. Woller, S.L. Kelly, C. Werner, & V. Morris
M. mirus Rehn & Hebard, 1916	ingroup	Scapularis Group	1	B	OR1321	yes	SC: Chesterfield Co., Carolina Sandhills NWR, [34.558056,-80.186667], 12-Jul-13, Fall Line sandhill, coll. J.G. Hill
M. scapularis Rehn & Hebard, 1916	ingroup	Scapularis Group	2	B	OR1310	yes	FL: Liberty Co., Torreya State Park, just inside SE edge of park, a short ways E of NW Torreya Park Rd., [30.558597,-84.950278], 2-X-2014, Field #PG162-1-A, classic sandhills on a gradient, coll. D.A. Woller & K. Woller
M. stegocercus Rehn & Hebard, 1916	ingroup	Scapularis Group	3	B	OR1316	yes	GA: Emanuel Co., Ohoopee Dunes N.A., [32.575556,-82.442500], 15-IX-2013, coll. J.G. Hill

Table 2-1 Continued.

F

Species (Sp.)	In/Outgroup	Historical s.s. Group	s.s. Group: # of Sp.	Modern Major Lineage	TAMUIC-IGC ID	Fresh DNA	Locality Data (GPS coordinates are in WGS84 format)
M. tumidicercus Hubbell, 1932	ingroup	Scapularis Group	4	B	OR1314	yes	GA: Treutlen Co., 0.5 miles N of Gillis Springs, just N of intersection of U.S. 221/771/56 and an unpaved road - on E. side, in elevated natural area between main road and Gillis Spring Rd./12, [32.464314,-82.490058], 19-V-2014, Field #PG139-2-A, dense scrubby undergrowth in pine forest, coll. D.A. Woller & E. Kosnicki
M. foxi Hebard, 1923	ingroup	Strumosus Group	1	B	OR1525	yes	GA: Seminole Co., Seminole State Park, far W side of park just SE of intersection of SR 39 and Hwy 253, [30.803703,-84.885235], 12-V-2015, Field #PG191-1-A, semi-overgrown sandhills, coll. J.G. Hill
M. strumosus Morse, 1904	ingroup	Strumosus Group	2	B	OR1330	yes	FL: Bay Co., Econfina Creek Wildlife Management Area, at S end of property just N of Hwy. 20 on E side of trail, [30.427695,-85.567802], 2-X-2014, Field #PG160-1-A, resembles sandhills, coll. D.A. Woller & K. Woller
M. childsi Otte, 2012 ("2011")	ingroup	Tequestae Group	1	D	OR1281	yes	FL: Highlands Co., Archbold Biological Station, Lake Annie Tract, just S of Lake Annie on E side of trail, [27.201654,-81.351544], 11-XII-2013, Field #PG109-5-D, fire-maintained scrub, coll. D.A. Woller & J.M. Noh

Table 2-1 Continued.

G

Species (Sp.)	In/Outgroup	Historical s.s. Group	s.s. Group: # of Sp.	Modern Major Lineage	TAMUIC-IGC ID	Fresh DNA	Locality Data (GPS coordinates are in WGS84 format)
M. sebringi Otte, 2012 ("2011")	ingroup	Tequestae Group	2	D	OR1282	yes	FL: Highlands Co., S end of Sebring, off E side of U.S.27 along the road, in vacant lot on embankment just NE of George Blvd. sign (on traffic light pole), [27.442255,-81.419021], 10-X-2013, Field #PG133-1-A, scrubby area near pine forest, coll. D.A. Woller
M. tequestae Hubbell, 1932	ingroup	Tequestae Group	3	D	OR1315	yes	FL: Polk Co., Allen David Broussard Catfish Creek Preserve State Park, along both edges of main trail a little ways SE of park entrance, [27.983279,-81.496190], 11-V-2013, Field #PG100-2-A, fire-maintained scrubby area, coll. D.A. Woller, S.L. Kelly, & E. Kelly
M. differentialis (Thomas, 1865)	outgroup	N/A	N/A	N/A	OR1189	yes	Mexico: Estado de Mexico, Teotihuacan ruins, [N 19°41.608',W 98°50.872'], 15-XII-2011, elev. 7,403 ft., scrub, coll. P. Fontana, P. Tirello, D.A. Woller, & R. Marino-Perez
M. mexicanus (Saussure, 1861)	outgroup	N/A	N/A	N/A	OR1188	yes	Mexico: Puebla, La Canada, near Libres, [N 19°30.614',W 97°46.379'], 3-XI-2011, elev. 8,680 ft., grassland in a pine forest, coll. P. Fontana, P. Tirello, D.A. Woller, & R. Marino-Perez
M. quercicola (Hebard, 1918)	outgroup	N/A	N/A	N/A	OR1230	no (kept in 100% EtOH)	FL: Liberty Co., Camel Lake, 13-X-2001, coll. T.C. & M.J. Justice
M. scudderi (Uhler, 1864)	outgroup	N/A	N/A	N/A	OR1325	yes	AL: Sumter Co., Univ. W. Alabama, [32°36'15"N 88°11'13"W], 19-IX-2013, restored Black Belt Prairie, coll. J.G. Hill

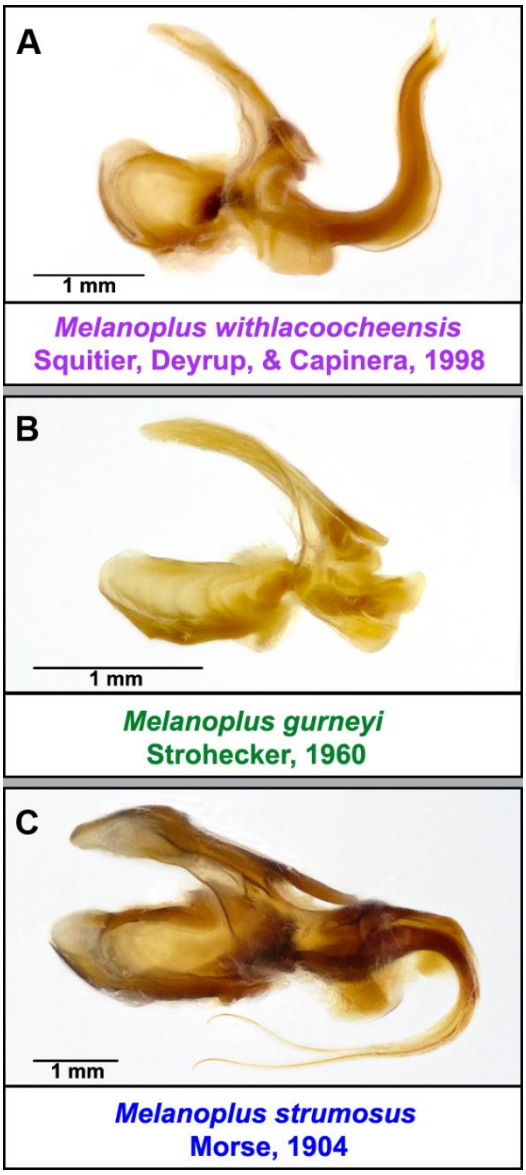

Figure 2-3. An example comparison of the extraordinary diversity present in the internal genitalia of the Puer Group. The right-most apical portion of varying shapes is the aedeagus and species names are colored by major lineage (see Fig. 2-6). **A.** *Melanoplus withlacoocheensis* (lineage D) represents the most extreme form of dorsally-curved aedeagi; **B.** *M. gurneyi* (lineage A) represents the most basic form of aedeagi; **C.** *M. strumosus* (lineage B) represents one of the most extreme forms of ventrally-curved aedeagi.

relationships of the PG species, and the diversification patterns of the PG and their potential correlation with the archipelago's geology. In this study, we present the most

comprehensive phylogenetic hypothesis of the PG to date based on molecular data and perform a rigorous biogeographic analysis aimed at explaining their present-day distribution based on a divergence time estimate built around the estimated geological ages of a few of Florida's major ridges. Specifically, we tested the following five hypotheses: **1)** the PG forms a monophyletic group and **2)** its six historical subgroups are monophyletic. Furthermore, due to the comparatively young geological age of peninsular Florida: **3)** the relative age and distribution of the species found in this region generally follow a north-south gradient, with the youngest towards the south, correlating with the geological age estimates of the ridges and **4)** these species are the youngest in the PG as a result of a relatively recent incursion from outside the region. Finally, **5)** part of the PG species that primarily reside in central-southern peninsular Florida, the Puer Group *sensu stricto* (hereafter referred to as the PGss) possesses a relatively high number of species that look comparatively similar (yet divergently unique) in terms of genitalic shapes and share close geographical connections, suggesting that this subgroup's species are generally the youngest in age because of recent, rapid radiation.

Materials and Methods

Taxon and Character Sampling

The 27 species in the PG compose the ingroup taxa for the phylogenetic analyses. Four outgroup species were also included that belong to *Melanoplus*: two of the more common and widely distributed brachypterous *Melanoplus* species in the southeast, which belong to two other species groups: *M. quercicola* (Hebard, 1918)

(Davisi Group - found within parts of peninsular Florida and Georgia) and *M. scudderi* (Uhler, 1864) (Scudderi Group - found not too far outside of Florida throughout many parts of the eastern U.S.) (Hill, 2015). Plus, two more morphologically (larger body size and macropterous) and geographically distant congenerics: *M. differentialis* (Thomas, 1865) and *M. mexicanus* (Saussure, 1861). The majority of the male specimens used for DNA extraction were recently collected by us (21) or colleagues (six, and only one of the outgroup species was not collected recently). Detailed taxon sampling information is provided in Table 2-1. DNA extracts and their corresponding specimens were deposited in the Texas A&M University Genomic Insect Collection (TAMU-IGC). To confirm the identity of species for DNA extractions and map construction, the internal genitalia of male specimens from each unique locality (679 sites in total) were examined and, when necessary, were removed and dissected further.

For the 31 taxa in the phylogenetic analyses, we generated nucleotide sequences via shotgun sequencing of genomic DNA using the Illumina platform. In order to extract high molecular weight DNA, we used the Gentra Puregene Tissue Kit (Qiagen) following the manufacturer's guidelines. The quality and concentration of DNA extracts were initially measured using either Qubit Fluorometer (Thermo Fisher Scientific) or DeNovix Spectrophotometer, and more thoroughly analyzed using Fragment Analyzer. For library preparation, we utilized the Nextera XT DNA Library Prep Kit and performed 150 bp paired-end (PE) sequencing using NextSeq500 or 125 bp PE sequencing using HiSeq2500. Library preparation and next generation sequencing (NGS) were conducted at either the Georgia Genomic Facility (NextSeq500) or Texas

A&M University's Genomics and Bioinformatics Service (HiSeq2500). The resulting raw reads were quality-trimmed in CLC Genomics Workbench 8 (Qiagen), followed by the use of the MITObim pipeline (Hahn et al., 2013) to assemble mtgenomes *de novo* from the NGS reads. All newly assembled mtgenomes were first uploaded as raw fasta files to MITOS (Bernt et al., 2013) to identify open reading frames (ORFs) and tRNAs. We also used tRNAscan-SE (Lowe and Eddy, 1997) to validate tRNA annotation. The resulting initial annotation from MITOS served as a guideline to delimit gene boundaries, with start and stop codons for each protein-coding gene manually identified in Geneious (v.10.0.9) (Biomatters) as recommended by Cameron (2014). We also extracted three nuclear genes, 18S ribosomal RNA (18S), 28S ribosomal RNA (28S), and histone 3 (H3), from the shotgun sequence data by using the "Map to Reference" tool in Geneious. Using an 18S sequence (KM853211) and H3 sequence (KM853654) from a grasshopper (*Melanoplus bivittatus* (Say, 1825)) and a 28S sequence (AY859541) from an unidentified gomphocerine (Orthoptera: Acrididae) downloaded from GenBank as references, we used the Geneious mapper with low sensitivity to search for short reads that mapped to the reference sequences. This was a very effective approach for extracting these three nuclear genes from all 31 taxa.

Phylogenetic Analyses

For protein-coding mitochondrial and nuclear genes, we aligned based on reading frame conservation by first translating into amino acids and aligning individually in MUSCLE (Edgar, 2004) using default parameters within Geneious. Transfer and

ribosomal RNA genes were individually aligned in MUSCLE (Katoh et al., 2005) using the E-INS-i algorithm in Geneious as well. All resulting individual alignments were then concatenated into a single matrix using SequenceMatrix (v.1.8) (Vaidya et al., 2011) and the data were divided into a total of 66 data blocks (13 mitochondrial protein-coding genes divided into individual codon positions, 22 tRNAs, 2 rRNAs, and the three nuclear genes). We used PartitionFinder (v.2.1.1) (Lanfear et al., 2012) to search for the best-fit scheme as well as to estimate the model of nucleotide evolution for each partition using "greedy" algorithm (heuristic search) with branch lengths estimated as "linked". The best-fit scheme from the PartitionFinder analysis divided the dataset into 11 partitions, and the final matrix consisted of 22,590 aligned bp and 31 taxa.

We performed Bayesian and maximum likelihood (ML) analyses on the total evidence dataset, with both run on XSEDE (Extreme Science and Engineering Discovery Environment, https://www.xsede.org) through the CIPRES Science Gateway (Miller et al., 2011). For the Bayesian analysis, we performed a mixed-model partitioned analysis using MrBayes (v.3.2.6) (Ronquist et al., 2012) with an appropriate model applied to each partition using default priors. We ran four runs with four chains each for 100 million generations, sampling every 2,500 generations. The likelihood trace for each run was then plotted to assess convergence with Tracer (v.1.6) (Tracer, 2003-2009), and an average of 25% of each run was discarded as burn-in. For the ML analysis, we used the best-fit partitioning scheme recommended by PartitionFinder with the GTRCAT model applied to each partition and analyzed using RAxML (v.7.2.8) (Stamatakis et al., 2008), with nodal support evaluated via 1,000 replications of rapid bootstrapping. The

resulting trees were visualized in FigTree (v.1.4.3) (Rambaut and Drummond, 2009) (Fig. 2-4). The aligned dataset, trees, and all associated data for all study analyses were deposited in Mendeley Data.

Divergence Time Estimation Analysis

In order to estimate timing and rates of divergence across the PG, we performed a divergence time estimate analysis using BEAST2 (Bouckaert et al., 2014). As there is no fossil available for the PG, we used the estimated geological age ranges of three Florida ridges to calibrate three internal clade nodes based on present-day close associations between one or more species in a clade and a ridge (Figs 2-4 and 2-1B): **1)** the clade formed by the sister species *M. indicifer* Hubbell, 1933 and *M. forcipatus* Hubbell, 1932 had its node calibrated using the Atlantic Coastal Ridge (0.0117-0.05 MYO) (Scott et al., 2001; Swaby et al., 2016; Scott, personal communication) because of its close association with *M. indicifer*; **2)** the clade formed by the sister species *M. ordwayae* Deyrup, 1997 and *M. nanciae* Deyrup, 1997 had its node calibrated using the Trail Ridge (0.006-2.21 MYO) (Burdette et al., 2013) because of its close association with *M. ordwayae*; and **3)** the clade formed by *M. tequestae* Hubbell, 1932, *M. childsi* Otte, 2012 ("2011"), and *M. sebringi* Otte, 2012 ("2011") had its node calibrated using Lake Wales Ridge (0.017-5.33 MYO) (Scott et al., 2001; Swaby et al., 2016) because of its close association with all three species. Geologic calibrations are difficult (Ho et al., 2015) and we fully acknowledge that future evidence could significantly revise this dating, but these age estimation data are currently the best known for these

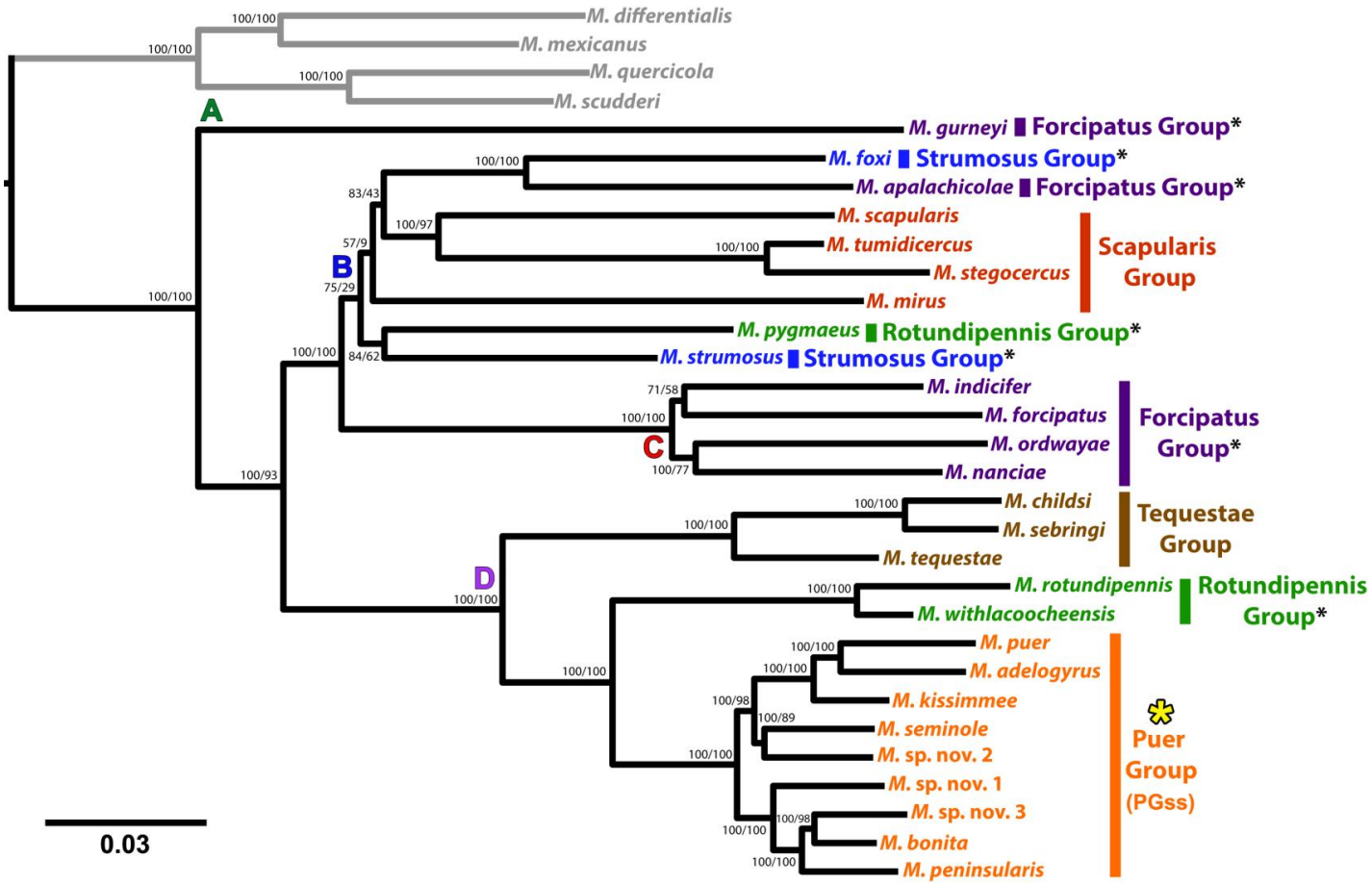

Figure 2-4. Molecular phylogeny of the Puer Group based on the entire mtGenome and three nuclear genes. The topology was identical between both Bayesian (first nodal support value and scale bar) and Maximum Likelihood (second nodal support value) frameworks. The four major lineages recovered are identified as A-D and are colored to correspond to the same in Fig. 2-6. The six historical subgroups are labeled, of which the Puer Group *sensu stricto* (PGss) (lineage D) is identified with a golden star. An ***** indicates paraphyly.

physiographic features. Moreover, while sea level curves are known for peninsular Florida, they were deemed not adequate enough to incorporate because they focused on the very southern end of Florida and the Keys (Muhs et al, 2013), which, except for a few isolated populations of a single species in the Everglades National Park (Fig. 2-1), are areas not yet colonized by the PG.

For this analysis, we used the total evidence dataset using the partitioning scheme and the models of nucleotide evolution recommended by PartitionFinder. We created an xml file in BEAUti (Drummond et al., 2012), specifying the priors and monophyly constraints. We used the relaxed clock log normal model for the clock model, the birth-death model with a uniform distribution as a tree prior and a log normal distribution as a distribution prior for geology-based calibration points. To assess convergence across independent runs, we conducted four separate analyses each for 100 million generations, sampling every 1,000 generations. We inspected the results using Tracer, discarded 75% of each run as burn-in due to computational constraints, and combined the trees using LogCombiner (v.2.4.5) (Rambaut and Drummond, 2007). A maximum clade credibility tree was summarized in TreeAnnotator (Rambaut and Drummond, 2007) and visualized in FigTree (Fig. 2-5).

Multispecies Coalescent Analyses

Due to its relatively young status (geologically speaking) and closely related nature of its members, a Puer Group species tree was estimated using the multilocus coalescent-based Bayesian approach with the *BEAST2 template within BEAUTi and

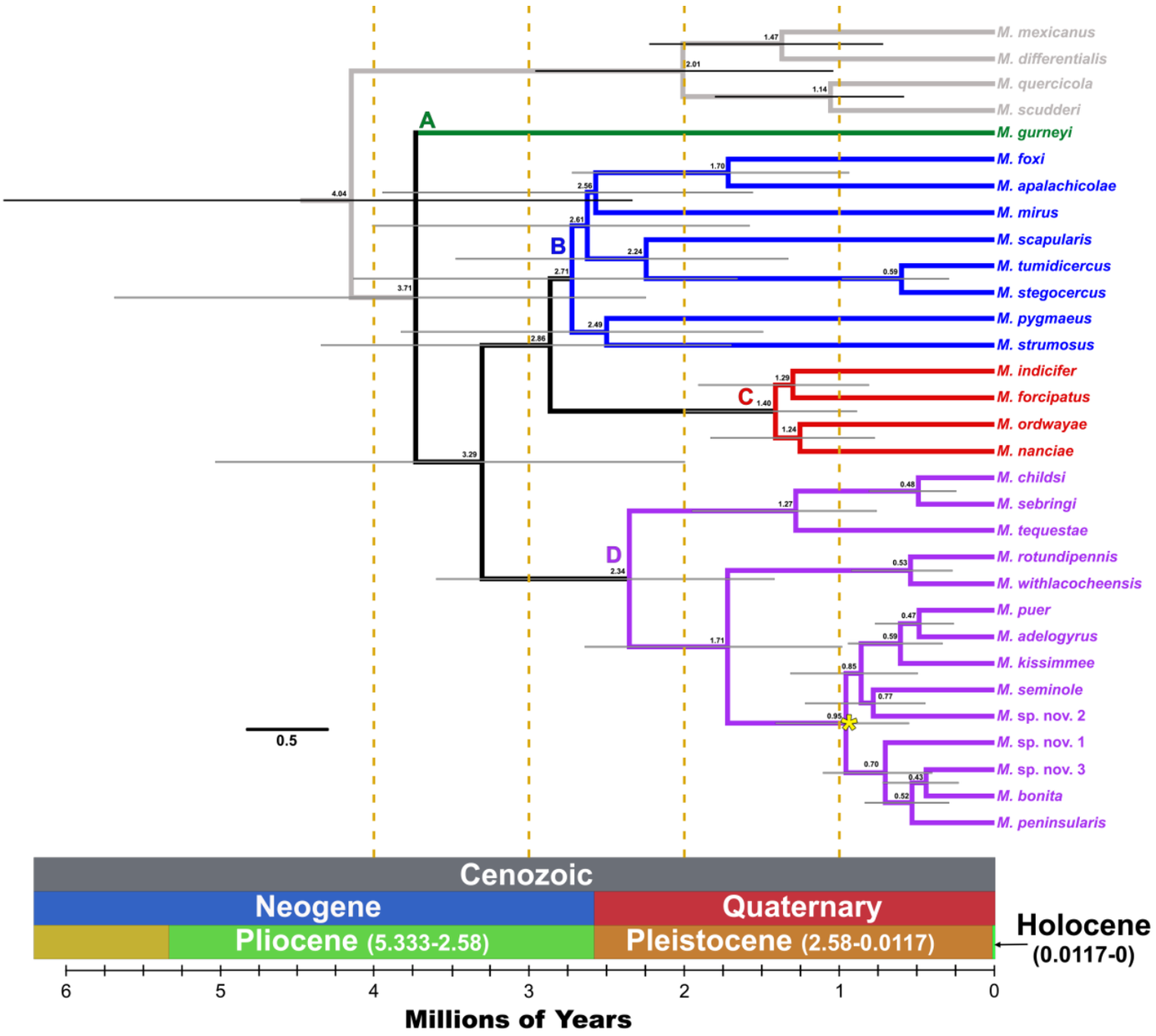

Figure 2-5. Bayesian-based divergence time estimation phylogeny that used the same genes from the concatenated approach. Nodal values correspond with estimated divergence times and nodal bars are relative confidence intervals. Major lineages of the Puer Group and their species are color-coded accordingly while the outgroups are in grey. Lineage D's Puer Group *sensu stricto* (PGss) is identified with a golden star.

BEAST2 (run on XSEDE via CIPRES). The same molecular data for the concatenated approach were used here, but were separated into 19 matrices: 13 individual protein-coding genes, a single tRNA set combined from 22 individual tRNA alignments (due to their smaller size), 12S rRNA, 16S rRNA, and the three individual nuclear genes. Within BEAUTi, all mitochondrial gene trees were linked for partitions, with the following selected for all four partitions: the selected population model was linear with constant root populations, the site models were estimated using the Beast Model Test package, the clock model was set to strict and the Birth Death Model was used for a prior; the length of the chain was set to 100,000,000, sampling every 10,000 generations across four independent runs (Heled and Drummond, 2014; Sanabria-Urbán et al., 2016; and Huw A. Ogilvie, personal communication). Parameter convergence of the runs was assessed with Tracer (each yielded more than acceptable ESS values), the tree files were then combined with LogCombiner, and TreeAnnotator summarized the maximum clade credibility tree, which was visualized in FigTree (Fig. 2-6).

BioGeoBEARS Analysis

We used the R package BioGeoBEARS (Biogeography with Bayesian (and Likelihood) Evolutionary Analysis in R Scripts) (Matzke, 2013) in R (R Core Team, 2013) to infer the biogeographical history of the PG, and to compare the fit of different biogeographical models. For biogeography analyses, the 27 ingroup taxa were used and the analyses were based on the divergence time estimation tree (Fig. 2-5) and the present-day geographical distribution map of the PG (Fig. 2-1). Model-based

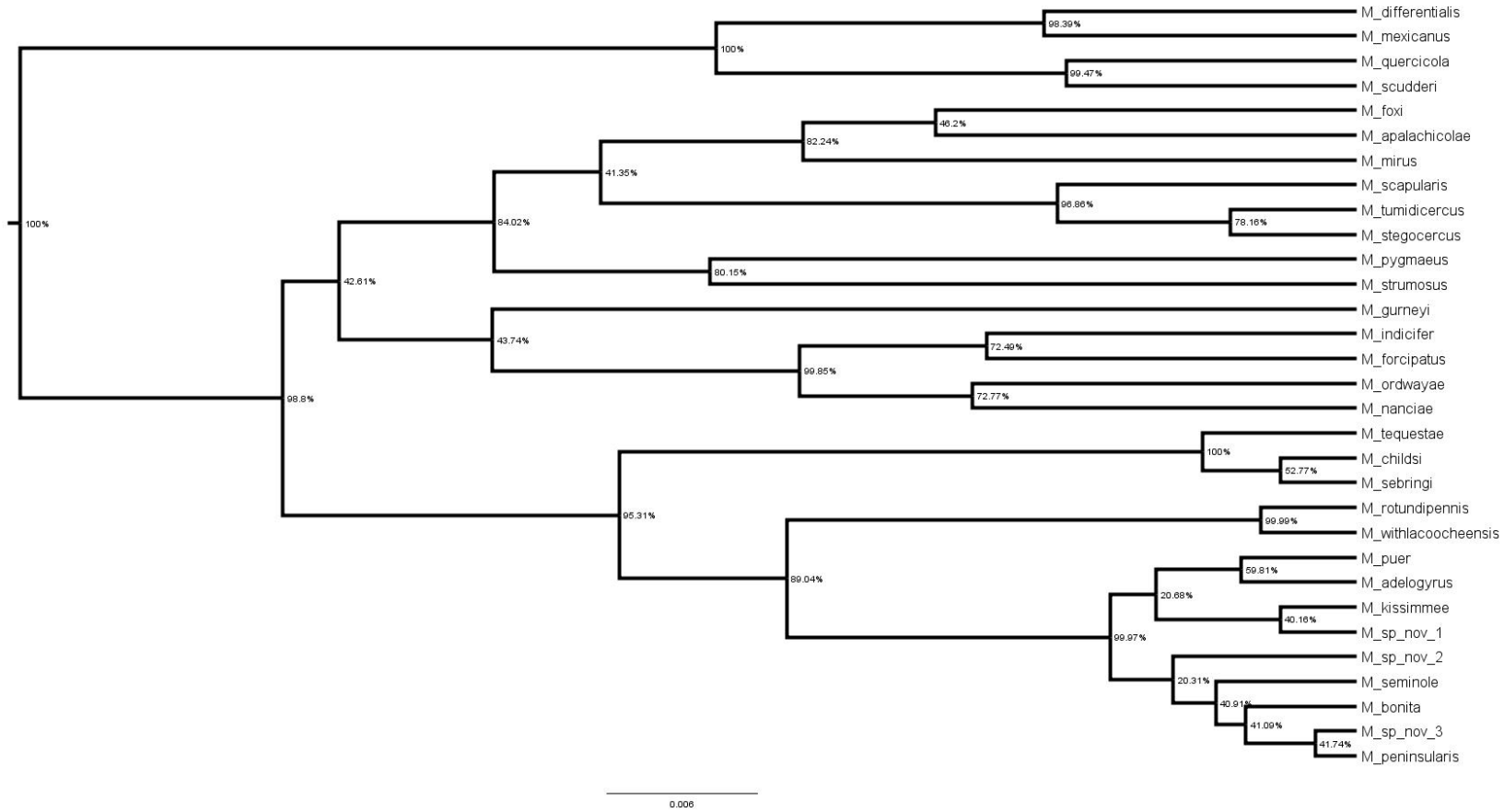

Figure 2-6. Bayesian-based phylogeny reconstructed from the multispecies coalescent analyses that used the same genes from the concatenated approach. Nodal support values correspond with posterior probability.

biogeographical inference as available in BioGeoBEARS (and in predecessor programs, such as Lagrange and DIVA) relies on characterizing geographic ranges as a series of presences and absences across a series of pre-defined, discrete areas. This is obviously a major simplification of reality, except perhaps in the simplest cases, such as oceanic islands. The choice of areas should attempt to capture the major patterns in the observed geographic ranges of the study clade, but the number of areas is quite strictly limited by computational restrictions. For example, a mere 11 areas can produce 2^11=2024 possible ranges, which means that the likelihood calculation involves exponentiation of a 2024x2024 matrix on each branch of the phylogeny each time the likelihood is calculated, and a Maximum Likelihood search involves iterating through hundreds of likelihood calculations (this can be reduced somewhat by limiting the maximum number of areas allowed in each range). The resulting compromise is unavoidable and will have some subjectivity regarding the choice of areas, taxa, and coding of taxon ranges. Peninsular Florida is a unique case within this system because the ridges/hill included in the analyses were once oceanic islands, but all species in this region have now expanded their present-day geographic distributions to at least partially include areas in-between that were formerly ocean. This is why we assumed that all species that appear to be strongly associated with these former oceanic islands dispersed outwards and not vice versa, a reasonable assumption given their present-day patterns of distribution (Fig. 2-1).

Therefore, six different BioGeoBEARS analyses were considered, with multiple models compared within each analysis, to see the effect of different decisions on the inferred biogeographical history of the PG. These analyses also had an emphasized focus

on peninsular Florida as it is the primary residence of a majority of the PG's species and offered the most interesting biogeographical scenarios due to its land-locked archipelago of ridges/hills. A synopsis of the six analyses (one coarse-scale and five fine-scale) can be found in Table 2 and are as follows: **1)** a coarse-scale discretization of eight geographical areas focused on the entire southeastern U.S., with five areas maximum per species (219 possible states), and all 27 species included. Five of the areas represented the southeast outside peninsular Florida and were delimited based on major river boundaries (Fig. 2-1A, 2-7), which seemed to correlate well with observed distributional patterns of PG species within these areas. The other three areas were major physiographic zones within peninsular Florida, the definition of which can vary, so the suggestions of White (1970) were followed, which loosely defines it in such a way that our use of the Apalachicola River of a western boundary for the area makes sense. Peninsular Florida was then divided up into three distinct sections according to White's (1970) concept of physiographic zones (Fig. 2-1B). Most of these areas can be considered to have been underwater at various points in the past and are distinguished by their general geological characteristics: **(i)** the northern, or proximal, zone, is characterized by continuous high ground; **(ii)** the central, or mid-peninsular, zone, is characterized by discontinuous highlands comprised of the majority of the previously mentioned ridges and hills; and **(iii)** the southern, or distal, zone, is characterized by a gently sloping plain that does not drain well. This analysis also included a connectivity matrix using the area's centroids, scoring the areas as either connected or having space between them.

Table 2-2. Summary of the six BioGeoBEARS analyses: **A.** Analyses 1 and 2; **B**. Analyses 3-6. Unconstrained models allowed dispersal between any of the areas, the DEC+x models used distance between areas to implement dispersal, and the DEC+w models used connectivity between areas to implement dispersal. All areas included are named in Fig. MAP. Statistical significance key:* = p < 0.05, ** = p < 0.01, *** = p < 0.001, ns = not significant (p > 0.05). Rows with values highlighted in blue are the best-fit model from each analysis.

A																				Pairwise Likelihood Ratio Tests								
																AICc (within)		Delta	relative	AICc weight	+j			+x			+w		
Analysis	# Areas	Areas Included	# Areas Max per Species	# Possible States	# Species	Species Excluded	Reason	Base Model	Constraints Model	Abbrev.	LnL	# Params.	d	e	j	x	w	value	weight	AICc	likelihood	(across)	deviance	p-value	sig.	deviance	p-value	sig.	deviance	p-value	sig.
1 Coarse-scale discretization focused on the entire southeastern U.S.	8	5 outside peninsular Florida + 3 physiographic zones within peninsular Florida	5	219	27	0	N/A	DEC	unconstrained	M0	-68.87	2	0.043	0.013	0	0	0	142.2	12%	20.56	3.43E-05	0%									
								DEC+J	unconstrained	M0	-65.7	3	0.033	8.60E-09	0.017	0	0	138.5	82%	16.77	2.29E-04	0%	6.34	0.012	*						
								DIVALIKE	unconstrained	M0	-71.58	2	0.055	0.041	0	0	0	147.7	1%	25.98	2.28E-06	0%									
								DIVALIKE+J	unconstrained	M0	-68.58	3	0.041	1.00E-12	0.019	0	0	144.2	5%	22.53	1.28E-05	0%	6.00	0.014	*						
								BAYAREALIKE	unconstrained	M0	-78.55	2	0.046	0.510	0	0	0	161.6	0%	39.92	2.14E-09	0%									
								BAYAREALIKE+J	unconstrained	M0	-72.86	3	0.035	1.00E-07	0.030	0	0	152.8	0%	31.09	1.78E-07	0%	11.38	7.42E-04	***						
								DEC+x	adjacent+distance	M4	-67.31	3	0.048	1.00E-12	0	-0.270	0	141.7	0%	19.99	4.57E-05	0%				3.12	0.077	ns			
								DEC+J+x	**adjacent+distance**	**M4**	**-55.93**	**4**	**0.180**	**1.00E-12**	**0.120**	**-2.250**	**0**	**121.7**	**85%**	**0.00**	**1.00E+00**	**46%**	**22.76**	**1.84E-06**	***	**19.54**	**9.85E-06**	***			
								DIVALIKE+x	adjacent+distance	M4	-70.35	3	0.062	0.035	0	-0.180	0	147.7	0%	26.07	2.19E-06	0%				2.46	0.117	ns			
								DIVALIKE+J+x	adjacent+distance	M4	-57.68	4	0.340	1.00E-12	0.200	-3.310	0	125.2	15%	3.50	1.74E-01	8%	25.34	4.81E-07	***	21.80	3.03E-06	***			
								BAYAREALIKE+x	adjacent+distance	M4	-69.66	3	0.760	0.510	0	-4.650	0	146.4	0%	24.69	4.36E-06	0%				17.78	2.48E-05	***			
								BAYAREALIKE+J+x	adjacent+distance	M4	-65.89	4	0.100	1.00E-07	0.084	-1.260	0	141.6	0%	19.92	4.73E-05	0%	7.54	0.006	**	13.94	1.89E-04	***			
								DEC+w	adjacent+connectivity	M5	-61.43	3	0.180	0.100	0	0	1.040	129.9	3%	8.23	1.64E-02	1%							14.88	0.000	***
								DEC+J+w	adjacent+connectivity	M5	-56.44	4	0.110	1.00E-12	0.064	0	1.390	122.7	93%	1.02	6.00E-01	28%	9.98	0.002	**				18.52	0.000	***
								DIVALIKE+w	adjacent+connectivity	M5	-66.69	3	0.110	0.010	0	0	0.460	140.4	0%	18.75	8.50E-05	0%							9.78	0.002	**
								DIVALIKE+J+w	adjacent+connectivity	M5	-59.52	4	0.160	1.00E-12	0.100	0	1.700	128.9	4%	7.18	2.76E-02	1%	14.34	1.53E-04	***				18.12	0.000	***
								BAYAREALIKE+w	adjacent+connectivity	M5	-78.44	3	0.041	0.330	0	0	0.160	163.9	0%	42.25	6.71E-10	0%							0.22	0.639	ns
								BAYAREALIKE+J+w	adjacent+connectivity	M5	-66.17	4	0.086	0.007	0.120	0	0.900	142.2	0%	20.48	3.57E-05	0%	24.54	7.28E-07	***				13.38	0.000	***
								DEC+w+x	adjacent+connectivity+distance	M6	-61.31	4	0.130	0.032	0	-0.530	0.490	132.4	1%	10.76	4.61E-03	0%				12.00	5.32E-04	ns	0.24	0.624	***
								DEC+J+w+x	adjacent+connectivity+distance	M6	-55.67	5	0.160	1.00E-12	0.088	-0.640	1.270	124.2	85%	2.52	2.84E-01	13%	11.28	7.83E-04	***	0.52	0.471	ns	1.54	0.215	ns
								DIVALIKE+w+x	adjacent+connectivity+distance	M6	-61.24	4	0.470	1.00E-12	0	-2.510	4.340	132.3	2%	10.62	4.94E-03	0%				18.22	1.97E-05	***	10.90	0.001	***
								DIVALIKE+J+w+x	adjacent+connectivity+distance	M6	-57.67	5	0.350	1.00E-12	0.200	-3.300	0.069	128.2	12%	6.52	3.84E-02	2%	7.14	0.008	**	0.02	0.888	ns	3.70	0.054	ns
								BAYAREALIKE+w+x	adjacent+connectivity+distance	M6	-69.21	4	0.600	0.500	0	-3.210	1.270	148.2	0%	26.56	1.71E-06	0%				0.90	0.343	***	18.46	0.000	ns
								BAYAREALIKE+J+w+x	adjacent+connectivity+distance	M6	-64.18	5	0.160	0.020	0.220	-1.180	1.050	141.2	0%	19.54	5.72E-05	0%	10.06	0.002	**	3.42	0.064	*	3.98	0.046	ns
2 Fine-scale discretization focused on the ridges and zones of peninsular Florida, and non-peninsular Florida as a whole	14	12 ridges within peninsular Florida + combo of 3 physiographic zones within peninsular Florida + combo of all 5 outside peninsular Florida	4	1,471	27	0	N/A	DEC	unconstrained	M0	-119.5	2	0.043	5.00E-08	0	0	0	243.5	56%	3.88	0.14	9%									
								DEC+J	unconstrained	M0	-119.5	3	0.043	8.50E-09	1.00E-05	0	0	246.1	16%	6.43	0.04	3%	0	1	ns						
								DIVALIKE	unconstrained	M0	-122.7	2	0.046	5.00E-08	0	0	0	250.0	2%	10.28	0.01	0%									
								DIVALIKE+J	unconstrained	M0	-122.7	3	0.046	1.00E-12	1.00E-05	0	0	252.5	1%	12.83	0.00	0%	0	1	ns						
								BAYAREALIKE	unconstrained	M0	-120.5	2	0.032	0.27	0	0	0	245.5	20%	5.88	0.05	3%									
								BAYAREALIKE+J	unconstrained	M0	-120.5	3	0.032	0.28	1.00E-05	0	0	248.1	6%	8.43	0.01	1%	0	1	ns						
								DEC+x	adjacent+distance	M4	-119.2	3	0.042	5.00E-04	0	-0.028	0	245.5	4%	5.83	0.05	3%				0.60	0.439	ns			
								DEC+J+x	**adjacent+distance**	**M4**	**-114.9**	**4**	**0.140**	**1.00E-12**	**1.00E-05**	**-0.670**	**0**	**239.7**	**74%**	**0.00**	**1.00**	**63%**	**8.6**	**0.003**	**	**9.20**	**2.42E-03**	**			
								DIVALIKE+x	adjacent+distance	M4	-118.6	3	0.140	1.00E-12	0	-0.600	0	244.3	7%	4.63	0.10	6%				8.20	4.19E-03	**			
								DIVALIKE+J+x	adjacent+distance	M4	-118.6	4	0.140	1.00E-12	1.00E-05	-0.600	0	247.1	2%	7.40	0.02	2%	0	1.000	ns	8.20	4.19E-03	**			
								BAYAREALIKE+x	adjacent+distance	M4	-118.6	3	0.048	0.270	0	-0.240	0	244.2	8%	4.63	0.10	6%				3.80	0.051	ns			
								BAYAREALIKE+J+x	adjacent+distance	M4	-117.7	4	0.062	0.240	1.00E-05	-0.400	0	245.2	5%	5.60	0.06	4%	1.8	0.180	ns	5.60	0.018	*			

Table 2-2 Continued.

B	# Areas	Areas Included	# Areas Max per Species	# Possible States	# Species	Species Excluded	Reason	Base Model	Constraints Model	Abbrev.	LnL	# Params.	d	e	j	x	w	AICc (within)		Delta AICc	relative likelihood	AICc weight (across)	Pairwise Likelihood Ratio Tests								
																								+j			+x			+w		
Analysis																		value	weight				deviance	p-value	sig.	deviance	p-value	sig.	deviance	p-value	sig.
3 Fine-scale discretization focused on peninsular Florida's ridges and the space in-between	15	12 ridges within peninsular Florida + 3 physiographic zones within peninsular Florida	4	1.941	20	7: *M. gurneyi*, *M. pygmaeus*, *M. mirus*, *M. stegocercus*, *M. tumidicercus*, *M. foxi*, *M. strumosus*	only found outside peninsular Florida	DEC	unconstrained	M0	-110.4	2	0.061	0.039	0	0	0	225.5	66%	4.90	8.63E-02	7%				2.00	0.157	ns			
								DEC+J	unconstrained	M0	-110	3	0.061	1.00E-12	1.00E-05	0	0	227.6	23%	7.00	3.02E-02	2%	8.80	0.003	**	10.00	1.57E-03	**			
								DIVALIKE	unconstrained	M0	-113.4	2	0.068	1.00E-12	0	0	0	231.5	3%	10.90	4.30E-03	0%				3.60	0.058	ns			
								DIVALIKE+J	unconstrained	M0	-113.4	3	0.068	1.00E-12	1.00E-05	0	0	234.3	1%	13.70	1.06E-03	0%	4.60	0.032	*	8.20	4.19E-03	**			
								BAYAREALIKE	unconstrained	M0	-112.9	2	0.072	0.580	0	0	0	230.6	5%	10.00	6.74E-03	1%				3.00	0.083	ns			
								BAYAREALIKE+J	unconstrained	M0	-113	3	0.073	0.600	1.00E-05	0	0	233.4	1%	12.80	1.66E-03	0%	0.00	1.000	ns	3.20	0.074	ns			
								DEC+x	adjacent+distance	M4	-109.4	3	0.066	1.00E-12	0	-0.062	0	226.3	5%	5.70	5.78E-02	5%				2.00	0.157	ns			
								DEC+J+x	**adjacent+distance**	**M4**	**-105**	**4**	**0.280**	**1.00E-12**	**1.00E-05**	**-0.890**	**0**	**220.6**	**92%**	**0.00**	**1.00E+00**	**82%**				**10.00**	**1.57E-03**	**			
								DIVALIKE+x	adjacent+distance	M4	-111.6	3	0.094	1.00E-12	0	-0.200	0	230.7	1%	10.10	6.41E-03	1%				3.60	0.058	ns			
								DIVALIKE+J+x	adjacent+distance	M4	-109.3	4	0.260	1.00E-12	1.00E-05	-0.750	0	229.3	1%	8.70	1.29E-02	1%				8.20	4.19E-03	**			
								BAYAREALIKE+x	adjacent+distance	M4	-111.4	3	0.210	0.570	0	-0.640	0	230.3	1%	9.70	7.83E-03	1%				3.00	0.083	ns			
								BAYAREALIKE+J+x	adjacent+distance	M4	-111.4	4	0.210	0.570	1.00E-05	-0.640	0	233.5	0%	12.90	1.58E-03	0%				3.20	0.074	ns			
4 Similar to #3, but also simulating the rising and falling of the ocean at various points in the past by excluding non-ridge distribution records	15	12 ridges within peninsular Florida + 3 physiographic zones within peninsular Florida	4	1.941	15	7: *M. gurneyi*, *M. pygmaeus*, *M. mirus*, *M. stegocercus*, *M. tumidicercus*, *M. foxi*, *M. strumosus* +5: *M. apalachicolae*, *M. scapularis*, *M. bonita*, *M.* sp. nov. 2, *M.* sp. nov. 3	7 only found outside peninsular Florida + 5 not currently known from any ridges	DEC	unconstrained	M0	-76.81	2	0.060	0.100	0	0	0	157.6	3%	6.80	3.34E-02	1%									
								DEC+J	unconstrained	M0	-72.47	3	0.037	1.00E-12	0.094	0	0	150.9	84%	0.10	9.51E-01	42%	11.38	7.42E-04	***						
								DIVALIKE	unconstrained	M0	-75.82	2	0.059	1.00E-12	0	0	0	155.6	8%	4.80	9.07E-02	4%									
								DIVALIKE+J	unconstrained	M0	-75.35	3	0.049	2.90E-08	0.025	0	0	156.7	5%	5.90	5.23E-02	2%	1.72	0.190	ns						
								BAYAREALIKE	unconstrained	M0	-81.6	2	0.110	1.010	0	0	0	167.2	0%	16.40	2.75E-04	0%									
								BAYAREALIKE+J	unconstrained	M0	-77.26	3	0.045	0.330	0.058	0	0	160.5	1%	9.70	7.83E-03	0%	8.95	0.003	***						
								DEC+x	adjacent+distance	M4	-75.09	3	0.220	0.120	0	-0.760	0	158.4	2%	7.60	2.24E-02	1%				3.44	0.064	ns			
								DEC+J+x	**adjacent+distance**	**M4**	**-69.4**	**4**	**0.210**	**1.00E-12**	**0.740**	**-1.090**	**0**	**150.8**	**90%**	**0.00**	**1.00E+00**	**44%**				**6.14**	**0.013**	*			
								DIVALIKE+x	adjacent+distance	M4	-74.07	3	0.170	1.00E-12	0	-0.640	0	156.3	6%	5.50	6.39E-02	3%				3.50	0.061	ns			
								DIVALIKE+J+x	adjacent+distance	M4	-73.21	4	0.180	1.00E-12	0.160	-0.820	0	158.4	2%	7.60	2.24E-02	1%				4.28	0.039	*			
								BAYAREALIKE+x	adjacent+distance	M4	-79.71564	3	0.449	1.154	0	-0.818	0	171.6	0%	20.80	3.04E-05	0%				3.77	0.052	ns			
								BAYAREALIKE+J+x	adjacent+distance	M4	-75.24	4	0.450	0.260	0.510	-1.330	0	162.5	0%	11.70	2.88E-03	0%				4.04	0.044	*			
5 Similar to #4, but also simulating the ridges acting as true islands surrounded by the ocean at some point in the past by excluding non-ridge distribution records and all non-ridge areas	13	12 ridges + 1 hill within peninsular Florida	4	1,093	15	7: *M. gurneyi*, *M. pygmaeus*, *M. mirus*, *M. stegocercus*, *M. tumidicercus*, *M. foxi*, *M. strumosus* +5: *M. apalachicolae*, *M. scapularis*, *M. bonita*, *M.* sp. nov. 2, *M.* sp. nov. 3	7 only found outside peninsular Florida + 5 not currently known from any ridges or hills	DEC	unconstrained	M0	-73.87	2	0.075	0.056	0	0	0	152.7	4%	6.70	3.51E-02	2%									
								DEC+J	unconstrained	M0	-69.51	3	0.051	1.00E-12	0.140	0	0	147.2	69%	1.20	5.49E-01	27%	11.12	8.54E-04	***						
								DIVALIKE	unconstrained	M0	-72.48	2	0.076	2.80E-08	0	0	0	150.0	17%	4.00	1.35E-01	7%									
								DIVALIKE+J	unconstrained	M0	-71.93	3	0.064	1.50E-08	0.037	0	0	152.0	6%	6.00	4.98E-02	2%	1.66	0.198	ns						
								BAYAREALIKE	unconstrained	M0	-81.5	2	0.086	0.650	0	0	0	168.0	0%	22.00	1.67E-05	0%									
								BAYAREALIKE+J	unconstrained	M0	-72.69	3	0.046	1.00E-07	0.370	0	0	153.6	3%	7.60	2.24E-02	1%	14.82	1.18E-04	***						
								DEC+x	adjacent+distance	M4	-72.57	3	0.230	0.057	0	-0.690	0	153.3	2%	7.30	2.60E-02	1%				2.60	0.107	ns			
								DEC+J+x	**adjacent+distance**	**M4**	**-67.01**	**4**	**0.260**	**1.00E-12**	**0.850**	**-1.060**	**0**	**146.0**	**82%**	**0.00**	**1.00E+00**	**50%**				**5.00**	**0.025**	*			
								DIVALIKE+x	adjacent+distance	M4	-71	3	0.240	1.00E-12	0	-0.720	0	150.2	10%	4.20	1.22E-01	6%				2.96	0.085	ns			
								DIVALIKE+J+x	adjacent+distance	M4	-70.17	4	0.220	1.00E-12	0.200	-0.810	0	152.3	4%	6.30	4.29E-02	2%				3.52	0.061	ns			
								BAYAREALIKE+x	adjacent+distance	M4	-78.26	3	0.460	1.220	0	-0.690	0	164.7	0%	18.70	8.70E-05	0%				6.48	0.011	*			
								BAYAREALIKE+J+x	adjacent+distance	M4	-70.85	4	0.160	1.00E-07	1.000	-0.780	0	153.7	2%	7.70	2.13E-02	1%				3.68	0.055	ns			
6 Similar to #5, but with the areas outside peninsular Florida acting collectively as a "mainland"	14	12 ridges + 1 hill within peninsular Florida + combo of all 5 outside peninsular Florida	4	1,471	24	3: *M. bonita*, *M.* sp. nov. 2, *M.* sp. nov. 3	not currently known from any ridges or hills	DEC	unconstrained	M0	-96.81	2	0.034	1.00E-12	0	0	0	200.6	5%	29.60	3.74E-07	0%									
								DEC+J	unconstrained	M0	-94.44	3	0.025	1.00E-12	0.025	0	0	196.1	48%	25.10	3.54E-06	0%	15.36	8.88E-05	***						
								DIVALIKE	unconstrained	M0	-96.39	2	0.039	1.00E-12	0	0	0	197.3	26%	26.30	1.95E-06	0%									
								DIVALIKE+J	unconstrained	M0	-95.52	3	0.032	7.80E-09	0.016	0	0	198.2	16%	27.20	1.24E-06	0%	13.82	2.01E-04	***						
								BAYAREALIKE	unconstrained	M0	-115.5	2	0.046	0.630	0	0	0	235.6	0%	64.60	9.38E-15	0%									
								BAYAREALIKE+J	unconstrained	M0	-96.86	3	0.023	1.00E-07	0.049	0	0	200.9	4%	29.90	3.22E-07	0%	57.00	4.36E-14	***						
								DEC+x	adjacent+distance	M4	-88.13	3	0.350	1.00E-12	0	-1.140	0	183.5	0%	12.50	1.93E-03	0%				19.74	8.87E-06	***			
								DEC+J+x	**adjacent+distance**	**M4**	**-80.45**	**4**	**0.500**	**1.00E-12**	**1.360**	**-1.650**	**0**	**171.0**	**98%**	**0.00**	**1.00E+00**	**98%**				**27.98**	**1.23E-07**	***			
								DIVALIKE+x	adjacent+distance	M4	-91.67	3	0.070	1.00E-12	0	-0.370	0	190.5	0%	19.50	5.83E-05	0%				9.44	2.12E-03	**			
								DIVALIKE+J+x	adjacent+distance	M4	-84.76	4	0.330	1.00E-12	0.310	-1.180	0	179.6	1%	8.60	1.36E-02	1%				21.52	3.50E-06	***			
								BAYAREALIKE+x	adjacent+distance	M4	-115	3	0.068	0.780	0	-0.100	0	237.3	0%	66.30	4.01E-15	0%				1.00	0.317	ns			
								BAYAREALIKE+J+x	adjacent+distance	M4	-86.5	4	0.350	1.00E-07	0.580	-1.350	0	183.1	0%	12.10	2.36E-03	0%				20.72	5.32E-06	***			

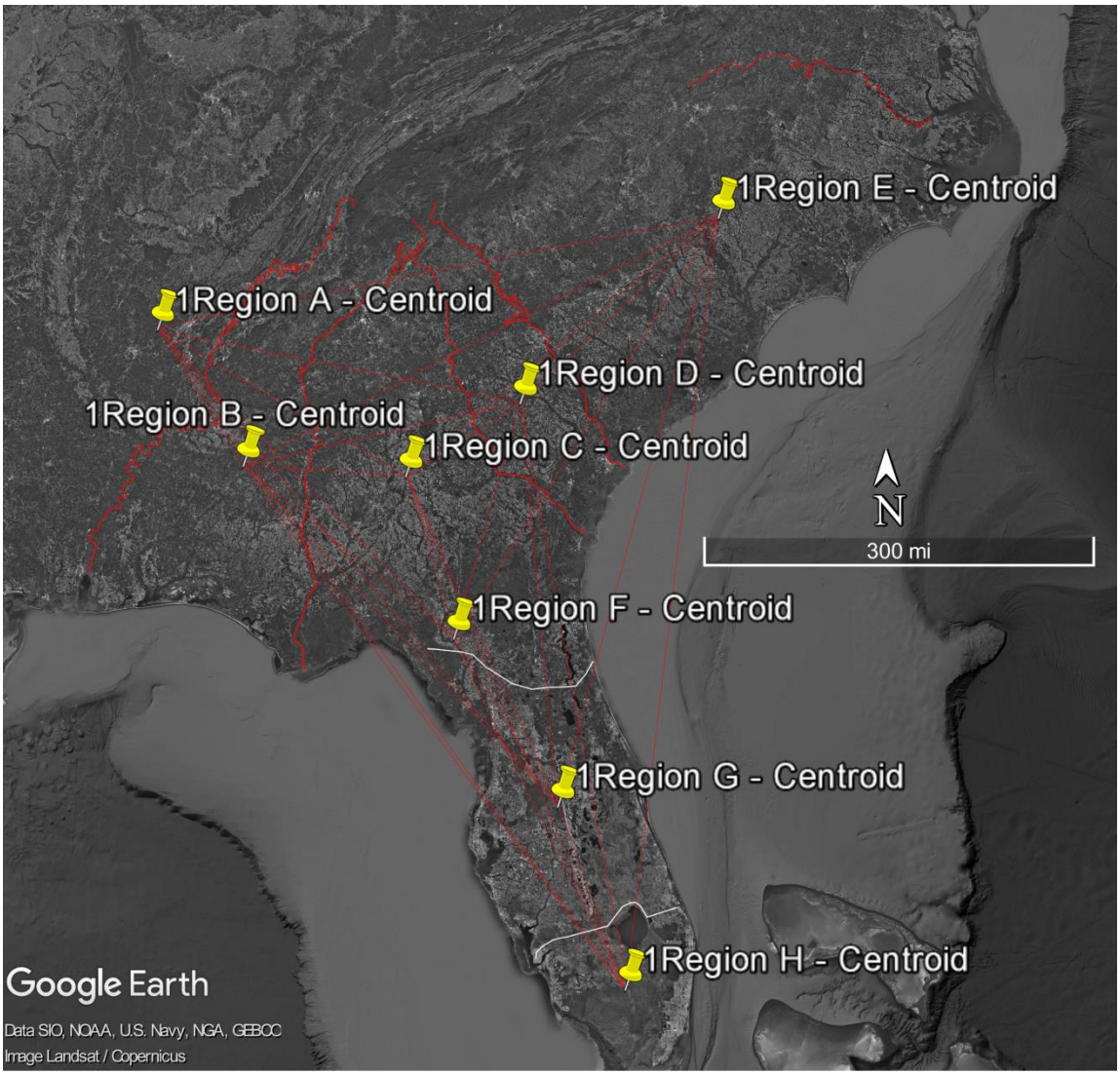

Figure 2-7. Map showing the eight geographical areas included in BioGeoBEARS analysis 1 and the location of their centroids. Letters A-H correspond with the locations seen in Fig. 2-1.

2) A fine-scale discretization of 14 geographical areas focused on the ridges and zones of peninsular Florida, and non-peninsular Florida as a whole, with four areas maximum per species (1,471 possible states), and all 27 species included. 12 of the areas were the primary ridges in peninsular Florida (Fig. 2-1B, 2-8), one was comprised of the

three physiographic zones from the first analysis, and the last one included a combination of all the non-peninsular Florida areas from analysis 1. **3)** A fine-scale discretization of 15 geographical areas focused on peninsular Florida's ridges and the space in-between, with four areas maximum per species (1,941 possible states), and 20 species included (seven are only found outside peninsular Florida – see Table 2 for the

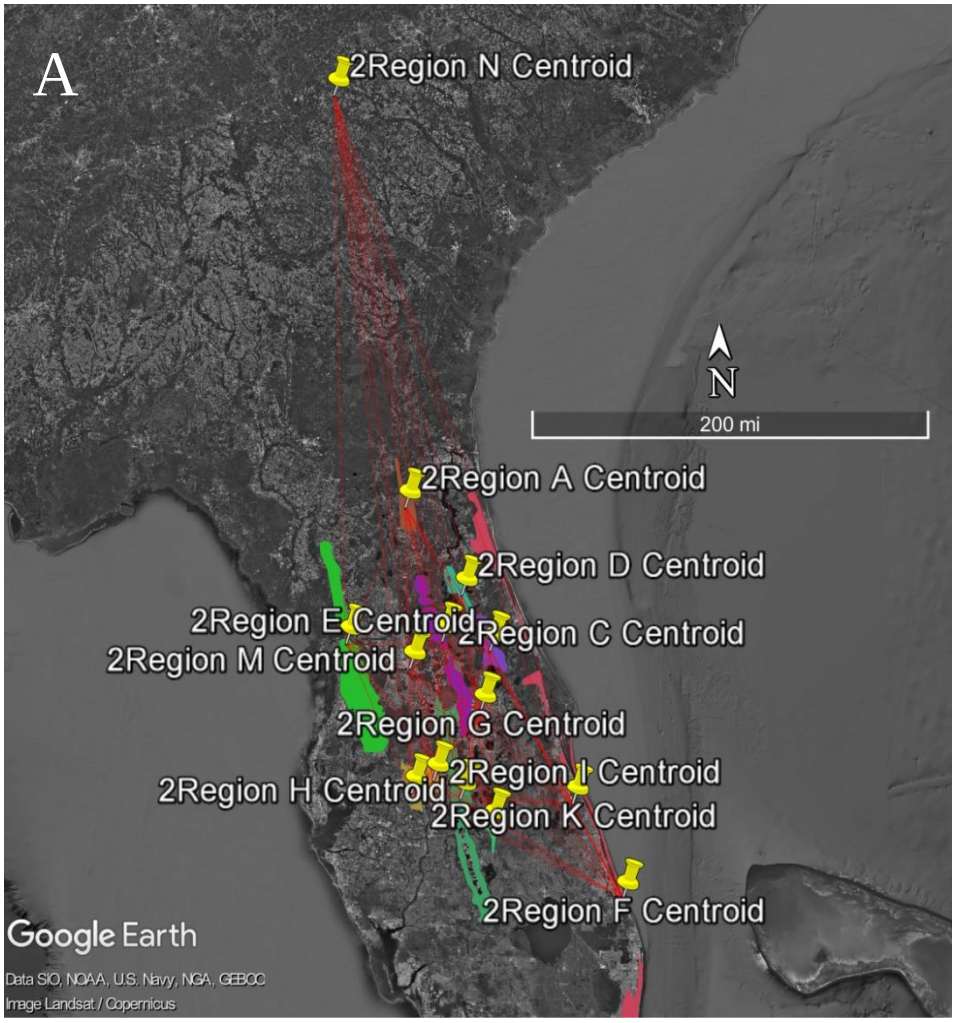

Figure 2-8. Maps showing the 14 geographical areas included in BioGeoBEARS analysis 2 and the location of their centroids. Letters A-N correspond with the locations seen in Fig. 2-1. A. Coarser view. B. Finer view.

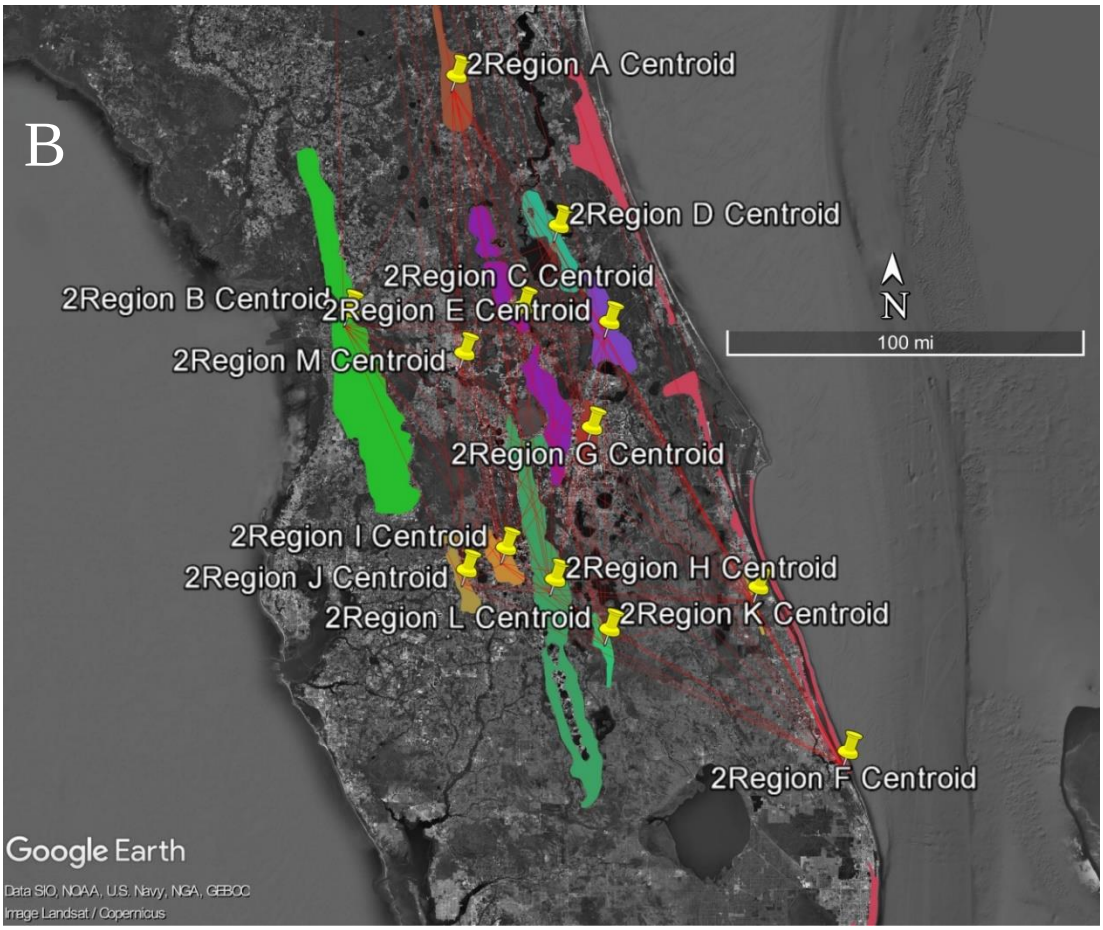

Figure 2-8 Continued.

list). 12 of the areas were the usual ridges and the other three were the individual physiographic zones from analysis 1 (Fig. 2-9). **4)** Similar to analysis 3 (Fig. 2-9), but also simulating the rising and falling of the ocean at various points in the past by excluding non-ridge distribution records. Only 15 species were included, so the same seven from outside peninsular Florida were removed along with five that are not currently known from any ridges (see Table 2 for the list). **5)** Similar to analysis 4, but also simulating the ridges acting as true islands surrounded by the ocean at some point in

the past by excluding non-ridge distribution records and all non-ridge areas. 13 areas only, with four areas maximum per species (1,093 possible states), and the areas included the typical 12 ridges, plus a hill strongly associated with one species (Fig. 2-10). **6)** Similar to analysis 5, but with the areas outside peninsular Florida (as in analysis

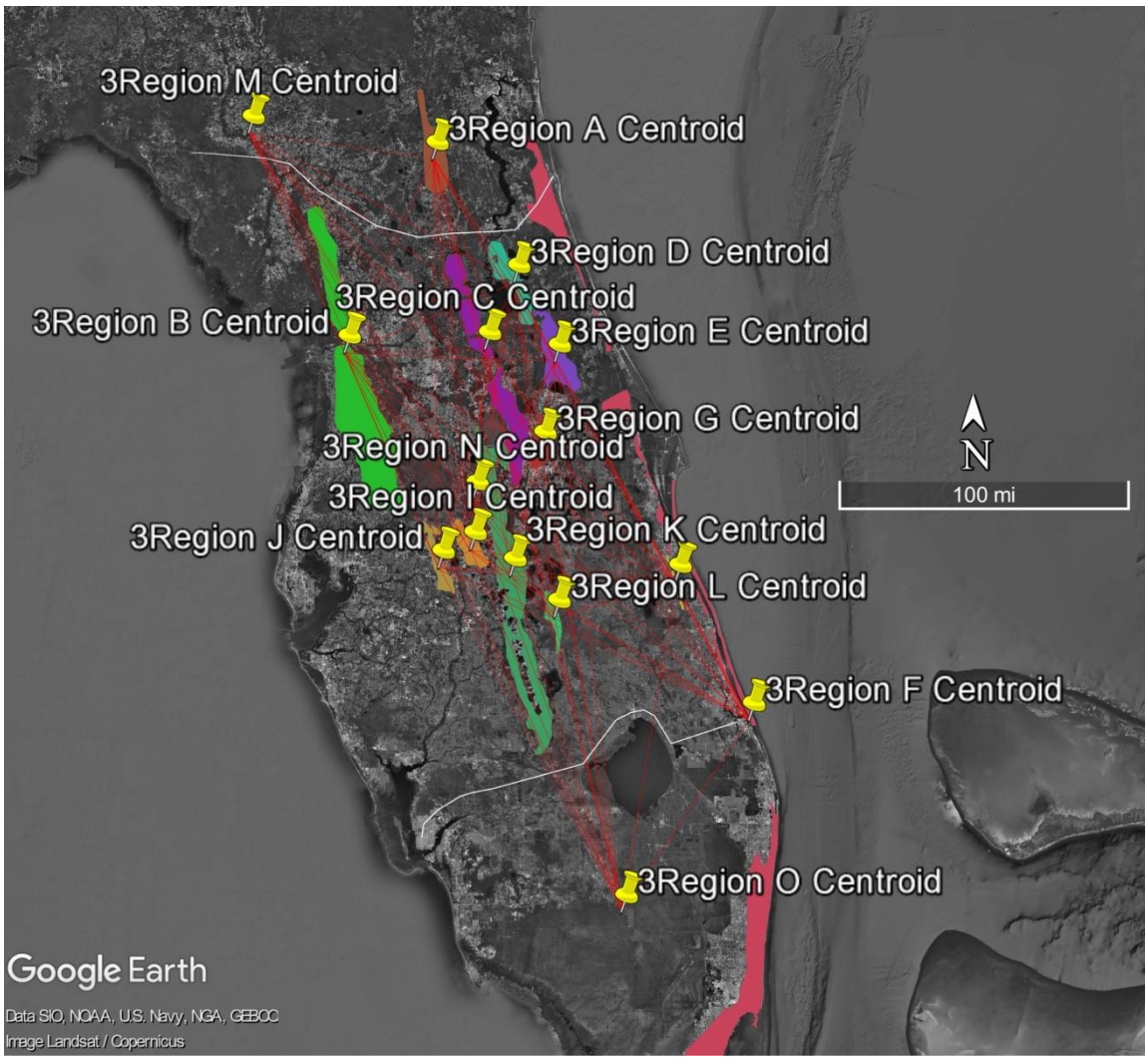

Figure 2-9. Maps showing the 15 geographical areas included in BioGeoBEARS analyses 3 and 4, and the location of their centroids. Letters A-O correspond with the locations seen in Fig. 2-1

1) acting collectively as a "mainland" (Fig. 2-11). There were four areas maximum per species (1,471 possible states) and only 24 species were included because three peninsular Florida species (see Table 2 for the list) are not currently found on any ridges or hills.

For analyses that include geographical distance as a predictor of dispersal rates (the *+x* model variant of Van Dam and Matzke 2016), the distance (in kilometers) between each geographic area in each was calculated (between the centroids of each area using Google Earth Pro, v. 7.1.8.3036. The centroid-to-centroid distance gives a rough overall measure of distance between discrete areas. We acknowledge that a number of other measures of distance between areas can be imagined (closest distance, amount of shared border, etc.). These could be explored in future studies, and would constitute additional hypotheses to test, although a larger dataset would be recommended for exploring the great many variant models that could be produced with multiple distance measures (in addition, various measures of geographic distance are likely to be substantially correlated). Here, our goal was simply to assess whether there was an obvious effect of distance on dispersal rates in this flightless clade. The between-area distances were divided by the smallest observed distance, so that the smallest rescaled distance was 1 (representing no effect on the base dispersal parameters). This was done to avoid scaling issues that might arise if, for example, absolute distances were used that were measured in a small unit such as meters; this might cause issues with maximum likelihood inference, when parameters hit minimum or maximum bounds before reaching the ML solution.

Due to computational and data limitations, some imaginable scenarios were not explored. For example, time stratification was not included in any of the analyses because the geologic age of peninsular Florida (where most PG species reside) and the relative age of the PG were estimated to be very recent at, respectively, 25 and 3.71 MYO. Furthermore, although it is known that significant sea level changes occurred in peninsular Florida, there is little data to support a clear, time-scaled reconstruction of paleogeography.

.

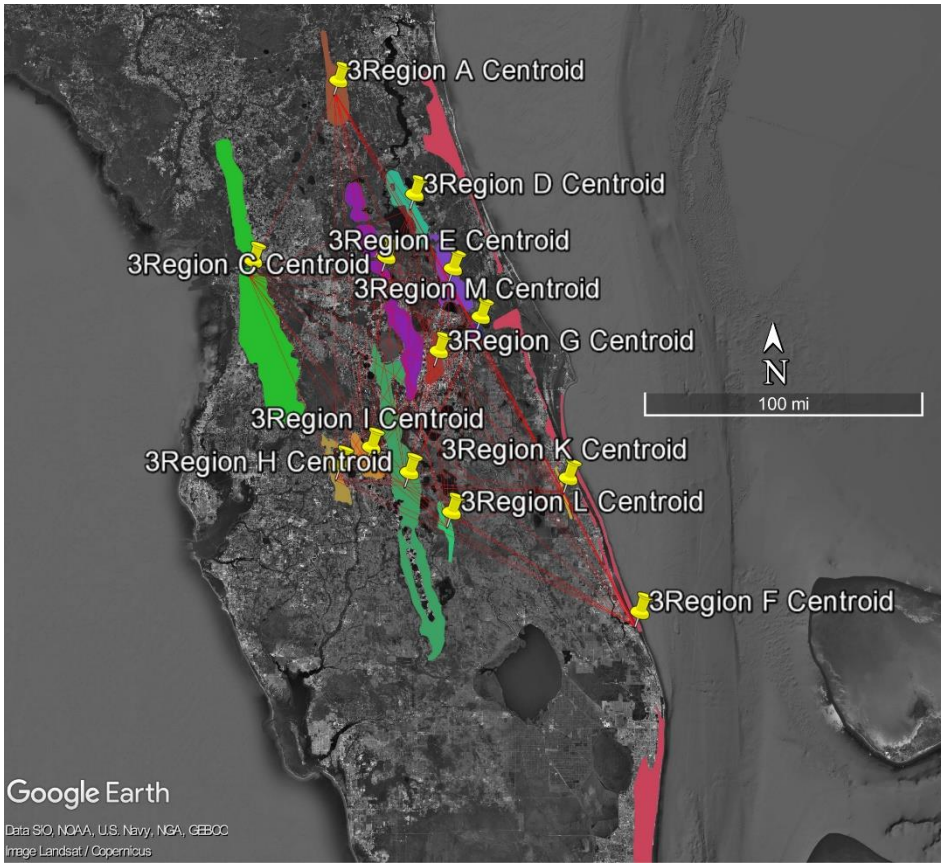

Figure 2-10. Maps showing the 13 geographical areas included in BioGeoBEARS analysis 5 and the location of their centroids. Letters A-M correspond with the locations seen in Fig. 2-1.

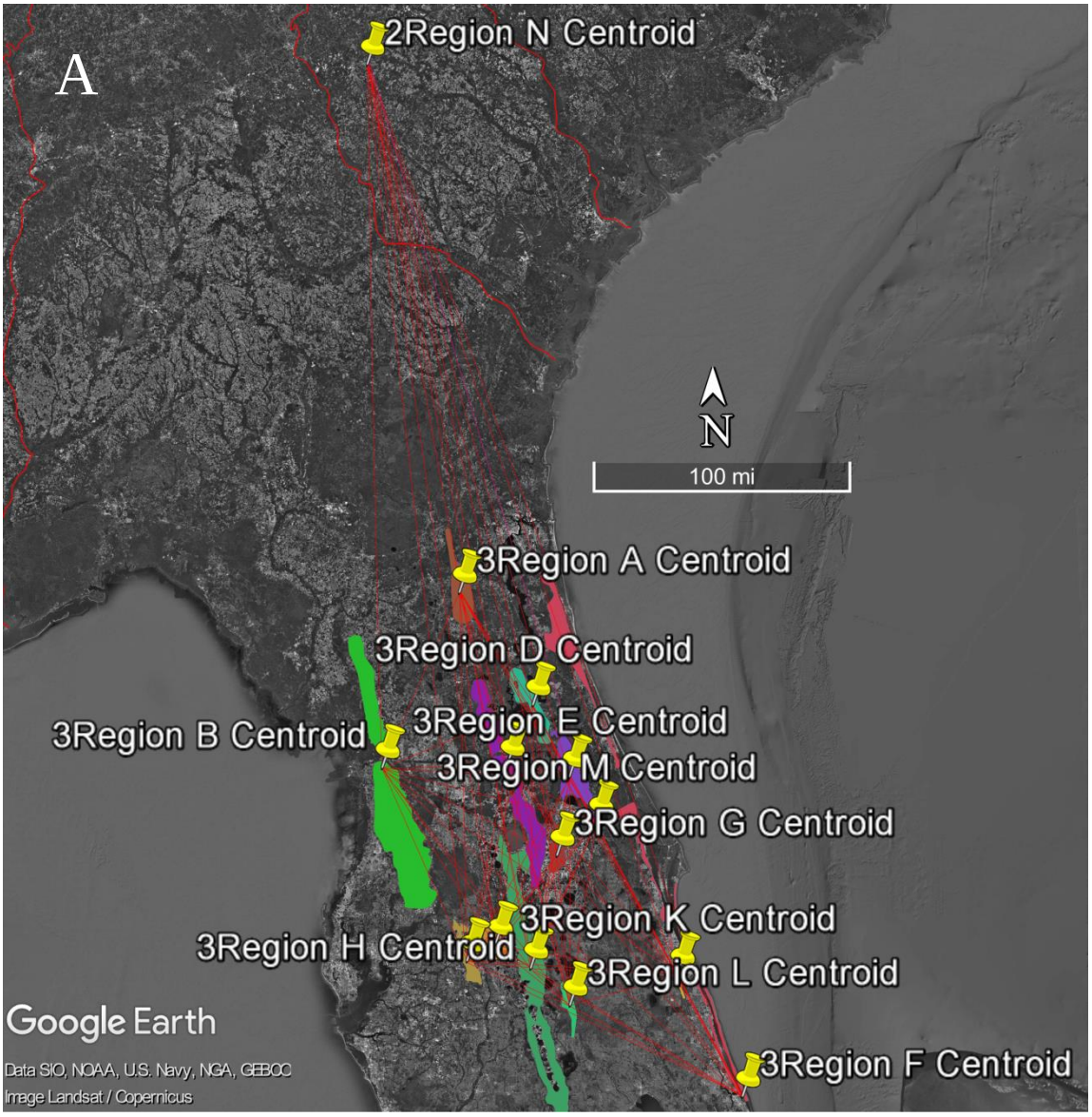

Figure 2-11. Maps showing the 14 geographical areas included in BioGeoBEARS analysis 6 and the location of their centroids. Letters A-N correspond with the locations seen in Fig. 2-1. A. Coarser view. B. Finer view.

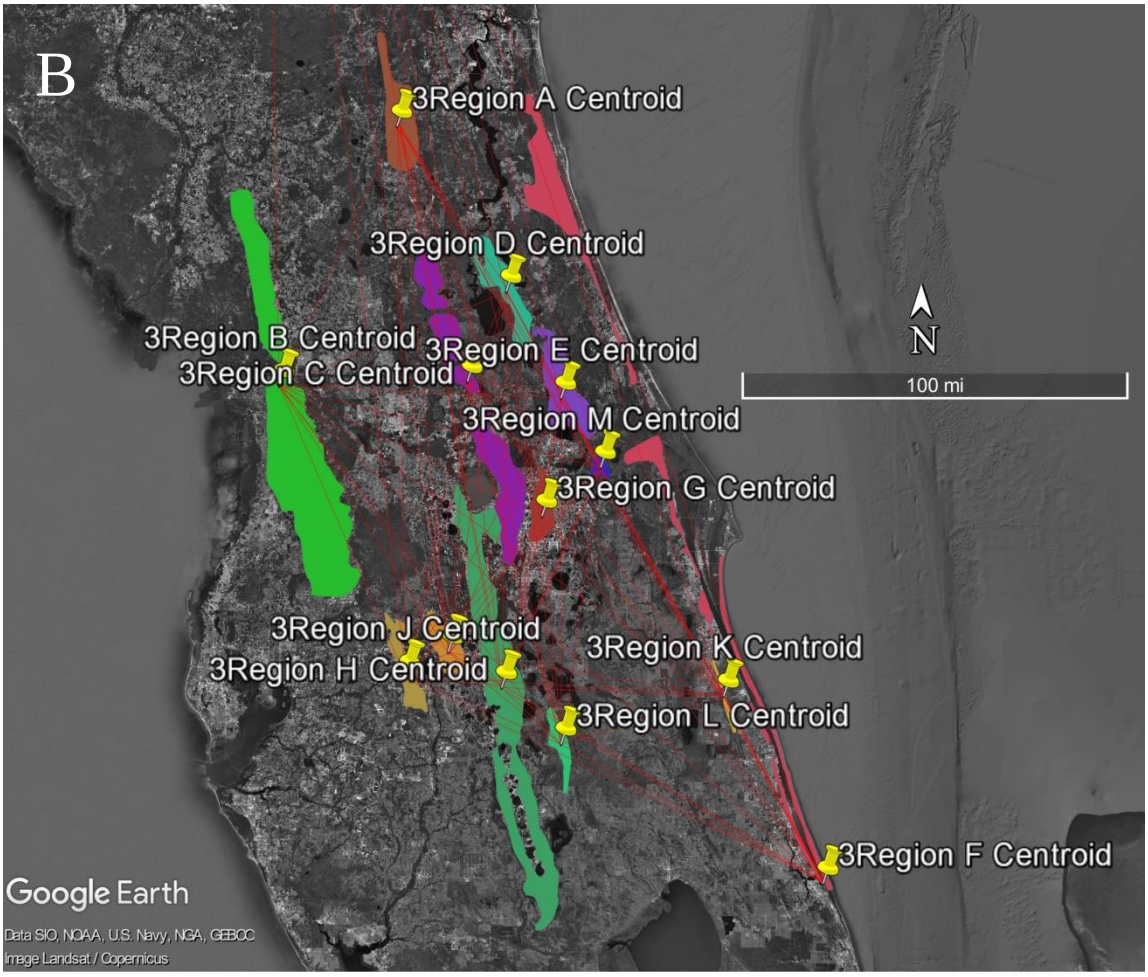

Figure 2-11 Continued.

Speciation Rate

Speciation rate (SR) was calculated according to the methods of McCune, 1997 (also used by Mendelson and Shaw, 2005, and inferred to have been used by Wessel et al., 2013) using our divergence time estimation tree. This tree can be classified as symmetrical/balanced in which bifurcations within all lineages occur with the same

frequency. Thus, the following equation was chosen, which assumes that there is no extinction due to the relatively young ages of the included clades:

$SR_{ln} = (\ln n)/t$

Where n = the number of extant species in a monophyletic clade and t = the estimated age of that clade. Speciation rate was then calculated for major PG lineages (Table 3).

Table 2-3. Speciation Rate (SR_{ln}) in species per million years for the PG's four major lineages (colors correspond to those in Fig. 2-4) and lineage D's three major clades and ordered within each category from lowest to highest rate. n = the number of species in a monophyletic clade and t = the estimated age of the associated clade.

Major Lineage	SR_{ln}	n	t
A	0	1	3.71
B	0.78	8	2.71
C	0.99	4	1.4
D	1.13	14	2.34
Major Clade			
Tequestae Group	0.87	3	1.27
M. rotundipennis-M. withlacoocheensis	1.31	2	0.53
Puer Group *sensu stricto*	2.31	9	0.95

Maps

The present-day geographical distribution map of the PG (Fig. 2-1) contains locality data compiled from 6,522 specimens across 17 collections (representing almost all known PG specimens) distilled down to 741 specimens representing 679 unique localities. The map was created with the web-based application Earth Point (http://www.earthpoint.us/), a tool for converting Microsoft Excel files (file format in which the Puer Group locality data resides) into Google Earth-enabled KML files. The

resulting KML was combined with county boundaries in KML form for the five included southeastern states (North and South Carolina, Georgia, Alabama, and Florida), downloaded from Google's Fusion Tables site (https://fusiontables.google.com), and also combined with a KMZ file of Florida's ridges and hills, from the Florida Department of Environmental Protection.

The map displaying the phylogeny overlaid onto the geography ("geophylogeny" – Fig. 2-12) was created in GenGIS (v.2.5.3) (Parks et al., 2013) using consensus coordinates for each species (only a single specimen per species can be included because, otherwise, the program will stochastically decide which one to use), identified by uploading all the locality data used to create the present-day map to Hamster Map's Quick Map feature (http://www.hamstermap.com/quickmap.php) and determining which specimen locality per species was the centroid. These data were combined with state outlines from Google's Fusion Tables (converted from KML to SHP files using MyGeodata's "Converter" feature: https://mygeodata.cloud/converter/) and the PG phylogeny (Bayesian phylogram) in Newick format with the outgroups pruned.

The historical maps used for the BioGeoBEARS analyses were based on the modern-day map (Fig. 2-1) and modified accordingly to suit the needs of the particular analysis.

Results

Phylogenetic and Multispecies Coalescent Analyses

We recovered identical topologies from total evidence analyses in both Bayesian and ML frameworks (Fig. 2-4), which were also quite similar to the multispecies coalescent analyses (the exceptions were the placements of: *M. gurneyi*. *M. mirus*, and some of the relationships within the PGss; nodal support was also lower, in general – Fig. 2-6). Therefore, we have referred to the Bayesian phylogram (Fig. 2-4) for subsequent discussions on phylogenetic relationships. We found the PG to be monophyletic with strong nodal support, which has diversified into four major lineages (Figs 2-4 and 2-5; Table 1): **A** (green) - the single earliest diverging species, restricted to Florida's panhandle: *M. gurneyi;* **B** (blue) - eight non-peninsular Florida species, with most primarily found in North and South Carolina, and Georgia, with some in Florida's panhandle, and specimens of two species crossing into Alabama; **C** (red) - four mostly northern/central peninsular Florida species; and **D** (purple) - the 14 mostly central/southern peninsular Florida species (which includes the PGss), with the sole exception being *M. rotundipennis* (Scudder, 1878), which is primarily found in the northern part of the peninsula, tangentially present in Florida's panhandle, and in parts of southern Georgia. Additionally, only two out of the six PG *sensu stricto* groups were recovered as monophyletic (Fig. 2-4): the Tequestae Group and the PGss. The remaining four historical subgroups (Forcipatus, Rotundipennis, Scapularis, and Strumosus Groups) were found to be paraphyletic (Fig. 2-4). Furthermore, lineage D can be further

separated into three major clades based mostly on these subgroups: **1)** the Tequestae Group, **2)** *M. rotundipennis-M. withlacoocheensis* (2/3 of the historical Rotundipennis Group), and **3)** the PGss (Fig. 2-4).

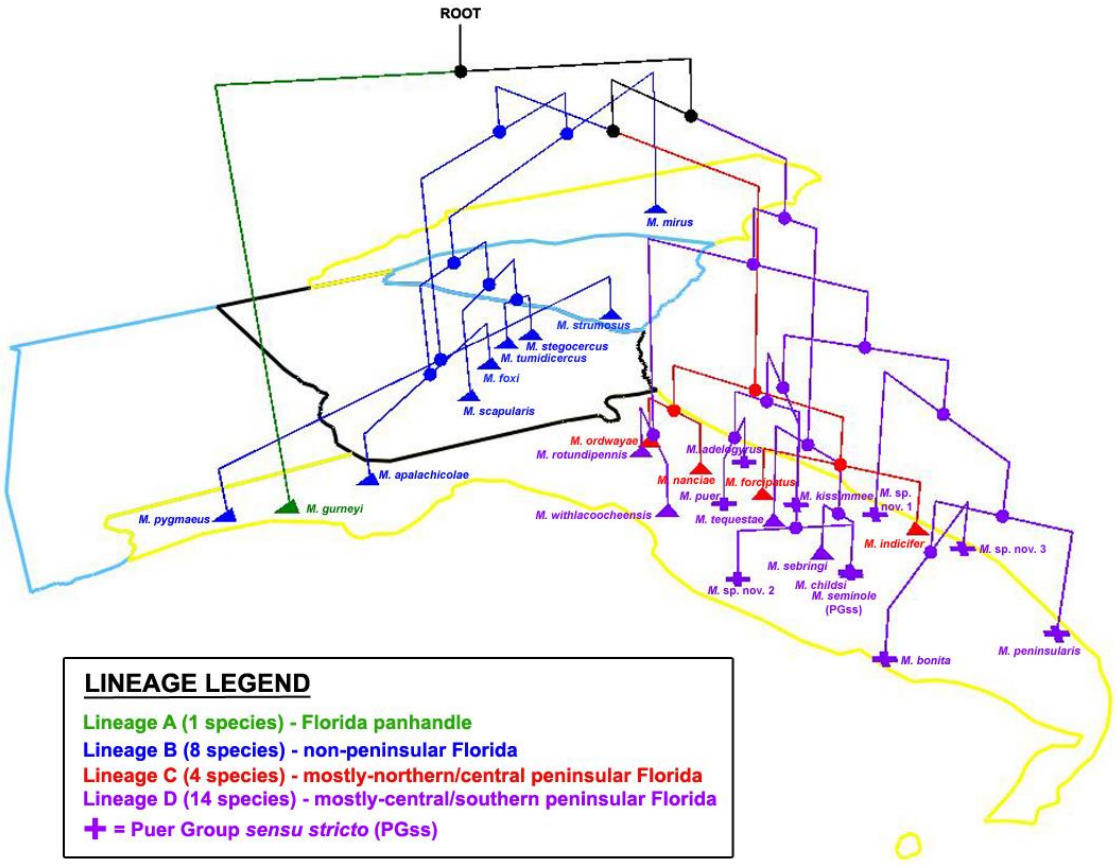

Figure 2-12. The phylogram of the Puer Group (see Fig. 2-4), minus the outgroups, overlaid onto the geography of the southeast to create a "geophylogeny". Each species point represents the center of that species range, many of which are very small in the first place. Lineage D's Puer Group *sensu stricto* (PGss) is identified using the symbol of a plus sign.

Lineages A, C, and D (Fig. 2-4) were well-supported overall with high nodal support values with the exception of relatively low nodal support for two Forcipatus

Group species in C: *M. indicifer* and *M. forcipatus*. Lineage B, though, had fairly low nodal support throughout with the exception of the clade formed by *M. foxi* Hebard, 1923 and *M. apalachicolae* Hubbell, 1932, as well as the clade (and its internal node) formed by *M. scapularis* Rehn & Hebard, 1916, *M. tumidicercus* Hubbell, 1932, and *M. stegocercus* Rehn & Hebard, 1916. The ancestral node joining lineages B and C had 100% support of both posterior probability and bootstrap values while the internal nodes possessed of relatively low support are borderline for relatively good support.

Divergence Time Estimation Analysis

The topology of the divergence time estimation analysis tree (Fig. 2-5) was slightly different from the phylogram (solely in the placement of the weakly supported *M. mirus*) and estimated that the PG diverged from the other included *Melanoplus* lineages around 4.71 MYO, but the 95% confidence interval (CI) was relatively wide. With regards to the relative ages of the four major lineages, lineage A was inferred to be the oldest as it also coincides with the estimated origin age of the PG. Lineage B was estimated to be the second-oldest at 3.71 MYO while lineage C was estimated to be the youngest at 2.4 MYO, the ancestral split between the two occurring a bit further back in time. Lineage D was estimated to be 3.34 MYO, with its ancestral split from lineages B and C happening a bit earlier. In general, the peninsular Florida species, represented by lineages C and D, contained the youngest lineages overall. In terms of PG s.s. groups, the PGss contained most of the youngest lineages, with fairly rapid radiation beginning

around 1.95 MYA, the most recent event of which was the ancestral split of the sister species *M.* sp. nov. 3 and *M. bonita*.

BioGeoBEARS Analysis

Despite the differences among the six BioGeoBEARS analyses (Figs. 2-13 to 2-18; Table 2), there were some general patterns that consistently stood out. First, though, it should be noted that our power to distinguish models was limited due to the rather small datasets that consisted of 15-27 species depending on the analysis. Still, in almost every analysis and based on AICc weighting of the models, DEC and DEC+J were the best-fitting base models. Adding the founder-event jump dispersal parameter (+*j*) almost always resulted in a statistically significant improvement in the model likelihood of DEC while adding a parameter for distance effect (+*x*) did the same for every analysis (albeit weakly in some cases). This means that, in all analyses, the model DEC+J+x was the best-fit in explaining the PG's current distribution. Taken together, these findings suggest that founder-events and geographical distance, particularly between peninsular Florida's ridges and hills, played important roles in that distribution (Fig. 2-1). Of the two, distance played the largest role because of its relative importance for predicting dispersal rates because founder-events were estimated to be minimal and did not even appear in analysis 2 (Fig. 2-14). In general, when founder-event speciation was suggested to have occurred, it was typically associated with the lineages C and D of peninsular Florida (the sole exceptions were lineage B's *M. mirus* and *M. apalachicolae* in analysis 1) and often appeared repeatedly in the same species/clades across analyses,

such as in lineage C's *M. ordwayae* and lineage D's sister species, *M. adelogyrus* and *M. puer*.

Furthermore, sympatric speciation events and range-expansion dispersal (parameter *d*) into areas of close proximity appeared to play the second-most important roles in the biogeography of this system. In stark contrast, extinction (parameter *e*), or range contraction, events were estimated to be rare, perhaps due to the relatively young age of the PG (Fig. 2-5) and peninsular Florida; also, DEC-type models are known to systematically underestimate *e* (Ree and Smith 2008). In addition, vicariance only played an occasional role in the speciation of the PG, the most likely instance being in lineage C, where vicariance was estimated to be likely in three of the analyses (Figs. 2-13 to 2-15).

In terms of lineage diversification, lineage A's split from the rest of the PG was estimated to be sympatric speciation (meaning only within-area speciation, which makes no statement about sympatry vs. allopatry at finer scales), but lineage A was only included in analyses 1, 2, and 6 (Figs 2-13, 2-14, and 2-18). Lineages B and C were included fully in the same three analyses, but also partially in analysis 3 (Figs 2-15). For analyses 1 and 2, the split between lineages B and C was estimated to most likely be a vicariance event and, in analysis 6, a founder event. In analysis 3, the divergence of lineages B and C was most likely sympatric, possibly as a result of only including two of lineage B's eight species (the two found in northern peninsular Florida). Lineage D's split from B and C was estimated to be most likely sympatric in all 6 analyses (Figs 2-13 to 2-18).

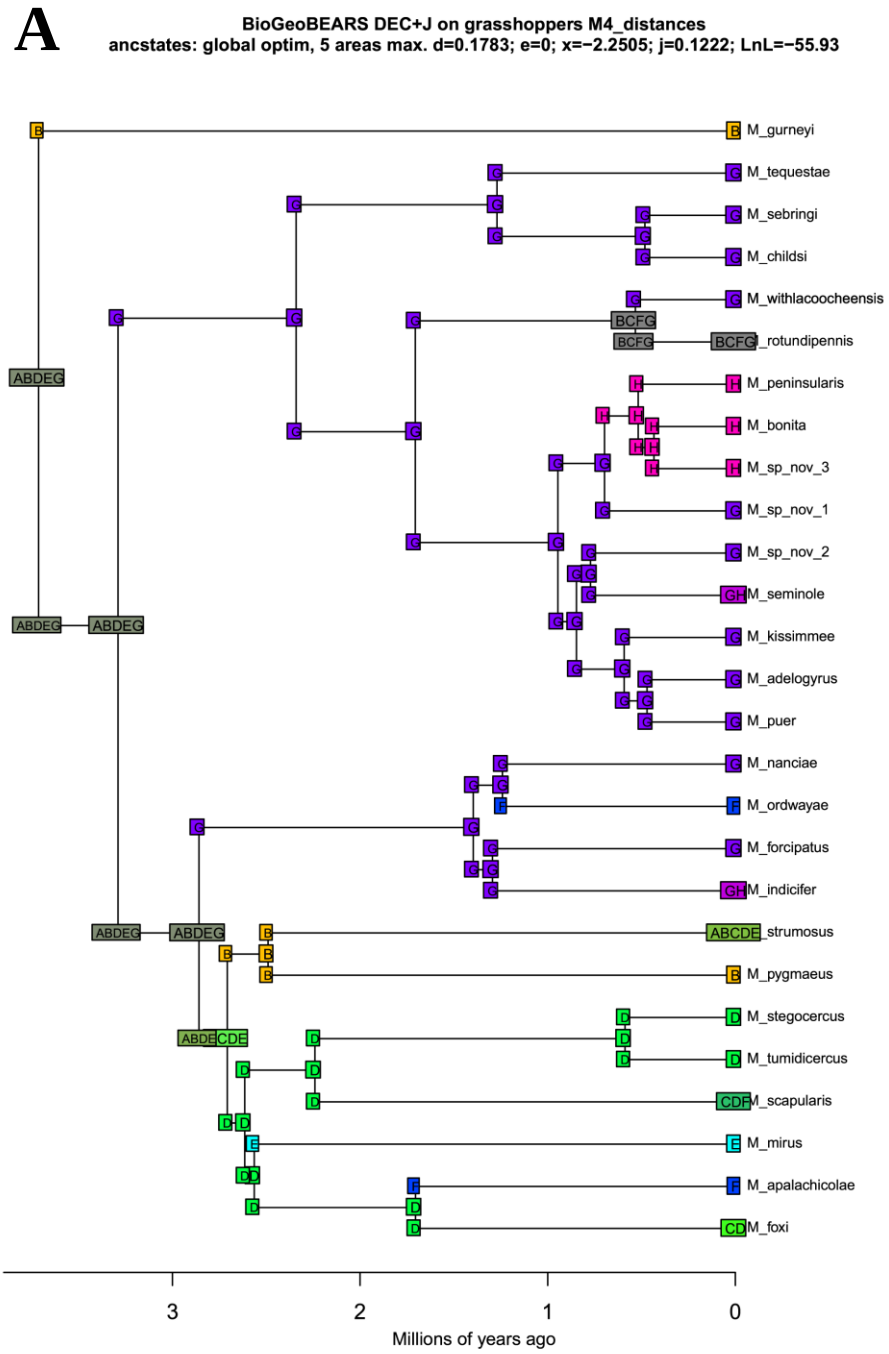

Figure 2-13. Ancestral state estimations for the Puer Group resulting from BioGeoBEARS analysis 1: **A.** Plot of the single-most-probable state (geographical range) at each node (just before speciation) and post-split (just after speciation). **B.** Pie charts represent the probabilities of each possible geographical range just before and after each speciation event.

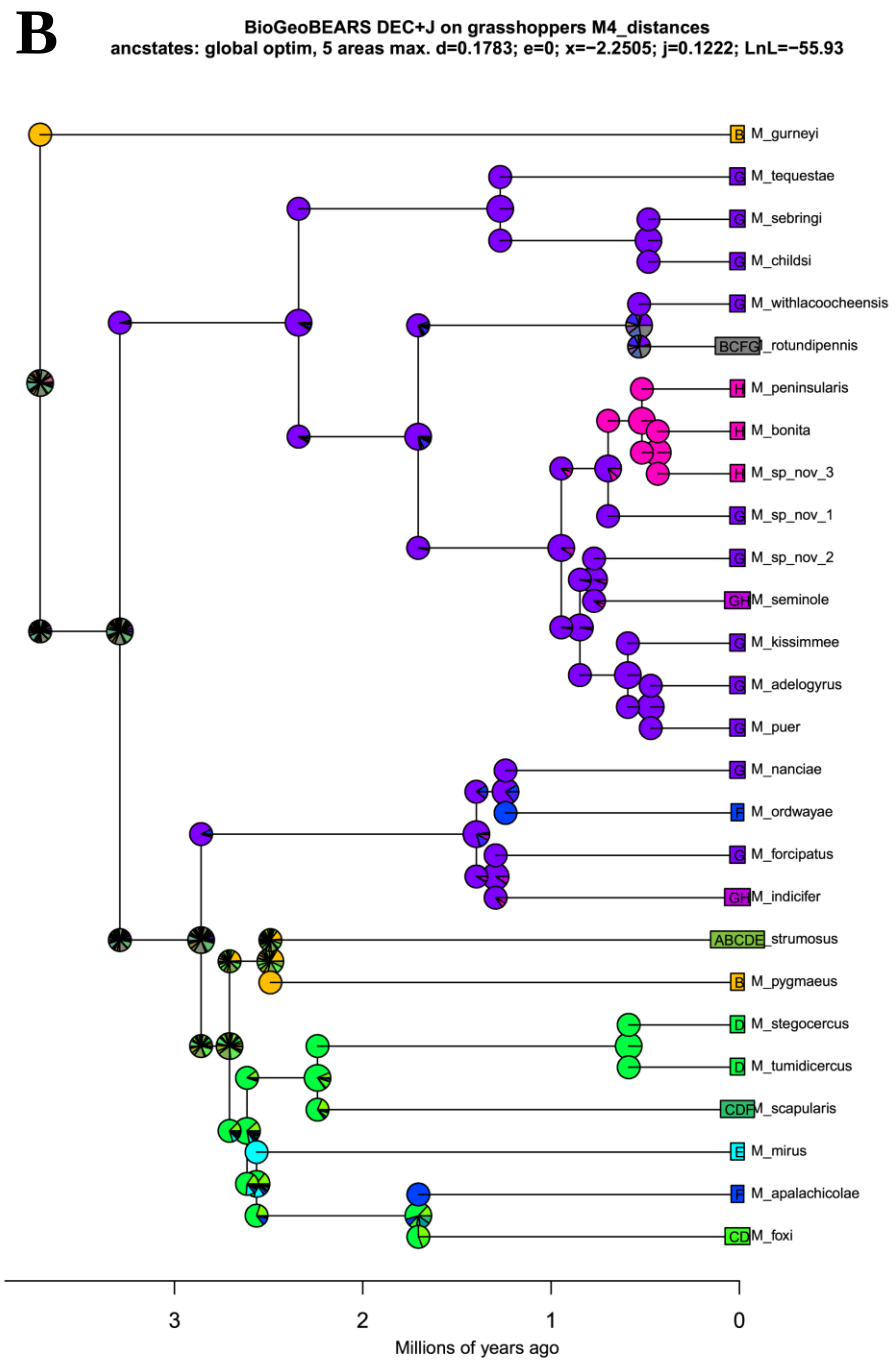

Figure 2-13 Continued.

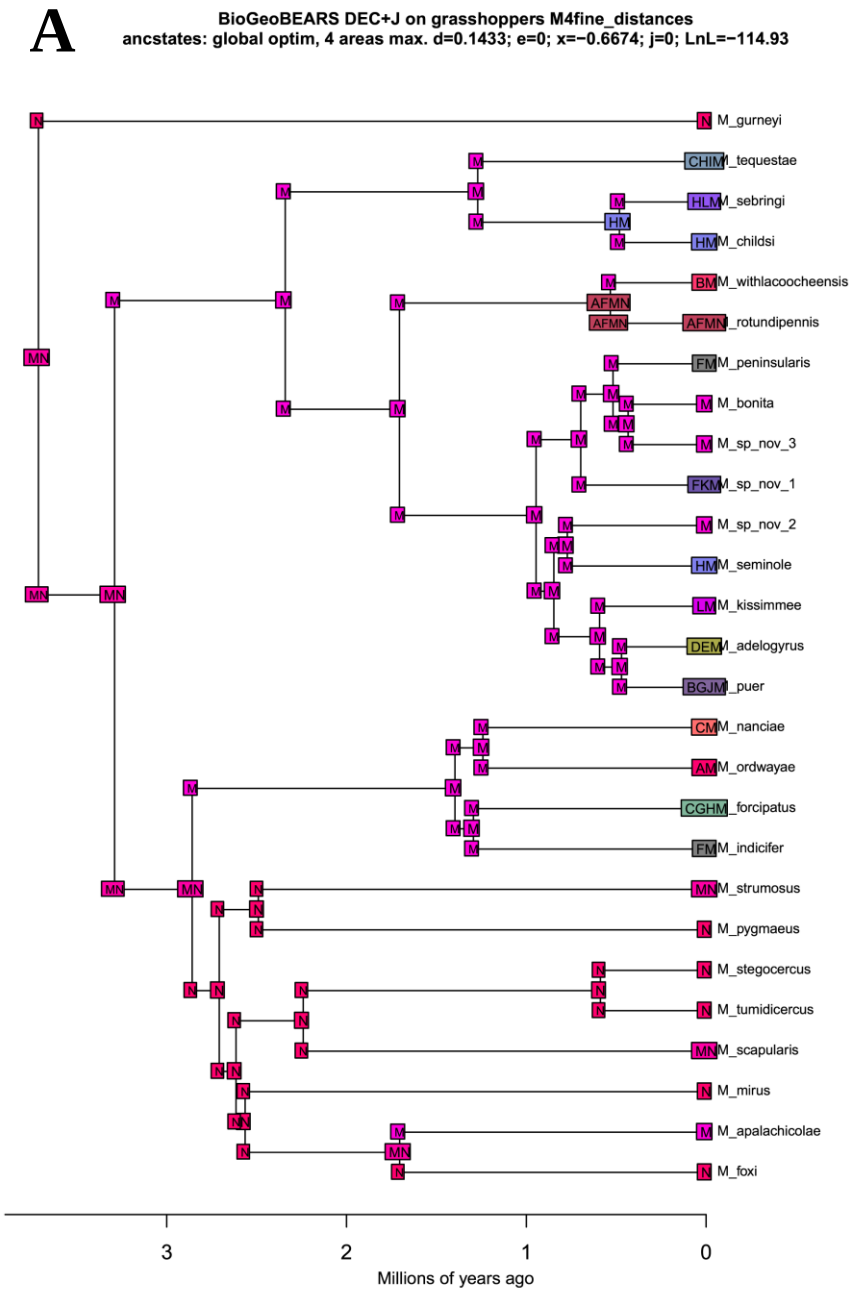

Figure 2-14. Ancestral state estimations for the Puer Group resulting from BioGeoBEARS analysis 2: **A.** Plot of the single-most-probable state (geographical range) at each node (just before speciation) and post-split (just after speciation). **B.** Pie charts represent the probabilities of each possible geographical range just before and after each speciation event.

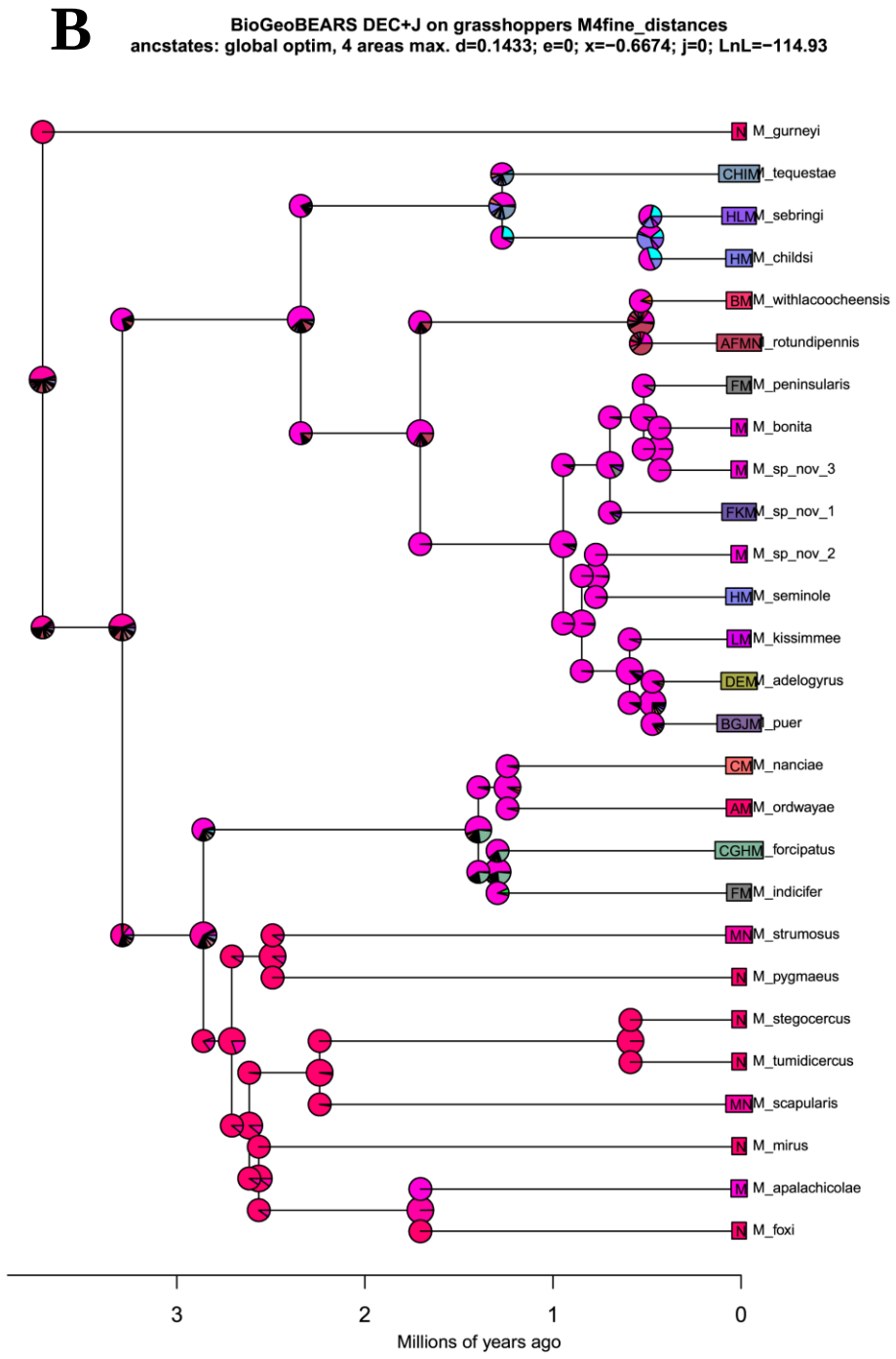

Figure 2-14 Continued.

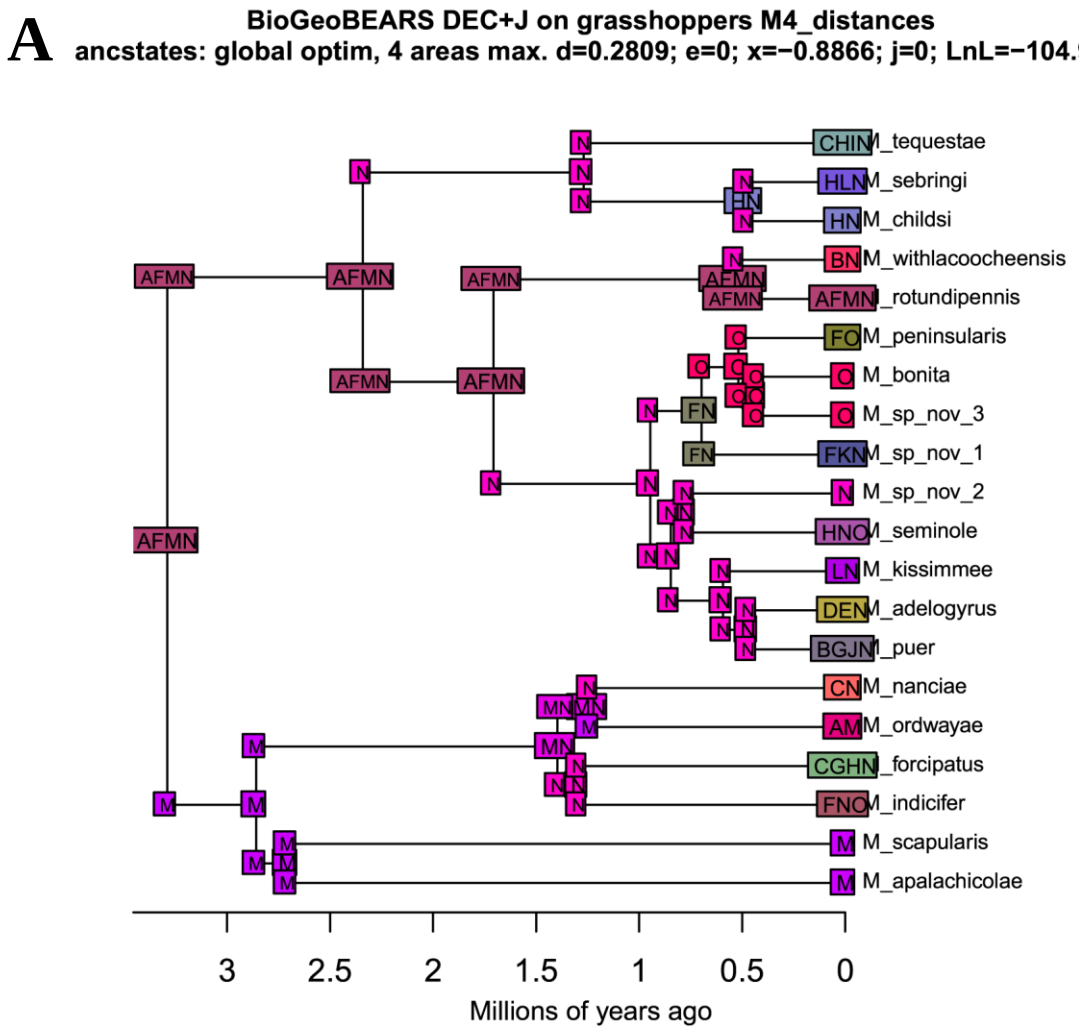

Figure 2-15. Ancestral state estimations for the Puer Group resulting from BioGeoBEARS analysis 3: **A.** Plot of the single-most-probable state (geographical range) at each node (just before speciation) and post-split (just after speciation). **B.** Pie charts represent the probabilities of each possible geographical range just before and after each speciation event.

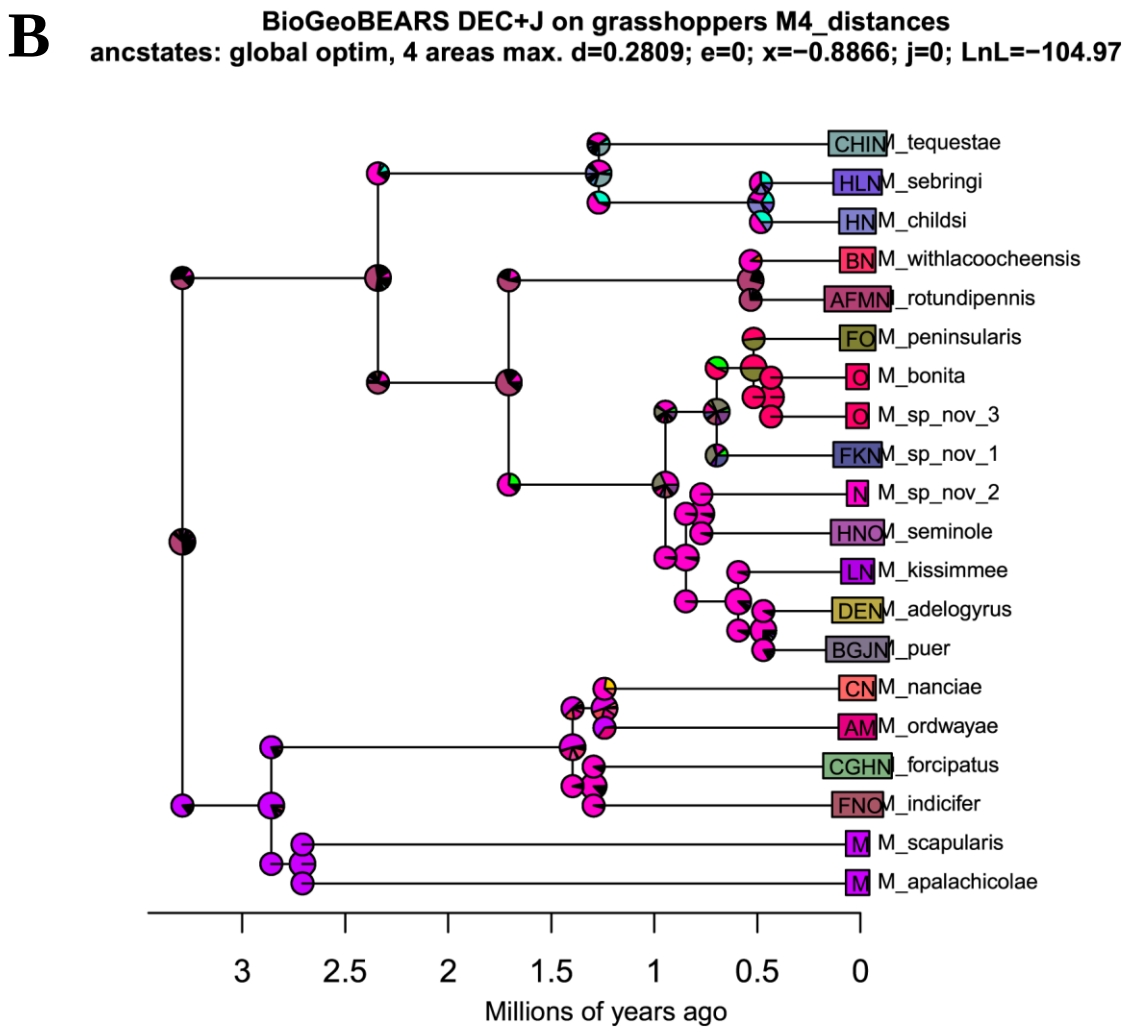

Figure 2-15 Continued.

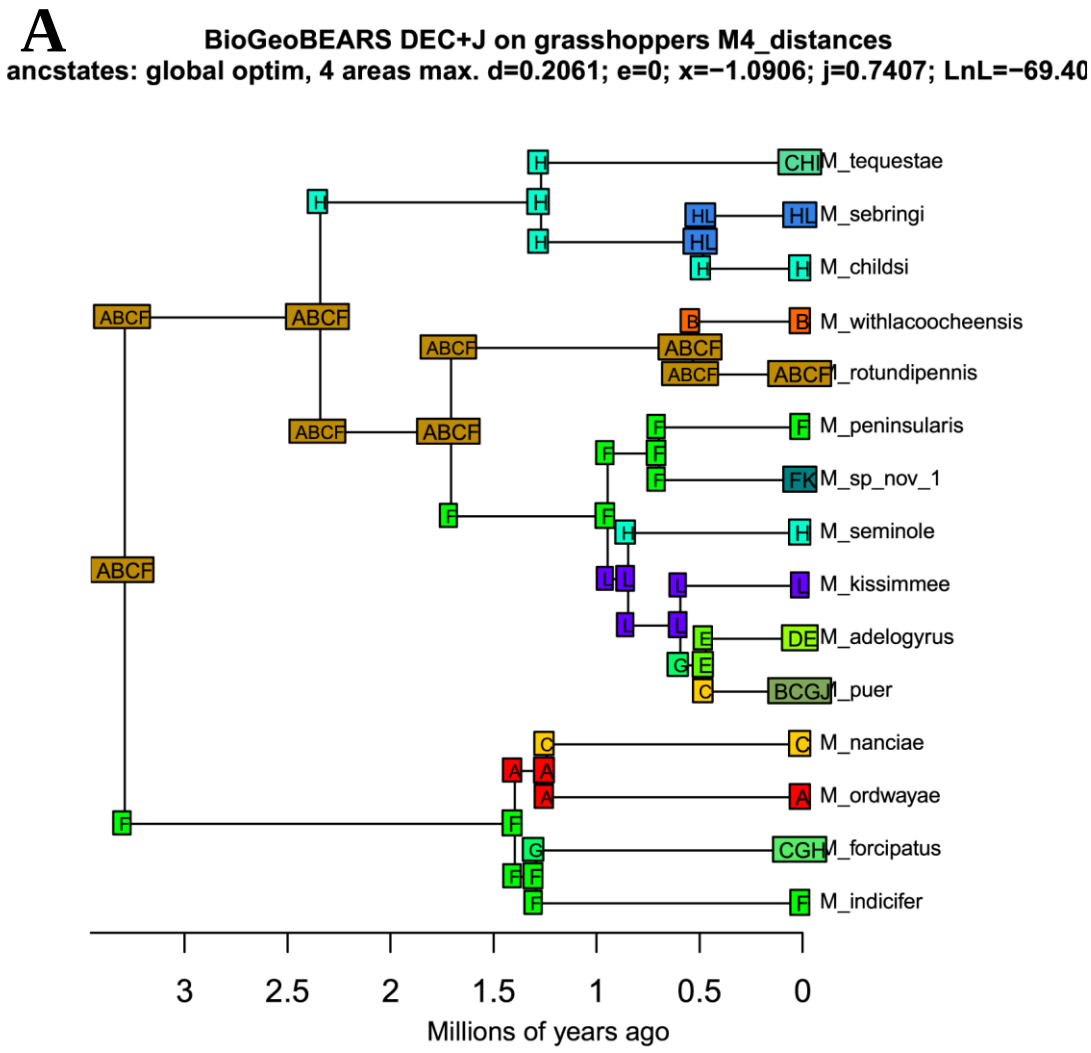

Figure 2-16. Ancestral state estimations for the Puer Group resulting from BioGeoBEARS analysis 4: **A.** Plot of the single-most-probable state (geographical range) at each node (just before speciation) and post-split (just after speciation). **B.** Pie charts represent the probabilities of each possible geographical range just before and after each speciation event.

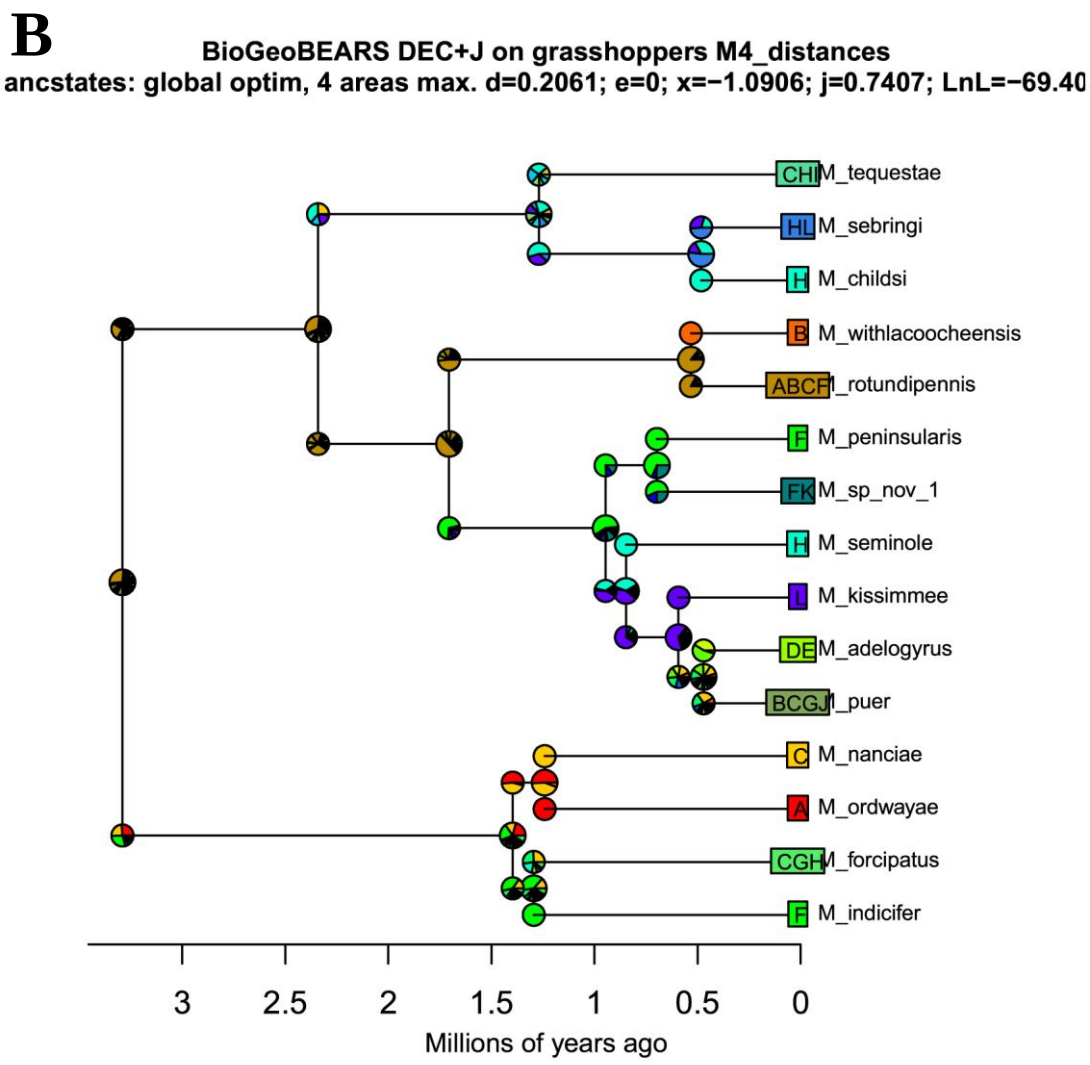

Figure 2-16 Continued.

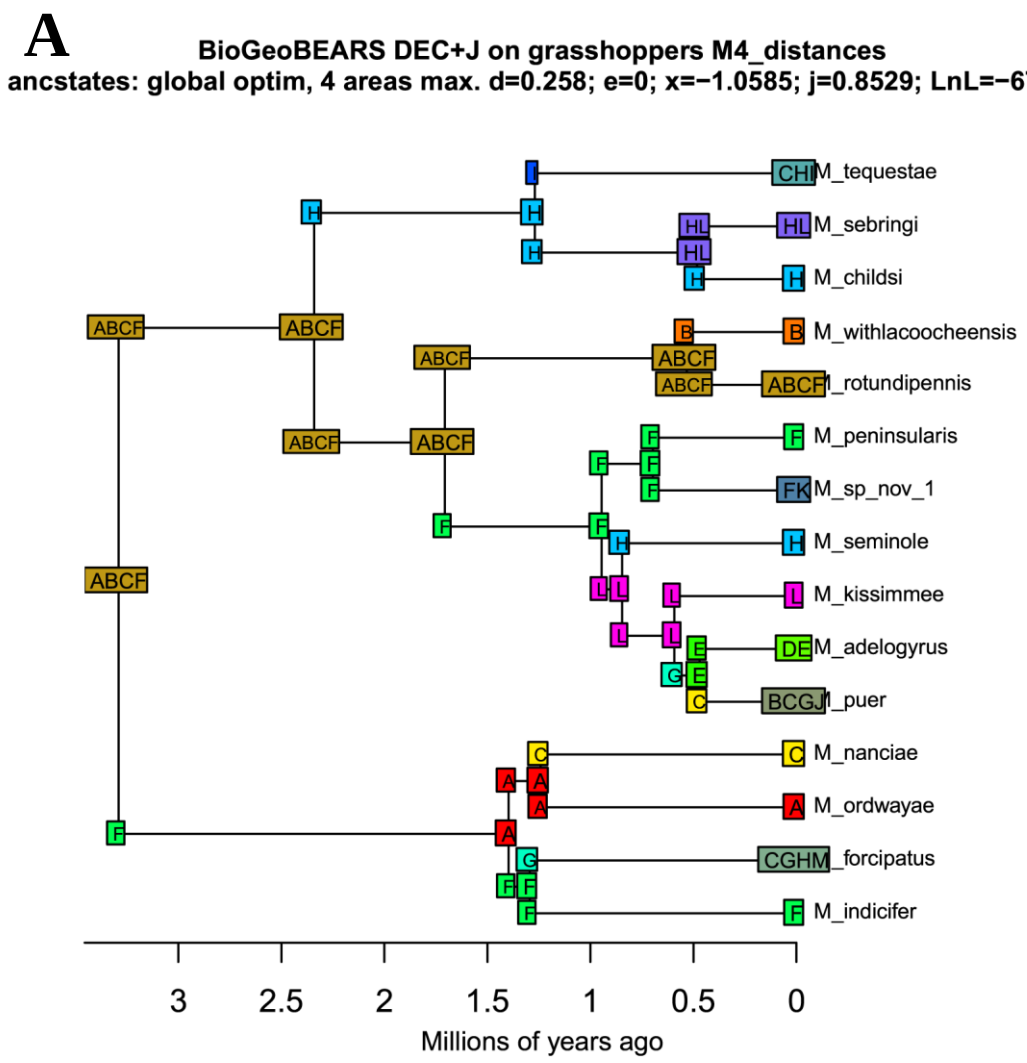

Figure 2-17. Ancestral state estimations for the Puer Group resulting from BioGeoBEARS analysis 5: **A.** Plot of the single-most-probable state (geographical range) at each node (just before speciation) and post-split (just after speciation). **B.** Pie charts represent the probabilities of each possible geographical range just before and after each speciation event.

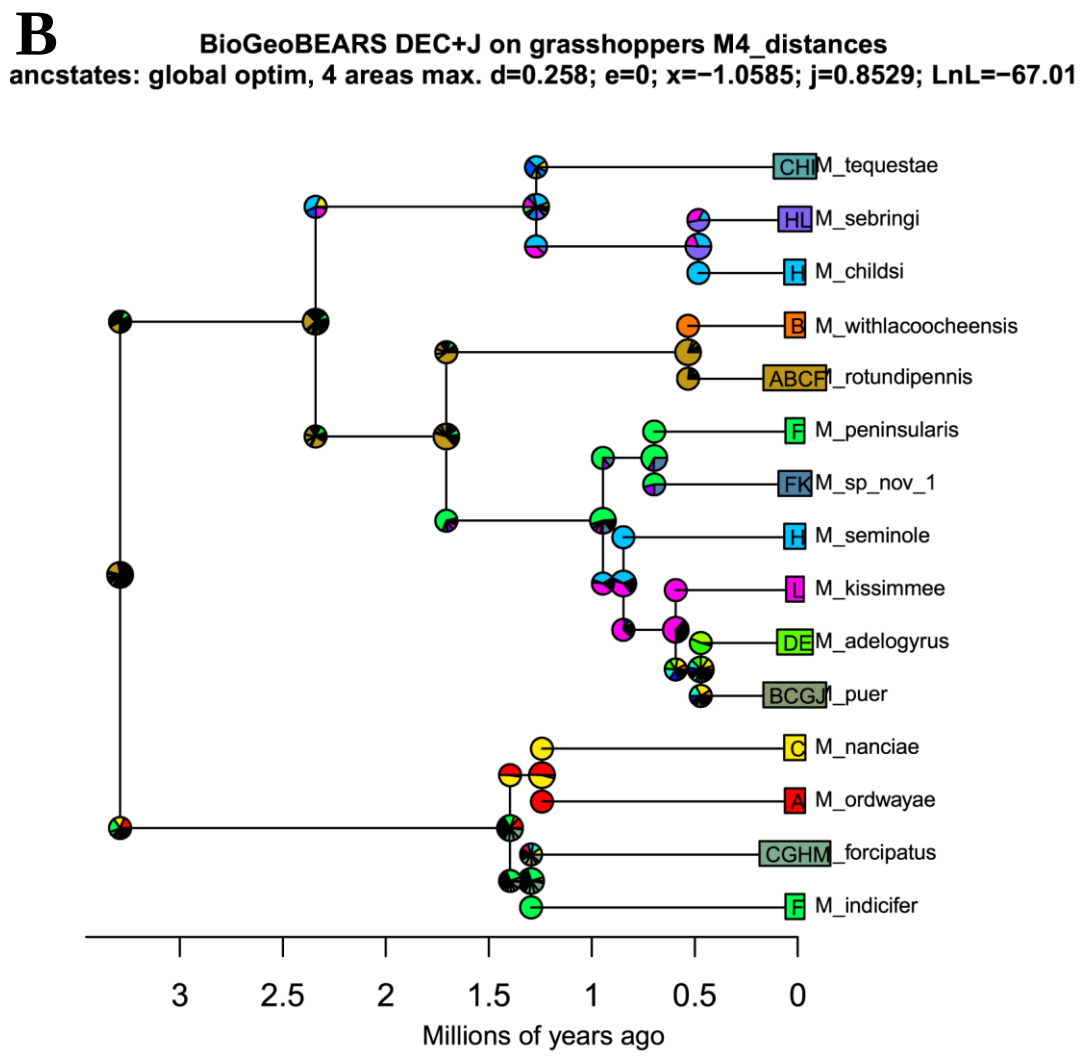

Figure 2-17 Continued.

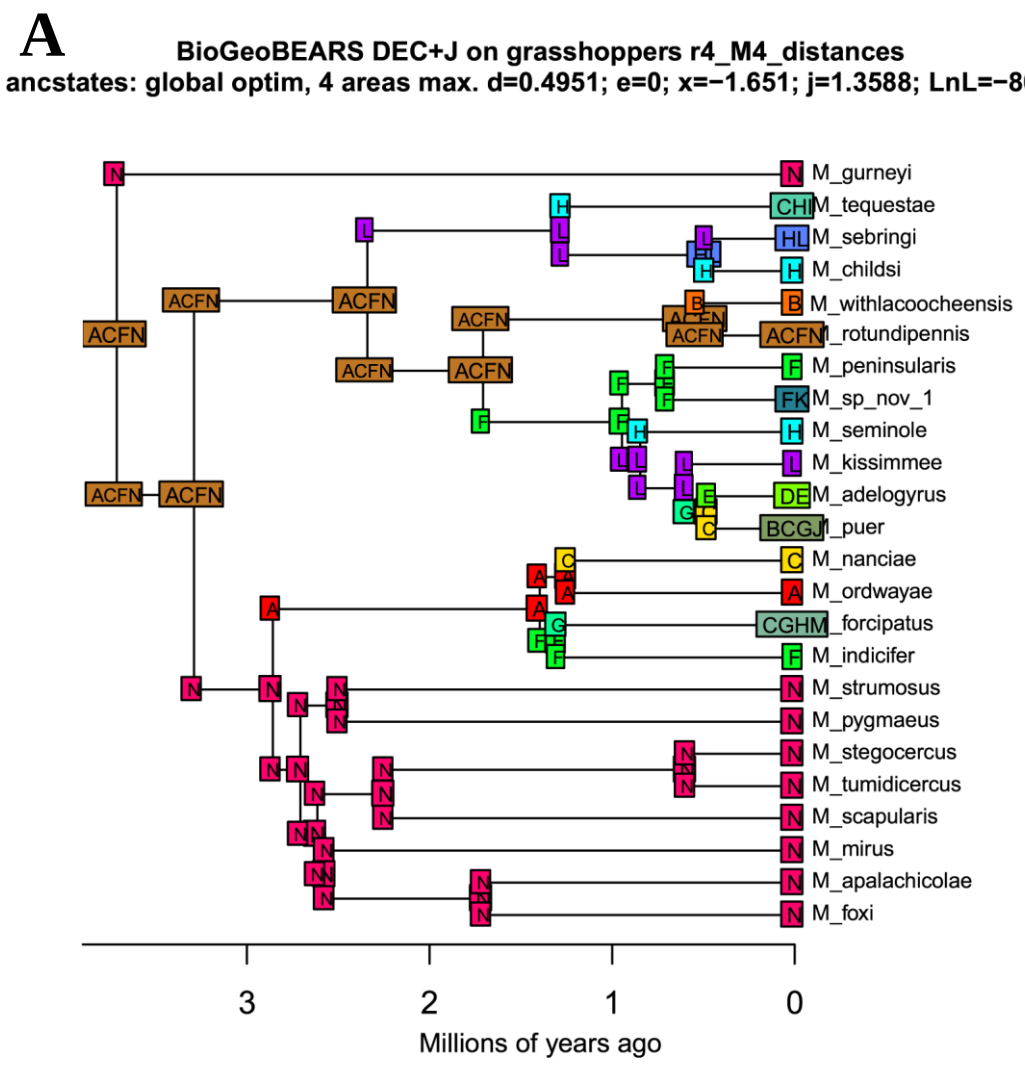

Figure 2-18. Ancestral state estimations for the Puer Group resulting from BioGeoBEARS analysis 6: **A.** Plot of the single-most-probable state (geographical range) at each node (just before speciation) and post-split (just after speciation). **B.** Pie charts represent the probabilities of each possible geographical range just before and after each speciation event.

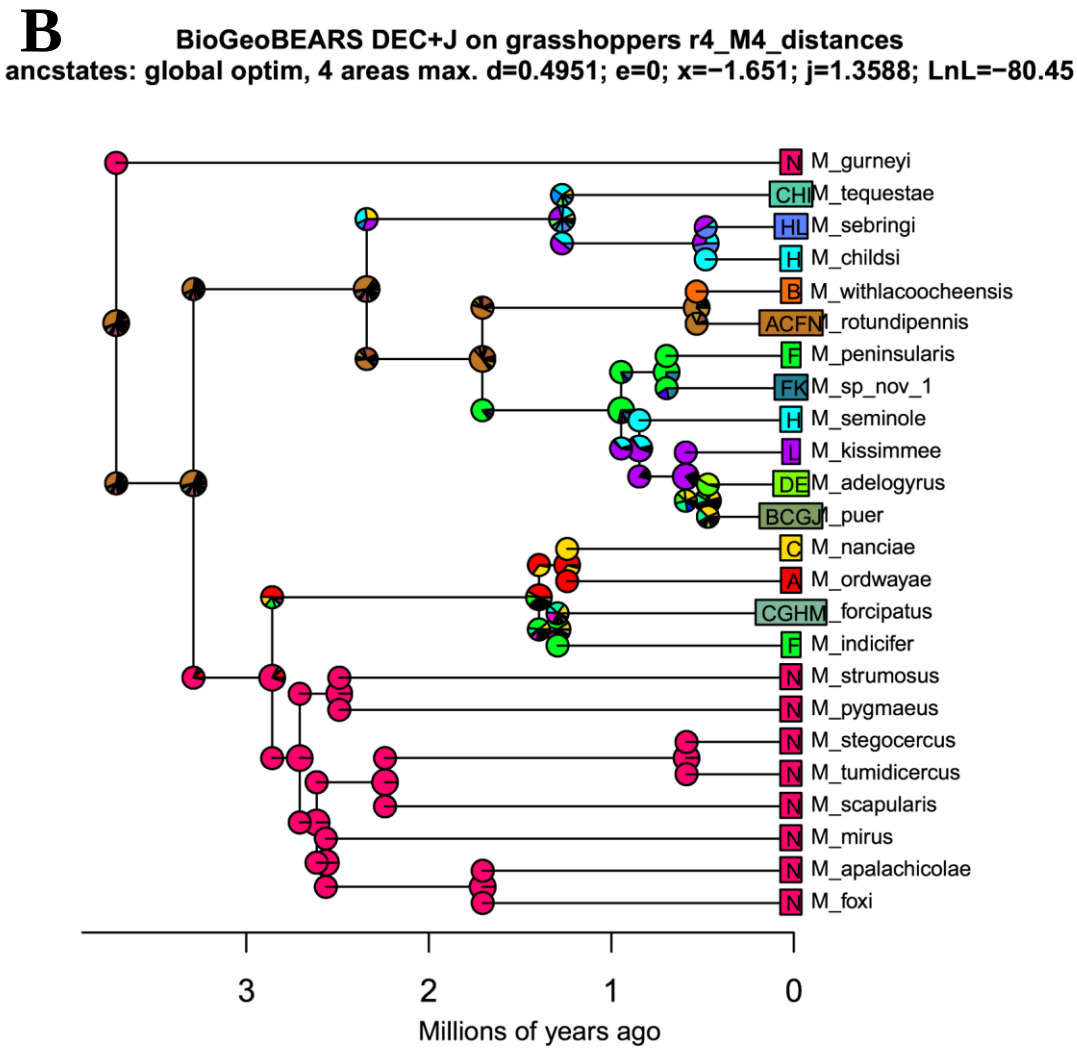

Figure 2-18 Continued.

In general, the probabilities of the most-likely ancestral ranges at each node on all generated trees (Fig. S2-13B to 2-18B) were often greater than 50%, except for nodes estimated to be older than two million years. An increase in node age often correlated with higher uncertainty in the ancestral range. This means that there is particularly high uncertainty about the ancestral geographic range for the common ancestor of PG. These

results are not unexpected: for a relatively small study clade, and a relatively large number of areas (due to a fairly detailed subdivision of the peninsular Florida's geography), uncertainty will be unavoidable. The most interesting results are those that are reasonably probable, and consistent across different analyses. Based on the ancestral ranges that appear repeatedly in different analyses, it can at least be said that the common ancestor was likely widespread. Most likely, based especially on the results of the coarse analysis (#1) (Fig. 2-13), the PG arose in northern areas and dispersed southwards. However, the estimation of which northern area is most likely ancestral depends on the scale of the analysis. For example, most of the fine-scale analyses essentially suggest that the northern areas of peninsular Florida, and beyond, may be the ancestral range of origin for the PG, while the coarse-scale analysis 1 suggests five areas: four outside of peninsular Florida, plus the central zone of peninsular Florida (Figs. 2-13 to 2-18).

Speciation Rate

Speciation rate was calculated for lineages A-D and D's three major clades (Fig. 2-5) and Table 3 summarizes the results. Lineage A's rate was found to be zero because it comprises a single species while the three highest rates were from within lineage D. Out of these seven calculations, the PGss Group had the highest overall rate at 2.3 species per million years.

Discussion

Monophyly of the Puer Group and its Historical Taxonomic Subgroups

We were fortunate to have access to the largest series of specimens of the PG yet compiled, which greatly enhanced our abilities to reconstruct a robust phylogeny of the PG as well as estimate and interpret historical biogeographical patterns. The status of the PG's monophyly has long been in question because there exist many other species of brachypterous *Melanoplus* in the southeastern U.S. that bear more than a passing resemblance to the group's 27 species. Despite the PG's similar morphology (especially non-genitalia) and present-day geographical distribution, even Hubbell (1932), in his seminal work on the PG, admitted to some difficulty (as did those that came before him – see Rehn and Hebard, 1916; Blatchley, 1920) in recognizing distinctive synapomorphies for the group. Due to this and the seemingly young age of the group, adequately reconstructing the relationships of the PG seemed daunting, but necessary for all subsequent analyses. We overcame these obstacles using a combination of the complete mtGenome and three nuclear genes for each species. These data enabled us to definitively determine that the PG is, indeed, a monophyletic group with internal nodes that were almost entirely well-supported across major lineages A, C, and D, but which were more poorly supported in lineage B's deeper nodes (Fig. 2-4).

The PG's internal relationships, though, were a different matter since only two of the six historical subgroups (Table 2-1) were found to be monophyletic: the Tequestae Group and the PGss (Fig. 2-4). These will also be the only two subgroups that we will

continue to refer to in a non-historical context. In 1932 (Hubbell), only four of the six historical subgroups existed: Rotundipennis, Scapularis, Strumosus, and Puer ss Groups, with the Forcipatus and Tequestae Groups arriving more recently (Hubbell, unpublished notes; Deyrup, 1996; Lamb and Justice, 2005; Otte, 2012 ("2011")). As previously mentioned, Hubbell (1932) sought to create order out of the relative morphological chaos of the PG and the subgroups are principally based on the unusual shapes of the phallic complex and other genital components, as well as relative geography. Even Hubbell (1932) acknowledged at the time that two of the historical groupings (Rotundipennis and Scapularis Groups) were not especially compelling, but their species were at least more similar to each other than species in the other historical subgroups. In fact, for the Scapularis Group (four species – Fig. 2-4; Table 2-1), Hubbell (1932) did not even have access to specimens of two of the group's existing species (*M. stegocercus and M. mirus*) when he erected two new species; thus, the group was partially based on species descriptions only and without any knowledge of internal genitalia. Despite the current paraphyly of most of these historical subgroup, Hubbell's (1932) knowledge and use of biogeography and genital morphology to differentiate species and infer relationships should be considered as cutting edge for the time. In fact, he is credited with being the first to use the internal genitalia characters of "New World" male grasshoppers to assess species status and relationships (Hubbell, 1985).

A Biogeographical History of the Puer Group Through the Lens of Lineage

The parameters and set-up of the six BioGeoBEARS analyses (Figs 2-8 to 2-11 and 2-13 to 2-18; Table 2-2) differed to varying degrees, but were united in the goal of improving our comprehension of the historical biogeographical scenarios that have led to the modern-day geographic distributions of the PG (Fig. 2-1). The analyses incorporated a phylogeny of estimated divergence times of PG species based on the best available data for the estimated ages of a few of peninsular Florida's ridges (Scott et al., 2001; Burdette et al., 2013; Swaby et al., 2016; Scott, personal communication). An emphasis was placed on lineages C and D due to the close associations of the majority of their species with peninsular Florida's landlocked archipelago and what their biogeographical patterns might tell us about the speciation process. BioGeoBEARS analysis 1 was the coarsest and focused on the entirety of the southeastern U.S. divided into eight regions that seemed to coincide well with current species distributions of the species. Peninsular Florida was divided into three major physiographic zones based on shared geological characteristics (White, 1970) (Fig. 2-1B) while the five regions beyond peninsular Florida were able to be separated naturally by five major rivers (Fig. 2-1A).

The historical biogeographical scenarios suggested by analysis 1 exemplified many of the repeating patterns estimated by the finer BioGEoBEARS analyses, which mainly focused on peninsular Florida and the ridges and hill with which the PG species in the region are most associated with. This is why analysis 1 is referred to the most often throughout this section, interspersed with mentions of conflicting or supplemental scenarios offered by the other, finer analyses. More of such analyses do not seem

possible at this time in the absence of more detailed knowledge of the geological history of this region, which would be difficult given the relatively young geological age of peninsular Florida (Swaby et al., 2016) and awareness of the multiple shifts in sea level during the Pliocene (2.58-5.333 MYA) and Pleistocene (0.0117-2.58 MYA) (Fig. 2-5) (Deyrup, 1989; Hine, 2009; Swaby et al., 2016).What follows is an overview examination of the most probable biogeographical history of the PG and its four major lineages, highlighting some of the more interesting biogeographical patterns suggested by our analyses.

Lineages A & B: Beyond Peninsular Florida

Lineages A and B (Fig. 2-5; Table 2-1) are found almost entirely outside of peninsular Florida throughout the rest of the southeast (the older regions), the exceptions being *M. scapularis* (mainly confined to Georgia) and *M. apalachicolae* (almost within Florida's panhandle) (Fig. 2-1). Although these lineages' species are integral to gaining a more complete understanding of the PG's biogeographical story, they do not seem to have as clear-cut ties to their surrounding geological features, less is known about their current distributions, in general, and they are not as species-rich. Therefore, these lineages were only completely included in half the BioGeoBEARS analyses (numbers one, two, and six, with two species – *M. scapularis* and *M. apalachicola* – also in the third one) and, as such, the biogeographical histories of these two lineages are unable to be conjectured on as strongly as lineages C and D. That being said, lineage A's history seems relatively straightforward compared to B's as it is composed of a single species, *M. gurneyi.* This species diverged the earliest in the PG (Fig. 2-5), is seemingly

restricted to Florida's panhandle (MAP), and most likely diverged from the rest of the PG via within-area speciation as a result of sympatry or allopatry (the effects of which can look similar at finer scales), as consistently suggested by the associated BioGeoBEARS analyses (Figs 2-13, 2-14, and 2-18; Table 2-2). Allopatry, via isolation on oceanic islands, might make the most sense given that several populations of *M. gurneyi* are still fairly secluded today, with some inhabiting coastal dunes right along the Gulf of Mexico in miniscule peninsular areas and at least one found on a tiny island not far from the coastline (Fig. 2-1A; Hubbell, unpublished notes; DAW, personal experience).

Lineages B and C were estimated to have diverged from lineage D (3.29 MYA) not long after the common ancestor of the Puer Group first split from lineage A (3.71 MYA) (Fig. 2-5). The common ancestor of lineage B then began speciating around 2.71 MYA, which is why its species were estimated to be older than the common ancestors of lineage C's species and lineage D's three major clades. These findings are congruent with the longer branch lengths of the majority of lineage B's species (compared to lineages C and D) (Fig. 2-5), which are also consistent with their geographical distributions being almost entirely within the older regions of the southeast (Fig. 2-1). The BioGeoBEARS analyses suggested that sympatric speciation played a large role overall, which is consistent with morphological patterns observed between closely related species and what is currently known about the relative geography of the same. At this time, based on our observations of the divergent genitalia within this lineage, it seems probable that sexual selection (Eberhard, 1985; Deyrup, 1996) has driven at least

some of this divergence. Furthermore, based on current distribution patterns alone (Fig. 2-1A), and knowing that the effects of sympatry and allopatry can resemble each other at finer scales, vicariance in the form of major river barriers probably also played a role in at least the initial diversification of lineage B. This might also suggest that founder-event jump dispersal may be revealed to be a speciation factor as well if finer analyses were able to be applied to the non-peninsular Florida regions. Finally, based on BioGeoBEARS analysis 1, it was estimated (with, admittedly, low probability) that the ancestral range for lineage B species could have been in any of the four non-peninsular areas included in the analysis except for the area between the Apalachicola and Altahama Rivers (Fig. 2-1A), which only contains two of the species. This suggestion makes much sense in light of the accumulated evidence before us, particularly the current distributions of lineage B's species in relation to the river boundaries, and some of the observed morphological evidence (more on the latter in a subsequent section).

Reviewing all of the evidence before us, we suggest that the most likely historical biogeographical scenario at this time for lineages A and B is that the PG's common ancestor came from outside of the southeast, possibly from the west based on the species richness of the region, its relative age, and on *M. gurneyi's* phylogenetic position and more basic genital morphology (see later section for more on this). Lineage B then diversified beyond Florida's panhandle into the rest of the southeast mainly via sympatry (and/or allopatry) and range-expansion dispersal, quite possibly in response to the greatly fluctuating sea levels of the Pliocene and Pleistocene (Fig. 2-5) (Deyrup, 1989; Hine, 2009; Swaby et al., 2016).

Lineages C and D: Within Peninsular Florida

Peninsular Florida, as mentioned before, is the youngest region in the southeast geologically speaking (Swaby et al., 2016). Based on all available age estimates of the primary ridges/hill examined in this study (coarse (based on surface strata): Scott et al., 2001 and Swaby et al., 2016; and fine: Burdette et al., 2013 and Scott, personal communication), Florida's peninsula can generally be described as being the oldest towards the northwest and the youngest towards the southeast. This means that the age of the peninsular species (across both lineages C and D) (Fig. 2-5), as predicted, do indeed broadly follow a north-south gradient (Figs 2-1, 2-5, and 2-12). This pattern is more than likely a result of the aforementioned numerous fluctuations in sea level that separated the ancient islands during the Pleistocene (Hubbell, 1932; Hubbell, 1961; Deyrup, 1989; Hine, 2009; Swaby et al., 2016), particularly during the relatively long passage of evolutionary time between the split of lineages B, C, and D, and the diversification of the clades within lineages C and D (Fig. 2-5).

Furthermore, we hypothesized that Florida's peninsula would contain the youngest PG species based on the relative geological age of the region and we found this to be the case (Fig. 2-5). Moreover, the fact that we recovered two independent lineages that reside in Florida's peninsula strongly suggests that two incursions into the region occurred in the recent past and not just a single one as we suspected. Determining which lineage arrived first, though, is a bit trickier. First, in terms of relational distribution lineages C and D actually overlap to some degree, mainly in the central (median age) portions of the region. Otherwise, lineage C is mainly associated with the more northern

(older) portions of the region (the exception being *M. indicifer*) while lineage D is more often found in the southern (younger) portions (the exception being *M. rotundipennis*) (Fig. 2-1). Based on where these species are found and their relative geographical relationships to one another (Fig. 2-12), it might seem that lineage C's ancestor arrived first. This is especially plausible given the observation that most of lineage D's species seem to be concentrated towards the mid-peninsular zone (White, 1970 – Fig. 2-1B), the heart of the archipelago, which may have been difficult to reach during sea level shifts. However, when relative age is taken into account (Fig. 2-5), it was estimated that the common ancestors of lineage D's species were older than those of lineage C. Hence, lineage D's common ancestor seems to actually represent the first incursion into peninsular Florida from outside the region despite lineage C's evolution (and current residence) in the older parts of peninsular Florida. We will delve into possible explanations of the historical biogeographical scenarios that may have led to these dual incursions in the following sections focused individually on lineage C and D.

Lineage C

In terms of biogeographic history, mainly based on the results of the BioGeoBEARS analyses, lineage C's two clades (Fig. 2-5; Table 2-1) offered some of the most compelling evidence for founder-event speciation given its disjointed distribution among four main ridges and one hill (Trail, Mt. Dora, Orlando, and Atlantic Coastal Ridges, and Geneva Hill: Fig. 2-1B) of peninsular Florida. This is especially noticeable for the *M. ordwayae-M. nanciae* clade, the younger of the two (slightly), and

with its species more comparatively restricted in their distribution. Jump (or active) dispersal plays an important role in the colonization of oceanic island systems (MacArthur and Wilson, 1967; Gillespie and Baldwin, 2009) and its estimated role in this lineage further confirms this importance, but also, potentially, in non-oceanic island systems (Matzke, 2014) depending on your perspective regarding such an unusual hybrid system. Proposing a most likely historical biogeographical scenario for the two clades would be difficult because the BioGeoBEARS analyses were not too consistent in their suggested explanations, only the probable mechanisms. However, this is not too surprising given the aforementioned disjointed distribution of the four species. The ancestral split between lineages B and C, though, had more consistent and probable explanations, and was estimated to be vicariance in two (Figs 2-13 and 2-14; Table 2-2) of the three BioGeoBEARS analyses in which all species from both lineages appeared together. Analysis six (Fig. 2-18; Table 2-2) suggested a founder-event took place. These results are actually quite compatible because the main difference between these two sets is that, in the first, all species were allowed to move freely between regions while analysis six simulated all of the included ridges/hill of peninsular Florida as oceanic islands and the other southeastern regions as a single mainland. Based on this and modern-day distributions (Fig. 2-1), it can be inferred that sea level shifts leading to isolation events caused lineage C to diverge from B, which led to the second incursion of the PG into Florida's peninsula. The cardinal direction from whence this incursion came is still debatable. In other words, did lineage C's common ancestor enter peninsular Florida from the north (and disperse southwards) or the west (and disperse northwards

and to the southeast)? Based solely on the relative age estimates of the clades, the latter seems to be the likelier of the two, but the relative distributions of the species in light of their phylogenetic relationships (Fig. 2-12) and our knowledge of the general age pattern of peninsula Florida point back to the alternate hypothesis. Obviously, future investigations are needed to dig deeper into this intriguing conundrum.

Lineage D

The three major clades in lineage D (Fig. 2-5; Table 2-1) collectively represent a majority of the youngest species in the entire PG. The most obvious reason for this is because lineage D's species are associated almost entirely with Florida's geologically young peninsula and its landlocked archipelago, the main exceptions being the widespread *M. rotundipennis* and three of the PGss species, which are not known to be associated with any ridges/hills (Fig. 2-1). Lineage C is also restricted to peninsular Florida and shows similar affinity for ridges and a hill, suggesting two possible reasons for lineage D's unique species age pattern: either something may be driving this relatively recent radiation (one possibility being a higher magnitude of sexual selection (Eberhard, 1985; Deyrup, 1996)) and/or it is simply an artifact of relative location since lineage C is restricted to the comparably older proximal zone (White, 1970 – Fig. 2-1B).

The BioGeoBEARS analyses revealed that lineage D as a whole has probably evolved through a combination of sympatric speciation (which, again, can resemble allopatric speciation at finer scales like most of those here) and range-expansion dispersal with the occasional founder-event (Figs 2-13 to 2-18). Examining the modern-

day distribution of the three clades (Fig. 2-1), with more closely-related species often found the nearest to each other, and given what we know about sea level changes in this region, it seems likely that allopatry in the form of isolating oceanic islands separated these clades (at least initially), jumpstarting the speciation process. Once isolated, it is quite possible that sexual selection took over as the dominant force driving speciation (based on our observations of the highly divergent genitalia between and within clades), which may have been further exacerbated once sea levels dropped and islands (and populations/species) were once again connected, allowing for movement between areas. The rise and fall of the ocean over time would have led to a repeating of these patterns, but speculating further at this time on the relative contributions of allopatry versus sympatry to the evolution of the species within this lineage would be difficult.

Adding further plausibility to these ideas is the fact that geographical distance played the largest role in predicting dispersal rates to explain the PG's overall distribution. This especially applies to the landlocked archipelago situation in peninsular Florida, which is mainly clustered in the central portion of the region and is also principally where lineage D's species are located (Fig. 2-1). Hubbell (1932, 1985) actually suggested that this mid-peninsular zone (White, 1970 - Fig. 2-1B) may have been the nexus of speciation activity for the peninsular PG species (based on the high species diversity in the region and their overlapping distributions) and it is possible he was correct. In fact, this is the very same biogeographical scenario that was estimated with high probability by the coarse BioGeoBEARS analysis 1 (Fig. 2-13) for lineage D: that this central area was the ancestral range for the lineage's common ancestor. The

other analyses more often suggested the ancestral range was to the north, which cannot be ruled out, but seems less likely given other available evidence. For instance, the relative age estimates of the three major clades within lineage D also point to the mid-peninsular zone scenario because the Tequestae Group was estimated to be the oldest and its species are restricted to this region (Fig. 2-1). Moreover, the age of the common ancestor between the other two clades was estimated to be even older and the PGss is also associated strongly with the mid-peninsular zone, from which, based largely on its internal relationships and their correlation with geography (Fig. 2-12), it seemingly speciated mainly southwards into the youngest parts of the southeast. In contrast, within this scenario, the *M. rotundipennis-M. withlacoocheensis* clade most likely dispersed westward and northward based on current distribution (Fig. 2-1).

Assuming Hubbell (1932, 1985) was correct in his hypothesis, how would lineage D have made its way into the mid-peninsular zone of Florida in the first place during the Pleistocene, an apparently chaotic time in the region's history? As it turns out, this scenario is actually more feasible than it initially seems for two reasons: **1)** it is known that Florida's peninsula was up to three times larger (particularly, as it turns out, towards the west) during this period with an ever-shifting coastline (Allen and Main, 2005; Swaby et al., 2016). **2)** Some have proposed that during the late Miocene (~11 MYA) or early Pleistocene (2.58-0.0117 MYA) glacial stages, non-flying organisms made the trek to the emerging Florida peninsula via one of three land bridge routes: Gulf Coastal, Atlantic Coastal, or from the north (Webb, 1990). Species found in the southwestern U.S. appear to have the strongest biogeographical connections to Florida,

giving additional support to the land bridge hypotheses, especially the Gulf Coast route. Examples of this connectivity include reptiles, like the gopher tortoise (*Gopherus Polyphemus*), plants, like the prickly pear cactus (*Opuntia* spp.) (Sharpe, 2010), and insects, like the desert cockroach, (*Arenivaga floridensis*) (Hubbell, 1961; Deyrup, 1989, 1990). Either one of these ideas probably also explains how the common ancestor for the entire PG initially arrived in the southeast.

Insect Speciation at (Possibly) Record Speed: the Puer Group *sensu stricto*

The effect of sexual selection (Eberhard, 1985; Deyrup, 1996) appears to be especially pronounced in the PGss (9 species, 0.95 MYO with relatively high confidence, Fig. 2-5), which not only has the youngest species overall, but has seemingly undergone rapid and recent radiation with a speciation rate of 2.31 species/million years (Sp/My) (Table 2-3), the highest in the PG and, possibly, for an insect group. Until recently, the record rate (4.17 Sp/My) belonged to a group of forest crickets (*Laupala* spp. – 6 species) from Hawai'i Island (Mendelson and Shaw, 2005). Wessel et al. (2013), however, pointed out that the estimated age of this island had since been revised to a million years (coincidentally, almost the same age as the common ancestor of the PGss), meaning that the rate was effectively reduced to 1.79 Sp/My. This, in turn, caused a subgroup of fruit flies on the same island (in the *Drosophila* "spoon tarsus" clade – 8 species) to temporarily have the honor at 2.08 Sp/My (extrapolated from Lapoint et al., 2011; Wessel et al., 2013). Wessel et al. (2013) then came close to that rate at 1.95 Sp/My (extrapolated by us) with another clade of insects (cave-associated planthoppers

within the *Oliarus polyphemus* species complex) from, yet again, the very same Hawaiian island. However, Wessel et al. (2013) further made the case that the younger ages of the involved geology (i.e., the caves in question) should increase the rate about 10 times higher since it was only being calculated based on the age of the island's emergence from the sea. Wessel et al. (2013) then advocated for a further 10-fold increase if the rate was calculated specifically for a particular three-species clade within the planthopper complex associated with an area estimated to only be 10,000 years old. Based on extrapolation, this extraordinarily high hypothetical rate would be 195 Sp/My.

Obviously, the PGss' speciation rate cannot compete with such a high rate, particularly because the ages of the areas with which it is associated are not yet able to be estimated with such apparent precision. We can, though, take solace in four factors that make our study still stand out from these three: **1)** all other mentioned speciation rates, even the varying rates for cichlid assemblages (the fastest known animal speciation rates: McCune, 1997; Mendelson and Shaw, 2005; Wessel et al., 2013) are at least suggested (or can be assumed) to being driven by sexual selection acting on secondary sexual characters of males, specifically color, sound, and/or visual cues used to attract mates (Seehausen and van Alphen, 1999; Mendelson and Shaw, 2005; Lapoint et al., 2011; Maruska et al., 2012; Wessel et al., 2013). Conversely, we have repeatedly suggested that sexual selection is also one of the driving forces behind PG speciation, but is acting on primary sexual characters (specifically, the intromittent aedeagi). Plus, classical mate attraction scenarios are unknown for the PG (and, possibly, all *Melanoplus*) and coercive mating is the norm (Otte, 1970; Bland 1987; Woller and Song,

2017 (see Ch. III)). From an evolutionary perspective, the rate of speciation on primary sexual characters would be expected to be slower because of all the environmental factors that could increase selective pressure on secondary characters, such as noisy habitats influencing songs to shift in volume or pitch (Deyrup, 1996; Olvido et al., 2010; Kraaijeveld, 2011). Conversely, contact between genitalia is effectively unaffected by these same sorts of external forces with the possible exception of environmental interruptions of copulation (Deyrup, 1996). And, yet, we seem to have strong evidence here that primary sexual characters in the PG have indeed evolved more rapidly than secondary characters if we only compare insect speciation rates based on the full number of species in a clade and use the maximum (i.e., conservative) estimated age for that same clade.

2) Our phylogeny might also be considered to be more robust, comparatively speaking, because the previous studies were unable to take full advantage, as we did, of the latest developments in next-generation sequencing technology for the phylogenetic reconstruction of younger lineages.

3) With the exception of Mendelson and Shaw's (2005) crickets, the number of species in the fruit fly (Lapoint et al., 2011) and planthopper (Wessel et al., 2013) clades used to estimate speciation rate was actually difficult to pin down (but not from their lack of trying) due to conflicting genetic signals between some individuals. While our own study was not classically phylogeographic in nature, our results are largely congruent with the lone previous PG molecular study which was (Lamb and Justice, 2005), we tried to include species representatives from the heart of each of their ranges

for maximum genetic coverage, and our robust gene inclusion should have helped resolve relationship limitations sometimes observed in phylogenies when using only a handful of genes (as we did during our initial attempt). Like many other insect species, the PG's species are based on the morphological species concept, which, in this case, mainly relies on the unique differences in genitalia, making the task of separating species fairly easy (especially when comparing aedeagi) as the structures are readily observable (Hubbell, 1985; Deyrup, 1996).

4) Compared to other biological systems restricted to typical islands, the PG system in peninsular Florida is quite unique from an archipelago standpoint. The Hawaiian Islands are currently oceanic islands while peninsular Florida's are most decidedly not, acting only as those types of islands in a relict capacity. Their landlocked nature, though, is what makes the PG's biogeographical story so much more compelling than a traditional island tale. While the insect clades of Hawai'i Island have essentially been trapped on that single landmass for at least one million years (Mendelson and Shaw, 2005; Lapoint et al., 2011; Wessel et al., 2013), the species in the PGss have probably been moving between near-by islands for almost the same amount of time, colonizing new areas (many formerly covered with water and probably more than once) and, possibly, re-colonizing former ones. And, yet, the PGss speciation rate is still on par, if not higher, than the Hawaiian clades.

To be fair, this could actually be a byproduct of the PGss essentially having an unlimited (although recent) area in which to speciate while oceanic island speciation may be constrained by island size once a hypothetical maximum capacity is reached

(MacArthur and Wilson, 1967; Losos and Schluter, 2000; Mendelson and Shaw, 2005). Then, again, peninsular Florida could still be considered to be acting like an oceanic island given its relatively narrow width, the fact that ocean surrounds it on three sides, and that the xeric habitats to the north differ fairly significantly. As a quick test of this effect on the PGss speciation rate, we can ignore three of the nine PGss species that are not yet known from any ridges or hills and assume the rest were part of a connected landmass at some point in the past. This gives us a revised rate of 1.86 Sp/My, which is still slightly higher than the revised rate for Mendelson and Shaw's (2005) crickets at 1.79 Sp/My, but now quite a bit lower than the rate for the other two insect groups (Lapoint et al., 2011; Wessel et al., 2013) if they are accepted at face value and at their most conservative.

Taxonomic Implications of Phylogeny and Historical Biogeography

Some of the taxonomic implications of the phylogenetic and biogeographical analyses are discussed herein, focusing on the paraphyletic historical subgroups spread across the lineages. As might be expected, there are many stories that might be of interest, but we will focus on the more intriguing ones, often tying them to the taxonomy of species, both historical and as suggested by our results.

Lineages A and B

The phylogenetic placement of Lineage A's sole species, *M. gurneyi*, appears to be logical from a morphological perspective because its genitalia are also some of the most basic within the PG, particularly the comparative shape of the cerci (not pictured)

and the aedeagus (Fig. 2-3B). Regarding lineage B, despite not ever physically reviewing any *M. stegocercus* specimens, Hubbell's (1932) concept of the historical Scapularis Group (Fig. 2-4; Table 2-1) was mostly supported with the exception of *M. mirus*. This may have been due to its low nodal support since it is also the lone species that changed its phylogenetic position when estimating divergence time (Figs 2-4 and 2-5). On the other hand, its genital morphology is quite unique in some ways, especially its aedeagus (the longest in the PG), but similar to the rest of the Scapularis Group's species in other ways (e.g., all lack furculae, components associated with the external genitalia).

Regarding the historical Strumosus Group (Fig. 2-4; Table 2-1), its two species, *M. foxi* and *M. strumosus*, do share some homologous features, but *M. foxi* was found to have more in common genetically (and, as it turns out, morphologically) with a member of the historical Forcipatus Group (Fig. 2-4; Table 2-1), *M. apalachicolae* (also within lineage B), which has far less in common with its former group. Similarly, *M. strumosus* was found to be the sister of *M. pygmaeus*, part of the historical Rotundipennis Group (Fig. 2-4; Table 2-1), which confirmed Hubbell's (1932) suspicion that this latter species probably belonged elsewhere. Oddly enough, these two species appear to share very little in common in terms of external morphology, but the similarities of their internal genitalia, especially their aedeagus (Fig. 2-3C), are intriguing and demand further investigation. All four species just mentioned appear to share an interesting biogeographical history; based on current distributions (Fig. 2-1), only *M. strumosus* and *M. pygmaeus* have overlapping ranges, but only in Florida's panhandle, to which *M. pygmaeus* appears to mainly be restricted. *M. strumosus*, on the other hand, has the

widest range of all PG species, being found in all five southeastern states (but almost no presence as of yet in Georgia), a claim no other species can yet make.

The wide, but unusual, distribution of *M. strumosus* may simply be an artifact of relatively poor collecting in regions outside of Florida, one of the best-collected states (thanks largely to the efforts of Hubbell, Deyrup, Hill, and DAW – personal observations), or may actually be due to sympatric speciation and range-expansion dispersal as suggested by BioGeoBEARS analyses 1, 2, and 6 (Figs 2-13, 2-14, and 2-18). In fact, a closer look at Fig. 2-1A supports the following historical biogeographical scenario proposed by analysis 1 in which the common ancestor of *M. strumosus*-*M. pygmaeus* possibly originated in Florida's panhandle (note, though, that the probability for this ancestral range received the most support, but under the desired 50% threshold), followed by the dispersal of *M. strumosus* throughout the rest of its known range. Quite possibly, the route it took to North Carolina (the furthest northwest edge of its range) aligned with the major river systems as shown in Fig. 2-1A, which would explain well its absence from the majority of Georgia.

As further evidence for *M. strumosus'* phylogenetic position, it is separated physically from *M. foxi*-*M. apalachicolae* (which are not too far from each other at the southwestern end of *M. foxi's* range) by the Apalachicola River (shown on Fig. 2-1A, but the scale makes it difficult to distinguish), suggesting that this barrier may have already been in place when *M. strumosus* began dispersing northwards. This same river is most likely the barrier over which a founder event occurred (suggested in BioGeoBEARS analysis 1 – Fig. 2-13) that may have caused the ancestral split between

M. foxi-M. apalachicolae , or, alternately, it may be the source of vicariance suggested to be the cause of the split by BioGeoBEARS analysis 2 (Fig. 2-14). This latter scenario, though, would imply a fairly young age for at least a portion of the Apalachicola River since the *M. foxi-M. apalachicolae* clade is only estimated to be 1.7 MYO. This would not necessarily fit with the proposed *M. strumosus* dispersal scenario either (unless it did not begin actively dispersing until more recently) since its common ancestor was estimated to have diverged from *M. pygmaeus* 2.49 MYA.

Lineage C

Lineage C, restricted to the peninsular Florida (mostly the northern-central portions), was recovered as having two major clades of a relatively young age: *M. indicifer-M. forcipatus* (with the lowest support) and *M. ordwayae-M. nanciae* (Fig. 2-5). These species comprise the majority of the six historical members of the historical Forcipatus Group (Hubbell, unpublished notes) (Fig. 2-4; Table 2-1) and are all relatively similar to one another morphologically, especially in terms of their genitalia. This group is intimately tied to the original concept of the Tequestae Group (Deyrup, 1996; Lamb and Justice, 2005), which included these four species and lineage D's *M. tequestae* on the basis of a handful of unique morphological characters shared by all five species: small body size, a white stripe on the lower edge of the femora, and an absence of furculae (Deyrup, 1996; Lamb and Justice, 2005). The present configuration of the Forcipatus Group in lineage C is based on Hubbell's unpublished thoughts (focused on, as usual, genital morphology and geography) is far more logical largely because the

unique, yet similar, aedeagi observed in the four species are far more similar to one another than to that of *M. tequestae*. Our findings also lend credence to Lamb and Justice's (2005) supposition that, based on their phylogeographic analyses, the original Tequestae Group was not monophyletic.

Despite these lines of evidence, Deyrup (1996) expressed incredulity at the notion that convergent evolution could have given rise to the handful of unique physical characters shared by species of the original Tequestae Group. To be fair, though, Deyrup (1996) did not have access to the amount of specimens we do and was only looking at five species versus seven (three now belong to the modern incarnation of the monophyletic Tequestae Group: Otte, 2012 ("2011") - Fig. 2-4; Table 2-1). With our enhanced data set, it was revealed that the body size was not always particularly small for these species compared to others in the PG (DAW, personal observations), like those, on average, in the PGss. The same, too, for the white stripe, which was found to be quite variable, even in an intraspecific sense, though it was more often distinct than not. Plus, the function of the furculae is currently unknown (Woller and Song, 2017), which means that it is difficult to say whether or not convergence on evolving a lack of these structures is even important in an evolutionary sense or, if so, what mechanism (if any) might be driving such evolution. Furthermore, the absence of furculae in North American *Melanoplus* species is not restricted to the PG (it is even lacking in some lineage B species), but is more uncommon than common (e.g., Otte, 2012 ("2011"); Hill, 2015; DAW personal experience). Therefore, as it stands, it seems to us that some

degree of morphological convergence has indeed occurred between the Forcipatus and Tequestae Groups.

Lineage D

The historical Rotundipennis Group (Fig. 2-4; Table 2-1) now apparently consists of only two species, one of which was described long after Hubbell (1932) suggested the group (*M. withlacoocheensis*). The species were recovered as strongly supported sisters to each other and as the sister clade to the PGss. Their shared morphology is quite strong as they possess two of the more obvious, and definitely related, aedeagi in the PG (Fig. 2-3A), and they were estimated to have split from each other quite recently (0.53 MYA – Fig. 2-5). In terms of their possible biogeographical history, the BioGeoBEARS analyses (Figs 2-13 to 2-18) were fairly congruent in that the group was estimated to have diversified via a combination of sympatric (which may be allopatric at finer scales) speciation and dispersal (the latter primarily for *M. rotundipennis*). This is plausible given their present distribution (Fig. 2-1) because *M. withlacoocheensis* is seemingly restricted to the Brooksville Ridge while *M. rotundipennis* is one of the most widespread PG species, and the widest when compared to all other peninsular Florida species. Also worth noting is the much shorter branch length of *M. withlacoocheensis* compared to its sister (Fig. 2-4).

Taken together and combined with historical biogeographical scenarios proposed earlier for lineage D, the following scenario is suggested: the clade's common ancestors were first separated from lineage D's two other major clades due to vicariance caused by

oceanic island barriers. The common ancestors were then confined to the proximal zone of peninsular Florida (White, 1970) and continued evolving until around 0.53 MYA when *M. withlacoocheensis* diverged from *M. rotundipennis*. This may, again, have been a result of allopatric speciation if *M. withlacoocheensis* became trapped on what may have soon been Brooksville Island (Squitier et al., 1998) while *M. rotundipennis* continued to disperse into other near-by areas. This scenario does not fully explain how *M. rotundipennis* became so widespread while other species in the region did not, but it gives additional weight to the simple idea that this species is just an excellent disperser comparatively speaking.

Perhaps most remarkable is the fact that little variation is seen in the morphology of *M. rotundipennis* despite its wide distribution (Squitier et al., 1998), quite the opposite of the pattern seen within the speciose PGss. While it is possible that sexual selection may have at least been the initial driver of the obvious divergence in genitalia between *M. rotundipennis* and *M. withlacoocheensis*, it is also possible that an element of ecological speciation may be at work here. While *M. withlacoocheensis* appears to be strongly correlated with the xeric habitat known as sandhills, *M. rotundipennis* does not seem to have as strong a preference for the same, being also found commonly in scrub, pine flatwoods, and other scrubby habitats, including disturbed ones (Hubbell, 1932; DAW, personal experience). In fact, Lamb and Justice (2005) had the same thought, supported by phylogeographic evidence, which displayed less defined structure compared to *M. puer* and its own wide-ranging conspecifics. This ability to persist in numerous types of habitats might also clarify why *M. rotundipennis* does not appear to

be associated strongly with any particular ridge/hill and how it came to dominate most of northern/central peninsular Florida and parts of Georgia. Then again, this ability may also be possessed by *M. withlacoocheensis*, but its relative restriction to the Brooksville Ridge (and just off it to the west – Fig. 2-1) may be obscuring it since it contains copious amounts of sandhills habitat.

Conclusions

We have demonstrated that the biogeographical history of the monophyletic and geologically young PG was complex and heavily influenced by the sea level changes of the Pliocene and Pleistocene (particularly during the latter) (Deyrup, 1989; Hine, 2009; Swaby et al., 2016). For at least the two peninsular Florida lineages, the system also strongly resembles classic oceanic island colonization scenarios (especially in terms of speciation and dispersal patterns) in rough accordance with the theory of island biogeography (MacArthur and Wilson, 1967; Gillespie and Baldwin, 2012). Furthermore, based on all evidence before us, the PG's common ancestor most likely entered the southeast from the west. We have additionally found consistent evidence (supported by high probability in many cases) that the four most influential factors and processes (starting with the top) that have shaped this unique system beyond general oceanic fluctuations were: **1)** relative proximity (distance) between estimated ancestral range(s) and closely related species (in direct contrast to the results of a previous study on a landlocked, island-like system: Van Dam and Matzke, 2016). **2)** Sympatric speciation events, which are strongly suspected to be driven largely by sexual selection

based on morphological evidence, although there is also some evidence to suggest an element of ecological speciation (Schluter 2001) may be at work based on some affinity among the species for particular xeric habitats (Hubbell, 1932; Deyrup, 1996; Squitier et al., 1998; Lamb and Justice, 2005; DAW, personal observations). A deeper investigation into the role of sexual selection in the PG is planned (in Ch. IV), using geometric morphometrics analyses focused on genital morphology. **3)** Range-expansion dispersal, which has enabled various PG species to colonize new (and possibly previous) islands and areas within the southeast. Extinction events were estimated to be very rare, but DEC-type models are known to underestimate these (Ree and Smith, 2008). Plus, if they occurred, they would most likely be associated with the non-peninsular Florida species as has been suggested for older lineages (Mendelson and Shaw, 2005). Our biogeographical resolution of the regions outside of Florida's peninsula, though, is still admittedly poor and in need of further enhancement, if possible. **4)** Allopatry (at least coarsely) for lineage C, in particular, and probably for the ancestral divergence of the three major clades of lineage D. Most likely, this was due to the isolation of populations on oceanic islands during sea level shifts.

Regarding the topic of biogeographical resolution, two phylogenetic issues have vexed us that necessitate further investigation. The first is that the placement of *M. mirus* appears to be in doubt (Figs 2-4 and 2-5) and clearly needs added resolution. The solution (that may also resolve the other less-than-optimal nodes in lineage B) may be to add more nuclear genes to the dataset given the somewhat older age of the species within lineage B. The second is that lineage C's peninsular Florida *M. indicifer-M. forcipatus*

clade was not optimally recovered, although their morphology is highly similar in many respects, marking this as a currently unexplainable anomaly in need of further exploration. The solution might be to try the phylogeographic approach and include multiple individuals from wide-ranging populations for each species to determine if the current situation is possibly clouded by subtle genetic differentiation at the population level.

Based on our investigation of the system, it seems that we could reasonably consider the Florida peninsula PG species to be classified as neo-autochthonous endemics (Schoville et al., 2011; Deyrup, 1990) given their estimation to have evolved in under 1.29 million years, and as suggested by their close associations with the region as a whole and with the former oceanic islands within the now-landlocked archipelago (based on current distribution patterns – see Fig. 2-1). The explosive radiation observed in the PGss with, possibly, one of the highest speciation rates known from an insect clade (let alone one not found on a classic oceanic archipelago), suggests that speciation is active in this subgroup and we may yet continue to discover new species in at least the PGss, if not the PG as a whole. Florida is "topographically monotonous" (Hubbell, 1932) and comparatively small in size for a state, but, unbelievably, there are still many unexplored areas (especially on the other ridges/hills not focused on here) to be investigated for PG presence (Fig. 2-1). Clearly, such a remarkable biogeographical system warrants further investigation and a revision of its taxonomic subgroups (with an emphasis on morphology) in light of our findings is clearly needed. We think it appropriate to allow Deyrup (1989) to have the final word since it was the following

sentence that inspired this study many years previous, which refers to the rapid loss of Florida's scrub habitats: "It is sad to think of North American biogeographers and evolutionary biologists preparing large scale grant proposals to study the biotic patterns of distant island chains, while their opportunities in Florida slip away."

CHAPTER III

INVESTIGATING THE FUNCTIONAL MORPHOLOGY OF GENITALIA DURING COPULATION IN THE GRASSHOPPER *MELANOPLUS ROTUNDIPENNIS* (SCUDDER, 1878) VIA CORRELATIVE MICROSCOPY*

Synopsis

A morphology renaissance is underway, revolutionized by powerful imaging technologies being harnessed in novel ways, particularly for examining insects. The frontier in greatest need of exploration is functional morphology, especially genitalia, studies of which would gain us great insight into animal genitalia evolution. One method of exploration is correlative microscopy, combining multiple imaging techniques to achieve greater understanding of morphological function. Here, we investigated probable functions of the interacting genital components of a male and a female of the flightless grasshopper species *Melanoplus rotundipennis* (Scudder, 1878) (frozen rapidly during copulation) by synergizing micro-computed tomography (micro-CT) with digital single lens reflex (DSLR) camera photography with focal stacking and scanning electron microscopy (SEM). To assign probable functions, we combined imaging results with observations of live and museum specimens, and function hypotheses from previous

*Reprinted with permission from "Investigating the functional morphology of genitalia during copulation in the grasshopper *Melanoplus rotundipennis* (Scudder, 1878) via correlative microscopy" by Woller, D.A. and Song, H. 2017. Journal of Morphology. 278(3):334–359. doi: 10.1002/jmor.20642.

studies, the majority of which focused on museum specimens with very few investigating hypotheses in a physical framework of copulation. For both sexes, detailed descriptions are given for each of the observed genital and other reproductive system components, the majority of which are involved in copulation, and we assigned probable functions to these latter components. The value of this synergistic imaging approach is immense in terms of the resulting knowledge gained. The correlative microscopy approach is highly effective for examining functional morphology in grasshoppers, so we suggest its use for other animals as well, especially when investigating body regions or events that are difficult to access and understand otherwise, as shown here with genitalia and copulation.

Introduction

The evolution of animal genitalia is one of the most active areas of research in evolutionary biology and it is generally accepted that sexual selection is the major driving force that explains the observed divergence of genital components often found among closely-related species (especially in males and particularly in insects), with these divergences playing a potentially significant role in speciation (Eberhard, 1985; Arnqvist et al., 2000; Arnqvist and Rowe, 2002; Hosken and Stockley, 2004; Ritchie, 2007; Hotzy et al., 2012; Richmond et al., 2012; Simmons, 2014). Insights into the underlying mechanisms of this evolutionary process, however, are difficult to gain for a number of reasons. For one, insect genitalia are extremely diverse and often relatively complex, especially in males, in terms of the number of components involved in copulation and

reproduction (Eberhard, 1985; Arnqvist, 1997; Eberhard, 2010). This relative complexity has often masked our ability to understand functional genital morphology, particularly during the copulation process. This process is difficult to examine intensely due to its often-hidden nature (internal components shielded from view by external components) and because it is often easily interrupted by active observation, but some studies investigating function have manipulated genitalia as a way around such issues (Briceño and Eberhard, 2009; Grieshop and Polak, 2012; Dougherty et al., 2015). Adding further complexity to understanding function, several studies have demonstrated that individual genital components may play different roles during copulation and evolve at different rates (Song and Wenzel, 2008; Song and Bucheli, 2010; Rowe and Arnqvist, 2011). Furthermore, when studying the evolution of genitalia, there has been a continued general bias towards examining the morphology of male genitalia for various reasons, including the difficulties in examining female genital morphology (Eberhard, 1985) (e.g. a common lack of rigidity), assumptions that female components do not appear to vary as much between conspecifics (which may also be true in some cases) (Eberhard, 1985; Ah-King et al., 2014), and because differences in male components are typically more obvious (Eberhard, 1985; Arnqvist, 1997). However, male and female genitalia have presumably co-evolved, and, therefore, should be studied together.

We are currently in the midst of an insect (and other invertebrates) morphology renaissance ever since a pioneering study in 2002 (Hörnschemeyer et al.) used micro-computed tomography (micro-CT) to examine beetle morphology. This powerful imaging technology is non-invasive and non-destructive and has been used by many to

investigate the morphology of insect morphology in novel ways (e.g. Jongerius and Lentink, 2010; Wipfler et al., 2011; Wojcieszek et al., 2012; Breeschoten et al., 2013; Faulwetter et al., 2013; Michalik et al., 2013; Beutel et al., 2014; Greco et al., 2014; Simonsen and Kitching, 2014). One of the primary benefits of micro-CT is the ability to build three-dimensional (3D) reconstructions of any anatomical component included in the high-resolution scanning process (Fig. 3-1A-D).

For this study, we couple this technology synergistically with two other imaging methods, digital single lens reflex (DSLR) camera photography with focal stacking and scanning electron microscopy (SEM), a method known as correlative microscopy (Caplan et al., 2011), to investigate the copulation process in the context of exploring the next frontier in morphological studies: functional morphology. Comprehending the function of morphology, principally how the male and female parts interact, is a key to better understanding genitalia evolution (Kelly and Moore, 2016). The copulation process in insects has previously been difficult to study in fine detail because of the cryptic nature of interactions between male and female genitalia and the invasive techniques that were necessary for examination. This frontier is ripe for exploration with relatively few studies focusing on functional genital morphology in insects (e.g. Eberhard and Ramirez, 2004; Briceño and Eberhard, 2009; Grieshop and Polak, 2012; Briceño et al., 2016; Rhebergen et al., 2016), with even fewer utilizing micro-CT to do so (e.g. Dougherty et al., 2015; Holwell et al., 2015; Mattei et al., 2015; Schmitt and Uhl, 2015). In terms of the order Orthoptera, only one other study of a similar nature has yet been undertaken (with *Metrioptera roeselii* (Hagenbach, 1822) (Ensifera:

Figure 3-1. Abdomina of original male and female *Melanoplus rotundipennis* specimens frozen *in copula* compared to their 3D reconstructions using micro-CT scanning (for all, female is above and male is below): **A.** left lateral view; **B.** right lateral view; **C.** left lateral view of 3D reconstructions; **D.** right lateral view of 3D reconstructions.

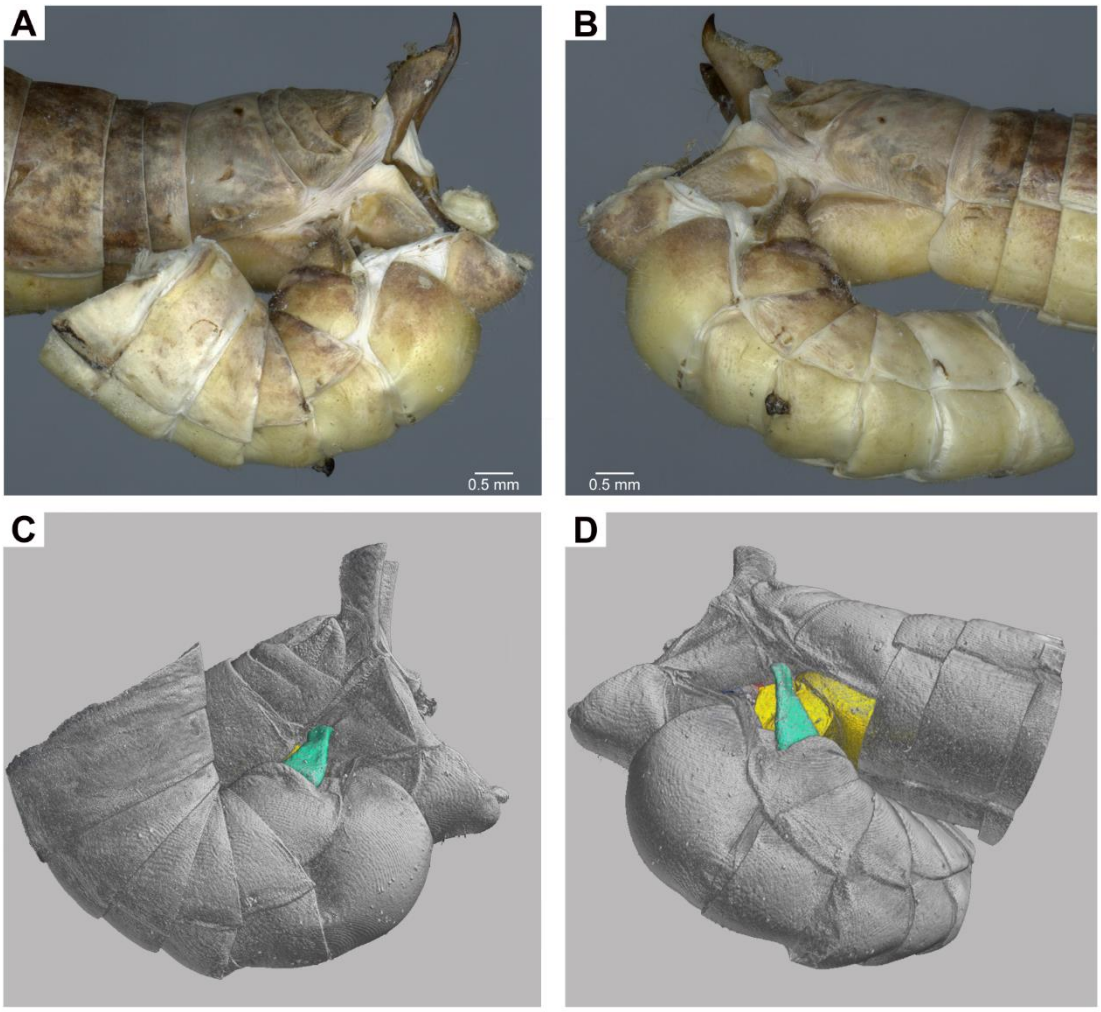

Tettigoniidae) in Wulff et al. (2015), but, to our knowledge, our study is the first to use micro-CT to examine functional morphology during the copulation process within the suborder Caelifera (true grasshoppers). Although this study is focused specifically on

elucidating the functional role of genital morphology during the copulation of grasshoppers, we think that our findings and methodology have wider implications for other animals, especially arthropods.

Our study subject, *Melanoplus rotundipennis* (Scudder, 1878) (Orthoptera: Caelifera: Acrididae: Melanoplinae) (Fig. 3-2A-C) is a member of the Puer Group (PG), a group of 24 small, flightless grasshoppers that reside in xeric habitats (e.g. scrub, pine flatwoods, and sandhills). Additionally, they appear to be strongly associated with scrubby oaks, are distributed across the southeastern U.S.A. (here defined as Alabama, North and South Carolina, Georgia, and Florida), and many are endemic to relatively small regions. Externally, all species resemble one another to a strong degree, but it is the male genitalia, primarily the aedeagus, that separate them due to their highly divergent forms (Hubbell, 1932). These collective factors make the PG an excellent system in which to examine the evolution of genitalia. Of all group members, *M. rotundipennis* was chosen for four reasons, the first being that it is the most widely-distributed (in both Florida and southern Georgia), meaning that locating populations, normally quite abundant, was easy and integral to encouraging specimens to mate in the lab within habitat boxes (Fig. 3-2C). The second is that intraspecific variation in male genitalia, especially in the aedeagi, is negligible (Squitier et al., 1998; pers. observ.), which may also be true for female genitalia. Third, the species is one of the largest in the PG with an average length of 15 mm in males and 20 mm in females and the aedeagus is males in also one of the most prominent, making this species one of the easiest to work with overall. Finally, the 58 named genital and other reproductive system components

across both sexes (33 male, 25 female) of *M. rotundipennis* can arguably be labeled as the most complex in the PG in terms of number and structural shape based on comparative observations, making this species interesting to study.

The general functions of grasshopper genitalia during copulation have been described and speculated on by numerous sources (Federov, 1927; Boldyrev, 1929; Snodgrass, 1935; Kyl, 1938; Roberts, 1941; Dirsh, 1956; Randell, 1963; Gregory, 1965; Otte, 1970; Pickford and Gillott, 1971; Whitman and Loher, 1984; Snodgrass, 1993; Eades, 2000; Chapman, 2012; Song and Mariño-Pérez, 2013), with the majority focused on museum specimens and many biased towards male anatomy. Only five of those studies (Boldyrev, 1929; Kyl, 1938; Gregory, 1965; Pickford and Gillott, 1971; Whitman and Loher, 1984) investigated hypotheses in a physical framework of copulation to better examine the largely-cryptic interactions of the external and internal components of both sexes. For further perspective, there are 12,219 species of Caelifera currently known worldwide (Cigliano et al., 2016) and each of the five previous framework studies focused on four different species and one subspecies across two families of grasshoppers (Acrididae and Romaleidae). This means that our collective understanding of functional genital morphology in grasshoppers is still quite poor, hence our decision to also utilize a physical framework of copulation to investigate previous findings and posited hypotheses by answering two broad questions: **1)** what role(s) do the genital and other reproductive system components of males play during copulation? Additionally, as noted previously, female morphology is frequently ignored, so female genitalia were intentionally made a focus of this study, both on their own and how they

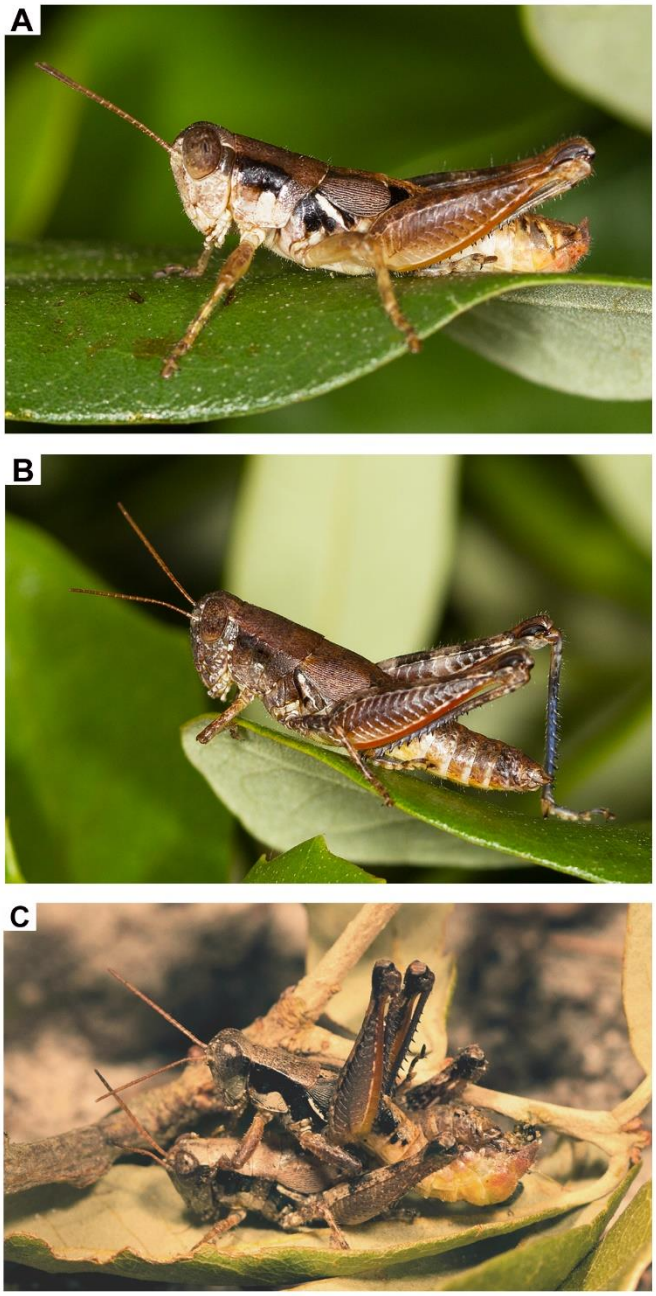

Figure 3-2. Live photos of *Melanoplus rotundipennis*: **A.** male; **B.** female; **C.** *in copula* pair.

interact with male genital morphology, leading us to ask: **2)** what role(s) do the genital and other reproductive system components of females play during copulation?

Furthermore, the majority of previous studies relied on standard dissections, drawings, and, occasionally, photographs, which were utilized well to gather evidence to support observations. Imaging technology, though, is continually advancing, so we harnessed the combined power of three of these technologies (DSLR with focal stacking, SEM, and micro-CT) and our own observations of live and museum specimens for two primary reasons: to investigate the general value of correlative microscopy and to decide if such an approach is more effective for examining genital morphology and function for at least grasshoppers.

Materials and Methods

Taxon Sampling

The present study is based on *Melanoplus rotundipennis* (Scudder, 1878) (Orthoptera: Caelifera: Acrididae: Melanoplinae). Utilized specimens mainly came from Florida with two from southern Georgia and included: museum, recently-collected, and laboratory-observed within habitat boxes. Specimens in the latter category were collected from different locations in Florida, with each box containing up to 10 individuals of mixed sex ratios, mainly to observe mating behavior. Specimen numbers and sexes used for each imaging technique are as follows: **1)** digital single lens reflex (DSLR) camera: 10♂,11♀; **2)** scanning electron microscopy (SEM): 5♂, 1♀; **3)** micro-computed tomography (micro-CT): 1♂, 1♀. Full locality and collection event data for all examined specimens are as follows (organized by type of investigation and image type) with pinned, curated specimens from the University of Michigan Museum of Zoology's

Insect Division (UMMZ) and the Florida State Collection of Arthropods (FSCA). Specimen label data from the UMMZ were databased by that museum's personnel with all other specimen data extracted and georeferenced by the first author. All entries have had data gaps filled in where necessary (e.g. current county) or had alterations made for the purposes of uniformity (e.g. dates). Pinned, curated specimens and some recently-collected specimens were georeferenced using Google Maps and with centroid points used in the case of coarse data, like city or county level while remaining newer specimens were georeferenced using a Pentax WG-III GPS Adventure Proof camera. All GPS coordinates are given in WGS84 decimal degrees format (latitude, longitude).

As they died naturally, recently-deceased specimens from living populations kept in habitat boxes in the lab were used to examine all aspects of male and female genitalia, primarily guided by micro-CT explorations. These specimens lack specific identifiers because none have yet been deposited in a curated insect collection and they reside within individual vials without a medium in the Song Lab in a -20°C freezer and are being utilized for further studies. The same applies for all PG species referenced here with “Field #PG”, which stands for “Field Notebook Number PG” followed by a unique code used to identify each site: e.g. “100-1-A” (site #, visit #, unique subsite I.D); these codes will eventually be placed on the locality labels of each specimen and will be linked to field notebook entries that will be digitized.

DSLR

Male: **FSCA20:** FL: Columbia Co. , Lake City, [30.179346, -82.639298], 21-VIII-1938; **Field #PG101-4-B:** FL: Lake Co., Rock Springs Run State Reserve, on both sides of Ethel Trail, mainly towards entrance along main park road (CR433), [28.804542,-81.453300], 22-VII-2014, coll. D.A. Woller; **Field #PG135-1-B:** FL: Lake Co., Seminole State Forest, down trail off W side of Hana Dr., [28.862681,-81.442285], 12-X-2013, coll. D.A. Woller & UCF Terrestrial Invertebrate Team; **Field #PG206-1-C:** FL: Levy Co., Manatee Springs State Park, just SW of intersection of NW 110 Ave. & 110 St., [29.488611,-82.955833], 19-V-2015, coll. D.A. Woller; **Field #PG207-1-A:** FL: Dixie Co., btwn SE CR 349 & SE 716 St., 0.5 miles W of Suwannee River, [29.467910,-83.014192], 19-V-2015, coll. D.A. Woller; **UMMZI-0051811:** FL: Levy Co., 1 mile SW Summer, [29.208185, -82.982071], 3-VIII-1938, coll. T.H. Hubbell & J.J. Friauf, Field #64; **UMMZI-0051947:** FL: Franklin Co., Carrabelle Beach, [29.832172, -84.684242], 28-X-1945, coll. T.H. Hubbell, Field #3; **UMMZI-0052007:** GA: Charlton Co., Folkston, [30.830772, -82.011289], 4-VIII-1939, coll. T.H. Hubbell and J. J. Friauf, Field #1.

Female: **Field #PG101-4-B** (see male); **Field #PG124-1-A (4♀):** FL: Putnam Co., Dunns Creek State Park, just off S side of main trail, [29.548218,-81.577550], 21-V-2013, coll. D.A. Woller, H. Song, & Integrative Bio. Class; **Field #PG206-1-C** (see male); **UMMZI-0051963:** FL: Taylor Co., Perry, [30.112088, -83.582508], 5-VIII-1925, coll. T.H. Hubbell, Field #4; **UMMZI-0052010:** GA: Charlton Co., Folkston, [30.830772, -82.011289], 4-VIII-1939, coll. T.H. Hubbell and J. J. Friauf, Field #1;

UMMZI-0052068: FL: Dixie Co., 6 mi S of Steinhetchie River, [29.560263, -83.360404], 5-VIII-1925, coll. T.H. Hubbell, Field #3.

Copulating: Live: Field #PG101-3-B (female): FL: Lake Co., Rock Springs Run State Reserve, on both sides of Ethel Trail, mainly towards entrance along main park road (CR433), [28.804542,-81.453300], 18-IV-2014, coll. D.A. Woller; **Field #PG127-2-B** (male): FL: Marion Co., Ocala National Forest, Big Scrub, 500 meters S of Big Scrub Campground on Forest Road 588/SE 241st Ave., [29.045266,-81.754964], 6-VII-2014, coll. D.A. Woller, E.C. Kerr-Woller, P.H. Woller, and K.L. Woller; **Deceased:** both Field #PG127-2-B.

SEM

Male: Field #PG101-1-A (2♂): FL: Lake Co., Rock Springs Run State Reserve, just off W side of a trail, [28.803126,-81.447415], 21-VI-2012, coll. D.A. Woller, S. Gotham, and C. Gale; **Field #PG115-1-A:** FL: Lake Co., Ocala National Forest, 1 mile SW of entrance to Alexander Springs, just off W side of 445 on a small ridge-like hill, [29.069117,-81.595417], 30-IX-2012, coll. D.A. Woller and C. Gale; **UMMZI-0051940:** FL: Alachua Co., Cross Creek, [29.486415, -82.165135], 4-X-1944, coll. T.H. Hubbell, Field #336; **UMMZI-0051948:** FL: Calhoun Co., 3.5 miles N of Blountstown, [30.504522, -85.047073], 22-VIII-1951, coll. I. J. Cantrall, Field #42.

Female: PG124-1-A: FL: Putnam Co., Dunns Creek State Park, just off S side of main trail, [29.548218,-81.577550], 21-V-2013, coll. D.A. Woller, H. Song, & Integrative Bio. Class.

Micro-CT Copulation

Field #PG105-1-A: FL: Orange Co., Wekiwa Springs State Park, a little ways E of 435, just off a trail that has a keyed gate, [28.720102,-81.487525], 15-IX-2012, coll. D.A. Woller.

Dissections

The internal genitalia and parts of the reproductive systems of male and female specimens were dissected from both freshly-collected and museum specimens (rehydrated by being dipped briefly into boiling water) and removed from the body using standard procedures for male grasshoppers (Hubbell, 1932) and female grasshoppers (Slifer, 1939) and the assistance of a Leica MZ16 microscope system. Intact dissected components were put in 0.65 ml vials containing a 10% KOH solution and placed into a boiling water bath for up to an hour to clear away obstructing tissues. The specimens were then removed and further dissected as necessary for examination and imaging. In the case of the male, this meant fully separating the epiphallus from the ectophallus and endophallus and, occasionally, the former from the latter. For the female, this meant removing all exterior abdominal segments to reveal hidden components.

Terminology

Terminology was derived and synthesized (and, in some cases, modified) from a number of sources: Snodgrass, 1935, 1993; Slifer, 1939, 1940a, 1940b, 1943; Roberts, 1941; Dirsh, 1956, 1965, 1973; Eades, 1961; Randell, 1963; Gregory, 1965; Uvarov,

1966; Ander, 1970; Amédégnato, 1976; Whitman and Loher, 1984; Key, 1989; Stauffer and Whitman, 1997; Eades, 2000; Gordh and Headrick, 2001; Chapman, 2012; and Song and Mariño-Pérez, 2013. The reproductive system is defined here as any anatomical components used by both sexes for the production of offspring, with genitalia defined as a subset of those components used specifically for copulation between a male and female. To aid in comprehension, the orientation of almost all of the DSLR and SEM images and 3D reconstructions was made uniform for both sexes (head facing left) and reflects the natural positions of all anatomy. Finally, the 3D reconstructions of male components were colored in shades of green, purple, and blue while female components were colored in shades of yellow, orange, pink, and red.

Imaging and 3D Reconstructions

DSLR

Digital images of anatomical components of freshly-collected and museum specimens were taken in the Song Laboratory of Insect Systematics and Evolution using a Visionary Digital imaging system equipped with a Canon EOS 6D DSLR camera combined with a 100mm/65mm lens (the latter often coupled with a 2x magnifier) to take multiple images at different focal lengths. The resulting files were converted from RAW to TIFF format using Adobe Lightroom (v.4.4), stacked into a single composite image using Zerene Stacker (v.1.04), and then Adobe Photoshop CS6 Extended was used to add a scale bar and adjust light levels, background coloration, and sharpness. Photographs of live specimens were taken in the same lab in a simulated habitat using a

Canon EOS 6D Digital SLR Camera equipped with a 100 mm lens and a Canon MT-24EX Macro Twin Lite Flash paired with two multi-directional halogen lights for additional lighting. Photographs of the specimens used for micro-CT scanning were taken by a colleague in Germany using a KEYENCE VHX-2000 series digital microscope.

SEM

Genitalia of both sexes came from specimens that had been cleared in KOH as described above. All images were taken with a JEOL JSM- 6480 after genitalia were attached to standard metal stubs with carbon glue and coated with 30 nm of gold palladium.

Micro-CT

Scanning was performed on a copulating pair of male and female specimens that were brought to the lab from the field, kept within a habitat box with other specimens of both sexes, fed Romaine lettuce daily, observed until copulating, carefully isolated into a smaller container, and then frozen rapidly in a -80°C freezer within 30 minutes of the male penetrating the female. Several other copulating pairs were also frozen this way and the set that looked the most intact was chosen to be the micro-CT subject. This specific pair was then prepared for the critical point drying process by removing the sample from the freezer and cutting through the entirety of their abdomens at or around segment 6. This smaller sample was then fully dehydrated over 24 hours within a 1.65 ml vial containing 100% ethanol. The sample was transferred next to a special microvial

punctured with a syringe for fluid/gas exchange and run through a Tousimis Samdri-790 Semi-Automatic Critical Point Drying Apparatus. Then, the final dried sample was scanned using an X-radia 400 (Carl Zeiss X-ray Microscopy, Inc., Pleasanton, USA) with absorption contrast and a spatial resolution of 2.6 μm. The resulting scans were mirrors of the sample.

3D Reconstructions

The micro-CT scanning process resulted in a stack of 1,943 TIFF images that was then imported into the program Amira (FEI, v. 6.0.1) and examined in three 2-dimensional (2D) planes (X-Y, X-Z, and Y-Z) in order to locate all desired anatomical structures, which were then transformed into 3-dimensional (3D) reconstructions using the Segmentation Editor. The file sizes of the four halves of the full exterior terminalia of the male and female seen only in the interactive reconstruction were found too large to work with, and thus, were made smaller with Resample module. Once created, each reconstruction was then isolated from the rest using the Surface View module and all were then exported as stereolithography (STL) files. The program Blender (v.2.76) was then used to apply smoothing algorithms to the individual STL files as follows: for almost all anatomical components, the Smooth Vertex option was applied with “1” as the Smoothing value and “30” as the Repeat value, but, for the four halves of the terminalia, “0.5” was the Smoothing value and “5” was the Repeat value. Smoothed reconstructions were then exported as updated STL files and imported back into Amira for color assignments using the Surface View module. Note that the smoothing process reduces

general roughness, which can disconnect objects formerly tightly connected. Blender was also used to mirror the STL files around the y-axis in order to match the original sample. All figures were assembled in Adobe Photoshop CS6 Extended and all reconstructions had their original backgrounds replaced with a uniform color. Photos of the original sample were taken in Germany once the micro-CT scanning process was completed in China. During the journey to Germany, the specimens shifted slightly, which is why they do not exactly match the reconstructions (Fig. 3-1).

Special Feature

The included interactive 3D figure (Fig. 3-S1) is special and requires a 3D PDF-enabled viewer such as Adobe Reader and is intended to simulate what we can see and do in Amira and to also assist the reader in better understanding how the anatomical components of both sexes interact because 2D images of such components can be difficult to mentally place spatially in relation to each other. The program PDF3D ReportGen (v. 2.13.0, Build 8317 x64) was used to accomplish this by combining all STL files generated in Amira and a text file (of the type IV) containing associated titles for each component that was modified from a template included with PDF3D. The color of each STL file was matched as closely as possible to the color of its 2D counterpart in the figures by using PDF3D's "pick screen color" option in the Visual Effects tab and clicking on the colors in the figures. Additionally, to reduce file size and optimize movement speed in the 3D PDF, the following simplification options within PDF3D (Advanced tab) were employed, all with a value of 150,000: threshold triangles count,

threshold line segments count, and threshold points count. Locations for placement of associated component titles were found using Amira by attaching the Line Probe module to each desired STL file, resulting in exact x, y, z coordinates.

High-resolution versions of the static figures (TIFF), interactive 3D figure (PDF), 3D reconstructions (STL – uncolored), and the micro-CT data used to build the 3D reconstructions (TIFF) are available for download at MorphoBank (O'Leary and Kaufman, 2012) under Project P2517: http://morphobank.org/permalink/?P2517.

Results

All terminology used for the genital and other reproductive system components are included in this section with occasional modifications from original sources to aid in uniformity and ease of understanding. Additionally, definitions are given for those components that are either not obviously delimited in referenced figures or are potentially unique to this species and/or the PG. Discoveries that are possibly novel are further elaborated on later. There are no intended statements of homology regarding terminology and given definitions, and they may only apply to this species and/or the PG. The genitalia and other reproductive system components of *M. rotundipennis* examined in this study are arguably the most complex compared to other PG species, consisting of 58 named components (many paired) for both sexes combined, 33 for males and 25 for females. To aid in comprehension, after a brief overview of mating behavior for this species is given, a detailed overview follows of the observed components of external and internal genitalia and other parts of the reproductive system

Figure 3-S1. Interactive 3D viewing window containing 3D reconstructions and associated labels of male and female components of genitalia and other parts of the reproductive system of *in copula Melanoplus rotundipennis* (male components are colored in maroon (Exterior) and shades of green, purple, and blue; female components are colored in white (Exterior) and shades of yellow, orange, pink, and red). The 3D PDF interface is filled with useful abilities and we welcome exploration, but here is a short guide to getting started quickly (the functionality of this guide depends on your version of Adobe Reader): at the top of the viewing window is a toolbar with shortcuts, of which the most useful is the one that resembles a phylogenetic tree called "Model Tree". Clicking on this icon opens the Model Tree pane to the left of the viewing window and, from here, you can check/uncheck boxes (clicking on "+" signs reveals full tree) associated with each component (name first, then body region, and then sex) as well as their associated labels ("LABELS-Anatomical_Components", naming scheme identical to components). These abilities are also present in the viewing window by right-clicking, choosing "Part Options", and then "Hide", and this function can be applied to both components and labels. There are also 15 pre-set views (Left Lateral View is Home) that we think you may find interesting and these can be accessed from the "View" dropdown menu of the viewing window toolbar, in a window below the model tree pane, or by right-clicking and choosing "Views". You may also change lighting schemes by clicking on the lamp icon (CAD Optimized Lights is default) in the viewing window toolbar. Finally, basic movements within the viewing window are as follows: hold down left mouse button to rotate in any direction, scroll middle mouse button to zoom in and out, hold down right mouse button and move mouse forward and back to more quickly zoom in and out (or hold Shift+left mouse button), and hold Ctrl+left mouse button to pan around. More movement abilities can be accessed from the far left arrowed icon of the viewing window toolbar or by right-clicking and looking in "Tools".

This area requires a 3D PDF enabled viewer such as Adobe Reader.

with orientation descriptions based on relative repose positions (i.e. when copulation is not occurring). The majority of these components were transformed into 3D reconstructions (e.g. Figs. 3-3 and 4) and an overview is provided separately for each sex, as well as for what components are touching while *in copula* (Figs. 3-3 and 4C) solely based on the 3D reconstructions. Additionally, further comprehension can be gained by exploring the interactive 3D reconstructions (Fig. 3-S1).

Mating Behavior

Habitat boxes often contained up to 10 *M. rotundipennis* individuals of mixed sex ratios, but mating did not seem to occur until at least two males were in the same habitat box with at least one female and then, occasionally, one would attempt copulation in a manner similar to what Bland (1987) observed in *M. childsi* Otte, 2012 ("2011") (formerly belonging to *M. tequestae* Hubbell, 1932) and what Otte (1970) observed in melanoplines in general. The male began his copulation attempt by moving slowly behind a female and then suddenly jumping on her back. The female would then often kick at him wildly with her hind tibiae and sometimes jump around the cage with the male clinging tight. Usually, the female would eventually calm down, allowing the male to position his abdomen under hers, invert his supra-anal plate to expose his phallic complex, and attempt to mate with her. The general *in copula* positions for grasshoppers (e.g. Figs. 3-3 and 4) are as follows: the male gains access to the female's internal genitalia by pulling down her subgenital plate with his epiphallus and then rotates his phallic complex anterodorsally around 90° (or more), inserting it through her vulva (e.g.

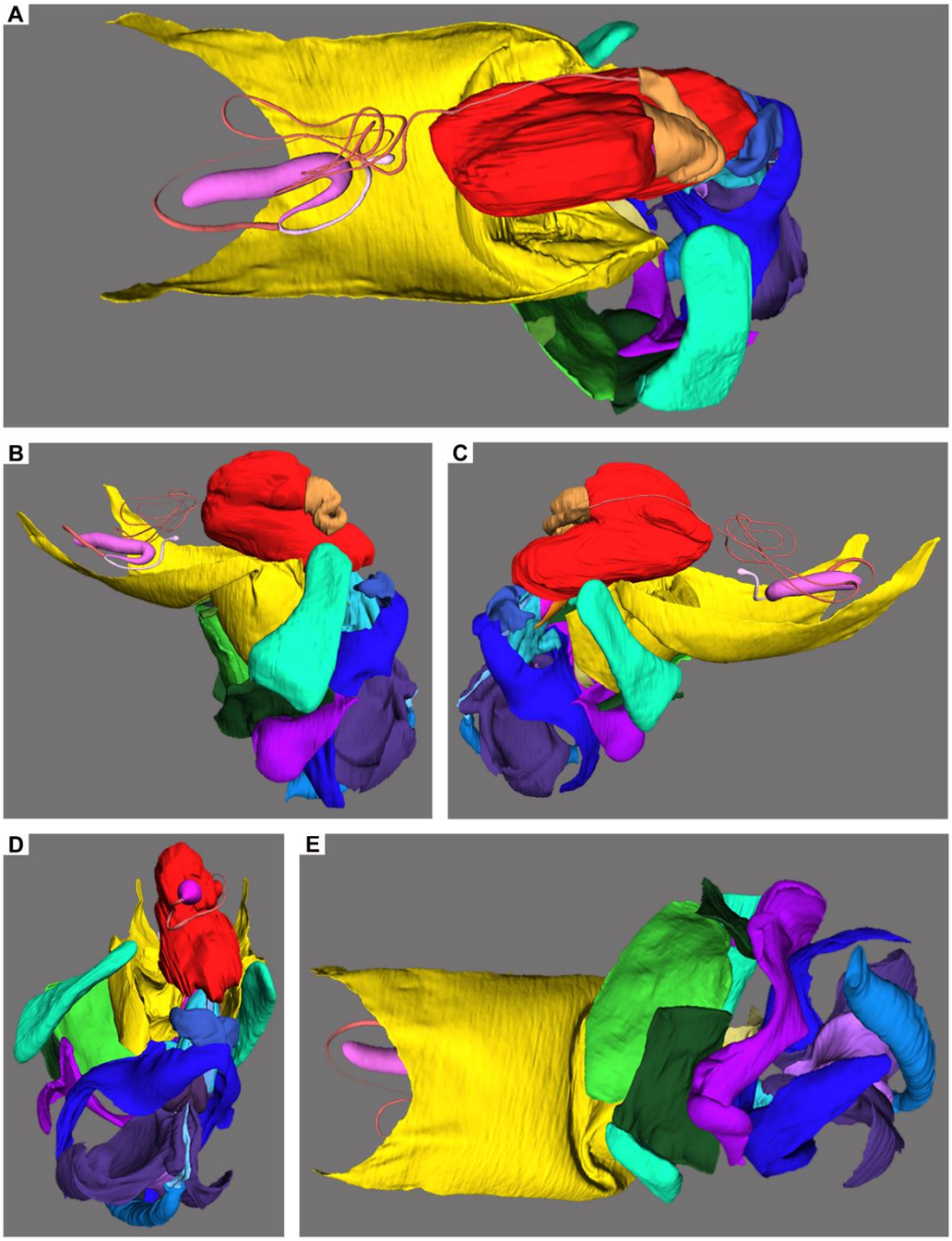

Figure 3-3. 3D reconstructions (*in copula* positions) of male and female components of genitalia and other parts of the reproductive system of *Melanoplus rotundipennis* (male components are colored in shades of green, purple, and blue; female components are colored in shades of yellow, orange, pink, and red): **A.** dorsal view, posterior to right; **B.** left lateral view, posterior to right; **C.** right lateral view, posterior to left; **D.** posterior view; **E.** ventral view, posterior to right.

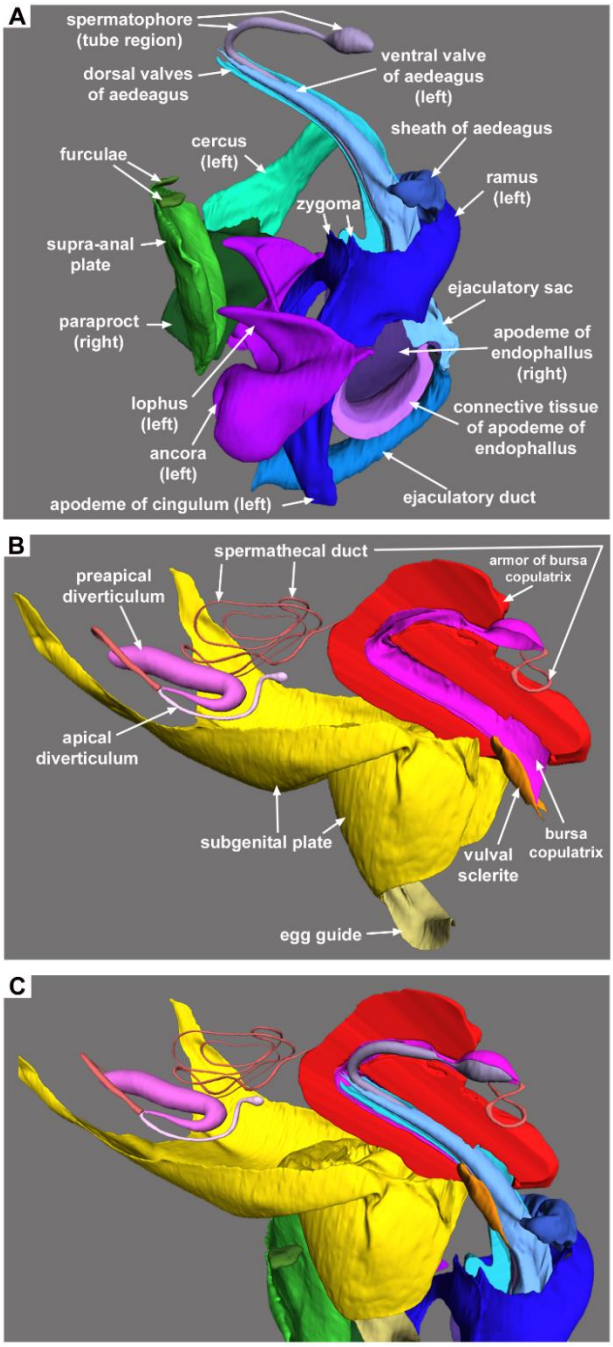

Figure 3-4. Left lateral, cut-away views of 3D reconstructions (*in copula* positions) of male and female components of genitalia and other parts of the reproductive system of *Melanoplus rotundipennis* (in all, posterior to right): **A.** male external and internal; **B.** female external and internal (muscle tissue of spermathecal complex removed); **C.** close-up view of combined male and female (muscle tissue of spermathecal complex removed).

Chapman, 2012). After successful mounting, defined here as a female allowing a male to insert his aedeagus into her for an uninterrupted period, (Figs. 3-2C) the *M. rotundipennis* pair were carefully transferred to a private container for periodic observations during which the pair would stay still or wander around slowly. We also observed the femora of both sexes vibrating intermittently along with periodic pulsations of both abdomens. Despite a female seeming to be receptive, some males were unsuccessful for unknown reasons, in either attempting to pull down the female's subgenital plate or inserting their adeagus. These rejected males would then dismount and wander away, sometimes not trying to mate again for hours or days, if at all.

Male: External and Internal Genitalia and Other Parts of the Reproductive System

External (Fig. 3-5): Seven anatomical components are present, three of which are paired. The furculae (Figs. 3-4A and 5A-E) are prominent and extend from the posterior margin of tergite 10 (Fig. 3-5C-E) and slightly across the base of the supra-anal plate (or epiproct) (Figs. 3-4A and 5A-E) that also emerges from tergite 10. The cerci (Figs. 3-4A, and 5A-E) extend posteriorly towards the cone-like pallium (Fig. 3-5C-E), the apex of the subgenital plate (Fig. 3-5D,E). The paraprocts (Figs. 3-4A and 5A-E) are in-between the supra-anal plate and the cerci, also extending laterally and posteriorly, and attach, via a membrane along the middle of their dorsal edge, to the base of the cerci. The subgenital plate resembles the general form found in many Acrididae species,

almost appearing to comprise two segments due to the medial transverse groove that can be stretched apart to a degree due to membranes in-between.

Internal (Fig. 3-6A): Two main anatomical components are present: the genital chamber (cavity enclosed by the supra-anal plate (Figs. 3-4A and 5A-E) dorsally and subgenital plate plus pallium (Fig. 3-5C-E), laterally, posteriorly, and ventrally) and the phallic complex (Fig. 6A), which comprises three subcomponents: epiphallus (Figs. 3-6B,C and 7F,G), ectophallus (Figs. 3-6D,E and 8A) and endophallus (Figs. 3-6F,G and 8A), each of which are divided further into more subcomponents. The epiphallus (Figs. 3-6B,C and 7F,G) consists of six subcomponents (five of which are paired) and is the most dorsal part of the phallic complex, resting above the ectophallus (Figs. 3-6D,E and 8A) and endophallus (Figs. 3-6F,G and 8A), connected to these two components via muscles and thick membranes. The ancorae (Figs. 3-4A, 6B,C, and 7F,G) curve ventrally at a steep angle and the anterior projections (Figs. 3-6B and 7F,G) curve inwards slightly while the posterior projections (Figs. 3-6B,C and 7F,G) do not. Additionally, the anterior projections have what appear to be multiple sensory receptors (not shown here) scattered about dorsally with more found in the median sclerotized cleft formed between the anterior projections and the ancorae. The bridge (Figs. 3-6B and 7F,G) is thick and bends strongly inwards in the middle when viewed anteriorly while the lateral plates (Fig. 3-6B,C and 7F) are also thick, but unremarkable. The lophi (Figs. 3-4A, 6B,C, and 7F,G) are covered with minute ridges that resemble fish scales that are oriented towards the anterior of the epiphallus (Fig. 3-9G).

The ectophallus (Figs. 3-6D,E and 8A) is the middle phallic complex component that is firmly connected to, and largely surrounds, the endophallus (Figs. 3-6F,G and 8A) via thin membranes and consists of one primary component, the cingulum (that would resemble the letter “H” if flattened (Roberts, 1941)) with four subcomponents (only two of which are typically paired). The apodemes of cingulum (Figs. 3-4A, 6D,E, 7B,C,E, and 9A) are of varying sizes and curvature while the zygoma (Figs. 3-4A, 6D,E, 7B,C, and 9A) can be described as double-layered and complete, though atypical (because it slightly extends posteriorly over the valves of aedeagus (Figs. 3-4A, 7B, and 9B), but just ventral to it is an almost-identical second region that contains a medial gap. The rami (Figs. 3-4A, 6D,E, 7B,D, and 9A) are well-developed, extend a little ways ventrally beyond the aedeagus, curve inwards slightly, and have what appear to be sensory receptors (not shown here) at the apex of the posterior region. The sheath of aedeagus (Figs. 3-4A, 6D,E, 7B-D, and 9A) is a somewhat misleading term for what is observed in this species because it is only vaguely sheath-like. In fact, it would be better described as two individual lobes that extend a little ways beyond the apices of the rami and are lightly-attached via membranes to the basal portion of the dorsal valves of aedeagus, but for ease of understanding, will be continued to be referred to as a single component. Additionally, the sheath of aedeagus curves upwards, almost reaching the top of the dorsal valves of aedeagus in some specimens (Fig. 3-7B), curve slightly inwards, and are also covered with tiny spines arranged in overlapping rows that point anteriorly (Fig. 3-9F).

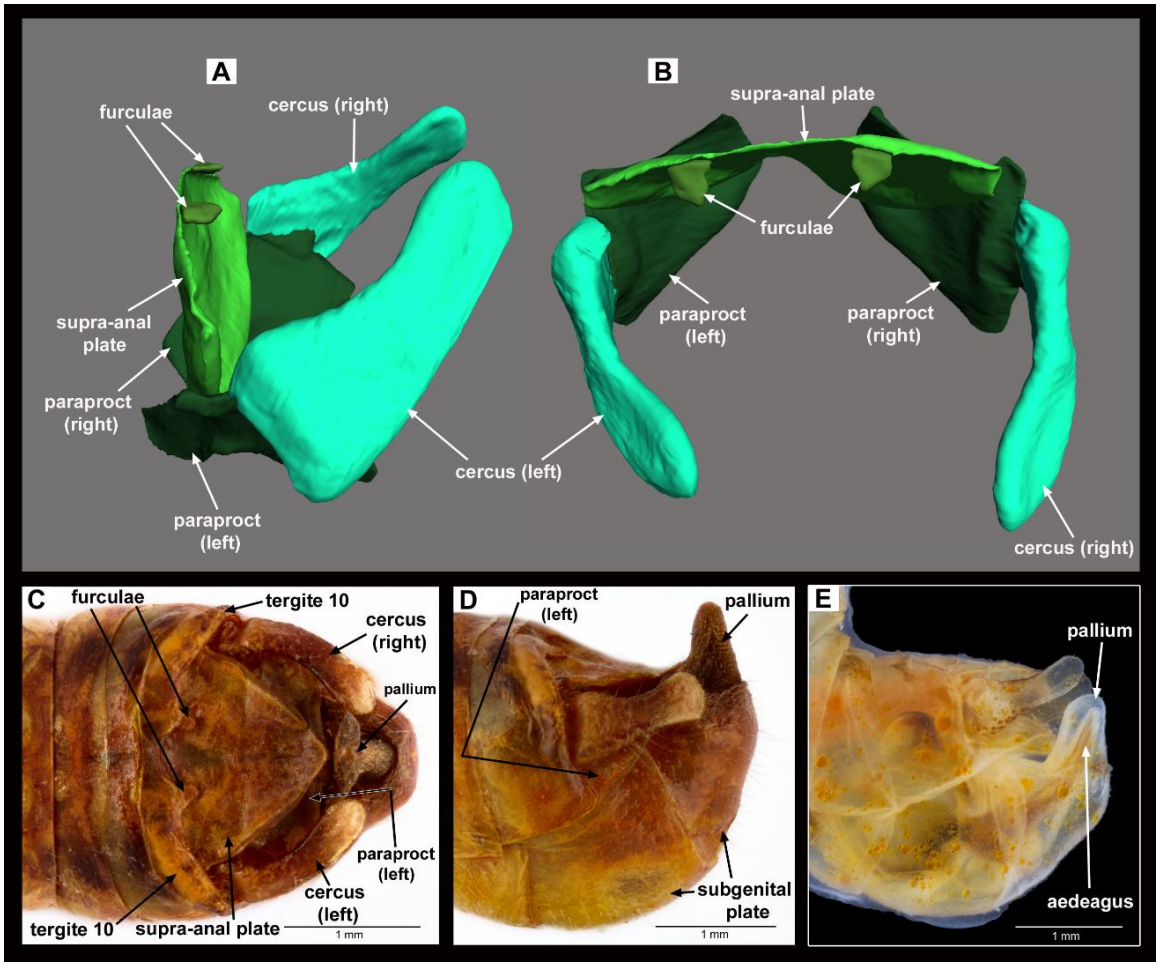

Figure 3-5. 3D reconstructions (*in copula* positions) and DSLR images of male external genitalic components of *Melanoplus rotundipennis*: **A.** 3D, left lateral view, posterior to right; **B.** 3D, dorsal view, posterior downwards; **C.** DSLR, dorsal view; **D.** DSLR, left lateral view; **E.** DSLR, left lateral view, made translucent with KOH.

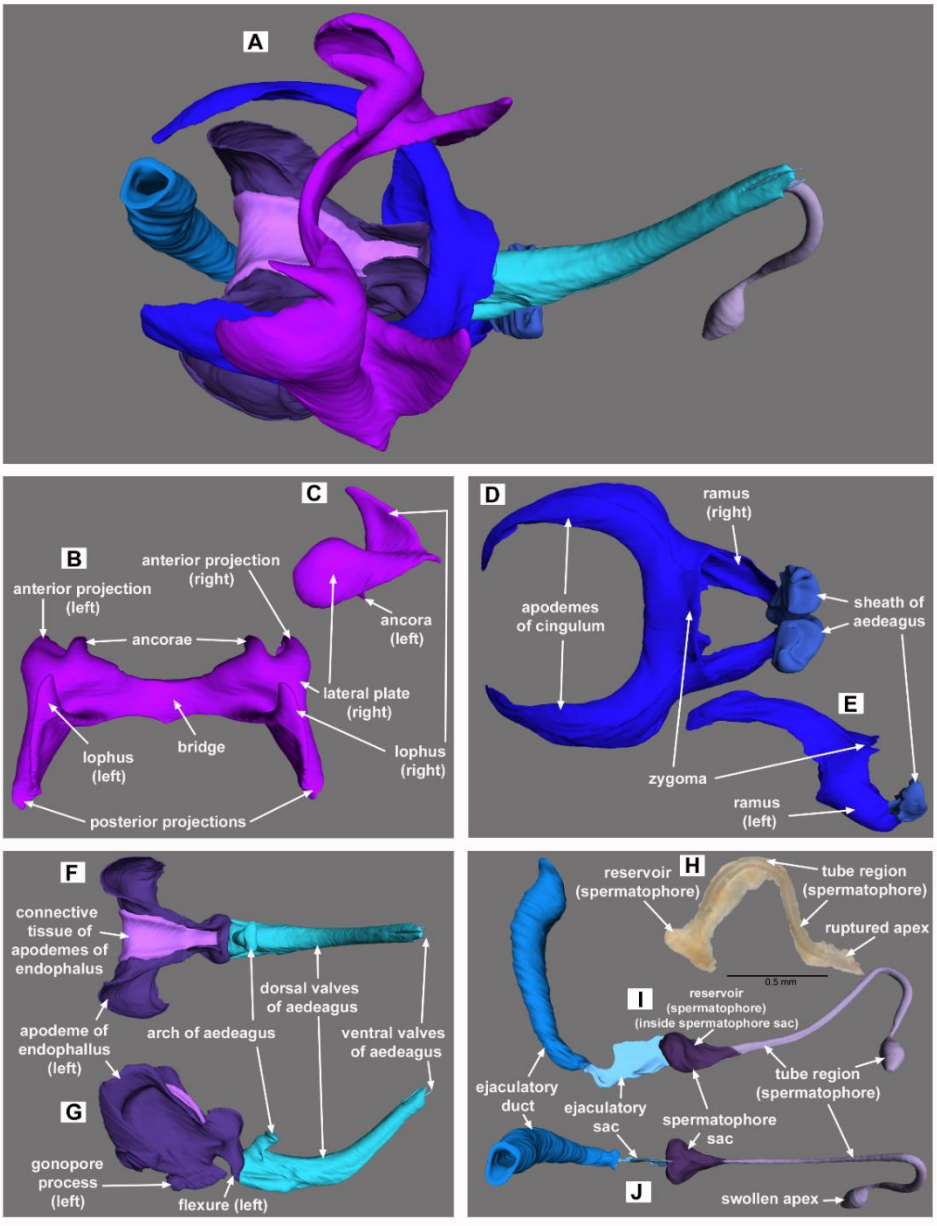

Figure 3-6. 3D reconstructions (based on in copula positions, but rotated into repose positions) and a DSLR image of male internal genitalia and greater reproductive system components of Melanoplus rotundipennis (posterior to right unless otherwise noted with one exception - spermatophore only present during copulation, so this component always points anteriorly): **A**. all components, quasi-dorsal view; **B**. epiphallus, dorsal view, posterior downwards; **C**. epiphallus, left lateral view; **D**. ectophallus, dorsal view; **E**. ectophallus, left lateral view; **F**. endophallus, dorsal view; **G**. endophallus, left lateral view; **H**. DSLR, discarded spermatophore, left lateral view; **I**. greater reproductive system, left lateral view; **J**. greater reproductive system, dorsal view.

The endophallus (Figs. 3-6F,G and 8A) is the most ventral part of the phallic complex and the primary portion that contains components of a species-specific nature,and consists of nine subcomponents (six of which are paired), with six more closely-connected that belong to the greater reproductive system (Fig. 3-7A). The apodemes of endophallus (Figs. 3-4A, 6F,G, 7B-E, 8B,D, and 9A) are typical for acridids as is its whitish, opaque connective tissue (Figs. 3-4A, 6F,G, 7C,E, and 8D), presumably, and, more than likely, so are the greater reproductive system components: ejaculatory duct (Figs. 3-4A, 6I,J, and 7A), ejaculatory sac (Figs. 3-4A, 6I,J, and 7A), gonopore (not pictured because it is a hole connecting the sacs), and spermatophore sac (Fig. 3-6 I,J). The duct and sacs can still be very difficult to see after dissection, being often obscured by vestiges of undissolved musculature (the whitish coloration of the components blends in well with the whitish musculature) and by their ethereal nature and relative plasticity of their shapes; therefore, we relied on the 3D reconstructions to guide us to the general shapes. The spermatophore (Fig. 3-4A and 6H-J) is a temporary creation of the greater reproductive system during copulation and, thus, its relative orientation is the opposite of other male internal components because the phallic complex is rotated around 90° (or more) during copulation (e.g. Fig. 3-4A,C). The spermatophore comprises two components (anterior to posterior): 1) tube region (the body, which is lightly-sclerotized) (Fig. 3-4A and 6H-J) and 2) reservoir (bulbous head) (Fig. 3-6H-J). Additionally, flexures (Figs. 3-6G, 7B, 8B, 9A, and 10E) are present and have obvious articulations (not labeled, but see Figs. 3-6G, 7B, 8B, and 10E) between them and the aedeagus while the gonopore processes (Figs. 3-6G, 7B,D, 8B, and 10E)

are near the apical end of the apodemes of endophallus and slope dorsally towards the flexures.

The aedeagus, the intromittent organ, is highly species-specific and, here, both its dorsal valves (Figs. 3-4A, 6F,G, 7B-E, 8B,D, 9A,B, and 10E) and ventral valves (Figs. 3-4A, 6F,G, 7B-E, 8B-E, 9B, and 10E) are quite long and gently curve upwards when viewed laterally. For this species, both sets of valves can be imagined as nested structures in which the concave dorsal valves almost fully encompass the tubular ventral valves. The dorsal valves are open along the entirety of their ventral side, fused for more than ¾ of their length with a thin, median dorsal cleft appearing for the remainder, and their entire outer surface is covered with microscopic leaf-like projections that are anteriorly-projected (Fig. 3-9A,D,E). The ventral valves are subcylindrical, apically-taper to points, and are enclosed by the dorsal valves on all sides except ventrally. However, the ventral valves can sometimes extend a bit beyond the start of the dorsal valves, and can also often be seen through the walls of the dorsal valves, especially laterally, when sclerotization is light or a specimen has been fully cleared in KOH (e.g. Fig. 3-7B). Often, these valves may appear to be attached for some length basally, but are actually only attached via light membranes. In fact, the valves can be fully separated into two nearly-identical halves, each appearing to be smooth, but, upon closer inspection, are actually quite rugose (Fig. 3-9C). Three length variations have been observed for the ventral valves: they do not extend beyond the apex of the dorsal valves (Figs 7B and 9A), they extend a little ways beyond the apex (Fig. 3-8A), and they extend quite a bit beyond the apex (Figs. 3-7A and 9B). Due to the unique shape of both valve

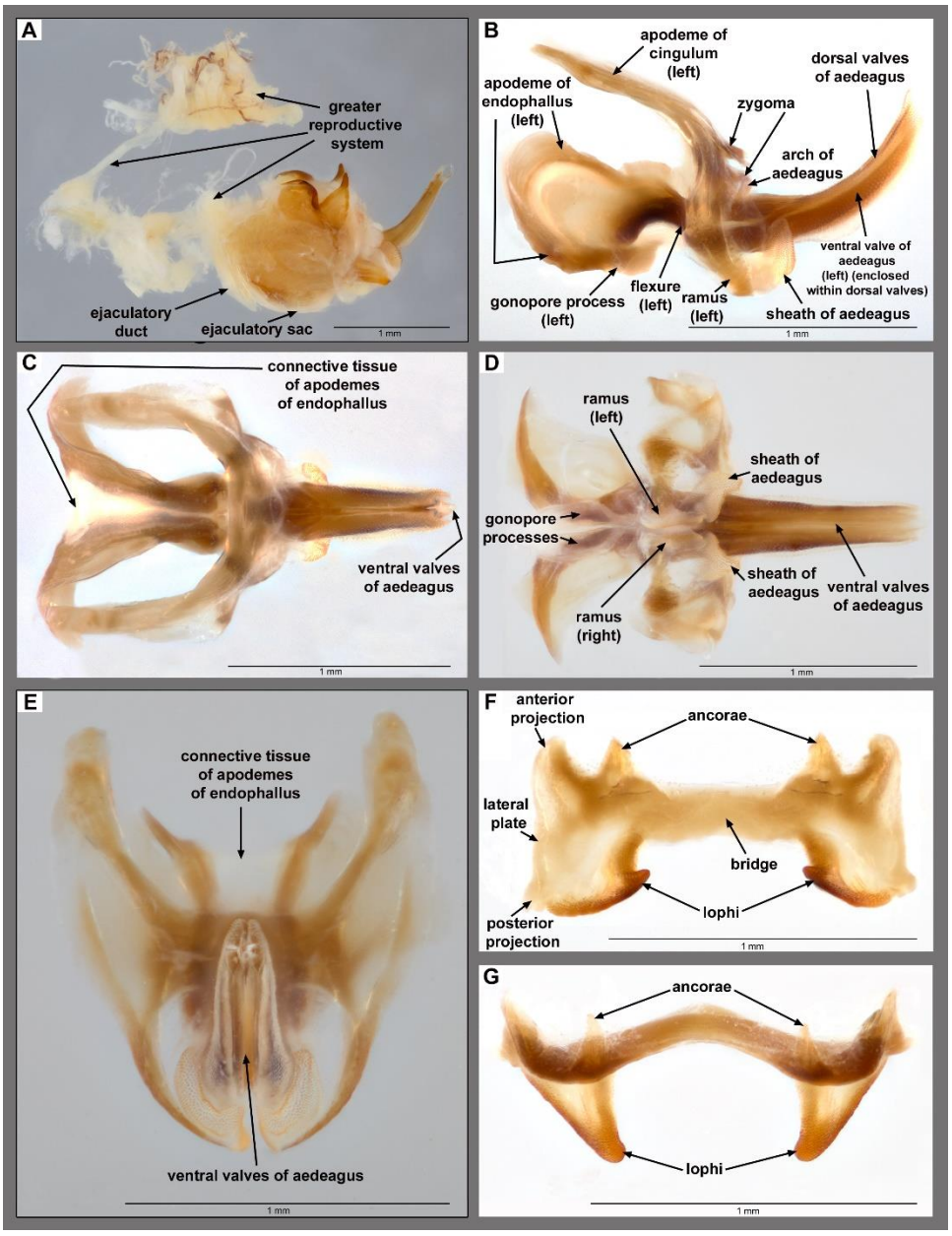

Figure 3-7. DSLR images of male internal genitalia and greater reproductive system components of *Melanoplus rotundipennis* (posterior to right unless otherwise noted): **A.** all components, left lateral view; **B.** phallic complex, left lateral view; **C.** phallic complex, dorsal view; **D.** phallic complex, ventral view; **E.** phallic complex, posterior view; **F.** epiphallus, dorsal view, posterior downwards; **G.** epiphallus, anterior view, dorsal downwards.

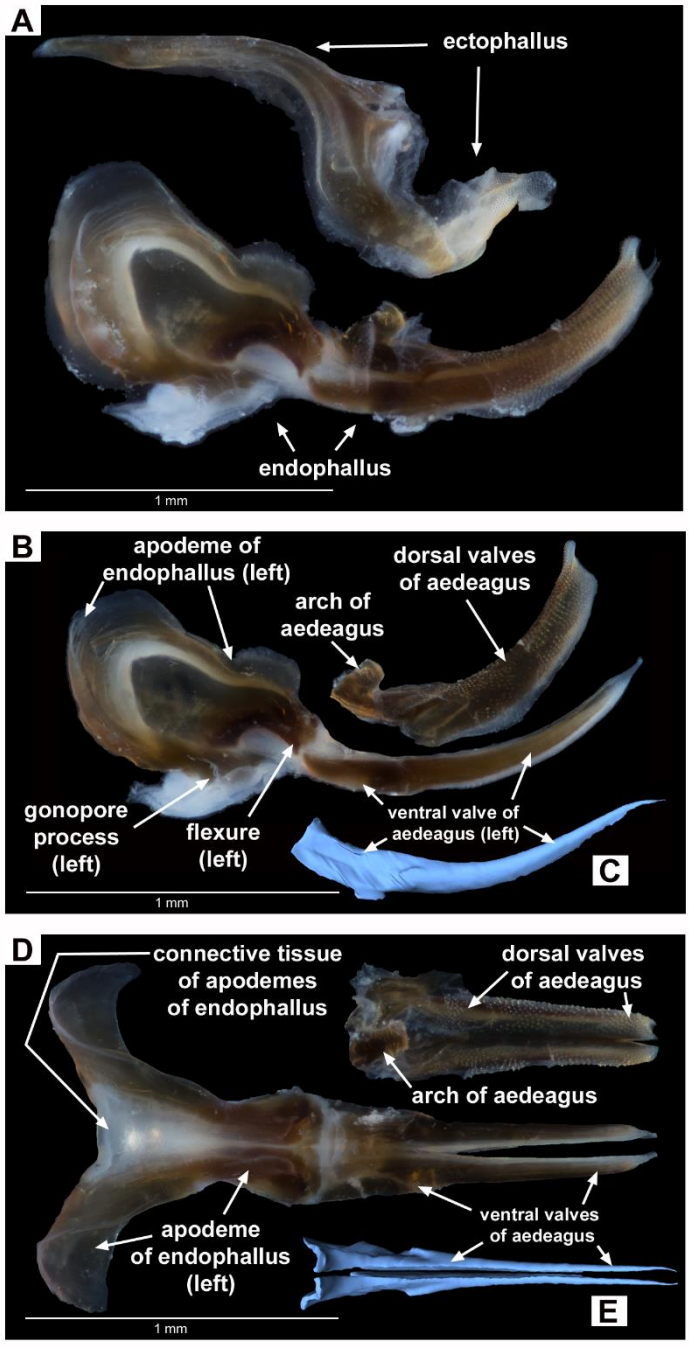

Figure 3-8. DSLR images and 3D reconstructions (based on *in copula* positions, but rotated into repose positions) of male internal genitalic components of *Melanoplus rotundipennis* (in all, posterior to right): **A.** DSLR, separated ectophallus and endophallus, left lateral view; **B.** DSLR, partially separated endophallus, left lateral view; **C.** 3D, ventral valve of aedeagus, left lateral view; **D.** DSLR, partially separated endophallus, dorsal view; **E.** 3D, ventral valves of aedeagus, dorsal view.

sets, the phallotreme (not labeled, but see Figs. 3-7B and 8A,B), the channel formed by the inner space of these valves through which the spermatophore (Fig. 3-4A and 6H-J) travels, is, thus, unique to this species. The arch of aedeagus (Figs. 3-6F,G, 7B, 8B,D, and 10C) rises from the median, dorsobasal region of the dorsal valves of aedeagus.

Female: External and Internal Genitalia, and Other Parts of the Reproductive System

External (Fig. 3-11): Nine anatomical components are present (six of which are paired) and one has two subcomponents (one of which is paired). The supra-anal plate (or epiproct) (Figs. 3-11A,B) is attached to tergite 10 (Fig. 3-11A,B) at its base with the cerci (Fig. 3-11A,B) extending posteriorly. The paraprocts (Figs. 3-11A,B) are similar to those in males, although larger and with a more rounded shape. Dorsal (Figs. 3-11A-C and 12B), inner (Fig. 3-11B), and ventral valves of ovipositor (Figs. 3-11A-D and 12A,B), and lateral basivalvular sclerites (Figs. 3-11B,C and 12A,B) are unremarkable and resemble those of other melanoplines, if not the majority of acridids that lay eggs in soil (Stauffer and Whitman, 1997). Similarly, the subgenital plate (Figs. 3-4B and 11B-H), which often has species-specific characters, such as the shape of its posterior margin, resembles that of all PG species with the margin possessing an ephemeral triangular projection that is attached firmly to the underside of the egg guide, extending about ¼ to ½ of its length (partially seen in Fig. 3-10A,B). The subgenital plate contains two subcomponents: the lophi receptacles (Fig. 3-11E-H) and egg guide (Figs. 3-4B and 11D-H), both of which also resemble those of all PG species. Additionally, the apical

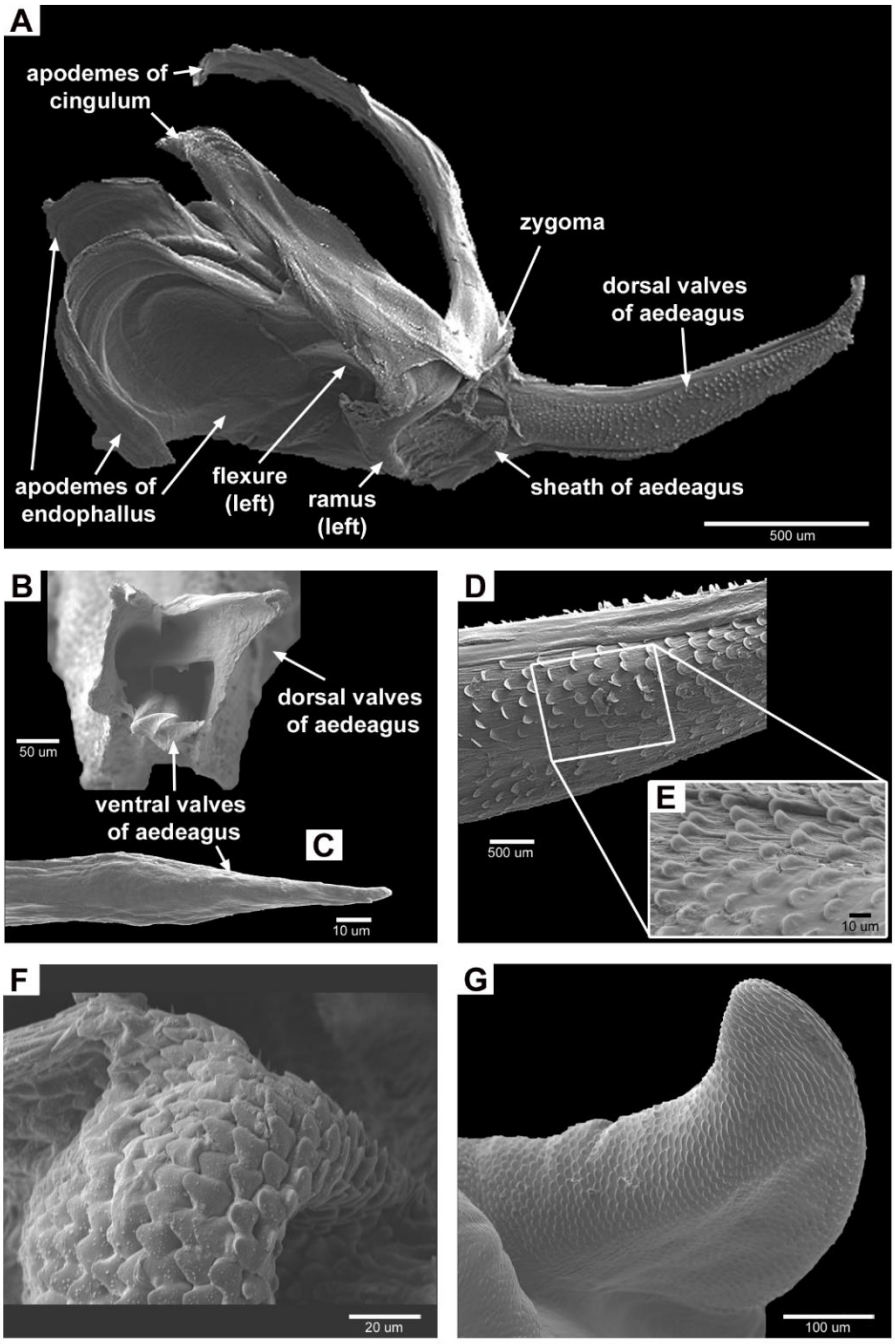

Figure 3-9. SEM images of male internal genitalic components of *Melanoplus rotundipennis*: **A.** ectophallus and endophallus, left lateral view, posterior to right; **B.** dorsal and ventral valves of aedeagus, posterior view; **C.** close-up, lateral view of left ventral valve of aedeagus; **D.** close-up, left lateral view of dorsal valves of aedeagus; **E.** further magnified close-up, left lateral view of dorsal valves of aedeagus; **F.** sheath of aedeagus, quasi-left lateral view, posterior to right; **G.** right lophus of epiphallus, quasi-left lateral view.

third of the subgenital plate that is bent downwards into the male's genital chamber during copulation (Fig. 3-4B) and contains the lophi receptacles is more heavily sclerotized than the rest (Fig. 3-11G,H).

Internal (Fig. 3-13A): Eight main anatomical components are present (three of which are paired) and two have subcomponents. The genital chamber is the cavity containing the internal genitalia and parts of the reproductive system, but can be difficult to delimit. Here, it seems to be delimited dorsally by the apodemes of ovipositor (Fig. 3-12A,B) and ventrally by the subgenital plate (Figs. 3-4B and 11B-H), with the spermathecal complex (Fig. 3-13H,I) as the most anterodorsal component, median oviduct (not pictured) as the most ventral, and vulval sclerite (Figs. 3-4B, 12A-E,G,H, and 13B-E) as the most posterior. The apodemes of ovipositor and anterior basivalvular sclerites (Fig. 3-12A,B) are unremarkable and resemble those of other melanoplines.

`The spermathecal complex (Fig. 3-13H,I), too, is essentially similar to other members of the PG and contains four subcomponents with one of these divided further into two more subcomponents. The entire complex is covered in what Snodgrass (1993) called a "muscular sheath" while Whitman and Loher (1984) referred to it as "glandular tissue" in *Taeniopoda eques* (Burmeister, 1838) (Romaleidae) and which a more detailed histological study by Ahmed and Gillott (1982) called a "small discrete bundle of muscle fibers". This is further supported by Lay et al. (1999) in which it is noted that "longitudinal and transverse muscles overlay" the entire complex. Here, we follow Gosálvez et al. (2010) in calling it the more general "muscle tissue" (partially

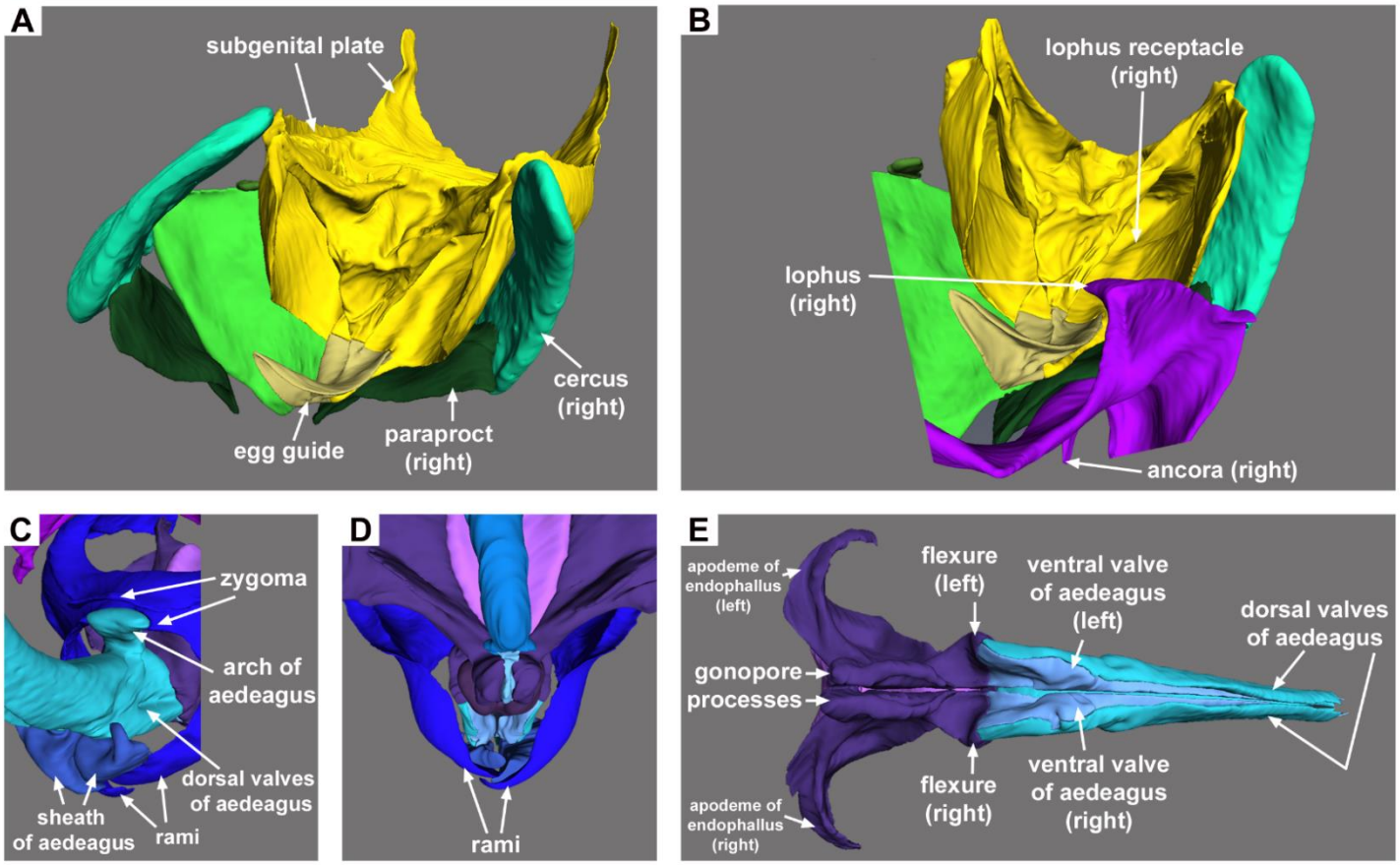

Figure 3-10. 3D reconstructions (A,B are *in copula* positions, C,D,E rotated into repose positions) of various genitalic components of *Melanoplus rotundipennis*: **A.** complete male and female external, posterior view; **B.** partial male external and internal, plus female external, posterior view; **C.** partial male phallic complex, quasi-right lateral view, posterior to left; **D.** partial male phallic complex, quasi-ventral view, posterior downwards; **E.** endophallus, ventral view, posterior to right.

seen in Figs. 3-12A and 13H). The spermathecae comprises two subcomponents: preapical and apical diverticula (Figs. 3-4B, 12A, and 13H,I), with the former very obvious, comparatively long, and slightly bulbous, and the latter only occasionally slightly bulbous at its apex, but often resembling the spermathecal duct (Fig. 3-4B, 12A, and 13H,I), for which the spermathecae form the apex. The duct itself appears to vary in length to a degree (Fig. 3-12A and 13H,I) and is typically compressed into loosely-tangled coils (Fig. 3-13H,I). Unlike in *Melanoplus sanguinipes* (Fabricius, 1798), *M. rotundipennis* and all other examined PG species do not have a U-shaped bend in the duct towards the basal end (Pickford and Gillott, 1971). Furthermore, for *M. rotundipennis* and other PG members, the spermathecae and spermathecal duct, though sometimes long, were not observed to extend beyond the basal arms of the subgenital plate (Fig. 3-3A-C,E), with spermathecal ducts typically compressed into loosely-tangled coils. The delimitation of the spermathecal aperture seems clear here and is the slit connecting the spermathecal duct to the bursa copulatrix (not labeled, but see Fig. 3-4B).

The bursa complex (Fig. 3-13A,E) comprises two subcomponents: the armor of bursa copulatrix (Figs. 3-4B, 12B-D,F,G, and 13E-G) and the bursa copulatrix (Figs. 3-4B, 12B-D,F,G, and 13E-G), and has the overall appearance of a scorpion's tail, with, approximately, its apical fourth being curved back on itself ventrally except in the 3D reconstructions (discussed later). Interestingly, this curvature was observed to point left or right (Fig. 3-12B) depending on the individual (and even within the same population)

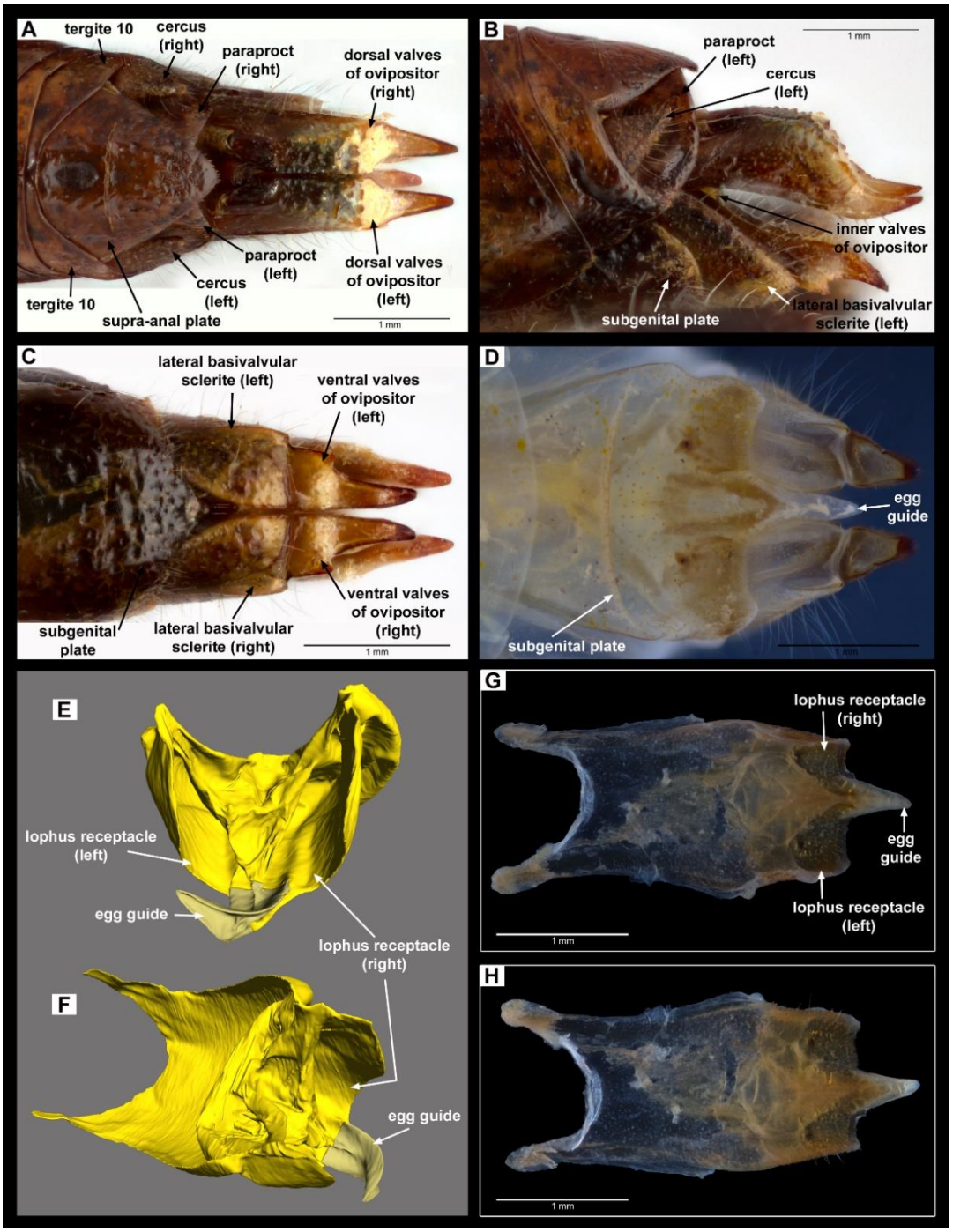

Figure 3-11. DSLR images and 3D reconstructions (*in copula* positions) of female external genitalia and greater reproductive system components of *Melanoplus rotundipennis* (posterior to right unless otherwise noted): **A.** DSLR, dorsal view; **B.** DSLR, left lateral view; **C.** DSLR, ventral view; **D.** DSLR, ventral view, made translucent with KOH; **E.** 3D, subgenital plate, posterior view; **F.** 3D, subgenital plate, quasi-left lateral view, posterior to right; **G.** DSLR, subgenital plate, dorsal view; **H.** DSLR, subgenital plate, ventral view.

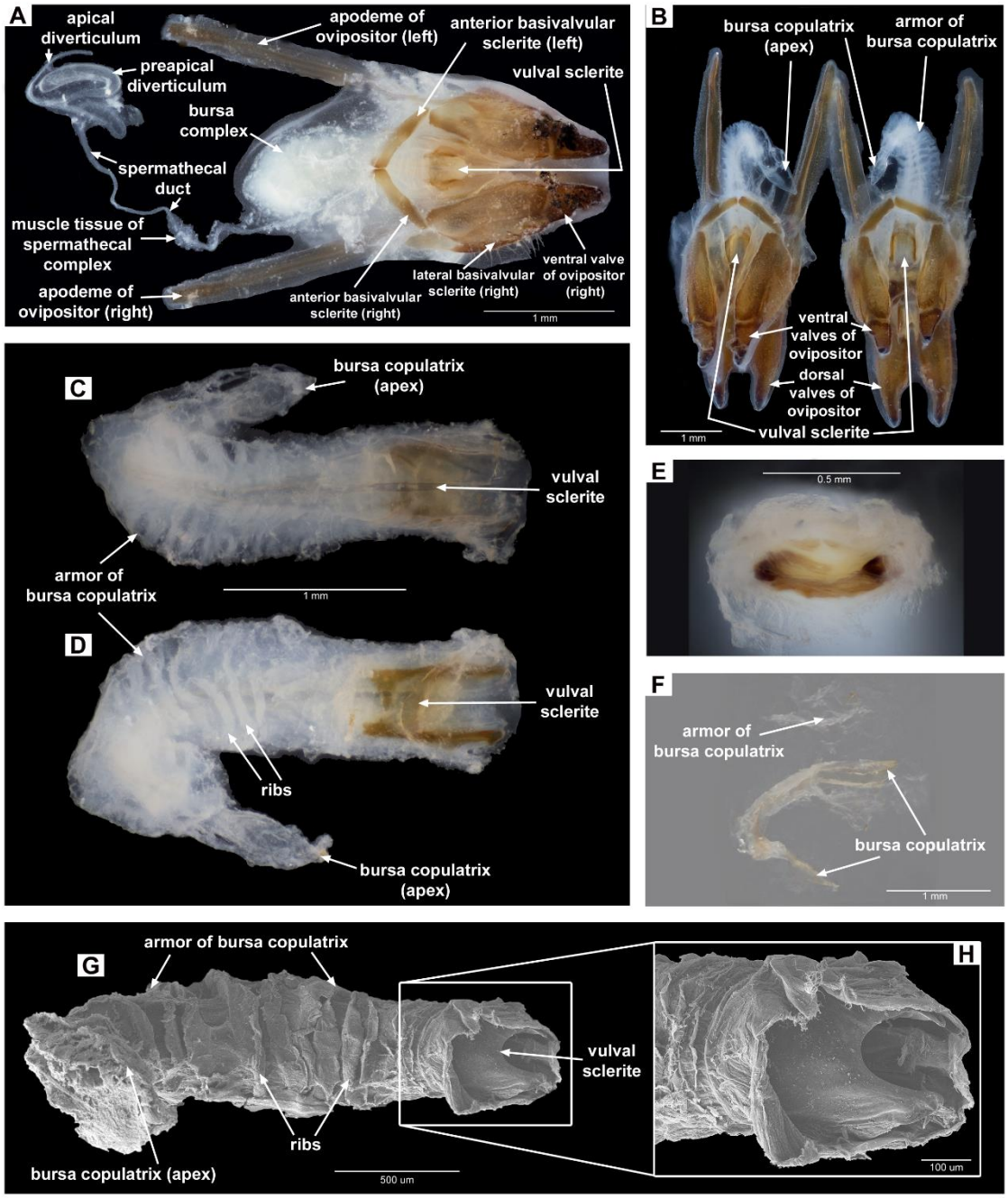

Figure 3-12. DSLR and SEM images of female external and internal genitalia, and greater reproductive system components of *Melanoplus rotundipennis* (posterior to right unless otherwise noted): **A.** DSLR, ventral view; **B.** DSLR, ventral view, posterior downwards; **C.** DSLR, bursa complex, dorsal view; **D.** DSLR, bursa complex, ventral view; **E.** DSLR, close-up of vulval sclerite, posterior view, dorsal upwards; **F.** DSLR, partially separated bursa complex, quasi-dorsal view; **G.** SEM, bursa complex, ventral view; **H.** SEM, close-up of posterior region of bursa complex, ventral view.

with no apparent pattern yet known. The armor of bursa copulatrix (Figs. 3-4B, 12B-D,F,G, and 13E-G) is an outer covering that surrounds the majority of the inner bursa copulatrix, has a ribbed appearance (Fig. 3-12D,G) with flexible membrane-like portions in-between. Furthermore, it is tough to the touch (of forceps), despite it not appearing to be heavily-sclerotized as in other components, and it also does not possess the yellowish coloration often associated with sclerotization (Fig. 3-12F). The bursa copulatrix (Figs. 3-4B, 12B-D,F,G, and 13E-G), on the other hand, does have the yellowish coloration (Fig. 3-12F), but is much weaker to the touch and only appears to be lightly-sclerotized, and to varying degrees among specimens. Overall, the bursa copulatrix is broadly tubular, but a portion just before its apex constricts into a narrower tube with its actual apex being quite bulbous (to varying degrees) and extending beyond the armor, sometimes quite extensively (Fig. 3-12B).

The vulval sclerite (Figs. 3-4B, 12A-E,G,H, and 13B-E) is found ventrally at the entrance to the bursa complex, also known as the vulva (not labeled, but see Fig. 3-12A-H), and often extending slightly beyond. Sclerotization levels for this component vary between specimens (Figs. 3-12D,E,G,H and 13B) and some may even be divided in two (Fig. 3-13C), but, in general, it is often plate-like, curves gently dorsally (lightly concave from an anterior view), has two lateral arms that extend posteriorly, and sometimes has slight anterodorsal protrusions (Fig. 3-13C). Finally, the Comstock-Kellog glands (not pictured) do not appear to be as obvious as in other *Melanoplus* species (Slifer and King, 1936; Slifer, 1940b), but are present in *M. rotundipennis*, are of a typical shape, and almost translucent (made even fainter with KOH).

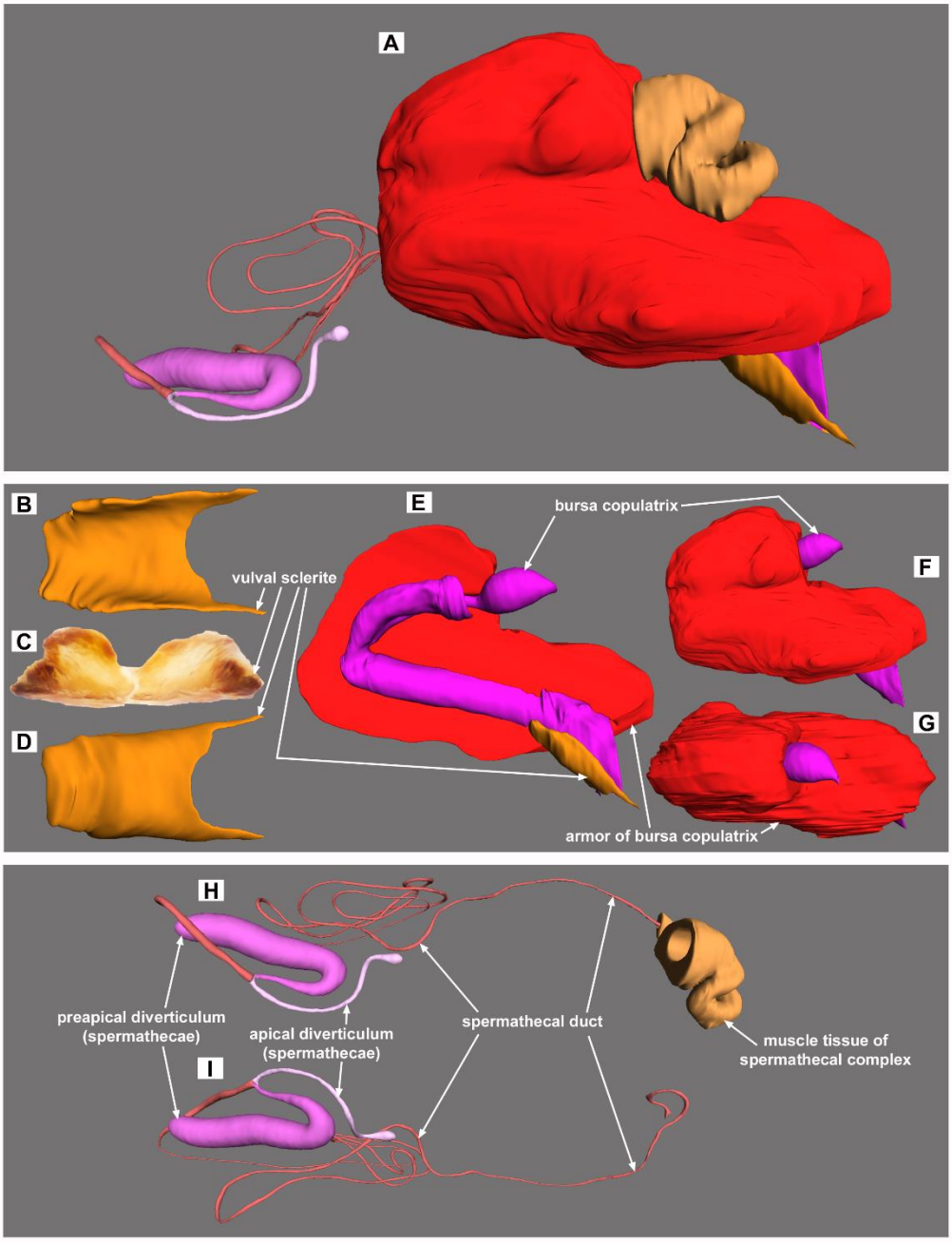

Figure 3-13. 3D reconstructions (*in copula* positions) and a DSLR image of female internal genitalia and greater reproductive system components of *Melanoplus rotundipennis* (posterior to right unless otherwise noted): **A.** all components, left lateral view; **B.** vulval sclerite, dorsal view; **C.** DSLR, vulval sclerite, posterior view, dorsal upwards; **D.** vulval sclerite, ventral view; **E.** bursa complex and vulval sclerite, left lateral, cut-away view; **F.** bursa complex, left lateral view; **G.** bursa complex, dorsal view; **H.** spermathecal complex, quasi-dorsal view; **I.** spermathecal complex, ventral view (muscle tissue of spermathecal complex removed).

In Copula

External: During copulation, the apical third of the female's subgenital plate is bent at an almost 90° angle ventrally, is wedged into the male's genital chamber, and is dominantly resting atop his right paraproct and basal end of his right cercus, but is not quite touching his folded-in supra-anal plate or furculae (Figs. 3-3C and 10A,B). Additionally, the apical half of the female's egg guide is bent upwards and to the left (Fig. 3-10A,B), most likely a result of encountering the muscles that surround the male's phallic complex. Finally, the male's cerci are pressing slightly on the female's abdomen towards the base of her lateral basivalvular sclerites (Fig. 3-1A-D).

Internal: During copulation, the right lophus of the male's epiphallus is inserted for some distance into the female's corresponding right lophus receptacle (Fig. 3-10B) while the majority of his aedeagus is inserted into her bursa complex, specifically coming into direct contact with her bursa copulatrix for some distance (Fig. 3-4C). The dorsal, concave surface of the female's vulval sclerite is entirely touching part of the basal, dorsal region of the male's dorsal valves of aedeagus (Fig. 3-4C). Finally, the male's spermatophore is emerging from between the apices of his dorsal and ventral valves of aedeagus, so that the rest of its tube region is extended through the remainder of the female's bursa copulatrix. Here, the apex of the tube region has swollen to completely fill the interior of the bulbous apex of the bursa copulatrix, presumably because it is close to rupturing (Fig. 3-4C).

Discussion

Functional Morphology

Unsurprisingly, but rarely demonstrated in action, external and internal anatomical components of the male and female reproductive system, mainly genital, in *M. rotundipennis* are involved in copulation, often appearing to possess multiple functions. Herein, the probable functions of 45 of the 58 named components will be discussed in more detail as well as other items of interest, like novel discoveries, starting, in general, with the male (32 male components) and then moving to the female (13 female components) (summarized in Table 1). 12 female components were not observed to be involved in copulation: tergite 10 (Fig. 3-11A,B), supra-anal plate (Figs. 3-11A,B), cerci (Fig. 3-11A,B), paraprocts (Fig. 3-11A,B), median oviduct (not pictured), dorsal, inner, and ventral valves of ovipositor (Figs. 3-11A-D and 12A,B), apodemes of ovipositor (Fig. 3-12A,B), lateral basivalvular sclerites (Figs. 3-11B,C and 12A,B), anterior basivalvular sclerites (Fig. 3-12A,B), and Comstock-Kellog glands (not pictured). Of these, the majority are most likely involved in laying eggs while others may be involved with structural support of the abdomen, assist in waste excretion, and/or sensory reception (possibly even during copulation) (Snodgrass, 1935; Eisner et al., 1966, Uvarov, 1966; Snodgrass, 1993; Stauffer and Whitman, 1997). For the males, the lone exception was the furculae (Figs. 3-4A and 5A-E), which were initially thought to be involved in copulation, but may not be. Observations were based on correlative microscopy combining DSLR and SEM images with micro-CT-based 3D reconstructions, as well as observations of museum specimens and live specimens, and

inferences based on past publications on other species of Acrididae, some within the same genus.

Male: External and Internal Genitalia, and Other Parts of the Reproductive System

External: All but one of the seven named external components that we observed appear to be involved in copulation. The primary probable function of the supra-anal plate, though, as in all other Acridoidea with eversible phallic complexes, is to act as the protective dorsal surface (a "roof") for the genital chamber and its contents. When swung downwards, however, it may also serve as an effective wall to ensure against the possibility of the female's subgenital plate (Figs. 3-4B and 11B-H), or even debris, making its way further anterior into the more delicate areas of the male's reproductive and digestive systems.

During observations of live copulation attempts the cerci (Figs. 3-4A and 5A-E) were able to be flipped inwards and outwards, most likely due to muscular action assuming the four muscles mentioned by Snodgrass (1935) are present that attach the cerci to both tergite 10 (Fig. 3-5C-E) and the supra-anal plate. Although not observed directly, a possible reason for cerci inversion is to assist in scooping the phallic complex up and out of the genital chamber, with the possible assistance of the supra-anal plate and paraprocts (Figs. 3-4A and 5A-E). In the *in copula* 3D reconstructions (Fig. 3-3A-E), the cerci are not inverted and are back in their original positions, which must occur at

Table 3-1. Summary of the probable functions of 45 (32 male, 13 female) of the 58 named genitalic and other reproductive system components/subcomponents involved in copulation in *Melanoplus rotundipennis* (Scudder, 1878), most of which have been reconstructed in 3D. For each function: 1 = observed in this study and previous studies; 2 = novel observation and/or hypothesis; 3 = hypothesized based on our observations, and evidence or hypotheses from previous study(ies); 4 = supported hypothesis from previous study(ies); 5 = only observed in previous study(ies)

Sex	Body region	Component	Subcomponent	Functions during copulation
Male	External (6)	tergite 10		Attachment point for furculae, supra-anal plate, cerci, and paraprocts[1]
		supra-anal plate		Closes off genital chamber at rest[1]; may protect anterior body regions during copulation[3]; may assist in phallic complex eversion[3]
		cerci		Push against female abdomen to act as supports during copulation and/or to assist in prevention of female leaving[3]; inversion ability may assist in phallic complex eversion[3]; act as sensory structures[5]; support female subgenital plate when pulled into genital chamber[2]
		paraprocts		Act as supports for female subgenital plate[2]; may assist in cerci inversion[3]; may assist in phallic complex eversion[3]
		pallium		Covers and protects aedeagus[1]
		subgenital plate		Stretches to allow for phallic complex eversion[1,2]
Male	Internal (26)	genital chamber		Encloses phallic complex[1]
		phallic complex (epiphallus)	ancorae	Hook onto and pull down female subgenital plate to gain access to vulva[1]; near-by sensory receptors may aid in this action[2]
			anterior projections	May serve as structural support and/or muscle attachment site[3]; scattered sensory receptors may aid in ancorae's action of pulling down female subgenital plate[2]
			posterior projections	May serve as structural support and/or muscle attachment site[3]
			bridge	May serve as structural support (can flex) and/or muscle attachment site[3]
			lateral plates	May serve as structural support and/or muscle attachment site[3]
			lophi	Pushed into female lophi receptacles to keep her subgenital plate pulled down for aedeagus insertion through her vulva[2,4]
		phallic complex (ectophallus)	apodemes of cingulum	General structural support for phallic complex[1]; attachment points for muscles[5]; leverage point for aedeagus[3]
			zygoma	Lower portion receives arch of aedeagus[1]; extended portion of upper region provides limited articulation and structural support for aedeagus[3]
			rami	May act as supports and attachment points for sheath of aedeagus[3]; Able to be laterally compressed inwards, which may tighten sheath of aedeagus for reason(s) unknown[2]; role of sensory receptors on posterior apices currently unknown[2]
			sheath of aedeagus	Covered in minute spines that may act as female-stimulators or as grippers[2]
		phallic complex (endophallus)	apodemes of endophallus	Attachment points for muscles[1]; contractions of muscles separate gonopore processes for transfer of spermatophore and may aid in pumping it into female[5]
			connective tissue of apodemes of endophallus	Acts like spring-loaded bellows to bring apodemes back to original position after contractions of muscles[2]
			flexures	Act as support and leverage points for the aedeagus[1]
			articulations	Act as support and leverage points for the aedeagus[1]
			gonopore processes	Laterally separate to open gonopore during contraction of muscles attached to apodemes of endophallus[5]
			dorsal valves of aedeagus	Assist in forming phallotreme for spermatophore formation[1]; external surface covered in microscopic leaf-like projections that act as female-stimulators or grippers[3]
			ventral valves of aedeagus	Assist in forming phallotreme for spermatophore formation[1]; assist in shaping spermatophore and guiding it into female[3]
			phallotreme	Channel between aedeagal valves that shapes spermatophore's tube region[1]
			arch of aedeagus	Provides limited articulation and structural support for aedeagus[3]

Table 3-1. Continued

Sex	Body region	Component	Subcomponent	Functions during copulation
		greater reproductive system	ejaculatory duct	1st step of spermatophore creation: uses accessory gland secretions to construct reservoir, then tube region, and then begins to fill with semen[5]
			ejaculatory sac	2nd step of spermatophore creation: enlarges reservoir/tube region and continues to fill with semen[5]
			gonopore	3rd step of spermatophore creation: when opened, allows for transfer of spermatophore from ejaculatory sac to spermatophore sac[5]
			spermatophore sac	4th step of spermatophore creation: via gonopore, receives spermatophore and surrounding muscles pump semen-filled tube region into phallotreme while reservoir stays within[5]
		greater reproductive system: spermatophore	tube region	Primary portion used to transfer semen to female[1]
			reservoir	In spermatophore sac, continually adds semen to tube region until empty[1]
Female	External (3)	subgenital plate		Blocks male's access to vulva[1]; apical third fits into male's genital chamber to allow him greater access to vulva by widening her genital chamber[2,4]
			lophi receptacles	Receive male lophi, possibly only one per copulation event[2,4]
			egg guide	Blocks access to vulva[1]; guides egg into intervalvular space[5]; provides support for male phallic complex to push against[2]
Female	Internal (10)	genital chamber		Encloses internal components[1]
		spermathecal complex	muscle tissue of spermathecal complex	May assist in moving sperm back toward eggs for fertilization[3]
			spermathecal duct	Duct through which sperm moves toward diverticula and then back for egg fertilization[5]
			spermathecal aperture	May serve as transfer point for sperm from spermatophore's tube region, swelling within apex of bursa copulatrix, to spermathecal duct[3]
		spermathecal complex: spermathecae	preapical diverticulum	Sperm receptacle[5]
			apical diverticulum	Sperm receptacle[5]
		bursa complex	armor of bursa copulatrix	During interactions with male aedeagus - strengthens bursa copulatrix and/or ribbing allows for expansion of bursa copulatrix[2]
			bursa copulatrix	Receives male aedeagus[1]; apex may alter size to accommodate swelling apex of spermatophore's tube region and may be rupture point for spermatophore[2,3]; may contain nerve endings for stimulation by male or lined with material for gripping by male[3]
		vulval sclerite		Connects vulva to bursa copulatrix[3]; reinforces entrance to bursa copulatrix[2]; support plate for male aedeagus[2]
		vulva		Opening to all other internal components[1]; receives male aedeagus[1]

some point during the process of copulation, because the cerci have been observed to push against the female's abdomen, possibly for support during copulation and/or to further prevent the female from leaving. Uvarov (1966) and Chapman (2012) mention something similar occurring across Acrididae, but use the term "grip" instead, although it is unclear if this suggests the cerci are pushing against the female (as we observed) or are actually pulling her towards the male. Kyl (1938) too, says the cerci "grasp the abdomen of the female" in *Melanoplus differentialis* (Thomas, 1865), but then goes further by describing that the effect of this action pulls down the egg guide, opening the genital chamber of the female slightly. We know now that, more than likely, the epiphallus is the component responsible for this in all grasshoppers, but Snodgrass (1935) seems to clarify the possible gripping role of the cerci by noting that they "grasp the base of the subgenital plate of the female". Boldyrev (1929) goes further and actually calls cerci "organs of attachment", specifically in reference to *Locusta migratoria* (Linnaeus, 1758), but also notes that their primary purpose is as "organs of orientation". Furthermore, it appears there might be a mild invagination towards the basal end of the female's lateral basivalvular sclerites (Figs. 3-11B,C and 12A,B) that the apices of the cerci might be able to push into slightly (Fig. 3-1A-D), but further investigation is needed to clarify this issue.

Moreover, cerci in numerous insects have been observed to be sensory structures, sensitive to sounds, movement of air, and touch, primarily due to the abundance of sensilla on them (Snodgrass, 1935; Uvarov, 1966; Snodgrass, 1993; Gordh and Headrick, 2001; Chapman, 2012). So far, for the PG, the presence of such sensilla has

yet to be confirmed, but the abundance of setae on the cerci of all species suggests it. Thus, it is quite possible that if such sensilla are present, they might be used as contact receptors during copulation and/or may even have functions not involved in copulation. Moreover, grasshopper cerci, which are often species-specific (particularly in *Melanoplus*) may be important for appropriate sensory stimulation and recognition of conspecific males by the female, a hypothesis in need of experimental investigation (Eberhard, 1985; Eades, pers. comm.). Finally, the cerci (at least the one on the right in this case), in conjunction with the paraprocts, appear to assist in supporting the posterior portion of the apical third of the female's subgenital plate when it is bent downwards into the male's genital chamber (Figs. 3-3C and 10A).

The paraprocts (Figs. 3-4A and 5A-E) may have at least two probable functions. The first one might be to assist in flipping the cerci down into the genital chamber due to their membranous connection (Fig. 3-5A,B). When the supra-anal plate is swung down into the genital chamber, it pushes the paraprocts downwards as well and brings the cerci with them. This proposed function, supported by experimentation with freshly-killed specimens in the lab using fine-tipped forceps, is less likely, if muscles turn out to be present at the base of the cerci. When the supra-anal plate was pushed inwards with forceps, the paraprocts were as well and pulled the cerci with them. Evidence contained in the 3D reconstructions (Figs. 3-3C and 10A) suggests the other possible function of the paraprocts (at least the one on the right in this case) is the same as the cerci: support for the posterior portion of the apical third of the female's subgenital plate when it is bent downwards into the male's genital chamber.

The obvious extension of the pallium (Fig. 3-5C-E) seems clear: because the aedeagus is one of the longest in the PG and is strongly curved upwards, it needs an extended cover for protection. When preparing for copulation, the rotators of phallus and retractors of pallium muscle, specifically the posterior portion (muscle 266, specifically 266B in Eades, 2000) pulls the pallium downwards, exposing the aedeagus' apex. The probable function of the subgenital plate (Fig. 3-5D,E) is not unique to this species and also seems clear: it is able to stretch ventroposteriorly to some degree via its medial membranous connection, which, most likely, assists in moving the phallic complex somewhat towards the posterior of the genital chamber, so the supra-anal plate, paraprocts, and cerci are able to swing inwards.

As mentioned, the function of the furculae (Figs. 3-4A and 5A-E) during copulation is still unknown at this time, although it is quite possible that they do not play a role. If they do, though, one suggestion is that they might possess sensory receptors (as seen on other male components) that might assist in assessing the location of a female's abdomen during copulation. However, preliminary SEM observations of the furculae of different PG species did not reveal their presence. Regardless, it can be unquestionably stated that the furculae in *M. rotundipennis* stay rigid and keep their original positions when the supra-anal plate (Figs. 3-4A and 5A-E) is swung downwards into the genital chamber (presumably via muscular action along tergite 10) (Fig. 3-3C). Numerous members of the PG possess species-specific furculae, but others lack them entirely, and the same observations can be applied to other Acrididae species, further suggesting that they may not play a role in copulation.

Internal: All the named internal components that we observed appear to be involved in copulation. The genital chamber encloses the phallic complex (Fig. 6A) until the male is ready to attempt copulation. Then, the external genital components are pushed out of the way (presumably via muscular action), so the phallic complex can be partially everted dorsally by muscular action and the inflation of surrounding membranes. The mechanism behind such inflation is currently unknown, but may be due to an increase in hemolymph-related hydrostatic pressure caused by muscular action (Whitman and Loher, 1984; Lawry, 2006; Chapman, 2012). Following that, the epiphallus (Figs. 3-6B,C and 7F,G) is pushed higher than the other phallic complex components because it is the most dorsal and not directly connected to the rest. The ancorae (Figs. 3-4A, 6B,C, and 7F,G) of the epiphallus are then used as hooks (maybe individually or together) to catch the posterior margin of the female's subgenital plate (Figs. 3-4B and 11B-H). This action pulls the subgenital plate down into the anterior of the male's genital chamber, thus opening access to the female's vulva. More than likely, the sensory receptors on the anterior projections (Figs. 3-6B, 7F,G) and near the ancorae (mentioned earlier and possibly seen here for the first time in acridids) play roles in this action. In the 3D reconstructions, also note that the epiphallus is not symmetrically-aligned with the female's subgenital plate, but, rather, skewed slightly towards the left (Fig. 3-10B). This is most likely due to the fact that even though a male is mounted on top of a female, he must lower his abdomen below and to either side of a female's abdomen, resulting in asymmetrical copulation (Fig. 3-2C), which, in the case of the male used for the 3D reconstructions, was from the left side of the female (Fig. 3-1A-D,

14).

After the apical third of the female's subgenital plate is pulled down into the anterior of the male's genital chamber, the entire phallic complex is swung dorsally in a quick motion, continuing in a counterclockwise arc anteriorly with the majority of the aedeagus (Figs. 3-4A, 7B,C, and 9A) entering the female's bursa complex through the vulva (not labeled, but see Fig. 3-12A-H). Such a motion means that all phallic complex components (previously described in a state of repose) (e.g. Fig. 3-6A) have rotated around 90° (or more), resulting in orientations that can now be described as ventral/anteriorly-projecting (e.g. Fig. 3-4A). In these new *in copula* positions (Fig. 3-3A-E, 4A,C, 5A,B, 10A,B) is how descriptions of the probable function(s) of the remaining components of the phallic complex will be described herein; referenced Figures should be carefully examined to maximize comprehension. Once rotation of the phallic complex has occurred, and (presumably) the aedeagus enters the female's bursa complex, at least one lophus on the male's epiphallus is able to be inserted into a female's corresponding lophus receptacle of the subgenital plate (Fig. 3-10B). There is little doubt that this pinning action ensures that the female's subgenital plate stays down to allow for continued access by the male to the female's internal genitalia. The scales observed on the lophi (Fig. 3-9G) all but confirm this hypothesis, especially in light of the fact that said scales are directed anteriorly (posteriorly during copulation) and would, thus, act as miniature friction anchors as a lophus is pushed into a receptacle and pulled down and back. If a female were found to possess similar structures that face in the opposite direction the friction effect should be even greater. The other three

subcomponents of the epiphallus: anterior projections, posterior projections, bridge, and lateral plates (Figs. 3-6B,C and 7F,G) appear to have no specialized function (a possible exception are the scattered sensory receptors on the anterior projections) other than 1) to potentially act as structural support during copulation, in some cases being able to flex to a degree as evident by the shape of the bridge, and 2) to possibly also serve as attachment sites for muscles (lateral plates: Eades, 2000; others: Eades, pers. comm.).

As mentioned previously, a male asymmetrically-copulates with a female, so, like the epiphallus, the ectophallus (Figs. 3-6D,E and 8A) and endophallus (Figs. 3-6F,G and 8A) are also asymmetrically-aligned with the female's internal genitalia. The particular male used for the 3D reconstructions entered the female from her left side (Fig. 3-1A-D, 14), so the phallic complex components are therefore skewed slightly at an angle to the right meaning that the aedeagus also enters the female's bursa complex at a slight angle (Fig. 3-3D). The fact that the phallic complex is able to be twisted a fair range manually with forceps supports the idea that asymmetrical entry is possible, but we do not think that it has been noted or demonstrated before. The probable functional role of the ectophallus overall is not fully clear compared to the other two phallic complex components. However, the apodemes of cingulum (Figs. 3-4A, 6D,E, 7B,C,E, and 9A) have a muscle attached to them called the protractors of cingulum (only found in *Melanoplus*) that, when combined with the retractors of cingulum muscle (attached to the zygoma: Figs. 3-4A, 6D,E, 7B,C, and 9A) (muscles 267XC and 278, respectively, in Eades, 2000) would most likely assist, in conjunction with other related muscles, in rotating the phallic complex for copulation and back again to its resting state (Eades,

2000). Additionally, the ectophallus acts as general structural support for the entire complex and most likely as a leverage point for the aedeagus, particularly during its insertion into the female's bursa complex (and extraction) and throughout spermatophore transfer during copulation. This leverage suggestion stems from the fact that the arch of aedeagus is inserted into the gap in the lower region of the zygoma (Fig. 3-7B and 10C) and it is quite possible that the upper region portion is extended to provide limited articulation and structural support (acting as a plate to push against) for the aedeagus during the copulation process.

For Melanoplinae, Eades (2000) made no mention of any muscles being attached directly to the rami (Figs. 3-4A, 6D,E, 7B,D, and 9A) and there do not seem to be any in this species (Fig. 3-7A), so it is strongly possible there are none meaning that the rami may just be supports and attachment points for the sheath of aedeagus (Figs. 3-4A, 6D,E, 7B-D, and 9A). Note, though, that the rami appear to be laterally compressed inwards during copulation as captured in the 3D reconstructions (Fig. 3-10C,D); such action may tighten the sheath around the dorsal valves of aedeagus for an unknown reason or may just be a by-product of muscle movement elsewhere. Additionally, it is currently unknown what role is played by the sensory receptors observed on the posterior apices of the rami. The probable function of the minute spines seen on the sheath of aedeagus (Fig. 3-9F) that are potentially new to science is also unknown at this time, but, given their placement in relation to the female's anatomy (Fig. 3-4C), it is feasible that they either play a role in stimulating the region surrounding the female's vulva (Eberhard, 1985) or act as additional grippers (possibly for gripping the ventral side of her

abdomen), further securing the male's aedeagus to the female, but they do not appear to be sensory receptors for the male's use.

The subcomponents of the endophallus (Figs. 3-6F,G, 8A-E, and 10E), and the associated subcomponents of the greater reproductive system (Fig. 3-6H-J and 7A), serve numerous probable functions during copulation. The apodemes of endophallus (Figs. 3-4A, 6F,G, 7B-E, 8B,D and 9A) provide attachment points for a number of muscles with many probable functions related to spermatophore production and insemination (Snodgrass, 1935; Roberts, 1941; Gregory, 1965; Hartmann, 1970; Pickford and Gillott, 1971; Whitman and Loher, 1984; Snodgrass, 1993; Eades, 2000), but the majority of these muscles will not be discussed here as it is outside of this study's scope. Insemination results from sperm contained within the semen contained in a male's spermatophore (Fig. 3-4A and 6H-J) and the process of its creation can differ from species to species, so it will only be briefly touched upon here, based upon synthesized evidence from studies of other grasshoppers, including some *Melanoplus* species (Boldyrev, 1929; Snodgrass, 1935; Kyl, 1938; Roberts, 1941; Gregory, 1965; Uvarov, 1966; Hartmann, 1970; Pickford and Gillott, 1971; Whitman and Loher, 1984; Snodgrass, 1993; Eades, 2000; Chapman, 2012). The first step in the process usually begins shortly after a male begins copulating with a female, which signals the transfer of accessory gland secretions to move into the ejaculatory duct (Figs. 3-4A, 6I,J, and 7A). These secretions are used to construct the spermatophore's reservoir (Fig. 3-6H-J), followed by its tube region (Fig. 3-4A and 6H-J), and then it begins to fill with semen. Next, the reservoir and tube region move to the ejaculatory sac (Figs. 3-4A, 6I,J, and

7A) where they are enlarged and continue to fill with semen. Then, the adductor of endophallic apodemes (muscle 283 in Eades (2000), extending between the two apodemes of endophallus) is contracted, laterally-separating the gonopore processes (Figs. 3-6G, 7B,D, 8B, and 10E) and opening the gonopore (not pictured). This transfers the spermatophore from the ejaculatory sac to the spermatophore sac (Fig. 3-6I,J) in which the spermatophore's reservoir will remain to continually add semen to the spermatophore's tube region during copulation until empty. Finally, via rhythmic contractions of the muscles surrounding the spermatophore sac, the semen-filled tube region is pumped through the phallotreme (which further shapes the spermatophore into its final tubular form), out of the aedeagus (Fig. 3-4A), and into the female (Fig. 3-4C), followed by the eventual ejection of the spermatophore from the body of both sexes upon the completion of sperm transferal. The exact sources of these muscular contractions are still being debated, but it has been suggested that one or more of the following muscles are responsible: adductor of endophallic apodemes, outer compressors of ejaculatory sac (muscle 281x in Eades, 2000), and/or inner compressors of ejaculatory sac (muscle 284 in Eades, 2000).

The probable function of the connective tissue of apodemes of endophallus (Figs. 3-4A, 6F,G, 7C,E, and 8D), seemingly not previously identified, named, or described (composition is reminiscent of the female's egg guide: Figs. 3-4B and 11D-H) by other studies, is not fully clear at this time. More than likely, though, based on examination with forceps and consideration, it serves to snap the apodemes back into their starting positions after each contraction by the adductor muscles (muscle 283 in Eades, 2000)

that cover most of it, so that further musculature is not needed to expand the apodemes again; in this way, the connective tissue would act in a similar manner as a spring-loaded bellows. The flexures (Figs. 3-6G, 7B, 8B, 9A, and 10E), the membranes connecting them to the valves of aedeagus (Fig. 3-8A,B), and the articulations between these subcomponents (not labeled, but see Figs. 3-6G, 7B, 8B, and 10E) possibly function, as other phallic complex components appear to, as support and leverage points for the dorsal and ventral valves, allowing the aedeagus greater movement and positioning ability (Whitman and Loher, 1984).

Based on the 3D reconstructions, the aedeagus can be inserted into the bursa complex almost entirely, its apex reaching just to the bend in the bursa complex, with essentially only the portion touching the sheath of aedeagus left outside the female (Fig. 3-4C). The mid-basal region of the dorsal valves of aedeagus appear to rest, and most likely push downwards, on the female's vulval sclerite (Fig. 3-4C). Such support may assist the male in guiding his aedeagus into the bursa complex and additionally offer purchase during insertion and extraction as well as spermatophore transfer. The tiny, leaf-like posterior-oriented projections observed all over the exterior of the dorsal valves (Fig. 3-9A,D,E) were seemingly observed for only the second time in at least Acridoidea and the first in Acrididae, despite Eades (2000) commenting that it was yet unknown if such microstructures were confined to the species they were originally found on (*T. eques* in Whitman and Loher, 1984) or if they might be found in other species of Acridomorpha. The probable function of these projections is not entirely clear here, but two possible explanations are as follows: 1) as stimulators for the interior of the female's

bursa copulatrix (Figs. 3-4B, 12B-D,F,G, and 13E-G) as suggested broadly by Eberhard (1985) and/or 2) as friction-structures for improved gripping while inserted into the bursa copulatrix as suggested for *T. eques* by Whitman and Loher (1984).

The only functions of the ventral valves (Figs. 3-4A, 6F,G, 7B-E, 8B-E, 9B, and 10E) hypothesized at this time for this species are assisting in the shaping and guiding of the spermatophore (Figs. 3-4A and 6H-J). As the semi-gelatinous spermatophore is exuded through the phallotreme during copulation it appears to mostly rest between the ventral valves, eventually passing further through them dorsally nearer to their apex, emerging beyond both sets of valves, and then into the apical remainder of the bursa copulatrix (Fig. 3-4C). The ventral valves of aedeagus, it should be noted, are quite soft and flexible compared to the much more rigid, and seemingly inflexible, dorsal valves, so it would make sense if the primary, if not only, probable functions of the ventral valves for this species are spermatophore shaping and guidance. Interestingly, in *T. eques*, the dorsal valves only possess transverse ridges while it is the ventral valves that have their exterior covered in microstructures that are described as backward-pointing spines. These spines serve multiple functions during copulation in *T. eques*, including anchoring the aedeagus to the basal region of the female's spermathecal duct (a bursa copulatrix is not present) and assisting in the removal of empty spermatophores, so that more can be transferred during a single copulation session (Whitman and Loher, 1984). In contrast, in *M. rotundipennis*, it is the dorsal valves that contain the microstructures, which are far from being spines (we have described them as "leaf-like projections") and are not as densely-packed. Furthermore, it is doubtful that these microstructures could

assist in spermatophore removal because the dorsal valves are fused for almost their entire length as opposed to the independently-articulating structures in *T. eques*. Finally, the ventral valves appear to lack any sort of ridges and only seem to be rugose (Fig. 3-9C), but, so far, only the apical third have been examined using SEM.

As a whole, the phallic complex is consistent in size and shape across the geographic range of the species. Slight differences do exist, though, particularly in the lophi of epiphallus (Figs. 3-4A, 6B,C, 7F,G) and apodemes of cingulum (Figs. 3-4A, 6D,E, 7B,C,E, and 9A) (Squitier et al., 1998; pers. observ.). Such differences in grasshoppers may be unique to an individual (pers. observ.), population-specific (e.g. in *Schistocerca lineata* Scudder, 1899 (Acrididae) (Song and Wenzel, 2008)), or even simply developmental in nature (e.g. in *S. americana* (Drury, 1770) (Song, 2004)).

Female: External and Internal Genitalia, and Other Parts of the Reproductive System

External: The only named external components that we observed that appear to be involved in copulation are the subgenital plate (Figs. 3-4B and 11B-H), its lophi receptacles (Fig. 3-11E-H), and, possibly, the attached egg guide (Figs. 3-4B and 11D-H) (its primary function appearing to be to guide an emerging egg upwards into the intervalvular space (Snodgrass, 1935)). The subgenital plate and its egg guide, in their normal state of repose, block entry to the vulva, which is centered just beneath the base of the ventral valves of ovipositor (Figs. 3-11A-D and 12A,B). The egg guide, at rest, passes dorsally between the ventral valves (Fig. 3-11D). When the male's ancorae (Figs.

3-4A, 6B,C, and 7F,G) pull the apical third of the female's subgenital plate and egg guide downwards into his genital chamber, her vulva is exposed through which the male is able to insert his aedeagus into the female's bursa complex (Fig. 3-4C). The lophi receptacles then receive at least one lophus from the male's epiphallus per copulation event (in this case, the right lophus: Fig. 3-10B), which most likely acts as a friction anchor to keep the subgenital plate and egg guide from being retracted and, thus, close the vulva. Note again that the heavier sclerotization of the apical third of the subgenital plate (Fig. 3-11G,H) is also the portion that is bent downwards at an approximately 90° angle (Figs. 3-4B and 11E,F). The fact that a bend takes place where the sclerotization level lessens is structurally logical, but also because the entire subgenital plate is quite long and would not fit into the male's genital chamber anyway.

In the 3D reconstructions, the egg guide, which is apparently highly flexible, can be seen being bent upwards and to the left near its middle (Fig. 3-10A,B). However, what the egg guide is pushing against is not shown and was not clearly observed, but, based on its position, just anterior to the male's apodemes of cingulum (Fig. 3-4C), it can be inferred to be the muscles that surround the ectophallus and endophallus of the male's phallic complex. The position of the egg guide gives rise to three possibilities: 1) that it is simply random chance, 2) the egg guide provides some level of support for the male to push against because the subgenital plate is essentially hollow, or 3) a mixture of both meaning that the position can change, but the egg guide could still be utilized by the male for support.

Internal: The only named internal components that we observed that appear to be involved in copulation are the genital chamber, bursa complex (Fig. 3-13A,E), and vulval sclerite (Figs. 3-4B, 12A-E,G,H, and 13B-E). The genital chamber, other than containing the internal genitalia and other parts of the greater reproductive system, seemingly plays only a single, but important, role in copulation: without the subgenital plate being pulled downwards by the male, thereby essentially widening the genital chamber dorsoventrally, he would not be able to access the vulva and begin the copulation process. Collectively, the bursa complex receives the male's aedeagus (Figs. 3-4A, 7B,C, and 9A) and spermatophore (Fig. 3-4A and 6H-J), although neither directly contact the armor of bursa copulatrix (Figs. 3-4B, 12B-D,F,G, and 13E-G). The ribbing of the armor (Fig. 3-12D,G) probably serve one to two functions, the first being reinforcement to strengthen the bursa copulatrix (Figs. 3-4B, 12B-D,F,G, and 13E-G) from either strong movements of the aedeagus during insertion and extraction as well as spermatophore transfer, or contact with the leaf-like projections that cover the male's dorsal valves of aedeagus (Fig. 3-9A,D,E). The second possible function could be expansion in that the ribs may allow for the flexible membrane-like portions between them to stretch, akin to an accordion, in order for the bursa copulatrix to better accommodate aedeagi, perhaps of varying sizes, and their movements (and possibly even those of the spermatophore).

The bursa copulatrix (Figs. 3-4B, 12B-D,F,G, and 13E-G) appears to function as the primary receptacle for the male's aedeagus (Figs. 3-4A, 7B,C, and 9A) and may be lined with nerve endings for the possible purpose of stimulation (Eberhard, 1985) by the

leaf-like projections on the aedeagus (Fig. 3-9A,D,E). Another possibility is that the bursa copulatrix is lined with rough material, possibly the aforementioned light sclerotization (Fig. 3-12F), that the male is able to grip onto via friction. The bulbous apex appears to be able to shift in size (Fig. 3-12B) and may do so to accommodate the increase in size of the apex of the male's spermatophore (Fig. 3-4A,B and 6I,J) as semen is continually added from the spermatophore's reservoir into its tube region (Fig. 3-4A and 6H-J). Presumably, the apex of the bursa copulatrix continues to expand until the spermatophore's apex ruptures (Fig. 3-6H), most likely sending semen into the spermathecal duct (Fig. 3-4B, 12A, and 13H,I) through the spermathecal aperture where the sperm would make their way towards the spermathecae (preapical and apical diverticula) (Figs. 3-4B, 12A, and 13H,I). In addition to the observations of the 3D reconstructions, this hypothesis is based on evidence from previous studies on other species, two also belonging to *Melanoplus*, in which a spermatophore (and in the non-*Melanoplus* species, the aedeagus) was introduced directly into the female's spermathecal duct where it ruptured either further in or at the first narrow U-shaped bend, a structurally-limiting situation similar to what we have observed in *M. rotundipennis* (Kyl, 1938; Gregory, 1965; Pickford and Gillott, 1971; Whitman and Loher, 1984; Lay et al., 1999). The muscle tissue of spermathecal complex (partially seen in Figs. 3-12A and 13H) is presumably responsible for moving the sperm back towards the eggs for the purpose of fertilization (Snodgrass, 1993). The vulval sclerite (Figs. 3-4B, 12A-E,G,H, and 13B-E) may be an uncommon component in grasshopper genitalia because it has only seemingly been identified once previously in a distantly-

related genus, *Praxibulus* Bolívar, 1906 ("dorsal sclerite of bursa copulatrix" in Key, 1989), and is only found in a few other PG species. In addition to seemingly serving as reinforcement to the entrance to the bursa copulatrix and as the connector between the latter and the vulva, this sclerite possibly also functions as a support plate for the male's aedeagus to slide along and push against during insertion and extraction as well as spermatophore transfer.

On the whole, the 3D reconstructions of all components of both sexes reflect the results gained using DSLR and SEM imaging methods with one difference for an internal female component: the "tail" of the bursa complex (so-called here because of its overall resemblance to a scorpion's tail as noted earlier) is bent ventrally at rest (e.g. Fig. 3-12B), but is bent dorsally when the aedeagus has been inserted and the spermatophore is being transferred (e.g. Fig. 3-4C). We know the entire bursa complex has not been rotated for two reasons: 1) the vulval sclerite (e.g. Figs. 3-12B and 13E) is oriented correctly and 2) the membranes anchoring the base of the bursa complex to the body (Fig. 3-12A) would not allow for full rotation, anyway. Before the 3D reconstructions were completed, it seemed apparent that the length and curvature of the aedeagus had evolved to fit better into the similarly long and curved bursa complex (the fact that it naturally bends left or right may not be a factor since it appears to be flexible: Fig. 3-12B). In fact, similarly-matched structures between the sexes also appear to exist in many of the PG species dissected and examined, but all of these situations require much further investigation. The final 3D reconstructions of *M. rotundipennis*, though, while not necessarily disputing the idea of corresponding genital structures, do complicate

matters. This is because it appears that even if the “tail” of the bursa complex was bent in the resting ventral position the aedeagus would barely curve into it anyway since almost the entirety of its length has already been inserted (Fig. 3-4C). The spermatophore, in the 3D reconstructions, is the structure that moves the rest of the way through the bursa complex and into the apex of the bursa copulatrix (Fig. 3-4C); it seems possible the spermatophore would do this regardless of “tail” orientation since it is essentially a tube being pushed through a slightly-larger tube. Therefore, a reason for the ventroposteriorly-curving nature of the complex is still unclear, but because at least population-level variation is known to exist (Squitier et al., 1998), it is plausible that variation in the length of aedeagi also exists. Another possible reason for the length of the bursa complex is to simply give the spermatophore more room to enter since it does not seem that the spermatophore would be able to move beyond the spermathecal aperture once its apex becomes engorged with semen.

As for why the 3D reconstructions and the other imaging methods differ, we offer two plausible explanations: 1) the freezing method used to capture copulation also caused the “tail” and spermatophore to shift. We know this occurred with the female’s valves of ovipositor (Fig. 3-11B) because the dorsoventral widening observed here (Fig. 3-1A-D) occurs on all female specimens frozen at -80°C. Normally, based on multiple observations of lab populations, the valves are kept in a “closed” state during copulation and such forced widening may also have affected musculature. This may also have shifted other linked components, though nothing other than the “tail” was noticed. 2) Pressure from the inserted aedeagus and/or the extruding spermatophore may have

shifted the “tail’s” position, meaning that the movement of this component is entirely natural. Clearly, as with many other discussed items, this situation warrants further investigation.

Conclusions

Foremost, a probable function(s) was able to be assigned to 45 (32 male, 13 female) of the 58 named genital and other reproductive system components involved in copulation in *M. rotundipennis*. Additionally, this study was the first to identify and describe some components in detail for both sexes (present in at least this species and some of the PG, if not in other species of Acrididae). Perhaps most importantly, many external and internal interactions of male and female components in a physical framework of copulation were observed and imaged for the first time in detail with the assistance of micro-CT. More specifically, an incredible amount of detail and information was gained about the morphology and probable function of the female genitalia and other reproductive system components of this species, both at rest and during copulation. These findings most likely apply to other PG species and, possibly, other acridids (at least).

Based on the imaging evidence included here, we think that the correlative microscopy approach combining DSLR, SEM, and micro-CT imaging was of immense value (especially micro-CT). We also suggest that correlative microscopy was more effective for gathering detailed information on probable functions compared to previous studies that also examined grasshopper morphology in-depth, but which only used

illustrations, one to two types of imaging, or a combination of both methods. However, we are aware that each type of imaging has its strengths (such as powerful magnification, high resolution, greater detail, and event-capturing 3D reconstructions) and weaknesses (such as training, cost, and time) with each offering unique perspectives. One weakness with micro-CT that may not be immediately obvious is the fact that reconstructing components in 3D to the extent shown here takes many months of painstaking work and an intimate knowledge of the subject(s) (in addition to the DSLR and SEM images, we were guided strongly by examining museum specimens with a microscope). A second weakness is that time constraints can sacrifice fine detail in some cases: e.g. compare the DSLR (Fig. 3-12D) and SEM (Fig. 3-12G) images of the armor of bursa copulatrix with the 3D reconstruction (Fig. 3-13A) and note the overall coarseness and loss of the ribs and in-between membrane-like portions. The 3D reconstruction could be made to look more like the non-3D images, but at the expense of large blocks of time, and the correlative microscopy approach already tells a comprehensive story.

Future Directions

While it is undeniably clear that many of the reproductive system components (especially genital ones) of grasshoppers perform integral functions during copulation, many still require further investigation. Specifically, micro-CT should be employed to examine more *M. rotundipennis* and/or other PG species at different times of the copulation process to further validate current ideas and add resolution to unresolved

issues, such as whether or not the re-orientation of the "tail" of the bursa complex observed in the 3D reconstructions is natural or a result of investigatory methods. More copulating *M. rotundipennis* specimens should also be combined with micro-CT to investigate whether or not invaginations truly exist on the female's abdomen for the male's cerci to push into and to clarify the functional role cerci play during copulation. In fact, the latter should be investigated further with comparisons between species because cerci shape widely varies. Additionally for *M. rotundipennis*, SEM and TEM should be utilized for multiple inquiries: both to determine if the setae that cover the cerci are functional sensilla, SEM to examine the lophi receptacles of the female's subgenital plate for the presence of microstructures that should correspond to similar structures on the male's lophi, and TEM to explore the potential function of the three sensory receptors found in the male. SEM and TEM might also be good tools to explore the interior of the female's bursa copulatrix in search of nerve endings and/or rough regions that the leaf-like projections on the male's aedeagus might be stimulating or rubbing against. Moreover, further SEM investigations (at higher magnifications) into the possibility of the presence of sensory receptors on male furculae in *M. rotundipennis* and other related species are needed to elucidate their role, if any, during copulation. SEM should also be used to examine the entirety of the ventral valves of males for the presence of microstructures, and both sets of valves of more grasshoppers, in general, should be examined for the presence of microstructures as previously suggested by Eades (2000). Additionally, the chemical composition of the female's egg guide and male's connective tissue of apodemes of endophallus should be investigated as they are

reminiscent of one another. Finally, further explorations should be undertaken of greater numbers of male and female specimens of PG species in search of further evidence to support possible observed correlations in genital components that might indicate coevolution.

By gaining a better understanding of functional morphology, we can also gain a better understanding of not only the evolution of genitalia, possibly one of the primary drivers of speciation within the PG, but also, by association, sexual selection. We have attempted to discover what occurs on the outside and inside in both sexes of *M. rotundipennis* during copulation via the results of three correlative microscopy methods and, in doing so, we have established a strong foundation on which to construct further in-depth studies similar to this one, particularly examining Melanoplinae species. The applications for correlative microscopy, especially micro-CT technology, are myriad and, in particular, it is enabling greater exploration of the genital frontier of functional morphology.

CHAPTER IV

INVESTIGATING THE EVOLUTION OF MALE GENITALIA OF XEROPHILIC FLIGHTLESS GRASSHOPPERS IN A PHYLOGENETIC FRAMEWORK

Introduction

One of the most widespread morphological patterns among animals is that the genitalia of closely related species are often considerably divergent. This is particularly noticeable in the male genitalia of insects, especially intromittent structures. In order to explain this intriguing pattern of genital divergence, sexual selection has been invoked as its primary evolutionary driver (Eberhard, 1985; Arnqvist et al., 2000; Arnqvist and Rowe, 2002; Hosken and Stockley, 2004; Ritchie, 2007; Song and Bucheli, 2010; Eberhard, 2010a; Eberhard, 2010b; Hotzy et al., 2012; Richmond et al., 2012; Simmons, 2014), which has often been linked to speciation because reproductive isolation is inferred from such divergences (West-Eberhard, 1983; Coyne and Orr, 2004; Ritchie, 2007; McPeek et al., 2008; Kraaijeveld et al., 2011; Barnard et al., 2017). These observations of highly divergent, species-specific genitalia have thus inspired the idea that the evolution of male genitalia is rapid in relative comparison to non-genital components within a given evolutionary time scale (Eberhard, 1985; Eberhard, 1996; Hosken and Stockley, 2004; Eberhard, 2009; Eberhard, 2010a; Eberhard, 2010b; Song and Bucheli, 2010; Rowe and arnqvist, 2011; Simmons, 2014). There is at least some

quantitative evidence to support the idea of rapid genital evolution (e.g., Arnqvist, 1998; Mutanen and Kaitala, 2006; Marquez and Knowles, 2007; Rowe and arnqvist, 2011). Simmons (2014) and Bond et al. (2003), though, have called for further studies to provide additional quantitative support for the continued claim of such rapidity by examining multiple lines of evidence, such as relative evolutionary rates and phylogenetic comparisons of genital morphology.

Compounding this issue is the fact that the genitalia of arthropods (especially insects) are often relatively complex, especially in males, in terms of the number of components involved in copulation and reproduction (Eberhard, 1985; Arnqvist, 1997; Eberhard, 2010b; Rowe and Arnqvist, 2011; Simmons, 2014; Frazee and Masly, 2015; Bennik et al., 2016). As an example, a recent study on the flightless grasshopper species *Melanoplus rotundipennis* (Scudder, 1878) (belonging to the Puer Group of the southeastern U.S.A.) determined that 45 of the 58 (32 male, 13 female) known reproductive system components (the majority genitalia) were involved in copulation alone (Woller and Song, 2017). Ascribing functions to genital morphology is often difficult without a physical framework of copulation to examine, something that can be tricky to create adequately and naturally, so such studies on insects have been relatively few and far between (e.g. Eberhard and Ramirez, 2004; Briceño and Eberhard, 2009; Briceño et al., 2016), although the increasing use of micro-CT has enabled greater advances in this arena (e.g. Dougherty et al., 2015; Wulff et al. 2015; Woller and Song, 2017). Several of these studies have also demonstrated that individual genital components play different roles during copulation, such as female-stimulation and

clasping, sperm transfer, and receptacles for male anatomy, suggesting they may potentially evolve at different rates because these functionally different components might be under different selective pressures (Marquez and Knowles, 2007; Song and Wenzel, 2008; Song and Bucheli, 2010; Rowe and Arnqvist, 2011; Simmons, 2014).

Woller and Song's (2017) investigative study with *M. rotundipennis* strongly pointed to these ideas (see Ch. III) (at least in *Melanoplus* grasshoppers related to the species due to shared morphology, like those in the Puer Group) because of the unique roles that the many genital components in both sexes play during copulation. For example, based on our findings (and the associated evidence of other studies whose findings we built upon), the internal aedeagus and its closely associated components (herein referred to as the aedeagal region, which includes the dorsal and ventral valves of aedeagus, arch of aedeagus, and sheath of aedeagus) appear to play the most significant role in copulation. This is because the aedeagal region (a collection of intromittent structures) not only stimulates the female before and during the copulatory process, but is also responsible for the direct transfer of the spermatophore to the female. Other internal genital components of note, such as the epiphallus (and its largest subcomponents, the lophi) and the ectophallus play indirect roles in spermatophore transfer by allowing a male to gain access to the female's internal genitalia by pulling down her subgenital plate to expose the vulva (epiphallus, in general), pinning down the subgenital plate during copulation (lophi specifically), and acting as general structural support for the entire phallic complex, especially in terms of being muscle attachment site. The cerci, in contrast, are a paired set of external genital components that are very

prominent and serve as taxonomically important species-identifiers in many cases. Yet, during copulation, they only appeared to act as general supports for the female's subgenital plate, and, seemingly, not directly in species recognition as might be expected, but further studies are needed. These five genital components are the focus of the quantitative assessments undertaken for this study. We also included a non-genital character, the tegmen (forewing), as a baseline comparison because, under the sexual selection hypothesis, differences in tegmen divergence should be relatively minor compared to those in the genitalia if the evolution of genitalia is rapid.

Furthermore, there is a pressing need to examine genital evolution and sexual selection in the context of a robust phylogeny because the findings would potentially provide explicit evidence for sexual selection's role in speciation and its relative rate of genital divergence. Such a study would also aid in more deeply investigating the two most widely accepted underlying mechanisms of sexual selection that would explain rapid divergence in genitalia: **1)** cryptic female choice (Eberhard, 1985; Eberhard, 1996; Arnqvist, 1997; Edvardsson and Arnqvist, 2000; Miller, 2003; Eberhard, 2004a; Bergsten and Miller, 2008; Briceno and Eberhard, 2009; Eberhard, 2009; Eberhard, 2010a; Eberhard, 2010b; Ah-King, 2014; Simmons, 2014) and **2)** sexually antagonistic coevolution (Parker, 1979; Arnqvist, 1997; Arnqvist et al., 2000; Arnqvist and Rowe, 2002; Chapman et al., 2003; Eberhard, 2004a; Eberhard, 2004b; Arnqvist and Rowe, 2005; Eberhard, 2009; Eberhard, 2010a; Eberhard, 2010b; Rowe and Arnqvist, 2011; Ah-King, 2014; Gavrilets, 2014; Simmons, 2014). The phylogenetic study of genital evolution is still rare with only a handful of studies to date explicitly focused on

quantifying the difference in the shape of arthropod genitalia in a phylogenetic framework through the aid of geometric morphometrics (Bond et al., 2003; Rönn et al., 2007; McPeek et al., 2008; Rowe and Arnqvist, 2011; Wojcieszek and Simmons, 2011). The reasons for this are most likely several when trying to identify a group of insects to investigate in this context: **1)** genitalia (of one or both sexes) should be obviously divergent across species; **2)** species should be closely related and ideally include relatively speciose clades and more sparse clades to better examine the tempo of genital evolution; **3)** estimated relative divergence times of species need to be known (using fossils and/or geologic features); **4)** the younger the group, the better in order to more easily rule out the possibility of complicating patterns caused by extinct species; and **5)** the probable functions of genital components during copulation should be known in order to gain a deeper understanding of their evolutionary role, particularly useful when interpreting and calculating relative rates of evolution.

The robustly monophyletic Puer Group *sensu lato* (s.l.) (PG) (see Ch. II and Table 1) fits these five criteria well and comprises 27 *Melanoplus* Stål, 1873 (Orthoptera: Acrididae: Melanoplinae*)* grasshopper species that are small and brachypterous, and distributed throughout the southeastern U.S. (here defined as Alabama, North and South Carolina, Georgia, and Florida), primarily in peninsular Florida (Figs. 4-1 and 4-2). Among grasshopper genera, *Melanoplus*, in general, is known to have some of the most extreme and divergent species-specific male genitalia and the PG exhibits this remarkably well, particularly their aedeagi, which are one of the primary characters that

Table 4-1. Taxonomic information, list of the anatomical components included in the geometric morphometrics analyses, and locality data for individual specimens included in this study belonging to the 27 species of the Puer Group. Specimens are organized by Modern Major Lineage and then in alpha order by specific name. "Spec." = Specimen.

Species (Sp.)	# of Spec./Sp.	Modern Major Lineage	Historical s.s. Group	Cercus (n = 265)	Ectophallus (n = 265)	Epiphallus (n = 266)	Lophus (n = 266)	Aedegal Region (n = 262)	Tegmen (n = 265)	Locality Data (GPS coordinates are in WGS84 format by latitude,longitude)
M. gurneyi Strohecker, 1960	1	A	Forcipatus Group	Included	Included	Included	Included	Included	Included	FL: Bay Co., about 2.5 mi. W. of intersection of Hwys. 20 and 231, in vacant lots along N and S sides of Hwy. 20, [30.436323,-85.475283], 2-X-2014, Field #PG161-1-A, coll. D.A. Woller & K. Woller, disturbed scrubby habitats
M. gurneyi Strohecker, 1960	2	A	Forcipatus Group	Included	Included	Included	Included	Included	Included	FL: Escambia Co., Big Lagoon SP, on W side of main park road (Bauer Rd.), [30.316064,-87.409317], 19-IX-2016, Field #PG216-1-A, coll. D.A. Woller, scrubby area with scrubby oaks, dense gopher apple patch, some scrub rosemary, and scattered pines (sand?)
M. gurneyi Strohecker, 1960	3	A	Forcipatus Group	Included	Included	Included	Included	Included	Included	FL: Okaloosa Co., Henderson Beach SP, along NE side of Nature Trail, [30.385330,-86.448392], 19-IX-2016, Field #PG218-1-B, coll. D.A. Woller, resembles scrub rosemary bald with dunes, many dense scrubby oak patches, and scattered gopher apple
M. gurneyi Strohecker, 1960	4	A	Forcipatus Group	Included	Included	Included	Included	Included	Included	FL: Walton Co., Topsail Hill Preserve SP, on dunes with Gulf of Mexico in view, [30.360377,-86.280157], 19-IX-2016, Field #PG219-1-D, coll. D.A. Woller, beach dunes with scattered gopher apple patches, occasional scrub rosemary, and some scrubby oak patches
M. gurneyi Strohecker, 1960	5	A	Forcipatus Group	Included	Included (R)	Included (R)	Included (R)	Included (R)	Included	FL: Walton Co., Grayton Beach SP, SE edge of park a ways down trail attached to beach parking lot, near Gulf of Mexico, [30.323698,-86.150695], 20-IX-2016, Field #PG220-1-A, coll. D.A. Woller, beach dunes with scattered, large clumps of scrubby oaks at apices, often surrounded by gopher apple patches, and some saw palmetto clumps
M. gurneyi Strohecker, 1960	6	A	Forcipatus Group	Included	Included	Included	Included	Included	Included	FL: Walton Co., Deer Lake SP, off E side of main boardwalk, Gulf of Mexico just to S, [30.300000,-86.077222], 20-IX-2016, Field #PG221-1-A, coll. D.A. Woller, beach dunes with scattered, large clumps of scrubby oaks at apices and along side, often surrounded by gopher apple patches, scattered scrub rosemary and magnolias also present
M. gurneyi Strohecker, 1960	7	A	Forcipatus Group	Included	Included	Included	Included	Included	Included	FL: Bay Co., St. Andrews SP, off NE side of beach parking lot, Gulf of Mexico just to SW, [30.132211,-85.741195], 20-IX-2016, Field #PG224-1-A, coll. D.A. Woller, short beach dunes covered with much vegetation, including a lot of young scrub rosemary, scattered scrubby oaks, and many lichens, but no gopher apple

Table 4-1 Continued.

Species (Sp.)	# of Spec./Sp.	Modern Major Lineage	Historical s.s. Group	Cercus (n = 265)	Ectophallus (n = 265)	Epiphallus (n = 266)	Lophus (n = 266)	Aedegal Region (n = 262)	Tegmen (n = 265)	Locality Data (GPS coordinates are in WGS84 format by latitude,longitude)
M. gurneyi Strohecker, 1960	8	A	Forcipatus Group	Included	Included	Included	Included	Included	Included	FL: Bay Co., Camp Helen SP, not too far down Oak Canopy Trail on S side across from service road entrance, [30.271863,-85.992725], 20-IX-2016, Field #PG223-1-A, coll. D.A. Woller, resembles mesic oak hammock with very dense canopy and lots of scattered scrubby oaks
M. gurneyi Strohecker, 1960	9	A	Forcipatus Group	Included	Included	Included	Included	Included	Included	FL: Bay Co., Panama City, 5-Nov-1938, coll. T. H. Hubbell, Field #1
M. gurneyi Strohecker, 1960	10	A	Forcipatus Group	Included	Included	Included	Included	Included	Included	FL: Santa Rosa Co., Santa Rosa I., 5-6-Nov-1938, coll. T. H. Hubbell, Field #1
M. apalachicolae Hubbell, 1932	1	B	Forcipatus Group	Included	Included (R)	Included	Included	Included (R)	Included	FL: Liberty Co., less than 1/4 mi. from SE edge of Torreya State Park, off W side of NW Torreya Park Rd., [30.551949,-84.945577], 2-X-2014, Field #PG163-1-A, coll. D.A. Woller & K. Woller, oak-pine forest w/scrubby oaks and gopher apple patches
M. apalachicolae Hubbell, 1932	2	B	Forcipatus Group	Included	Included	Included	Included	Included	Included	FL: Liberty Co., Camp Torreya, 29-Jul-1925, coll. T.H. Hubbell, Field #64
M. apalachicolae Hubbell, 1932	3	B	Forcipatus Group	Included	Included	Included	Included	Included	Included	FL: Liberty Co., Camp Torreya, 29-Jul-1925, coll. T.H. Hubbell, Field #64
M. apalachicolae Hubbell, 1932	4	B	Forcipatus Group	Included	Included	Included	Included	Included	Included	FL: Liberty Co., Camp Torreya, 30-Jul-1925, coll. T.H. Hubbell, Field #66
M. apalachicolae Hubbell, 1932	5	B	Forcipatus Group	Included	Included	Included	Included	Included	Included	FL: Liberty Co., Camp Torreya, 28-Jul-1925, coll. T.H. Hubbell, Field #58
M. apalachicolae Hubbell, 1932	6	B	Forcipatus Group	Included	Included	Included	Included	Included	Included	FL: Liberty Co., Camp Torreya, 29-Jul-1925, coll. T.H. Hubbell, Field #59
M. apalachicolae Hubbell, 1932	7	B	Forcipatus Group	Included	Included	Included	Included	Included	Included	FL: Liberty Co., Camp Torreya, 29-Oct-1925, coll. T.H. Hubbell, Field #82
M. apalachicolae Hubbell, 1932	8	B	Forcipatus Group	Included	Included	Included	Included	Included	Included	FL: Liberty Co., Alum Bluff, 1-Nov-1931, coll. T.H. Hubbell, Field #94
M. apalachicolae Hubbell, 1932	9	B	Forcipatus Group	Included	Included	Included	Included	Included	Included	FL: Liberty Co., 20-Aug-1941
M. apalachicolae Hubbell, 1932	10	B	Forcipatus Group	Included	Included	Included	Included	Included	Included	FL: Liberty Co., Torreya State Park, 27-Sep-1946
M. foxi Hebard, 1923	1	B	Strumosus Group	Included	Included	Included	Included	Included	Included	GA: Seminole Co., Seminole State Park, far W side of park just SE of intersection of SR 39 and Hwy 253, [30.803703,-84.885235], 13-V-2015, Field #PG191-2-A, coll. D.A. Woller & J.G. Hill, somewhat overgrown sandhills
M. foxi Hebard, 1923	2	B	Strumosus Group	Included	Included	Included	Included	Included	Included	GA: Bibb Co., Macon, 3-I-1937
M. foxi Hebard, 1923	3	B	Strumosus Group	Included	Included	Included	Included	Included	Included	GA: Seminole Co., Dry Oakland. dist 21, lot 171, 13-Jun-1953, coll. T.H. Hubbell, Field #74
M. foxi Hebard, 1923	4	B	Strumosus Group	Included	Included	Included	Included	Included	Included	GA: Seminole Co., Dry Oakland. dist 21, lot 171, 13-Jun-1953, coll. T.H. Hubbell, Field #74

Table 4-1 Continued.

Species (Sp.)	# of Spec./Sp.	Modern Major Lineage	Historical s.s. Group	Cercus (n = 265)	Ectophallus (n = 265)	Epiphallus (n = 266)	Lophus (n = 266)	Aedegal Region (n = 262)	Tegmen (n = 265)	Locality Data (GPS coordinates are in WGS84 format by latitude,longitude)
M. foxi Hebard, 1923	5	B	Strumosus Group	Included	Included	Included	Included	Included	Included	GA: Seminole Co., High Pine, Dist 21, Lot 143, 13-Jun-1953, coll. T.H. Hubbell, Field #70
M. foxi Hebard, 1923	6	B	Strumosus Group	Included	Included	Included	Included	Included	Included	GA: Wheeler Co., 4.5 mi. S Dodge Co. Line, on US Hwy 441, 19-Jun-1953, coll. T. H. Hubbell, Field #83
M. foxi Hebard, 1923	7	B	Strumosus Group	Included	Included	Included	Included	Included	Included	GA: Seminole Co., Dist 21, Lot 211, 5.3 mi. SW Reynoldsville, 16-Jun-1956, coll. T. J. Cohn & P.B. Kannowski, Field #14
M. foxi Hebard, 1923	8	B	Strumosus Group	Included	Included	Included	Included	Included	Included	GA: Seminole Co., Dist 21, Lot 211, 5.3 mi. SW Reynoldsville, 15-Jun-1956, coll. T. J. Cohn & P.B. Kannowski, Field #13
M. foxi Hebard, 1923	9	B	Strumosus Group	Included	Included	Included	Included	Included	Included	GA: Seminole Co., Dist. 21, Lot 172, 10-Jun-1953, coll. T. H. Hubbell, Field #57
M. foxi Hebard, 1923	10	B	Strumosus Group	Included	Included	Included	Included	Included	Included	GA: Seminole Co., Dist 21, Lot 172, 13-Jun-1953, coll. T. H. Hubbell, Field #71
M. mirus Rehn & Hebard, 1916	1	B	Scapularis Group	Included	Included	Included	Included	Included	Included	SC: Chesterfield Co., Carolina Sandhills NWR, [34.558056,-80.186667], 12-Jul-2013, coll. J.G. Hill, Fall Line sandhill
M. mirus Rehn & Hebard, 1916	2	B	Scapularis Group	Included	Included	Included	Included	Included	Included	SC: Chesterfield Co., Carolina Sandhills NWR, [34.558056,-80.186667], 12-Jul-2013, coll. J.G. Hill, , Fall Line sandhill
M. mirus Rehn & Hebard, 1916	3	B	Scapularis Group	Included	Included	Included	Included	Included	Included	SC: Chesterfield Co., Carolina Sandhills NWR, [34.558056,-80.186667], 12-Jul-2013, coll. J.G. Hill, , Fall Line sandhill
M. mirus Rehn & Hebard, 1916	4	B	Scapularis Group	Included	Included	Included	Included	Included	Included	NC: Halifax Co., Weldon, 24-VII-1913, coll. R. and H.
M. mirus Rehn & Hebard, 1916	5	B	Scapularis Group	Included	Included	Included	Included	Included	Included	NC: Bladen Co., Jones Lake S.P., [34.701393,-78.621362], 13-Aug-2009, coll. J.G. Hill, xeric sand scrub
M. mirus Rehn & Hebard, 1916	6	B	Scapularis Group	**No**	Included	Included	Included	Included	**No**	NC: Caldwell Co., Pilot Mtn., 19-Jul-1931, coll. B.B. Fulton
M. pygmaeus Davis, 1915	1	B	Rotundipennis Group	Included	Included	Included	Included	Included	Included	FL: Escambia Co., Big Lagoon SP, along S side of main park road (Bauer Rd.) near Big Lagoon, [30.310790,-87.412203], 19-IX-2016, Field #PG216-1-B, coll. D.A. Woller, resembles overgrown flatwoods with short scrubby oaks, scattered pines (longleaf?), and near-by gopher apple patch
M. pygmaeus Davis, 1915	2	B	Rotundipennis Group	Included	Included	Included	Included	Included	Included	FL: Okaloosa Co., Henderson Beach SP, just W of Eglin AFB fenced area on W side of Nature Trail entrance, close to Gulf of Mexico, [30.384690,-86.448242], 19-IX-2016, Field #PG218-1-A, coll. D.A. Woller, unusual habitat: dominated by sandy/vegetated dunes with a short Magnolia, scruby oaks, and some gopher apple patches
M. pygmaeus Davis, 1915	3	B	Rotundipennis Group	Included	Included	Included	Included	Included	Included	FL: Walton Co., Topsail Hill Preserve SP, on S side of paved road, not far from nature trail entrance, [30.367096,-86.280002], 19-IX-2016, Field #PG219-1-B, coll. D.A. Woller, unusual mix of scattered sand pines and saw palmetto, some gopher apple, and scrubby oak patches
M. pygmaeus Davis, 1915	4	B	Rotundipennis Group	Included	Included	Included	Included	Included	Included	FL: Walton Co., Grayton Beach SP, just NE of campground spot #48, with a slough just to the E, [30.330963,-86.154350], 20-IX-2016, Field #PG220-1-B, coll. D.A. Woller, resembles overgrown sandhills

Table 4-1 Continued.

Species (Sp.)	# of Spec./Sp.	Modern Major Lineage	Historical s.s. Group	Cercus (n = 265)	Ectophallus (n = 265)	Epiphallus (n = 266)	Lophus (n = 266)	Aedegal Region (n = 262)	Tegmen (n = 265)	Locality Data (GPS coordinates are in WGS84 format by latitude,longitude)
M. pygmaeus Davis, 1915	5	B	Rotundipennis Group	Included	Included	Included	Included	Included	Included	AL: Baldwin Co., Gulf State Park, [30.271389,-87.654722], 4-Oct-2013, coll. J.G. Hill, edge of maritime forest
M. pygmaeus Davis, 1915	6	B	Rotundipennis Group	Included	Included	Included	Included	Included	Included	FL: Okaloosa Co., Crestview, 3.3 mi. E of rest stop off I-1-W, 17-II-2000, coll. T.C. & M.J. Justice
M. pygmaeus Davis, 1915	7	B	Rotundipennis Group	Included	Included	Included	Included	Included	Included	FL: Walton Co., 5 mi. NE DeFuniak Springs, 14-Nov-1938, coll. I. J. Cantrall, Field #12
M. pygmaeus Davis, 1915	8	B	Rotundipennis Group	Included	Included	Included	Included	Included	Included	FL: Okaloosa Co., Delaco, 11-12-Aug-1935, coll. T.H. and G.G. Hubbell, Field #2
M. pygmaeus Davis, 1915	9	B	Rotundipennis Group	Included	Included	Included	Included	Included	Included	FL: Okaloosa Co., 1.7 mi. E Niceville on Fla. 20, 21-Aug-1951, coll. I. J. Cantrall, Field #35
M. pygmaeus Davis, 1915	10	B	Rotundipennis Group	Included	Included	Included	Included	Included	Included	FL: Okaloosa Co., Niceville, 6-Nov-1939, coll. T.H. Hubbell, Field #2
M. scapularis Rehn & Hebard, 1916	1	B	Scapularis Group	Included	Included	Included	Included	Included	Included	GA: Appling Co., Moody Forest WMA, not far E of intersection of Jake Moody Rd. and East River Rd. along trail just E of old abandoned buildings, [31.906389,-82.311111], 14-V-2015, Field #PG195-1-A, coll. D.A. Woller, disturbed Pinus taeda forest w/fairly dense understory mainly composed of grapevine, blackberry, and various grasses w/some poison ivy
M. scapularis Rehn & Hebard, 1916	2	B	Scapularis Group	Included	Included	Included	Included	Included	Included	GA: Appling Co., Moody Forest WMA, in elevated portion of forest on W side of Jake Moody Rd., just SW of "A", [31.904167,-82.311111], 14-V-2015, Field #PG195-1-B, coll. D.A. Woller, resembles sandhills, but sign calls it "Pinus palustris woodland" - burned recently w/sparse understory of ferns, grasses, wiregrass, smilax, inkberry, etc.
M. scapularis Rehn & Hebard, 1916	3	B	Scapularis Group	Included	Included (R)	Included	Included	Included (R)	Included	FL: Liberty Co., Camp Torreya, 29-Jul-1925, coll. T.H. Hubbell, Field #57
M. scapularis Rehn & Hebard, 1916	4	B	Scapularis Group	Included	Included	Included	Included	Included	Included	FL: Liberty Co., Camp Torreya, 30-Jul-1925, coll. T.H. Hubbell, Field #66
M. scapularis Rehn & Hebard, 1916	5	B	Scapularis Group	Included	Included	Included	Included	Included	Included	FL: Liberty Co., Old Camp Torreya, 4-Sep-1954, coll. T.H. Hubbell and I.J. Cantrall, Field #71
M. scapularis Rehn & Hebard, 1916	6	B	Scapularis Group	Included	Included	Included	Included	Included	Included	FL: Liberty Co., 29-Jul-1925, coll. T.H. Hubbell, Field #57
M. scapularis Rehn & Hebard, 1916	7	B	Scapularis Group	Included	Included	Included	Included	Included	Included	FL: Liberty Co., 29-Jul-1925, coll. T.H. Hubbell, Field #54
M. scapularis Rehn & Hebard, 1916	8	B	Scapularis Group	Included	Included	Included	Included	Included	Included	GA: Coffee Co., 11.2 mi. N Broton, 30-Sep-1945, coll. T.H. Hubbell, Field #1
M. scapularis Rehn & Hebard, 1916	9	B	Scapularis Group	Included	Included	Included	Included	Included	Included	GA: McIntosh Co., 0.9 mi. N Darien, 20-Oct-1947, coll. T.H. Hubbell, Field #2
M. scapularis Rehn & Hebard, 1916	10	B	Scapularis Group	Included	Included	Included	Included	Included	Included	GA: Chatham Co., Sandfly, 13-Jun-1922

Table 4-1 Continued.

Species (Sp.)	# of Spec./Sp.	Modern Major Lineage	Historical s.s. Group	Cercus (n = 265)	Ectophallus (n = 265)	Epiphallus (n = 266)	Lophus (n = 266)	Aedegal Region (n = 262)	Tegmen (n = 265)	Locality Data (GPS coordinates are in WGS84 format by latitude,longitude)
M. stegocercus Rehn & Hebard, 1916	1	B	Scapularis Group	Included	Included	Included	Included	Included	Included	GA: Emanuel Co., Ohoopee Dunes WMA, South Natural Area, not far NW of CR 160, [32.530000,-82.455278], 14-V-2015, Field #PG194-1-A, coll. D.A. Woller & J.G. Hill, resembles sandhills
M. stegocercus Rehn & Hebard, 1916	2	B	Scapularis Group	Included	Included	Included	Included	Included	Included	GA: Emanuel Co., Ohoopee Dunes WMA, South Natural Area, not far NW of CR 160, [32.530000,-82.455278], 14-V-2015, Field #PG194-1-A, coll. D.A. Woller & J.G. Hill, resembles sandhills
M. stegocercus Rehn & Hebard, 1916	3	B	Scapularis Group	Included	Included	Included	Included	Included	Included (R)	GA: Emanuel Co., Ohoopee Dunes WMA, South Natural Area, not far NW of CR 160, [32.530000,-82.455278], 14-V-2015, Field #PG194-1-A, coll. D.A. Woller & J.G. Hill, resembles sandhills
M. stegocercus Rehn & Hebard, 1916	4	B	Scapularis Group	Included	Included	Included	Included	Included	Included (R)	GA: Emanuel Co., Ohoopee Dunes WMA, South Natural Area, not far NW of CR 160, [32.530000,-82.455278], 14-V-2015, Field #PG194-1-A, coll. D.A. Woller & J.G. Hill, resembles sandhills
M. stegocercus Rehn & Hebard, 1916	5	B	Scapularis Group	Included	Included	Included	Included	Included	Included	GA: Chatham Co., Groveland, 21-Sep-1917, coll. R. & H.
M. stegocercus Rehn & Hebard, 1916	6	B	Scapularis Group	Included	Included	Included	Included	Included	Included	GA: Emanuel Co., Swainsboro, 18-Jun-2002, coll. Mark Deyrup, Ohoopee Dunes Natural Area, scrub habitat, Miss. State Cross Competition
M. stegocercus Rehn & Hebard, 1916	7	B	Scapularis Group	Included	Included	Included	Included	Included	Included	GA: Emanuel Co., Swainsboro, 18-Jun-2002, coll. Mark Deyrup, Ohoopee Dunes Natural Area, scrub habitat, Miss. State Cross Competition
M. stegocercus Rehn & Hebard, 1916	8	B	Scapularis Group	Included	Included (R)	Included	Included	Included (R)	Included	GA: Emanuel Co., Swainsboro, 18-Jun-2002, coll. Mark Deyrup, Ohoopee Dunes Natural Area, scrub habitat, Miss. State Cross Competition
M. stegocercus Rehn & Hebard, 1916	9	B	Scapularis Group	Included	Included	Included	Included	Included	Included	GA: Chatham Co., Groveland, 21-I-1917, coll. R&H
M. stegocercus Rehn & Hebard, 1916	10	B	Tequestae Group	Included	Included	Included	Included	Included	Included	GA: Chatham Co., Groveland, 21-I-1917, coll. R&H
M. strumosus Morse, 1904	1	B	Strumosus Group	Included	Included	Included	Included	Included	Included	FL: Bay Co., Econfina Creek Wildlife Management Area, at S end of property just N of Hwy. 20 on E side of trail, [30.427695,-85.567802], 2-X-2014, Field #PG160-1-A, coll. D.A. Woller & K. Woller, reminiscent of sandhills
M. strumosus Morse, 1904	2	B	Strumosus Group	Included	Included	Included	Included	Included	Included	FL: Santa Rosa Co., vacant lot on N. side of Frontera St., just E. of intersection w/Andorra St., behind a Publix grocery store, [30.404722,-86.878611], 6-VI-2015, Field #PG211-1-A, coll. D.A. Woller, overgrown scrubby area w/dense scrubby oak patches and scattered mature and immature Pinus palustris

Table 4-1 Continued.

Species (Sp.)	# of Spec./Sp.	Modern Major Lineage	Historical s.s. Group	Cercus (n = 265)	Ectophallus (n = 265)	Epiphallus (n = 266)	Lophus (n = 266)	Aedegal Region (n = 262)	Tegmen (n = 265)	Locality Data (GPS coordinates are in WGS84 format by latitude,longitude)
M. strumosus Morse, 1904	3	B	Strumosus Group	Included	Included	Included	Included	Included	Included	FL: Walton Co., Point Washington State Forest, just NE of intersection of E Lamb Rd. and Goldsby Rd., [30.391134,-86.295813], 7-VI-2015, Field #PG213-1-A, coll. D.A. Woller, overgrown, dense Pinus palustris flatwoods w/young and mature pines, scattered wiregrass, and dense patches of scrubby oaks and gopher apple
M. strumosus Morse, 1904	4	B	Strumosus Group	Included	Included	Included	Included	Included	Included	FL: Washington Co., 4.2 mi. E of Ebro, [30.440000,-85.803056], 27-Oct-2015, coll. J.G. Hill, roadside sandhill remnant
M. strumosus Morse, 1904	5	B	Strumosus Group	Included	Included	Included	Included	Included	Included	FL: Bay Co., Pine Log State Forest, Crooked Creek Trail, , 14-X-2001, coll. T. Lamb and J.C. Justice
M. strumosus Morse, 1904	6	B	Strumosus Group	Included	Included	Included	Included	Included	Included	FL: Jackson Co., Freeman Road, Off 231 , Near Compass Lake, , 14-X-2001, coll. T. Lamb and J.C. Justice
M. strumosus Morse, 1904	7	B	Strumosus Group	Included	Included	Included	Included	Included	Included	FL: Walton Co., DeFuniak Springs, 5-Jun-1924, coll. T.H. Hubbell, Field #1
M. strumosus Morse, 1904	8	B	Strumosus Group	Included	Included	Included	Included	Included	Included	AL: Calhoun Co., Camp MacClellan, Chocolocco Mt., 13-Jul-1925, coll. H.D. Smith, Field #3
M. strumosus Morse, 1904	9	B	Strumosus Group	Included	Included	Included	Included	Included	Included	FL: Holmes Co., Ponce de Leon, 3-Aug-1925, coll. T.H. Hubbell, Field #1
M. strumosus Morse, 1904	10	B	Strumosus Group	Included	Included	Included	Included	Included	Included	FL: Calhoun Co., Chipola R., 5-Nov-1911, coll. T.H. Hubbell, Field #2
M. tumidicercus Hubbell, 1932	1	B	Scapularis Group	Included	Included	Included	Included	Included	Included	GA: Treutlen Co., 0.5 miles N. of Gillis Springs, just N of intersection of U.S 221/771/56 and an unpaved road - on E side, in elevated natural area between main road and Gillis Spring Rd./12, [32.464314,-82.490058], 19-V-2014, Field #PG139-2-A, coll. D.A. Woller & E. Kosnicki, "island" of habitat w/Pinus clausa forest and dense scrubby undergrowth
M. tumidicercus Hubbell, 1932	2	B	Scapularis Group	Included	Included	Included	Included	Included	Included	GA: Treutlen Co., 0.5 miles N. of Gillis Springs, just N of intersection of U.S 221/771/56 and an unpaved road - on E side, in elevated natural area between main road and Gillis Spring Rd./12, [32.464314,-82.490058], 4-X-2014, Field #PG139-3-A, coll. D.A. Woller & K. Woller, "island" of habitat w/Pinus clausa forest and dense scrubby undergrowth
M. tumidicercus Hubbell, 1932	3	B	Scapularis Group	Included	Included	Included	Included	Included	Included	GA: Treutlen Co., 0.5 miles N. of Gillis Springs, just N of intersection of U.S 221/771/56 and an unpaved road - on E side, in elevated natural area between main road and Gillis Spring Rd./12, [32.464314,-82.490058], 4-X-2014, Field #PG139-3-A, coll. D.A. Woller & K. Woller, "island" of habitat w/Pinus clausa forest and dense scrubby undergrowth

Table 4-1 Continued.

Species (Sp.)	# of Spec./Sp.	Modern Major Lineage	Historical s.s. Group	Cercus (n = 265)	Ectophallus (n = 265)	Epiphallus (n = 266)	Lophus (n = 266)	Aedegal Region (n = 262)	Tegmen (n = 265)	Locality Data (GPS coordinates are in WGS84 format by latitude,longitude)
M. tumidicercus Hubbell, 1932	4	B	Scapularis Group	Included	Included	Included	Included	Included	Included	GA: Treutlen Co., 0.5 miles N. of Gillis Springs, just N of intersection of U.S 221/771/56 and an unpaved road - on E side, in elevated natural area between main road and Gillis Spring Rd./12, [32.464314,-82.490058], 4-X-2014, Field #PG139-3-A, coll. D.A. Woller & K. Woller, "island" of habitat w/Pinus clausa forest and dense scrubby undergrowth
M. tumidicercus Hubbell, 1932	5	B	Scapularis Group	Included	Included	Included	Included	Included	Included	GA: Treutlen Co., 0.5 miles N. of Gillis Springs, just N of intersection of U.S 221/771/56 and an unpaved road - on E side, in elevated natural area between main road and Gillis Spring Rd./12, [32.464314,-82.490058], 4-X-2014, Field #PG139-3-A, coll. D.A. Woller & K. Woller, "island" of habitat w/Pinus clausa forest and dense scrubby undergrowth
M. tumidicercus Hubbell, 1932	6	B	Scapularis Group	Included	Included	Included	Included	Included	Included	GA: Treutlen Co., 0.5 miles N. of Gillis Springs, just N of intersection of U.S 221/771/56 and an unpaved road - on E side, in elevated natural area between main road and Gillis Spring Rd./12, [32.464314,-82.490058], 4-X-2014, Field #PG139-3-A, coll. D.A. Woller & K. Woller, "island" of habitat w/Pinus clausa forest and dense scrubby undergrowth
M. tumidicercus Hubbell, 1932	7	B	Scapularis Group	Included	Included	Included	Included	Included	Included	GA: Treutlen Co., 0.5 miles N. of Gillis Springs, just N of intersection of U.S 221/771/56 and an unpaved road - on E side, in elevated natural area between main road and Gillis Spring Rd./12, [32.464314,-82.490058], 4-X-2014, Field #PG139-3-A, coll. D.A. Woller & K. Woller, "island" of habitat w/Pinus clausa forest and dense scrubby undergrowth
M. tumidicercus Hubbell, 1932	8	B	Scapularis Group	Included	Included	Included	Included	Included	Included	GA: Treutlen Co., 0.5 miles N. of Gillis Springs, just N of intersection of U.S 221/771/56 and an unpaved road - on E side, in elevated natural area between main road and Gillis Spring Rd./12, [32.464314,-82.490058], 4-X-2014, Field #PG139-3-A, coll. D.A. Woller & K. Woller, "island" of habitat w/Pinus clausa forest and dense scrubby undergrowth
M. tumidicercus Hubbell, 1932	9	B	Scapularis Group	Included	Included	Included (R)	Included	Included	Included	GA: Treutlen Co., 0.5 miles N. of Gillis Springs, just N of intersection of U.S 221/771/56 and an unpaved road - on E side, in elevated natural area between main road and Gillis Spring Rd./12, [32.464314,-82.490058], 4-X-2014, Field #PG139-3-A, coll. D.A. Woller & K. Woller, "island" of habitat w/Pinus clausa forest and dense scrubby undergrowth
M. tumidicercus Hubbell, 1932	10	B	Scapularis Group	Included	Included	Included	Included	Included	Included	GA: Treutlen Co., 0.5 miles N. of Gillis Springs, just N of intersection of U.S 221/771/56 and an unpaved road - on E side, in elevated natural area between main road and Gillis Spring Rd./12, [32.464314,-82.490058], 14-V-2015, Field #PG139-4-A, coll. D.A. Woller, "island" of habitat w/Pinus clausa forest and dense scrubby undergrowth

Table 4-1 Continued.

Species (Sp.)	# of Spec./Sp.	Modern Major Lineage	Historical s.s. Group	Cercus (n = 265)	Ectophallus (n = 265)	Epiphallus (n = 266)	Lophus (n = 266)	Aedegal Region (n = 262)	Tegmen (n = 265)	Locality Data (GPS coordinates are in WGS84 format by latitude,longitude)
M. forcipatus Hubbell, 1932	1	C	Forcipatus Group	Included	Included	Included	Included	Included	Included	FL: Seminole Co., Chuluota Wilderness Area, on both sides of trail, [28.619361,-81.056057], 13-V-2014, Field #PG123-2-B, coll. D.A. Woller & H. Song, overgrown scrub along perimeter of very dense pine flatwoods
M. forcipatus Hubbell, 1932	2	C	Forcipatus Group	Included	Included	Included	Included	Included	Included	FL: Seminole Co., Geneva Wilderness Area, on both sides of trail towards southern end of property, [28.699623,-81.125005], 31-VII-2014, Field #PG149-1-A, coll. D.A. Woller, overgrown scrub
M. forcipatus Hubbell, 1932	3	C	Forcipatus Group	Included	Included	Included	Included	Included	Included	FL: Lake Co., Clermont, along trail just beyond the end of Sawgrass Bay Blvd., [28.400988,-81.672299], 26-IX-2014, Field #PG159-1-A, coll. D.A. Woller, very overgrown scrub w/many pines
M. forcipatus Hubbell, 1932	4	C	Forcipatus Group	Included	Included	Included (R)	Included	Included	Included	FL: Seminole Co., Black Hammock Wilderness Area, along trail at N end of park just S of private neighborhood entrance, [28.719993,-81.149591], 7-X-2014, Field #PG174-1-A, coll. D.A. Woller, overgrown scrubby flatwoods
M. forcipatus Hubbell, 1932	5	C	Forcipatus Group	Included	Included	Included	Included	Included	Included	FL: Orange Co., Orlando, 30-Aug-1924, coll. F.W. Walker, Field #38
M. forcipatus Hubbell, 1932	6	C	Forcipatus Group	Included	Included	Included	Included	Included	Included	FL: Lake Co., 4.5 mi.. E Eustis , 25-Aug-1938, coll. Hubbell and Friauf, Field #184
M. forcipatus Hubbell, 1932	7	C	Forcipatus Group	Included	Included	Included	Included	Included	Included	FL: Lake Co., 5.5 mi. NE Cassia, 26-Aug-1938, coll. Hubbell and Friauf, Field #186
M. forcipatus Hubbell, 1932	8	C	Forcipatus Group	Included	Included	Included	Included	Included	Included	FL: Lake Co., 3 mi. E Altoona, 28-Aug-1938, coll. Hubbell and Friauf, Field #196
M. forcipatus Hubbell, 1932	9	C	Forcipatus Group	Included	Included	Included	Included	Included	Included	FL: Lake Co., 1.7 mi. E. Lisbon, 24-Aug-1938, coll. Hubbell and Friauf, Field #175
M. forcipatus Hubbell, 1932	10	C	Forcipatus Group	Included	Included	Included	Included	Included	Included	FL: Lake Co., 3 mi. NW Fullerville, 29-Aug-1938, coll. Hubbell and Friauf, Field #208
M. indicifer Hubbell, 1933	1	C	Forcipatus Group	Included	Included	Included	Included	Included	Included	FL: Brevard Co., Malabar Scrub Sanctuary, along sides of various trails, but primarily at coordinates, [28.004746,-80.581205], 15-VIII-2014, Field #PG151-1-A, coll. D.A. Woller, B. Silverman, & S.L. Kelly, somewhat overgrown classic scrub
M. indicifer Hubbell, 1933	2	C	Forcipatus Group	Included	Included	Included	Included	Included	Included	FL: Brevard Co., Titusville, just S of old Carousel Roller Rink (4745 Apollo Rd.), 16-V-2001, coll. T.L. Justice
M. indicifer Hubbell, 1933	3	C	Forcipatus Group	Included	Included	Included	Included	Included	Included	FL: Palm Beach Co., Jupiter, 30-Oct-1934, coll. T.H. Hubbell, Field #4
M. indicifer Hubbell, 1933	4	C	Forcipatus Group	Included	Included	Included	Included	Included	Included	FL: St. Lucie Co., Ft. Pierce, 30-Oct-1934, coll. T.H. Hubbell, Field #2
M. indicifer Hubbell, 1933	5	C	Forcipatus Group	Included	Included	Included	Included	Included	Included	FL: Palm Beach Co., Kelsey City, 30-Oct-1934, coll. T.H. Hubbell, Field #2
M. indicifer Hubbell, 1933	6	C	Forcipatus Group	Included	Included	Included	Included	Included	Included	FL: Martin Co., Fruita, 30-Oct-1934, coll. I. J. Cantrall, Field #1

Table 4-1 Continued.

Species (Sp.)	# of Spec./Sp.	Modern Major Lineage	Historical s.s. Group	Cercus (n = 265)	Ectophallus (n = 265)	Epiphallus (n = 266)	Lophus (n = 266)	Aedegal Region (n = 262)	Tegmen (n = 265)	Locality Data (GPS coordinates are in WGS84 format by latitude,longitude)
M. indicifer Hubbell, 1933	7	C	Forcipatus Group	Included	Included	Included	Included	Included	Included	FL: Palm Beach Co., Jupiter Lighthouse, 2-Aug-1930, coll. R. H. Beamer
M. indicifer Hubbell, 1933	8	C	Forcipatus Group	Included	Included	Included	Included	Included	Included	FL: Volusia Co., 5.4 mi. W New Smyrna, 31-Aug-1938, coll. T.H. Hubbell & J.J. Friauf, Field #212
M. indicifer Hubbell, 1933	9	C	Forcipatus Group	Included	Included	Included	Included	Included	Included	FL: Brevard Co., 1.75 mi. S Melbourne, 9-Aug-1938, coll. T.H. Hubbell & J.J. Friauf, Field #104
M. indicifer Hubbell, 1933	10	C	Forcipatus Group	Included	Included	Included	Included	Included	Included	FL: St. Lucie Co., Viking, 18-Oct-1991, coll. Deyrup & Fitzpatrick, yellow sand scrub with *Dicerandra immaculata*
M. nanciae Deyrup, 1997	1	C	Forcipatus Group	Included	Included	Included	Included	Included	Included	FL: Marion Co., Ocala National Forest, Big Scrub, 500 meters South of Big Scrub Campground on Forest Road 588/SE 241st Ave., [29.045266,-81.754964], 26-V-2013, Field #PG127-1-B, coll. D.A. Woller & E. Kosnicki, close to classic scrub - maintained w/roller-chopping and with dense Pinus clausa (?) forest near-by
M. nanciae Deyrup, 1997	2	C	Forcipatus Group	Included	Included	Included	Included	Included	Included	FL: Marion Co., Ocala National Forest, 1.3 miles Northwest of entrance to Juniper Springs Recreation Area, not far down vehicle-sized trail on west side of Forest Road 33, [29.184393,-81.729991], 6-VII-2014, Field #PG130-2-B, coll. D.A. Woller, E. Kerr-Woller, P. Woller, & K. Woller, within dense pine forest on both sides of trail
M. nanciae Deyrup, 1997	3	C	Forcipatus Group	Included	Included	Included	Included	Included	Included	FL: Marion Co., Ocala national Forest, 2-Sep-1938, coll. T. H. Hubbell & J.J. Friauf, Field #219
M. nanciae Deyrup, 1997	4	C	Forcipatus Group	Included	Included	Included	Included	Included	Included	FL: Marion Co., Ocala National Forest, 27-Jul-1938, coll. T. H. Hubbell & J.J. Friauf, Field #34
M. nanciae Deyrup, 1997	5	C	Forcipatus Group	Included	Included	Included	Included	Included	Included	FL: Marion Co., Ocala National Forest, 8-Jun-1938, coll. T. H. Hubbell & J.J. Friauf, Field #19
M. nanciae Deyrup, 1997	6	C	Forcipatus Group	Included	Included	Included	Included	Included	Included	FL: Marion Co., Ocala National Forest, 24-Jul-1938, coll. T. H. Hubbell & J.J. Friauf, Field #5
M. nanciae Deyrup, 1997	7	C	Forcipatus Group	Included	Included	Included	Included	Included	Included	FL: Marion Co., Ocala National Forest, 24-Jul-1938, coll. T. H. Hubbell & J.J. Friauf, Field #6
M. nanciae Deyrup, 1997	8	C	Forcipatus Group	Included	Included (R)	Included	Included	Included (R)	Included	FL: Marion Co., Ocala National Forest, 8-Jun-1938, coll. T. H. Hubbell & J.J. Friauf, Field #15
M. nanciae Deyrup, 1997	9	C	Forcipatus Group	Included	Included	Included	Included	Included	Included	FL: Marion Co., Ocala National Forest, Juniper Springs, 3-Sep-1938, coll. T. H. Hubbell & J.J. Friauf, Field #224
M. nanciae Deyrup, 1997	10	C	Forcipatus Group	Included	Included	Included	Included	Included	Included	FL: Lake Co., 7 mi. SW Astor, 28-Aug-1938, coll. T. H. Hubbell & J.J. Friauf, Field #200
M. ordwayae Deyrup, 1997	1	C	Forcipatus Group	Included	Included	Included	Included	Included	Included	FL: Clay Co., Mike Roess Gold Head Branch State Park, along the trail just NE of park entrance, [29.847725,-81.961243], 15-X-2012, Field #PG118-1-A, coll. C. Gale, sandhills
M. ordwayae Deyrup, 1997	2	C	Forcipatus Group	Included	Included	Included	Included	Included	Included	FL: Clay Co., Mike Roess Gold Head Branch State Park, mainly on E side of the trail just NE of park entrance, [29.847725,-81.961243], 18-IX-2014, Field #PG155-1-A, coll. D.A. Woller, classic sandhills, although a bit overgrown

Table 4-1 Continued.

Species (Sp.)	# of Spec./Sp.	Modern Major Lineage	Historical s.s. Group	Cercus (n = 265)	Ectophallus (n = 265)	Epiphallus (n = 266)	Lophus (n = 266)	Aedegal Region (n = 262)	Tegmen (n = 265)	Locality Data (GPS coordinates are in WGS84 format by latitude,longitude)
M. ordwayae Deyrup, 1997	3	C	Forcipatus Group	Included	Included	Included	Included	Included	Included	FL: Putnam Co., Ordway Preserve, 2-I-2001
M. ordwayae Deyrup, 1997	4	C	Forcipatus Group	Included	Included	Included	Included	Included	Included	FL: Clay Co., Kingsley lake, 30-Oct-1938, coll. T. H. Hubbell, Field #2
M. ordwayae Deyrup, 1997	5	C	Forcipatus Group	Included	Included	Included	Included	Included	Included	FL: Clay Co., Kingsley lake, 30-Oct-1938, coll. T. H. Hubbell, Field #2
M. ordwayae Deyrup, 1997	6	C	Forcipatus Group	Included	Included	Included	Included	Included	Included	FL: Putnam Co., Putnam Hall, 28-Oct-1938, coll. T. H. Hubbell, Field #8
M. ordwayae Deyrup, 1997	7	C	Forcipatus Group	Included	Included	Included	Included	Included	Included	FL: Putnam Co., Putnam Hall, 28-Oct-1938, coll. T. H. Hubbell, Field #8
M. ordwayae Deyrup, 1997	8	C	Forcipatus Group	Included	Included	Included	Included	Included	Included	FL: Putnam Co., Clay Springs, 29-Oct-1938, coll. T. H. Hubbell, Field #7
M. ordwayae Deyrup, 1997	9	C	Forcipatus Group	Included	Included	Included	Included	Included	Included	FL: Clay Co., Gold Head Br. St. P., 29-Oct-1942, coll. T. H. Hubbell , Field #7
M. ordwayae Deyrup, 1997	10	C	Forcipatus Group	Included	Included	Included	Included	Included	Included	FL: Putnam Co., 9-11-Feb-1959, coll. R.E. Woodruff
M. adelogyrus Hubbell, 1932	1	D	Puer Group	Included	Included	Included	Included	Included	Included	FL: Brevard Co., Merritt Island National Wildlife Refuge, a little ways down Scrub Trail, E of Courtenay Pkwy N/Kennedy Pkwy N and just W of Clark Slough, [28.694973,-80.716039], 19-VI-2013, Field #PG131-1-A, coll. D.A. Woller, I. Kutch, G. Alava, R. Marino-Perez, S. Evans, A. Kladke, J.M. Noh, & S. Gotham, overgrown scrub next to a slough
M. adelogyrus Hubbell, 1932	2	D	Puer Group	Included	Included	Included	Included	Included	Included	FL: Volusia Co., Lake George State Forest, just SE of intersection of State Forest Roads 7 & 19, just off both sides of road, [29.180483,-81.503633], 25-V-2103, Field #PG126-1-B, coll. D.A. Woller & E. Kosnicki, managed Pinus clausa (?) with numerous scrubby oaks
M. adelogyrus Hubbell, 1932	3	D	Puer Group	Included	Included	Included	Included	Included	Included	FL: Brevard Co., Kennedy Space Center, Tel-4 Tract, not far S of E Crisafulli Rd. on both sides of trail, [28.461667,-80.670800], 5-VIII-2014, Field #PG150-1-B, coll. D.A. Woller & I.J. Stout, overgrown scrubby flatwoods
M. adelogyrus Hubbell, 1932	4	D	Puer Group	Included	Included	Included	Included	Included	Included	FL: Brevard Co., Kennedy Space Center, Happy Creek section, a short ways N of Happy Creek Rd. on W side of A Ave. NE trail, [28.626265,-80.663714], 14-X-2014, Field #PG150-2-A, coll. D.A. Woller & I.J. Stout, maintained scrubby flatwoods with distant, scattered cabbage palms

Table 4-1 Continued.

Species (Sp.)	# of Spec./Sp.	Modern Major Lineage	Historical s.s. Group	Cercus (n = 265)	Ectophallus (n = 265)	Epiphallus (n = 266)	Lophus (n = 266)	Aedegal Region (n = 262)	Tegmen (n = 265)	Locality Data (GPS coordinates are in WGS84 format by latitude,longitude)
M. adelogyrus Hubbell, 1932	5	D	Puer Group	Included	Included	Included	Included	Included	Included	FL: Brevard Co., Kennedy Space Center, Happy Creek section, about 1/4 mi. N of Happy Creek Rd. on W side of trail, [28.622742,-80.672879], 14-X-2014, Field #PG150-2-C, coll. D.A. Woller & I.J. Stout, overgrown and dense scrubby flatwoods w/few trees
M. adelogyrus Hubbell, 1932	6	D	Puer Group	Included	Included	Included	Included	Included	Included	FL: Volusia Co., Blue Spring State Park, not too far S of head of Pine Island Trail, [28.940209,-81.338076], 10-X-2014, Field #PG177-1-A, coll. D.A. Woller, resembles a pine flatwoods, although wetter
M. adelogyrus Hubbell, 1932	7	D	Puer Group	Included	Included	Included	Included	Included	Included	FL: Volusia Co., Blue Spring State Park, just NW of intersection of Becker Rd. and turnoff to 1st camping area, [28.948768,-81.334222], 10-X-2014, Field #PG177-1-B, coll. D.A. Woller, odd habitat - a disturbed scrubby grassland?
M. adelogyrus Hubbell, 1932	8	D	Puer Group	Included	Included	Included	Included	Included	Included	FL: Volusia Co., Lyonia Preserve, NE side of Deltona, [28.928000,-81.225374], 10-X-2014, Field #PG176-1-A, coll. D.A. Woller, fairly overgrown classic scrub
M. adelogyrus Hubbell, 1932	9	D	Puer Group	Included	Included	Included	Included	Included	Included	FL: Volusia Co., Emporia, 3-May-1931, coll. T.H. Hubbell, Field #5
M. adelogyrus Hubbell, 1932	10	D	Puer Group	Included	Included	Included	Included	Included	Included	FL: Putnam Co., Welaka, 3-Jul-1940, coll. J.J. Friauf, Field #H-8
M. bonita Otte, 2012 ("2011")	1	D	Puer Group	Included	Included	Included	Included	Included	Included	FL: Collier Co., just W. of the perimeter of Railhead Scrub Preserve, W of I-75 & E of Old 41 Rd. off Sun Century Rd., mainly on E side of railroad tracks, [26.305475,-81.791579], 24-IV-2014, Field #PG136-1-A, coll. D.A. Woller & S.L. Kelly, scrubby oaks sparse, but gopher apple patches tall and abundant; scrub rosemary bald nearby (no hoppers)
M. bonita Otte, 2012 ("2011")	2	D	Puer Group	Included	Included	Included	Included	Included	Included	FL: Lee Co., 3 mi. SW Estero, 12-13-Aug-1938, coll. T.H. Hubbell & J.J. Friauf, Field #121
M. bonita Otte, 2012 ("2011")	3	D	Puer Group	Included	Included	Included	Included	Included	Included (R)	FL: Lee Co., Fort Myers, 13-15-Sept-1917, coll. Rehn & Hebard
M. bonita Otte, 2012 ("2011")	4	D	Puer Group	Included	Included	Included	Included	Included	Included	FL: Collier Co., Naples, 30-Aug-1951, coll. I. J. Cantrall, Field #75
M. bonita Otte, 2012 ("2011")	5	D	Puer Group	Included	Included	Included	Included	Included	Included	FL: Collier Co., 12 mi. S Naples, 30-Aug-1951, coll. I. J. Cantrall, Field #74
M. bonita Otte, 2012 ("2011")	6	D	Puer Group	Included	Included	Included	Included	Included	Included	FL: Lee Co., Fort Myers, 13-15-Sept-1917, coll. Rehn & Hebard
M. bonita Otte, 2012 ("2011")	7	D	Puer Group	Included	Included	Included	Included	Included	Included	FL: Lee Co., Fort Myers, 25-Aug-1937
M. bonita Otte, 2012 ("2011")	8	D	Puer Group	Included	Included	Included	Included	Included	Included	FL: Lee Co., Fort Myers, 25-Aug-1937
M. bonita Otte, 2012 ("2011")	9	D	Puer Group	Included	Included	Included	Included	Included	Included	FL: Collier Co., Marco Island, 15-Oct-1955

Table 4-1 Continued.

Species (Sp.)	# of Spec./Sp.	Modern Major Lineage	Historical s.s. Group	Cercus (n = 265)	Ectophallus (n = 265)	Epiphallus (n = 266)	Lophus (n = 266)	Aedegal Region (n = 262)	Tegmen (n = 265)	Locality Data (GPS coordinates are in WGS84 format by latitude,longitude)
M. bonita Otte, 2012 ("2011")	10	D	Puer Group	Included	Included	Included	Included	Included	Included	FL: Lee Co., Bonita Beach, 24-Oct-1993, coll. Stephen & Glenn Lenberger, FL scrub habitat
M. childsi Otte, 2012 ("2011")	1	D	Tequestae Group	Included	Included	Included	Included	Included	Included	FL: Highlands Co., Archbold Biological Station, Lake Annie Tract, just S of Lake Annie on E side of trail, [27.201654,-81.351544], 26-VIII-2014, Field #PG109-8-D, coll. D.A. Woller, fire-maintained classic scrub w/scattered pines
M. childsi Otte, 2012 ("2011")	2	D	Tequestae Group	Included	Included	Included	Included	Included	Included	FL: Highlands Co., Lake June-In-Winter Scrub State Park, short distance from parking lot on E side of northern trail, [27.298352,-81.420267], 23-IX-2014, Field #PG156-1-A, coll. D.A. Woller & S.L. Kelly, overgrown scrub, but fire-maintained; just W. of Lake June in Winter
M. childsi Otte, 2012 ("2011")	3	D	Tequestae Group	Included	Included	Included	Included	Included	Included	FL: Highlands Co., about 3.25 mi. N. of Venus , just off W side of U.S 27, [27.110100,-81.332154], 18-X-2014, Field #PG182-1-A, coll. D.A. Woller & S.L. Kelly, overgrown scrub on a gradient
M. childsi Otte, 2012 ("2011")	4	D	Tequestae Group	Included	Included	Included	Included	Included	Included	FL: Highlands Co., about 3 mi. N. of Venus , just off W side of U.S 27, [27.106631,-81.332602], 23-X-2014, Field #PG182-2-B, coll. D.A. Woller & S.L. Kelly, overgrown scrub w/scattered dense gopher apple patches and lots of Opuntia humifusa
M. childsi Otte, 2012 ("2011")	5	D	Tequestae Group	Included	Included	Included	Included	Included	Included	FL: Highlands Co., about 3.5 mi. N. of Venus, just off E side of U.S 27, [27.118833,-81.330515], 30-X-2014, Field #PG186-1-A, coll. D.A. Woller, scrubby patch w/dense gopher apple patch and scrubby oaks w/priarie beyond
M. childsi Otte, 2012 ("2011")	6	D	Tequestae Group	Included	Included	Included	Included	Included	Included	FL: Highlands Co., about 4.25 mi. N. of Venus, just off E side of U.S 27, [27.135584,-81.328831], 30-X-2014, Field #PG187-1-A, coll. D.A. Woller, low, scrubby habitat w/gopher apple patches surrounded by scrubby oaks w/orange groves just N.
M. childsi Otte, 2012 ("2011")	7	D	Tequestae Group	Included	Included	Included	Included	Included	Included	FL: Highlands Co., off W. side of U.S.27 along the road, just S of Josephine Creek, [27.371539,-81.400733], 11-XII-2013, Field #PG132-2-B, coll. D.A. Woller & J.M. Noh, scrubby lot w/scrub rosemary, scrubby oaks, and larger oaks - found mainly in and around "oak islands"
M. childsi Otte, 2012 ("2011")	8	D	Tequestae Group	Included	Included	Included	Included	Included	Included	FL: Highlands Co., Archbold Biological Station, not far from the Station along a trail, [27.183075,-81.351118], 10-X-2013, Field #PG109-3-B, coll. D.A. Woller & M. Deyrup, scrubby area with many scrubby oaks
M. childsi Otte, 2012 ("2011")	9	D	Tequestae Group	Included	Included	Included	Included	Included	Included	FL: Highlands Co., Archbold Biological Station, just off S side of SR70, across the fence from a Lake Annie Tract trail, [27.209126,-81.357030], 10-X-2013, Field #PG109-3-C, coll. D.A. Woller, scrubby area w/dense gopher apple patch, a lot of scrubby oaks, bigger oaks, and abundant cacti

Table 4-1 Continued.

Species (Sp.)	# of Spec./Sp.	Modern Major Lineage	Historical s.s. Group	Cercus (n = 265)	Ectophallus (n = 265)	Epiphallus (n = 266)	Lophus (n = 266)	Aedegal Region (n = 262)	Tegmen (n = 265)	Locality Data (GPS coordinates are in WGS84 format by latitude,longitude)
M. childsi Otte, 2012 ("2011")	10	D	Tequestae Group	Included	Included	Included	Included	Included	Included	FL: Highlands Co., Archbold Biological Station (Childs), 6-Aug-1930, coll. R. H. Beamer
M. kissimmee Otte, 2012 ("2011")	1	D	Puer Group	Included	Included	Included	Included	Included	Included	FL: Orange Co., University of Central Florida Natural Area ("Arboretum"), mainly between Wildflower Loop Trail and Fire Loop Trail , [28.603303,-81.189410], 18-III-2014, Field #PG119-4-C, coll. D.A. Woller & C. Gale, pine flatwoods
M. kissimmee Otte, 2012 ("2011")	2	D	Puer Group	Included	Included	Included	Included	Included	Included	FL: Orange Co., Split Oak Forest Wildlife and Environmental Area, entrance at the curve of Clapp Simms Duda Rd., on both sides of Trail #1, [28.351667,-81.206111], 14-V-2014, Field #PG138-1-A, coll. D.A. Woller, C. Gale, & J.M. Noh, overgrown scrub
M. kissimmee Otte, 2012 ("2011")	3	D	Puer Group	Included	Included (R)	Included	Included	Included (R)	Included	FL: Osceola Co., Disney Wilderness Preserve, about 1/2 mile east of visitor center on edge of trail, [28.127964,-81.424187], 27-IV-2013, Field #PG122-1-A, coll. D.A. Woller, pine flatwoods
M. kissimmee Otte, 2012 ("2011")	4	D	Puer Group	Included	Included	Included	Included	Included	Included	FL: Osceola Co., Lake Lizzie Conservation Area, N end of park, on W side of an unmarked tail between North Trail Loop (N) and Lake Lizzie Trail (S), [28.246465,-81.166838], 8-XI-2014, Field #PG188-1-A, coll. D.A. Woller, E.C. Kerr-Woller, S.L. Kelly, & E. Kelly, unusual habitat - dense swaths of Lyonia ferruginea w/scattered *Pinus palustris* along trail edges w/more classic scrub further back
M. kissimmee Otte, 2012 ("2011")	5	D	Puer Group	Included	Included	Included	Included	Included	Included	FL: Seminole Co., Econ River Wilderness Area, not far from intersection of 2 trails, about 1/4 mi. S of Fawn Run and directly across from the backs of some homes, [28.617493,-81.166616], 30-VIII-2012, Field #PG103-1-A, coll. D.A. Woller , fairly dense pine flatwoods
M. kissimmee Otte, 2012 ("2011")	6	D	Puer Group	Included	Included	Included	Included	Included	Included	FL: Osceola Co., 2.6 mi. SE St. Cloud, 6-Aug-1938, coll. T.H. Hubbell & J.J. Friauf, Field #84
M. kissimmee Otte, 2012 ("2011")	7	D	Puer Group	Included	Included	Included	Included	Included	Included	FL: Orange Co., Christmas, little ways off off N side of E Colonial Dr./SR50, [28.539097,-81.034881], 11-VII-2015, coll. A. Orfinger
M. kissimmee Otte, 2012 ("2011")	8	D	Puer Group	Included	Included	Included	Included	Included	Included	FL: Orange Co., Econlockhatchee Sandhills Conservation Area, along trail about 1/4 of a mi. NW of main trail, [28.604075,-81.154069], 1-VI-2016, coll. A. Orfinger
M. kissimmee Otte, 2012 ("2011")	9	D	Puer Group	Included	Included	Included	Included	Included	Included	FL: Orange Co., Savage-Christmas Creek Preserve, along W side of a trail little ways NW of entrance , [28.558628,-81.034025], 20-II-2016, coll. A. Orfinger
M. kissimmee Otte, 2012 ("2011")	10	D	Puer Group	Included	Included	Included	Included	Included	Included	FL: Osceola Co., Disney Wilderness Preserve, [28.068333,-81.406944], 17-June-2015, coll. J.G. Hill and J.A. Barone, collected in sandy, dry flatwoods
M. peninsularis Hubbell, 1932	1	D	Puer Group	Included	Included	Included	Included	Included	Included	FL: Miami-Dade Co., Miami., 23-Jul-1938
M. peninsularis Hubbell, 1932	2	D	Puer Group	Included	Included	Included	Included	Included	Included	FL: Monroe Co., Long Pine Key, 5-Aug-1938, coll. H.F.S. Strohecker

Table 4-1 Continued.

Species (Sp.)	# of Spec./Sp.	Modern Major Lineage	Historical s.s. Group	Cercus (n = 265)	Ectophallus (n = 265)	Epiphallus (n = 266)	Lophus (n = 266)	Aedegal Region (n = 262)	Tegmen (n = 265)	Locality Data (GPS coordinates are in WGS84 format by latitude,longitude)
M. peninsularis Hubbell, 1932	3	D	Puer Group	Included	Included	Included	Included	Included	Included	FL: Broward Co., Fort Lauderdale, 29-Aug-1925, coll. T.H. Hubbell, Field #3
M. peninsularis Hubbell, 1932	4	D	Puer Group	Included	Included	Included	Included	Included	Included	FL: Miami-Dade Co., Miami., 27-Mar-1910
M. peninsularis Hubbell, 1932	5	D	Puer Group	Included	Included	Included	Included	Included	Included	FL: Miami-Dade Co., Miami. Beach, 12-Mar-1915
M. peninsularis Hubbell, 1932	6	D	Puer Group	Included	Included	Included	Included	Included	Included	FL: Miami-Dade Co., Coconut Grove, [25.733897,-80.239649], 9-Aug-1930, coll. L.D. Tuthill
M. peninsularis Hubbell, 1932	7	D	Puer Group	Included (R)	Included	Included	Included	Included	Included	FL: Broward Co., Pompano Beach, [26.243044,-80.128175], 4-Jul-1935, coll. I. J. Cantrall, Field #59
M. peninsularis Hubbell, 1932	8	D	Puer Group	Included	Included	Included	Included	Included	Included	FL: Miami-Dade Co., 2 mi.W of Perrine, [25.600635,-80.394863], 21-Oct-1967
M. peninsularis Hubbell, 1932	9	D	Puer Group	Included	Included	Included	Included	Included	Included	FL: Broward Co., Ft. Lauderdale, 15-May-1948
M. peninsularis Hubbell, 1932	10	D	Puer Group	Included	Included	Included	Included	Included	Included	FL: Dade Co., Miami. Beach, 8-Nov-1936
M. puer (Scudder, 1878)	1	D	Puer Group	Included	Included	Included	Included	Included	Included	FL: Citrus Co., Withlacoochee State Forest, Citrus Tract, just SE of intersection of Trail 13 and 20 and just SW of Tillis Hill Campground, [28.723992,-82.417703], 1-XI-2014, Field #PG148-2-C, coll. D.A. Woller, S.L. Kelly, A. Orfinger, & B. Silverman, classic sandhills
M. puer (Scudder, 1878)	2	D	Puer Group	Included	Included	Included	Included	Included	Included	FL: Hernando Co., Withlacoochee State Forest, Richloam Tract, clearing between 2 unmarked roads short ways N of intersections w/Dark Stretch Rd., [28.481700,-82.147401], 25-XI-2014, Field #PG148-3-D, coll. D.A. Woller, S.L. Kelly, & A. Orfinger, odd habitat - grassy clearing w/tall oaks around perimeter w/scattered scrubby oaks
M. puer (Scudder, 1878)	3	D	Puer Group	Included	Included	Included	Included	Included	Included	FL: Orange Co., Wekiwa Springs State Park, a ways NW of N parking lot, mainly on E side of trail, [28.734514,-81.479778], 15-IX-2012, Field #PG107-1-A, coll. D.A. Woller, scrubby flatwoods
M. puer (Scudder, 1878)	4	D	Puer Group	Included	Included	Included	Included	Included	Included	FL: Alachua Co., Archer, 22-Aug-1924, coll. F.W. Walker, Field #172
M. puer (Scudder, 1878)	5	D	Puer Group	Included	Included	Included	Included	Included	Included (R)	FL: Alachua Co., Newberry, 12-Oct-1924, coll. F.W. Walker, Field #122
M. puer (Scudder, 1878)	6	D	Puer Group	Included	Included	Included	Included	Included	Included	FL: Sumter Co., 3.4 mi. N Mable, 21-Aug-1938, coll. T.H. Hubbell & J.J. Friauf, Field #170
M. puer (Scudder, 1878)	7	D	Puer Group	Included	Included	Included	Included	**No**	Included	FL: Hernando Co., 11 mi. W Brooksville, 21-Aug-1938, coll. T.H. Hubbell & J.J. Friauf, Field #168

Table 4-1 Continued.

Species (Sp.)	# of Spec./Sp.	Modern Major Lineage	Historical s.s. Group	Cercus (n = 265)	Ectophallus (n = 265)	Epiphallus (n = 266)	Lophus (n = 266)	Aedegal Region (n = 262)	Tegmen (n = 265)	Locality Data (GPS coordinates are in WGS84 format by latitude,longitude)
M. puer (Scudder, 1878)	8	D	Puer Group	Included	Included	Included	Included	Included	Included	FL: Orange Co., Isle of Pine Preserve, off S side of a trail little ways SE of Lacebark Pine Rd. entrance, [28.359854,-81.162224], 14-V-2015, coll. A. Orfinger
M. puer (Scudder, 1878)	9	D	Puer Group	Included	Included	Included	Included	Included	Included	FL: Hernando Co., 3.8-4.2 mi. E Bayport, 9-Nov-1946, coll. T.H. Hubbell , Field #1
M. puer (Scudder, 1878)	10	D	Puer Group	Included	Included	Included	Included	Included	Included	FL: Orange Co., Orlando, 28-Aug-1924, coll. F.W. Walker, Field #30
M. rotundipennis (Scudder, 1878)	1	D	Rotundipennis Group	Included	Included (R)	Included	Included	Included (R)	Included	Fl: Brevard Co., Titusville, on N side of trail about 1/4 E from entrance to Titusville Wellspring, [28.550942,-80.816723], 14-X-2014, Field #PG178-1-A, coll. D.A. Woller & I.J. Stout, in dense gopher apple patch outside of a dense oak/*Pinus elliotti* forest
M. rotundipennis (Scudder, 1878)	2	D	Rotundipennis Group	Included	**No**	Included (R)	Included	**No**	Included	FL: Levy Co., Manatee Springs SP, just W of park entrance on both sides of NW 115 St., [29.495055,-82.970884], 19-V-2015, Field #PG206-1-A, coll. D.A. Woller, N. side resembles overgrown sandhills while S. side resembles dense mesic hardwood forest
M. rotundipennis (Scudder, 1878)	3	D	Rotundipennis Group	Included	Included	Included	Included	Included	Included	FL: Clay Co., Mike Roess Gold Head Branch State Park, mainly on E side of the trail just NE of park entrance, [29.847725,-81.961243], 18-IX-2014, Field #PG155-1-A, coll. D.A. Woller, classic sandhills, although a bit overgrown
M. rotundipennis (Scudder, 1878)	4	D	Rotundipennis Group	Included (R)	Included	Included	Included	Included	Included	FL: Osceola Co., Kissimmee, in vacant lot slightly NE of intersection of Sinclair Rd. and Connector Rd., [28.296426,-81.599393], 26-IX-2014, Field #PG158-1-A, coll. D.A. Woller, in vacant lot with dense pine canopy and dense needle bed; reminiscent of sandhills
M. rotundipennis (Scudder, 1878)	5	D	Rotundipennis Group	Included	Included	Included	Included	Included	Included	FL: Marion Co., Ocala National Forest, Big Scrub, 500 meters South of Big Scrub Campground on Forest Road 588/SE 241st Ave., [29.045266,-81.754964], 6-VII-2014, Field #PG127-2-B, coll. D.A. Woller, E. Kerr-Woller, P. Woller, & K. Woller, close to classic scrub maintained w/roller-chopping and with dense Pinus clausa (?) forest near-by
M. rotundipennis (Scudder, 1878)	6	D	Rotundipennis Group	Included	Included	Included	Included	Included	Included	FL: Lake Co., Rock Springs Run State Reserve, on both sides of Ethel Trail, mainly towards entrance along main park road (CR433), [28.804542,-81.453300], 22-VII-2014, Field #PG101-4-B, coll. D.A. Woller, overgrown, "classic" scrub on N. side w/scattered pines and more traditional sandhills on S. side
M. rotundipennis (Scudder, 1878)	7	D	Rotundipennis Group	Included	Included	Included (R)	Included	Included	Included	FL: Gilchrist Co., Thomas Farm, not far SW of fossil dig site, [29.860000,-82.832222], 18-V-2015, Field #PG205-1-A, coll. D.A. Woller, edge of an oak forest in grasses - scrubby area just S.
M. rotundipennis (Scudder, 1878)	8	D	Rotundipennis Group	Included	Included	Included	Included	Included	Included	FL: St. Johns Co., Moses Creek Conservation Area, about 0.5 miles down trail from E trailhead, [29.762624,-81.282995], 15-V-2015, Field #PG199-1-A, coll. D.A. Woller, S.L. Kelly, & A. Orfinger, large classic scrub w/some wet sections surrounded by w/Pinus clausa forests

Table 4-1 Continued.

Species (Sp.)	# of Spec./Sp.	Modern Major Lineage	Historical s.s. Group	Cercus (n = 265)	Ectophallus (n = 265)	Epiphallus (n = 266)	Lophus (n = 266)	Aedegal Region (n = 262)	Tegmen (n = 265)	Locality Data (GPS coordinates are in WGS84 format by latitude,longitude)
M. rotundipennis (Scudder, 1878)	9	D	Rotundipennis Group	Included	Included	Included	Included	Included	Included	FL: St. Johns Co., Faver-Dykes SP, just S of main park road and not far NE of Pellicer Creek, [29.667222,-81.268056], 15-V-2015, Field #PG196-1-B, coll. D.A. Woller, S.L. Kelly, & A. Orfinger, Pinus palustris savannah
M. rotundipennis (Scudder, 1878)	10	D	Rotundipennis Group	Included	Included	Included	Included	Included	Included	FL: St. Johns Co., along trails behind power station on N. side of SR206, just S of Moses Creek Conservation Area, [29.758326,-81.291557], 15-V-2015, Field #PG198-1-A, coll. D.A. Woller, S.L. Kelly, & A. Orfinger, overgrown classic scrub
M. sebringi Otte, 2012 ("2011")	1	D	Tequestae Group	Included	Included	Included	Included	Included	Included	FL: Highlands Co., S. end of Sebring, off E side of U.S27 along the road, in vacant lot on embankment just NE of George Blvd. sign (on a traffic light pole), [27.442255,-81.419021], 5-VI-2014, Field #PG133-3-A, coll. D.A. Woller & B. Hall, scrubby area just in front of a pine forest in an urban area
M. sebringi Otte, 2012 ("2011")	2	D	Tequestae Group	Included	Included	Included	Included	Included	Included	FL: Highlands Co., N. end of Sebring, off E side of U.S27 along the road, in vacant lot flanked by a Denny's & a Holiday Inn Express, [27.523486,-81.496962], 5-VI-2014, Field #PG137-2-A, coll. D.A. Woller & B. Hall, unusual - scrubby to a degree with odd mix of groundcover, including sand lace; scrubby oaks and larger oaks scattered
M. sebringi Otte, 2012 ("2011")	3	D	Tequestae Group	Included	Included	Included	Included	Included	Included	FL: Highlands Co., S. end of Sebring, off E side of U.S27 along the road, in vacant lot on embankment just NE of George Blvd. sign (on a traffic light pole), [27.442255,-81.419021], 5-VI-2014, Field #PG133-3-A, coll. D.A. Woller & B. Hall, scrubby area just in front of a pine forest in an urban area
M. sebringi Otte, 2012 ("2011")	4	D	Tequestae Group	Included	Included	Included	Included	Included	Included	FL: Highlands Co., Highlands Hammock State Park, at SE corner of park, across from CR635, [27.456321,-81.515914], 5-VI-2014, Field #PG147-1-A, coll. D.A. Woller & B. Hall, recently-burned classic scrub with dense understory
M. sebringi Otte, 2012 ("2011")	5	D	Tequestae Group	Included	Included	Included	Included	Included	Included	FL: Highlands Co., Carter Creek South, [27.51925,-81.40756], 1-Apr-2009, coll. M. Deyrup, H. Otte, & A. May, sandhill/scrub habitat
M. sebringi Otte, 2012 ("2011")	6	D	Tequestae Group	Included	Included	Included	Included	Included	Included	FL: Highlands Co., Flamingo Villas Preserve, [27.44231,-81.37822], 25-May-2009, coll. M. Deyrup, A. May, & D. Otte, Townes trap, scrub habitat
M. sebringi Otte, 2012 ("2011")	7	D	Tequestae Group	Included	Included	Included	Included	Included	Included	FL: Highland Co., Sebring, "High Oak" Lakeview Place Subdividion - btwn. Micco & Shontee Aves., 7-Jan-1927, coll. F.W. Walker
M. sebringi Otte, 2012 ("2011")	8	D	Tequestae Group	Included	Included	Included	Included	Included	Included	FL: Highlands Co., Lake Pythias, Avon Park, 28-29-Oct-1934, coll. T.H. Hubbell, Field #1
M. sebringi Otte, 2012 ("2011")	9	D	Tequestae Group	Included	Included	Included	Included	Included	Included	FL: Highlands Co., Sebring, 29-Oct-1934, coll. T.H. Hubbell, Field #2

Table 4-1 Continued.

Species (Sp.)	# of Spec./Sp.	Modern Major Lineage	Historical s.s. Group	Cercus (n = 265)	Ectophallus (n = 265)	Epiphallus (n = 266)	Lophus (n = 266)	Aedegal Region (n = 262)	Tegmen (n = 265)	Locality Data (GPS coordinates are in WGS84 format by latitude,longitude)
M. sebringi Otte, 2012 ("2011")	10	D	Tequestae Group	Included	Included	Included	Included	Included	Included	FL: Highlands Co., 2 mi. S. Sebring, 2-I-1936, coll. Rehn & Rehn
M. seminole Hubbell, 1932	1	D	Puer Group	Included	Included	Included	Included	Included	Included	FL: Charlotte Co., Charlotte Harbor Preserve State Park, a little bit W off an unmarked trail, about 0.5 mi. W of Rotonda Blvd. S, [26.874849,-82.280707], 11-XI-2014, Field #PG189-1-C, coll. D.A. Woller, A. Orfinger, & A. Perilla, resembles overgrown scrubby flatwoods w/dense patches of gopher apple
M. seminole Hubbell, 1932	2	D	Puer Group	Included	Included	Included	Included	Included	Included	FL: Glades Co., Palmdale, vacant lot bordered by 5th St., Main St., Pine Ave., & 3rd St., [26.941892,-81.306959], 18-X-2014, Field #PG180-1-A, coll. D.A. Woller & S.L. Kelly, odd habitat - "southern sandhills?" or "scrub-like sandhills?"
M. seminole Hubbell, 1932	3	D	Puer Group	Included	Included	Included	Included	Included	Included	FL: Glades Co., Palmdale Forestry Site, N side of 29, very close to intersection w/U.S27, [26.923434,-81.315410], 23-X-2014, Field #PG184-1-A, coll. D.A. Woller & S.L. Kelly, rollerchopped, disturbed scrubby area surrounded by tall oaks
M. seminole Hubbell, 1932	4	D	Puer Group	Included	Included	Included	Included	Included	Included	FL: Charlotte Co., Amberjack Environmental Park, around central area of Purple Trail, just W of Charlotte Harbor State Park, [26.867487,-82.298308], 11-XI-2014, Field #PG190-1-A, coll. D.A. Woller, A. Orfinger, & A. Perilla, unusual habitat - reminiscent of typical scrub combined w/pine flatwoods and sandhills (coastal scrub?)
M. seminole Hubbell, 1932	5	D	Puer Group	Included	Included	Included	Included	Included	Included	FL: Charlotte Co., Charlotte Harbor Preserve State Park, a little ways S of Rotonda Trace off E side of a trail beyond Gate 5, [26.833573,-82.213721], 11-XI-2014, Field #PG189-1-A, coll. D.A. Woller, A. Orfinger, & A. Perilla, unusual habitat - reminiscent of typical scrub combined w/pine flatwoods and sandhills (coastal scrub?) w/*Cassytha filiformis* dominating undergrowth
M. seminole Hubbell, 1932	6	D	Puer Group	Included	Included	Included	Included	Included	Included	FL: Charlotte Co., Charlotte Harbor Preserve State Park, not on a trail, just E of Amberjack Environmental Park and a short ways NE of gated entrance on Arlington Dr., [26.866293,-82.295916], 11-XI-2014, Field #PG189-1-B, coll. D.A. Woller, A. Orfinger, & A. Perilla, dense pine flatwoods
M. seminole Hubbell, 1932	7	D	Puer Group	Included	Included	Included	Included	Included	Included	FL: Glades Co., 2 mi. W Ortona, 12-Aug-1938, coll. T.H. Hubbell & J.J. Friauf, Field #120
M. seminole Hubbell, 1932	8	D	Puer Group	Included	Included	Included	Included	Included	Included	FL: DeSoto Co., Arcadia, 12-Sep-1917, coll. R&H, Field #148
M. seminole Hubbell, 1932	9	D	Puer Group	Included	Included	Included	Included	Included	Included	FL: Okeechobee Co., 2 mi. N Okeechobee, 24-May-1931, coll. T.H. Hubbell, Field #1
M. seminole Hubbell, 1932	10	D	Puer Group	Included	Included	Included	Included	Included	Included	FL: Highlands Co., Venus, 19-Apr-1958

Table 4-1 Continued.

Species (Sp.)	# of Spec./Sp.	Modern Major Lineage	Historical s.s. Group	Cercus (n = 265)	Ectophallus (n = 265)	Epiphallus (n = 266)	Lophus (n = 266)	Aedegal Region (n = 262)	Tegmen (n = 265)	Locality Data (GPS coordinates are in WGS84 format by latitude,longitude)
M. sp. nov. 1	1	D	Puer Group	Included	Included	Included	Included	Included	Included	FL: Okeechobee Co., in general vicinity of Fort Drum, on W. side of U.S. 441/15 , not too far N of Fort Drum General Store, [27.532674,-80.807697], 18-X-2014, Field #PG183-1-A, coll. D.A. Woller & S.L. Kelly, dense and overgrown scrubby patch in mostly-urban area
M. sp. nov. 1	2	D	Puer Group	Included	Included	Included	Included	Included	Included	FL: Brevard Co., St. Sebastian River Preserve SP, along Scrub Jay Link Trail, trailhead just N of Fellsmere Rd./CR 512, [27.770833,-80.565000], 16-V-2015, Field #PG200-1-A, coll. D.A. Woller, S.L. Kelly, & A. Orfinger, overgrown scrub
M. sp. nov. 1	3	D	Puer Group	Included	Included	Included (R)	Included	Included	Included	FL: Brevard Co., Malabar Scrub Sanctuary, along sides of various trails, but primarily at coordinates, [28.004746,-80.581205], 15-VIII-2014, Field #PG151-1-A, coll. D.A. Woller, B. Silverman, & S.L. Kelly, somewhat overgrown classic scrub
M. sp. nov. 1	4	D	Puer Group	Included	Included	Included	Included	Included	Included	FL: Brevard Co., 5 mi. W Melbourne, 24-May-1931, coll. T.H. Hubbell, Field #1
M. sp. nov. 1	5	D	Puer Group	Included	Included	Included	Included	Included	Included	FL: Brevard Co., 1.75 mi. S Melbourne, 9-Aug-1938, coll. T.H. Hubbell & J.J. Friauf, Field #104
M. sp. nov. 1	6	D	Puer Group	Included	Included	Included	Included	Included	Included	FL: Indian River Co., Sebastian, 24-May-1931, coll. T.H. Hubbell, Field #1
M. sp. nov. 1	7	D	Puer Group	Included	Included	Included	Included	Included	Included	FL: Indian River Co., Fort Pierce, 5-Jul-1935, coll. I. J. Cantrall, Field #66
M. sp. nov. 1	8	D	Puer Group	Included	Included	Included	Included	Included	Included	FL: Okeechobee Co., Olney, 24-May-1931, coll. T.H. Hubbell
M. sp. nov. 1	9	D	Puer Group	Included	Included	Included	Included	Included	Included	FL: Okeechobee Co., 23 mi. N. Okeechobee near Olney, 24-May-1931, coll. T.H. Hubbell, Field #2
M. sp. nov. 1	10	D	Puer Group	Included	Included	Included	Included	Included	Included	FL: Martin Co., 17-Apr-1962
M. sp. nov. 2	1	D	Puer Group	Included	Included	Included	Included	Included	Included	FL: Hillsborough Co., Little Manatee River State Park, 5 miles S of Sun City, on both sides of trail slightly NE of park entrance off of Lightfoot Rd., [27.658500,-82.374083], 27-III-2013, Field #PG121-1-A, coll. D.A. Woller & S.L. Kelly, unusual - pine flatwoods-esque with more oaks than pines
M. sp. nov. 2	2	D	Puer Group	Included	Included	Included	Included	Included	Included	FL: Hillsborough Co., Little Manatee River State Park, 5 miles S of Sun City, on both sides of trail slightly NE of park entrance off of Lightfoot Rd., [27.658500,-82.374083], 27-III-2013, Field #PG121-1-A, coll. D.A. Woller & S.L. Kelly, unusual - pine flatwoods-esque with more oaks than pines
M. sp. nov. 2	3	D	Puer Group	Included	Included	Included	Included	Included	Included	FL: Hillsborough Co., Little Manatee River, US Hwy 41, 18-Aug-1938, coll. T.H. Hubbell & J.J. Friauf, Field #129
M. sp. nov. 2	4	D	Puer Group	Included	Included	Included	Included	Included	Included	FL: Hillsborough Co., Little Manatee River, US Hwy 41, 18-Aug-1938, coll. T.H. Hubbell & J.J. Friauf, Field #129

Table 4-1 Continued.

Species (Sp.)	# of Spec./Sp.	Modern Major Lineage	Historical s.s. Group	Cercus (n = 265)	Ectophallus (n = 265)	Epiphallus (n = 266)	Lophus (n = 266)	Aedegal Region (n = 262)	Tegmen (n = 265)	Locality Data (GPS coordinates are in WGS84 format by latitude,longitude)
M. sp. nov. 2	5	D	Puer Group	Included	Included	Included	Included	Included	Included	FL: Glades Co., Sarasota, 17-Feb-1911
M. sp. nov. 2	6	D	Puer Group	Included	Included	Included	Included	**No**	Included	FL: Glades Co., Sarasota, 17-Feb-1911
M. sp. nov. 2	7	D	Puer Group	Included	Included	Included	Included	Included	Included	FL: Manatee Co., Manatee, 22-Aug-1925, coll. T.H. Hubbell, Field #36
M. sp. nov. 2	8	D	Puer Group	Included	Included	Included	Included	Included	Included	FL: Manatee Co., 28-Apr-1955, coll. H.A. Denmark
M. sp. nov. 2	9	D	Puer Group	Included	Included	Included	Included	Included	Included	FL: Manatee Co., Lake Manatee State Rec. Area, 26-Oct-1991, coll. M. Deyrup, scrubby flatwoods
M. sp. nov. 2	10	D	Puer Group	Included	Included	Included	Included	Included	Included	FL: Manatee Co., S.R. 675 at radio tower, 25-Oct-1991, coll. M. Deyrup, sandhill habitat
M. sp. nov. 3	1	D	Puer Group	Included	Included	Included	Included	Included	Included	FL: Martin Co., Jonathan Dickinson SP, across from a parking lot and SE of Park Rd./SE Jonathan Dickinson Way, [26.992974,-80.144831], 16-V-2015, Field #PG201-1-A, coll. D.A. Woller, S.L. Kelly, & A. Orfinger, pine flatwoods (possibly Pinus elliottii var. densa)
M. sp. nov. 3	2	D	Puer Group	Included	Included	Included	Included	Included	Included	FL: Martin Co., Jonathan Dickinson SP, across from a parking lot and SE of Park Rd./SE Jonathan Dickinson Way, [26.992974,-80.144831], 16-V-2015, Field #PG201-1-A, coll. D.A. Woller, S.L. Kelly, & A. Orfinger, pine flatwoods (possibly Pinus elliottii var. densa)
M. sp. nov. 3	3	D	Puer Group	Included	Included	Included	Included	Included	Included	FL: Martin Co., Jonathan Dickinson SP, not far from parking lot along Kitching Creek Nature Trail, [26.993056,-80.147222], 16-V-2015, Field #PG201-1-B, coll. D.A. Woller, S.L. Kelly, & A. Orfinger, pine flatwoods (possibly *Pinus elliottii var. densa*)
M. sp. nov. 3	4	D	Puer Group	Included	Included	Included	Included	Included	Included	FL: Martin Co., Jonathan Dickinson SP, not far from parking lot along Kitching Creek Nature Trail, [26.993056,-80.147222], 16-V-2015, Field #PG201-1-B, coll. D.A. Woller, S.L. Kelly, & A. Orfinger, pine flatwoods (possibly Pinus elliottii var. densa)
M. sp. nov. 3	5	D	Puer Group	Included	Included	Included	Included	Included	Included	FL: Martin Co., Jonathan Dickinson SP, not far from parking lot along Kitching Creek Nature Trail, [26.993056,-80.147222], 16-V-2015, Field #PG201-1-B, coll. D.A. Woller, S.L. Kelly, & A. Orfinger, pine flatwoods (possibly *Pinus elliottii var. densa*)
M. sp. nov. 3	6	D	Puer Group	Included	Included	Included	Included	Included	Included	FL: Martin Co., Jonathan Dickinson SP, just SE of Park Rd. and an unamed road, [27.005278,-80.140278], 16-V-2015, Field #PG201-1-C, coll. D.A. Woller, S.L. Kelly, & A. Orfinger, pine flatwoods (possibly *Pinus elliottii var. densa*) w/sections of temporary wetlands
M. sp. nov. 3	7	D	Puer Group	Included	Included	Included	Included	Included	Included	FL: Martin Co., Jonathan Dickinson SP, just SE of Park Rd. and an unamed road, [27.005278,-80.140278], 16-V-2015, Field #PG201-1-C, coll. D.A. Woller, S.L. Kelly, & A. Orfinger, pine flatwoods (possibly *Pinus elliottii var. densa*) w/sections of temporary wetlands

Table 4-1 Continued.

Species (Sp.)	# of Spec./Sp.	Modern Major Lineage	Historical s.s. Group	Cercus (n = 265)	Ectophallus (n = 265)	Epiphallus (n = 266)	Lophus (n = 266)	Aedegal Region (n = 262)	Tegmen (n = 265)	Locality Data (GPS coordinates are in WGS84 format by latitude,longitude)
M. sp. nov. 3	8	D	Puer Group	Included	Included	Included	Included	Included	Included	FL: Martin Co., Jonathan Dickinson SP, just SE of Park Rd. and an unamed road, [27.005278,-80.140278], 16-V-2015, Field #PG201-1-C, coll. D.A. Woller, S.L. Kelly, & A. Orfinger, pine flatwoods (possibly *Pinus elliottii var. densa*) w/sections of temporary wetlands
M. sp. nov. 3	9	D	Puer Group	Included	Included	Included	Included	Included	Included (R)	FL: Martin Co., Jonathon Dickinson State Park, 31-VIII-2001, coll. T.C. Justice
M. sp. nov. 3	10	D	Puer Group	Included	Included	Included	Included	Included	Included	FL: Martin Co., Jonanthan Dickinson State Park, 18-V-2001, coll. T.C. Justice
M. tequestae Hubbell, 1932	1	D	Tequestae Group	Included	Included	Included	Included	Included	Included	FL: Orange Co., Orlando, Fenton St. conservation easement, just N of W Fenton Street, 1.5 miles NW of Interstate 4, [28.406074,-81.505922], 22-IX-2012, Field #PG112-1-A, coll. D.A. Woller, overgrown scrub
M. tequestae Hubbell, 1932	2	D	Tequestae Group	Included (R)	Included	Included	Included	Included	Included	FL: Polk Co., Sun Ray (unincorporated area SW of Frostproof), just off E side of U.S 27 not far N of Sun Ray water tower, [27.715188,-81.560500], 26-VIII-2014, Field #PG152-1-B, coll. D.A. Woller, open scrubby area with dense understory mainly composed of *Opuntia humifusa*
M. tequestae Hubbell, 1932	3	D	Tequestae Group	Included	Included	Included	Included	Included	Included	FL: Polk Co., 1/4 mi. N. of entrance to Warner University, just off W side of U.S 27 , [27.829357,-81.591989], 26-VIII-2014, Field #PG153-1-A, coll. D.A. Woller, overgrown scrubby area with dense gopper apple patches
M. tequestae Hubbell, 1932	4	D	Tequestae Group	Included	Included	Included	Included	Included	Included	FL: Polk Co., N. edge of Lake Wales Ridge State Forest in a Fish & Wildlife Management Area, off W side of U.S 27, just S of The Vanguard School and turn-off to Bok Tower , [27.918426,-81.605210], 23-X-2014, Field #PG185-1-A, coll. D.A. Woller & S.L. Kelly, very scrubby habitat w/few trees
M. tequestae Hubbell, 1932	5	D	Tequestae Group	Included	Included	Included	Included	Included	Included	FL: Polk Co., Saddle Blanket Lakes Preserve, not far from entrance and just S of Avon Park Cut Off Rd., [27.671529,-81.576138], 17-V-2015, Field #PG202-1-A, coll. D.A. Woller, A. Orfinger, A. Perilla, & R. Ridenbaugh, fairly classic scrub w/lots of sand lace and logs
M. tequestae Hubbell, 1932	6	D	Tequestae Group	Included	Included	Included	Included	Included	Included	FL: Polk Co., Hickory Lake Scrub , about 2 miles slightly SW of Frostproof off NW side of SR 17, [27.697500,-81.538611], 17-V-2015, Field #PG204-1-A, coll. D.A. Woller, A. Orfinger, A. Perilla, & R. Ridenbaugh, somewhat overgrown scrub w/lots of cactus and scattered Pinus clausa and large oaks

Table 4-1 Continued.

Species (Sp.)	# of Spec./Sp.	Modern Major Lineage	Historical s.s. Group	Cercus (n = 265)	Ectophallus (n = 265)	Epiphallus (n = 266)	Lophus (n = 266)	Aedegal Region (n = 262)	Tegmen (n = 265)	Locality Data (GPS coordinates are in WGS84 format by latitude,longitude)
M. tequestae Hubbell, 1932	7	D	Tequestae Group	Included	Included	Included	Included	Included	Included	FL: Polk Co., about 0.5 miles S. of Avon Park Cut Off Rd., habitat "island" surrounded by agriculture fields and E of Saddle Blanket Lakes Preserve, [27.666110,-81.559368], 17-V-2015, Field #PG203-1-A, coll. D.A. Woller, A. Orfinger, A. Perilla, & R. Ridenbaugh, scrubby area transforming into oak hammock
M. tequestae Hubbell, 1932	8	D	Tequestae Group	Included	Included	Included	Included	Included	Included	FL: Orange Co., Apopka , between West Orange Trail, Clarcona-Ocoee Rd., and Forest Lake Golf Club, [28.605279,-81.532499], 10-VII-2014, Field #PG146-1-A, coll. D.A. Woller and S.L. Kelly, classic scrub surrounded by urban growth - primarily found specimens amongst grapevine
M. tequestae Hubbell, 1932	9	D	Tequestae Group	Included	Included	Included	Included	Included	Included	FL: Polk Co., Allen David Broussard Catfish Creek Preserve State Park, along both edges of main trail a little ways SE of park entrance , [27.983279,-81.496190], 9-V-2012, Field #PG100-1-A, coll. D.A. Woller, R. Marino-Perez, & L. Faucher, primarily in scrubby oaks/gopher apple
M. tequestae Hubbell, 1932	10	D	Tequestae Group	Included	Included	Included	Included	Included	Included	FL: Polk Co., Lake Wales Ridge State Forest, Walk-In-The-Water Wildlife Management Area, 2 miles E of Frostproof, [27.800262,-81.471137], 19-X-2013, Field #PG120-3-2-1, coll. D.A. Woller & Restoration Ecology Class, sandhills, amongst young scrubby oaks and gopher apple
M. withlacoocheensis Squitier, Deyrup, & Capinera, 1998	1	D	Rotundipennis Group	Included	Included	Included	Included	Included	Included	FL: Citrus Co., Withlacoochee State Forest, Citrus Tract, less than a mile S of 44 of E side of Forest Road 13, [28.848646,-82.419326], 10-VII-2014, Field #PG148-1-A, coll. D.A. Woller, S.L. Kelly, C. Werner, & V. Morris, classic sandhills
M. withlacoocheensis Squitier, Deyrup, & Capinera, 1998	2	D	Rotundipennis Group	Included (R)	Included	Included	Included	Included	Included	FL: Citrus Co., Withlacoochee State Forest, Citrus Tract, less than a mile S of 44 of E side of Forest Road 13, [28.848646,-82.419326], 10-VII-2014, Field #PG148-1-A, coll. D.A. Woller, S.L. Kelly, C. Werner, & V. Morris, classic sandhills
M. withlacoocheensis Squitier, Deyrup, & Capinera, 1998	3	D	Rotundipennis Group	Included	Included	Included	Included	Included	Included	FL: Citrus Co., Withlacoochee State Forest, Citrus Tract, about 1/4 of a mile S of Forest Road 10 and not too far E of Holder Mine Campground, [28.796592,-82.393544], 10-VII-2014, Field #PG148-1-B, coll. D.A. Woller, S.L. Kelly, C. Werner, & V. Morris, classic sandhills
M. withlacoocheensis Squitier, Deyrup, & Capinera, 1998	4	D	Rotundipennis Group	Included	Included	Included	Included	Included	Included	FL: Citrus Co., Withlacoochee State Forest, Citrus Tract, about 1/4 of a mile S of Forest Road 10 and not too far E of Holder Mine Campground, [28.796592,-82.393544], 10-VII-2014, Field #PG148-1-B, coll. D.A. Woller, S.L. Kelly, C. Werner, & V. Morris, classic sandhills

Table 4-1 Continued.

Species (Sp.)	# of Spec./Sp.	Modern Major Lineage	Historical s.s. Group	Cercus (n = 265)	Ectophallus (n = 265)	Epiphallus (n = 266)	Lophus (n = 266)	Aedegal Region (n = 262)	Tegmen (n = 265)	Locality Data (GPS coordinates are in WGS84 format by latitude,longitude)
M. withlacoocheensis Squitier, Deyrup, & Capinera, 1998	5	D	Rotundipennis Group	Included	Included	Included	Included	Included	Included	FL: Citrus Co., Withlacoochee State Forest, Citrus Tract, just SE of intersection of Trail 13 and 20 and just SW of Tillis Hill Campground, [28.723992,-82.417703], 1-XI-2014, Field #PG148-2-C, coll. D.A. Woller, S.L. Kelly, A. Orfinger, & B. Silverman, classic sandhills
M. withlacoocheensis Squitier, Deyrup, & Capinera, 1998	6	D	Rotundipennis Group	Included	Included	Included	Included	Included	Included	FL: Citrus Co., Withlacoochee State Forest, Citrus Tract, just N of Trail 2, W of Trail 13, and E of Trail 15 (and county landfill), [28.844943,-82.431752], 25-XI-2014, Field #PG148-3-E, coll. D.A. Woller, S.L. Kelly, & A. Orfinger, a scrubby "island" surrounded by dense medium-sized oaks and Pinus clausa w/sandhills further off
M. withlacoocheensis Squitier, Deyrup, & Capinera, 1998	7	D	Rotundipennis Group	Included	Included	Included	Included	Included	Included	FL: Hernando Co., Chassahowitzka Wildlife Management Area, just SW of Cortez Blvd./SR50, [28.527933,-82.589110], 18-VII-2015, coll. A. Orfinger
M. withlacoocheensis Squitier, Deyrup, & Capinera, 1998	8	D	Rotundipennis Group	Included	Included	Included (R)	Included	**No**	Included	FL: Hernando Co., just outside of Chassahowitzka Wildlife Management Area, Weeki Wachee, off W side of Allen Dr., [28.554117,-82.578582], 18-VII-2015, coll. A. Orfinger
M. withlacoocheensis Squitier, Deyrup, & Capinera, 1998	9	D	Rotundipennis Group	Included	Included	Included	Included	**No**	Included	FL: Hernando Co., Along S.R. 50, 15-I-1997, coll. J.M. Squitier
M. withlacoocheensis Squitier, Deyrup, & Capinera, 1998	10	D	Rotundipennis Group	Included	Included	Included	Included	Included	Included	FL: Hernando Co., Along S.R. 50, 8-X-1998, coll. J.L. Capinera

been historically used to define the species (Hubbell, 1932; Strohecker, 1960; Deyrup, 1996; Squitier et al., 1998; Otte, 2012 ("2011")). In terms of non-genital morphology, though, PG species tend to strongly resemble one another. Peninsular Florida, in general, is relatively young in terms of geology and biology (Hubbell, 1932; Hubbell, 1961; Webb 1990), and these facts, coupled with a robust dated molecular phylogeny (Fig. 4-3) and previous, insightful biogeographical analyses of the group (see Ch. II), further position the PG as a prime candidate to investigate the potential effects of the sexual selection hypothesis in a phylogenetic framework. Based on the aforementioned phylogeny, the PG can be further divided into four lineages (A-D, Fig. 4-3), with the one comprised of central-southeastern peninsular Florida species (lineage D) containing three major clades. The most speciose of these is collectively known as the Puer Group *sensu stricto* (herein referred to as the PGss) (Fig. 4-3; Table 1) and is estimated to have diverged very recently in geological terms (0.95 million years ago). Based on the estimated biogeographical history of the PGss (see Ch. II), sympatric speciation and range-expansion dispersal had the greatest influence on its formation. Combined with the fact that the subgroup's nine species evolved over such a short period of time at a very rapid speciation rate (2.31 species per million years) has led us to the supposition that sexual selection has been an active (if not the primary) driver of speciation in the PGss (West-Eberhard 1983; Kraaijeveld et al., 2011).

Melanoplus species, including those in the PG, exhibit coercive mating, in which a male stealthily approaches a female and attempts to mount her without any obvious pre-copulatory signal(s). Once coupled, copulation can last up to several hours, after

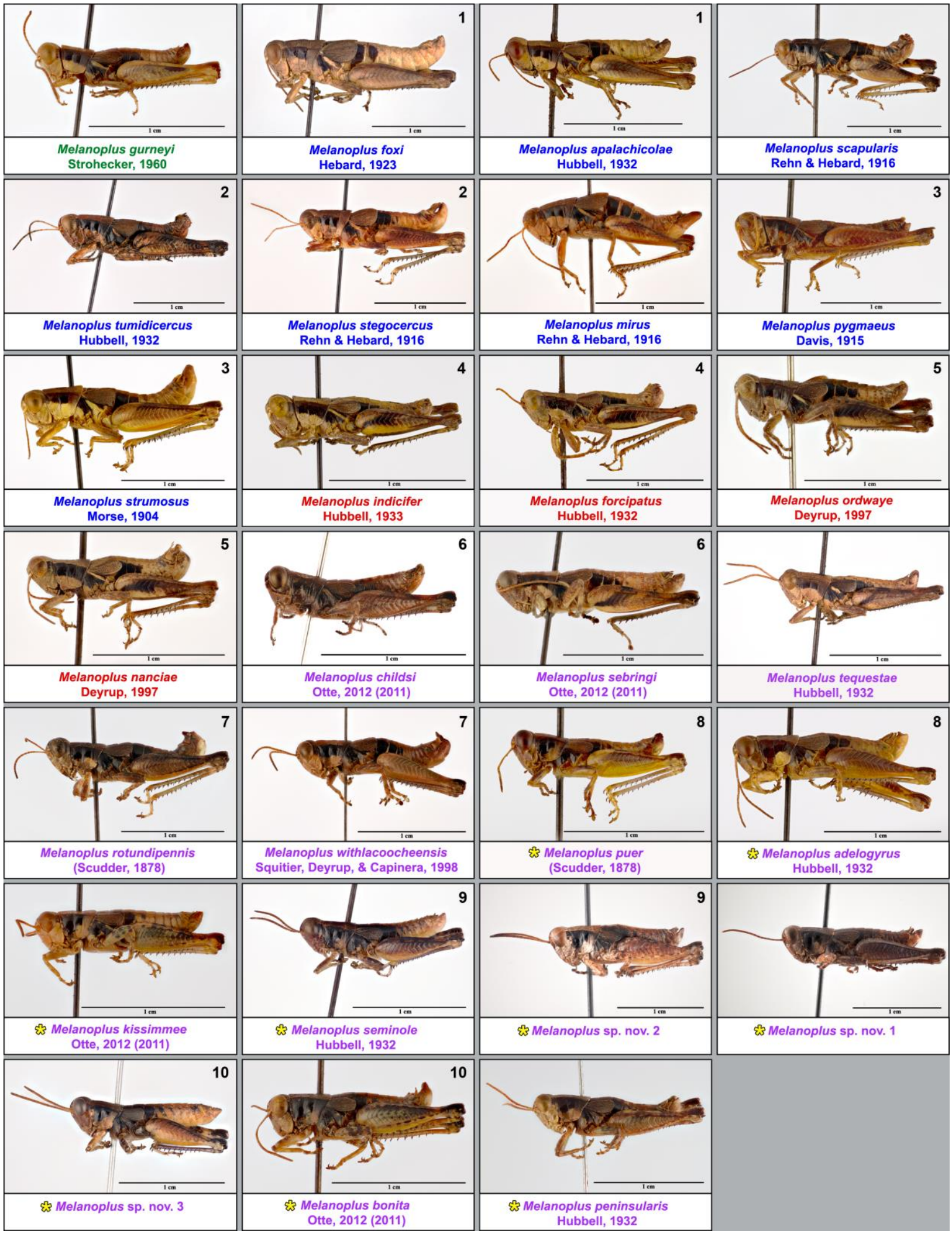

Figure 4-1. Left lateral habitus of adult males of all 27 species of the Puer Group. Note their cerci, which often differ and can aid in identifying species. Species are grouped and their names colored in accordance with their major lineage, and organized, from top to bottom and left to right, in descending order of the phylogenetic tips (Fig. 4-3). The numbers in the upper right hand corner of most images correspond with pairs of sister species (see Fig. 4-3). Puer Group sensu stricto species are identified by golden stars to the left of their names

which both sexes will disconnect and often try again elsewhere (Otte, 1970; Bland 1987; Woller and Song, 2017). Based on this, of the two leading hypotheses of genital evolution, the cryptic female choice hypothesis currently seems best-suited to explain the wildly divergent genitalia seen in the males of the PG species. The hypothesis posits that male genitalia are an internal courtship device in non-monogamous mating systems that conspecific females use to judge the quality of a male based on his genital shape and/or its related performance. Receptive females are then able to bias paternity following copulation in multiple ways (e.g., re-mating and sperm choice), which may result in offspring similarly equipped as the male fathers that were deemed to be superior (Eberhard, 1985; Eberhard, 1996; Hosken and Stockley, 2004; Briceno and Eberhard, 2009; Eberhard, 2009; Eberhard, 2010b; Simmons, 2014). This then suggests that observed morphological divergence could be a byproduct of Fisherian runaway selection (Lande, 1981; Kirkpatrick, 1982; West-Eberhard, 1983; Eberhard, 1985; Eberhard, 1996; Eberhard, 2010b; Song and Bucheli, 2010), which, by proxy, further implies that genital shapes will be more divergent in more closely related species (Lande, 1981; Eberhard, 1985; Eberhard, 1996; Hosken and Stockley, 2004; Eberhard, 2009; Eberhard, 2010a; Eberhard, 2010b; Song and Bucheli, 2010; Simmons, 2014). A number of empirical studies have examined the evolution of male genitalia from the context of cryptic female choice and are generally supportive of the hypothesis (Briceno and Eberhard, 2009; reviewed in Eberhard, 2009; and more recently in Firman et al., 2017).

For the plethora of reasons outlined, the males of the PG lend themselves extraordinarily well towards investigating the relative rate of evolution of genital

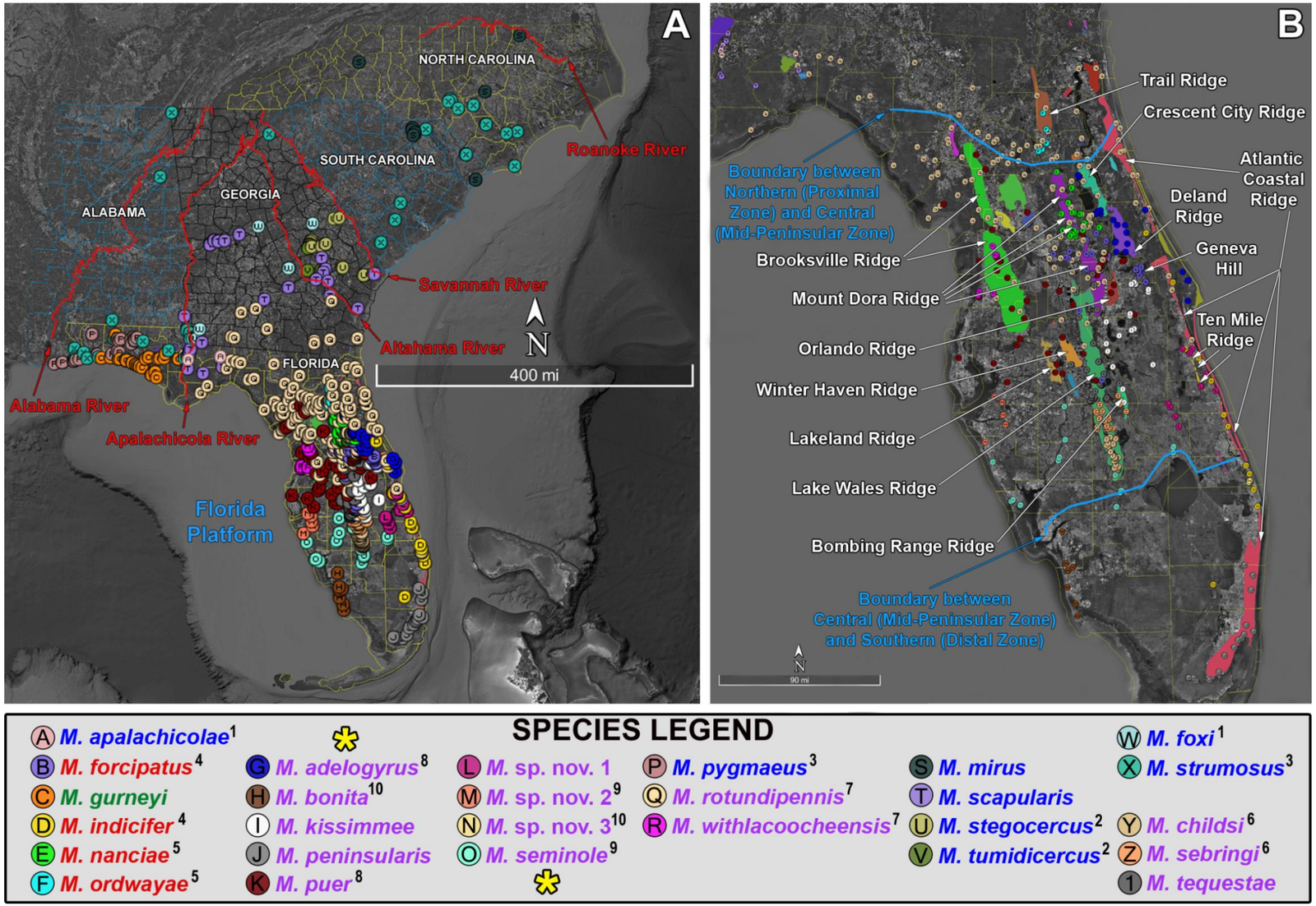

Figure 4-2. Modern-day geographical distributions of the Puer Group: A. The five states comprising the southeastern U.S.A. as defined in this study are identified along with the five major river boundaries dividing the species in the regions beyond peninsular Florida. The Florida Platform is labeled for increased understanding and is far beneath the ocean. B. Peninsular Florida, plus all of its major ridges and hills, with the 12 ridges and one hill labeled that are the focus of this study. Also included are the three major physiographic zones of this region (White, 1970). *The Species Legend is organized into columns according to historical subgroup in alpha order (see Table 4-1): 1 = Forcipatus Group, 2/3 = Puer Group sensu stricto (PGss) – bookended by golden stars, 4 = Rotundipennis Group, 5 = Scapularis Group, 6 = Strumosus and Tequestae Groups. Within each subgroup, species are in alpha order by specific name and colored by major lineage (see Fig. 4-3; Table 4-1). The superscript numbers correspond with pairs of sister species (see Fig. 4-3).

components, the degree of shape divergence among species, and the role (and its comparative impact) that sexual selection via cryptic female choice has played in the speciation of the group. If sexual selection is a primary driver of speciation in the PG overall, we can test the following hypotheses quantitatively with the aid of geometric morphometric analyses and the latest additions to the continually expanding phylogenetic comparative toolkit (Denton and Adams, 2015): 1) Different components of the male genitalia evolve at different rates and those components that are likely under strong sexual selection, such as intromittent structures (i.e., the aedeagal region), are evolving more rapidly relative to other components. 2) Due to Fisherian runaway selection, the male genitalia of sister species should be more divergent from each other compared to non-sister pairs in terms of evolutionary time. 3) If sexual selection is the primary driver of the recent and rapid radiation of the PGss clade, then the genitalia of its nine species should be the most divergent between each other relative to other PG species in terms of evolutionary time, as well as the most rapidly evolving genitalia overall.

Materials and Methods

Taxon and Character Sampling

We included an average of 10 specimens (a mix of recently collected and museum-curated) for each of the 27 species of the PG (Fig. 4-1; Table 4-1), representing, when possible, the full geographic range and intraspecific variation of each

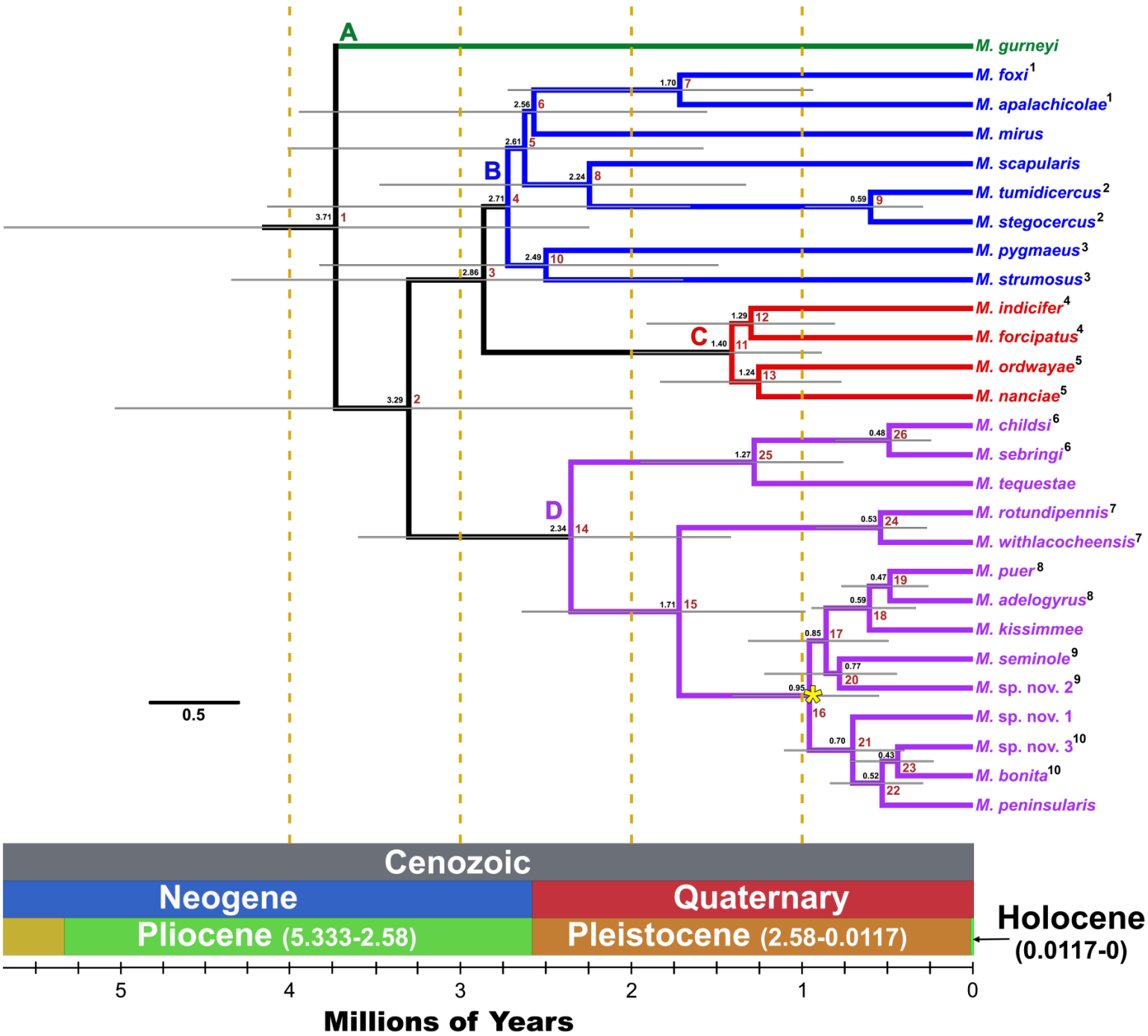

Figure 4-3. Bayesian-based divergence time estimation phylogeny that used the same genes from the concatenated approach. Nodal values to the left correspond with estimated divergence times while numbers to the right correspond with those in the phylomorphospaces (Figs. 4-22 to 4-28). The nodal bars are relative confidence intervals. Major lineages of the Puer Group and their species are color-coded accordingly while the outgroups are in grey. Lineage D's Puer Group sensu stricto (PGss) is identified with a golden star. Sister species are identified by paired superscript numbers to the right of their names.

species (Fig. 4-2). We chose these candidate specimens from a pool of 6,522 across 17 collections (representing almost all known PG specimens). Six anatomical components, the relative positions in which they were imaged, and the numbers quantified of each using landmark-based geometric morphometric methods (e.g., see Denton and Adams, 2015) were as follows (some components were not represented by all 266 specimens due to damaged or missing components) (Fig. 4-4): **external genitalia: 1)** left lateral view of cercus (n = 265); and **internal genitalia: 2)** left lateral view of ectophallus (n = 265), **3)** left half of epiphallus in dorsal view (n = 266) – note that this view includes the lophus in part, but does not fully capture its diversity, **4)** left lophus from posterior view and at 45° angle tilted anteriorly to capture the majority of its diversity (n = 266), and **5)** left lateral view of aedeagal region (n = 262); and **external, non-genitalic character: 6)** left lateral view of tegmen (n = 265). It should be noted that the aedeagal region was chosen as a whole due to the high variability of its four individual components (dorsal and ventral valves of aeadeagus, arch of aedeagus, and sheath of aedeagus) among the PG species and the degree of difficulty involved in delimiting these components for some species. This, in turn, also makes it problematic to identify homologous landmarks on the separate components, but, as a whole, such landmarking is possible. The lateral view of the aedeagal region (the leftmost apical portion of the endo/ectophallus in Fig. 4-5) is also not the most ideal because it fails to fully capture the intricate apices of the valves of aedeagus because they are often twisting in multiple directions. Micro-computed tomography (micro-CT) for 3D geometric morphometrics was the only other option, but the 2D left lateral view of the aedeagal region was deemed to be the least time-intensive

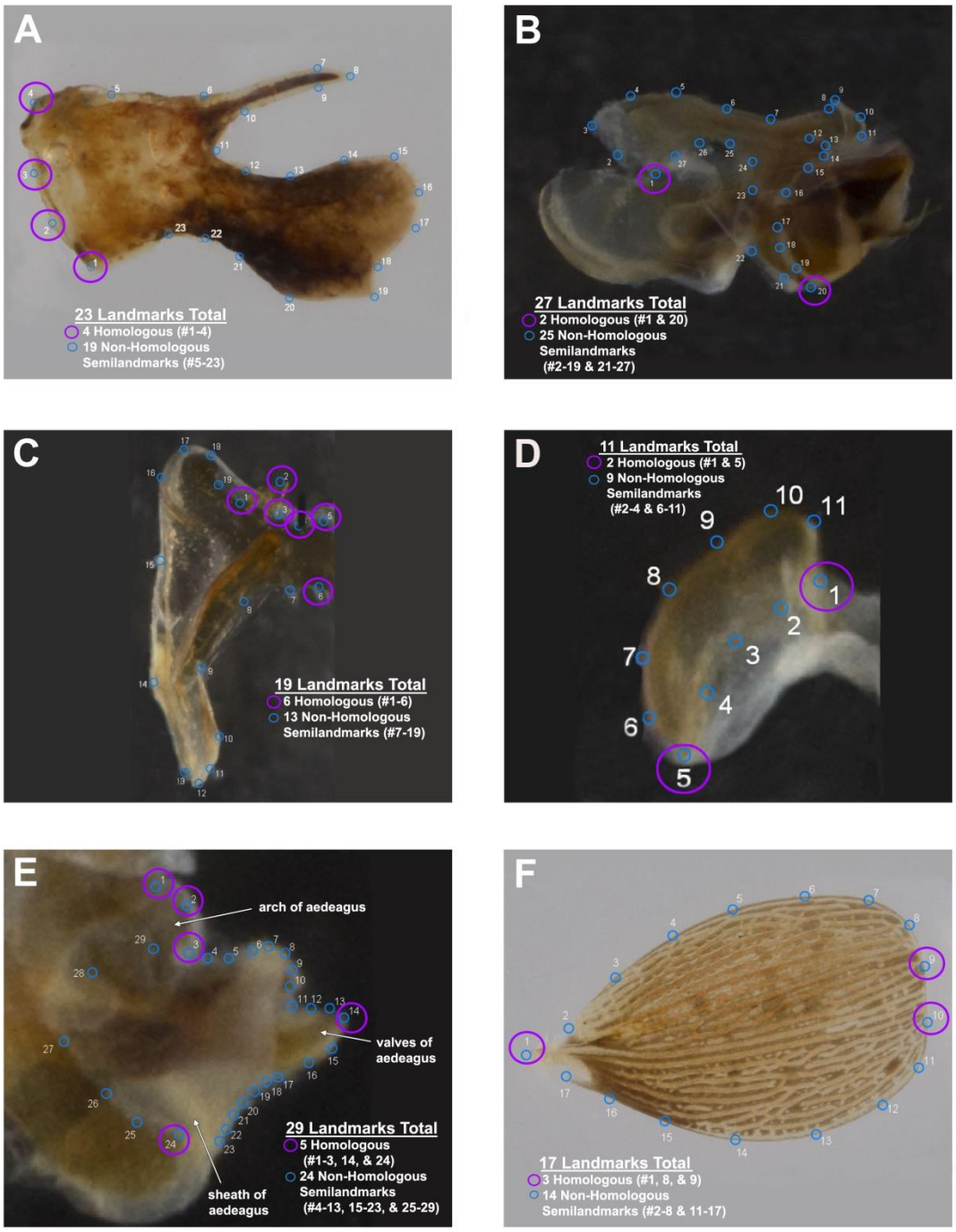

Figure 4-4. Exemplar specimens displaying the landmarks utilized for all specimens (see full list in Table 4-1) included in the geometric morphometrics analyses for each of the six shapes: **A.** cercus, **B.** ectophallus, **C.** epiphallus, **D.** lophus, **E.** aedeagal region, and **F.** tegmen.

and cost-effective, and the results strongly indicate that enough of the observed diversity was captured effectively.

For dissections, museum specimens were rehydrated by being dipped briefly into boiling water while recently collected specimens were placed into a -20° C freezer as they were collected. Dissecting scissors were used to remove the tegmen and cercus while the internal genitalia (phallic complex) were removed from the body using standard dissecting procedures for male grasshoppers (Hubbell, 1932) and the assistance of a Leica MZ16 microscope system. Dissected phallic complexes were put in 0.65 ml vials containing a 10% KOH solution and placed into a boiling water bath in batches of 10 vials for up to an hour to clear away obstructing tissues. The cleared components were then removed and examined further using the microscope to verify species identity before including in the study, and were then preserved in glycerin and kept with the original specimens.

The robust divergence time estimation phylogeny of the PG (Fig. 4-3) and maps (Fig. 4-2) were generated for Chapter II and used in all geometric morphometric analyses that incorporated phylogeny. We excluded the phylogeny's outgroup species from our geometric morphometric analyses because their distant relationships with each other and to the PG biased the results in the preliminary analyses we conducted.

Imaging

A mix of specimens that were recently collected and preserved in museum collections were used to image the full external lateral view and internal genitalia

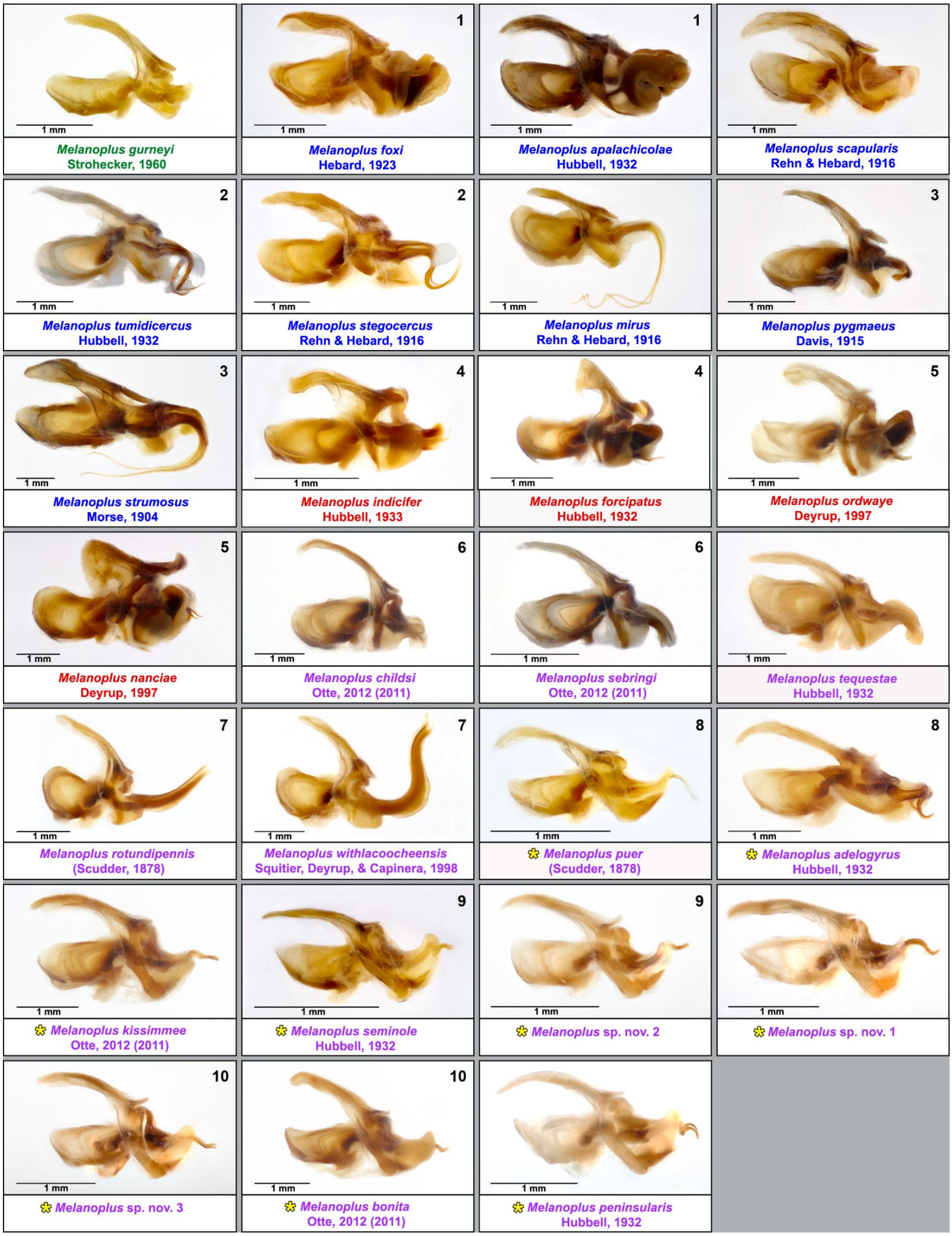

Figure 4-5. The extraordinary diversity present in the internal genitalia of the 27 species of the Puer Group. The right-most apical portion of wildly diverging shapes is the aedeagus, the most obvious component of the aedeagal region (see Fig. 4-4E), and which is one of the primary characters used to identify species. Species are grouped and their names colored in accordance with their major lineage, and organized, from top to bottom and left to right, in descending order of the phylogenetic tips (Fig. 4-3). The numbers in the upper right hand corner of most images correspond with pairs of sister species (see Fig. 4-3). Puer Group *sensu stricto* species are identified by golden stars to the left of their names.

representing adult males of each species (Figs 4-1 and 4-2; Table 4-1). Photography was done in the Song Laboratory of Insect Systematics and Evolution using a Visionary Digital imaging system equipped with a Canon EOS 6D DSLR camera combined with a 100mm or an MP-E 65mm lens (the latter often coupled with a 2x magnifier) to take multiple images at different focal lengths. The resulting files were converted from RAW to TIFF format using Adobe Lightroom (v.4.4), stacked into a single composite image using Zerene Stacker (v.1.04), and then Adobe Photoshop CS6 Extended was used to add a scale bar and, as needed, adjust light levels, background coloration, and sharpness.

For the single-shot images from which landmark data were acquired, the MP-E 65mm lens was used due to the very small nature of the anatomical components involved and all images for each shape were captured at the same scale to enable easier landmarking. When possible, each species had its complete set of components for each shape imaged simultaneously for more rapid processing. For the tegmen and cercus, this entailed spreading a thin layer of hand sanitizer (to aid in arrangement and prevent loss) on a standard slide in a consistent 3x4 arrangement to prevent specimen confusion. In the case of the cercus, a second slide was placed on top to flatten the components in order to capture the maximum dimensions of the shapes because they often bend inwards when attached to the body. All PG tegmina are slightly convex, so the tegmen component was allowed to remain unflattened in order to retain as much of the actual dimensions of the shapes as possible. The remaining four components belong to the internal genitalia and were imaged in a similar manner to the tegmina and cerci, but were

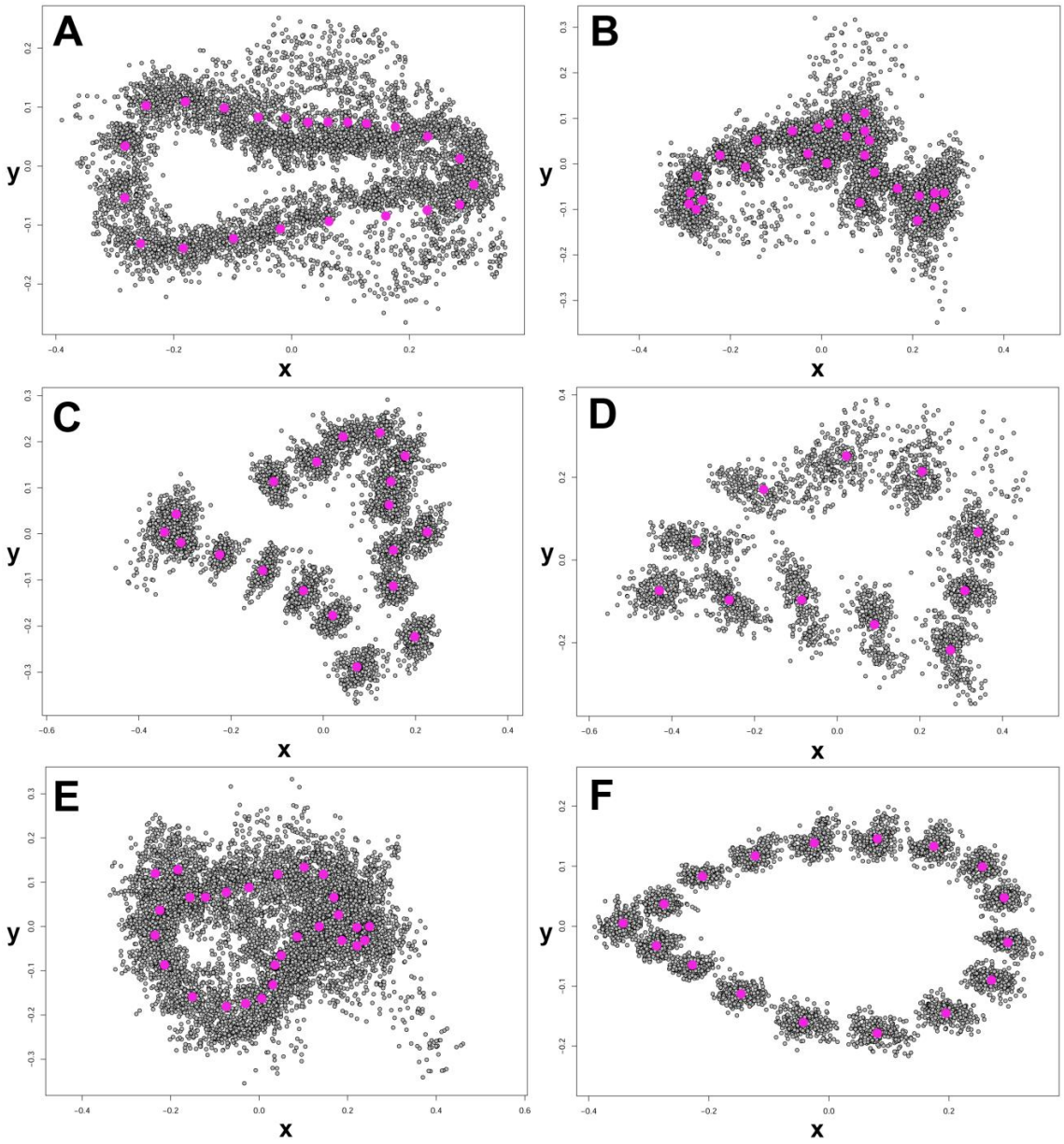

Figure 4-6. Results from the generalized Procrustes analyses (GPA) for each of the six shapes: **A.** cercus, **B.** ectophallus, **C.** epiphallus, **D.** lophus, **E.** aedeagal region, and **F.** tegmen. Note that C and D have been rotated about 90° clockwise (see Fig. 4-4C and D for comparison).

embedded in hand sanitizer within a micro watch glass and covered with 100% ethanol to create a glassy layer for optimal imaging. In rare cases, the damaged anatomical

components of some specimens were replaced with their mirrored counterparts (Table 4-1).

For all shape sets, only a single image at an optimal focus level was necessary to see the details required to assign landmarks. After completing all imaging, species sets were virtually divided up in Photoshop into individual specimen photos for each shape set. Additionally, Photoshop was used to adjust contrast as needed and orient replaced components in a manner that matched all others in a shape set.

Geometric Morphometric Analyses

Landmarks were assigned separately to each shape set using the thin plate spline (TPS) suite (Rohlf, 2017), specifically the modules tps Utility program (tpsUtil, v.1.74) and Relative warps (tpsRelw, v.1.67). The geomorph package (v.3.0.5) (Adams et al., 2017) for R was then used to assign semilandmarks ("sliders", landmarks that are not necessarily homologous) and run all of the subsequent analyses. Semilandmarks were slid by minimizing bending energy due to the relatively high amount of variation apparent in the majority of the shape sets (Gunz and Mitteroecker, 2013). The number of total landmarks (homologous landmarks + semilandmarks) for the six shapes are as follows (Fig. 4-4): **1)** tegmen: 17 (3 +14), **2)** cercus: 23 (4+19), **3)** epiphallus: 19 (6+13), **4)** lophus: 11 (2+9), **5)** ectophallus: 27 (2+25), and **6)** aedeagal region: 29 (5+ 24).

For each shape, a number of analyses were undertaken separately and together, beginning with the superimposition method known as generalized Procrustes analysis (GPA) (function "gpagen" in geomorph) that forms the basis for all subsequent analyses.

GPA translates the original coordinates of all specimen shapes to the origin in "morphospace" and uses unit centroid size to scale them (to remove size biases). Then, GPA rotates each shape around the origin (the consensus shape position) with a least-squares criterion in order to minimize shape differences by optimally aligning corresponding points relative to the consensus shape and included specimens (akin to fitting points to a regression line) (Webster and Sheets, 2010; Adams et al., 2013; Klingenberg, 2013). The resulting Procrustes tangent coordinates (Fig. 4-6) were treated as a set of shape variables for each specimen, with the means of these coordinates calculated for each species for use in later analyses. Next, Principal Components Analyses (PCA) (function "plottangentspace") were performed for all the GPA-aligned specimens for each species. After calculating residuals, a PCA essentially rotates the GPA data around the axis in morphospace in order to remove correlations and plot the axes (each is a shape variable) of greatest variation against each other (Polly, 2013) (Figs 4-7 to 4-12; Table 4-2).

Morphological disparity (function "morphol.disparity") was then calculated for each shape set by utilizing the absolute differences in Procrustes variances as test statistics to calculate overall relative disparity values for each species compared to the consensus shape and build pairwise comparison matrices of all species (Adams et al., 2017) (Figs 4-13B to 4-18B; Tables 4-3 and 4-4). Pairwise calculation of morphological disparity over time was then calculated in Microsoft Excel by dividing the previous disparity values by the most recent estimated age of divergence between each species comparison using the dated phylogeny (Figs 4-3 and 4-13B to 4-18B).

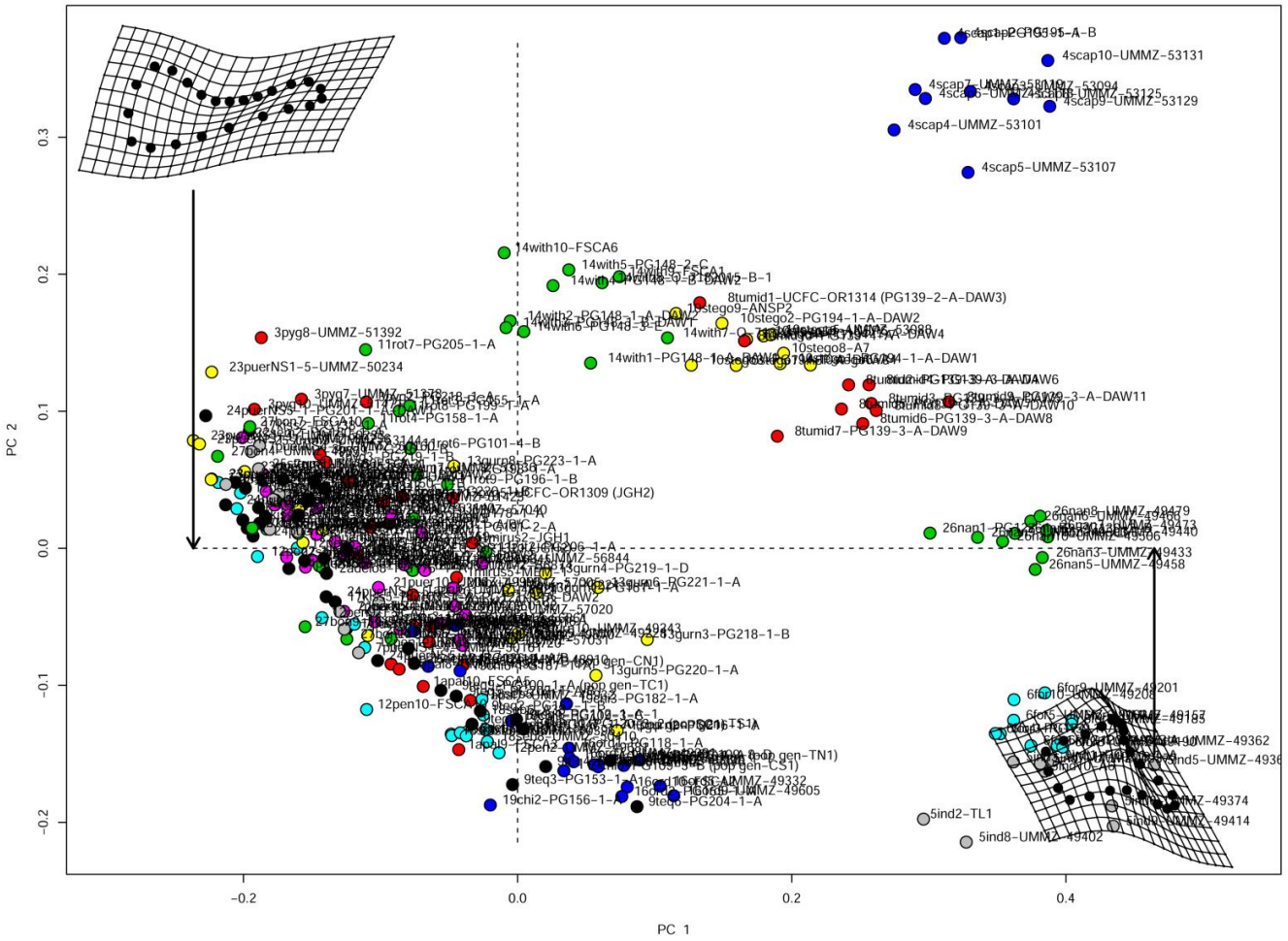

Figure 4-7. Individual specimen results from principal components analysis (PCA) for the cercus (PC1 vs. PC2). Species were randomly color-coded by the R package *geomorph* and the specimen names are codes used to identify each individual.

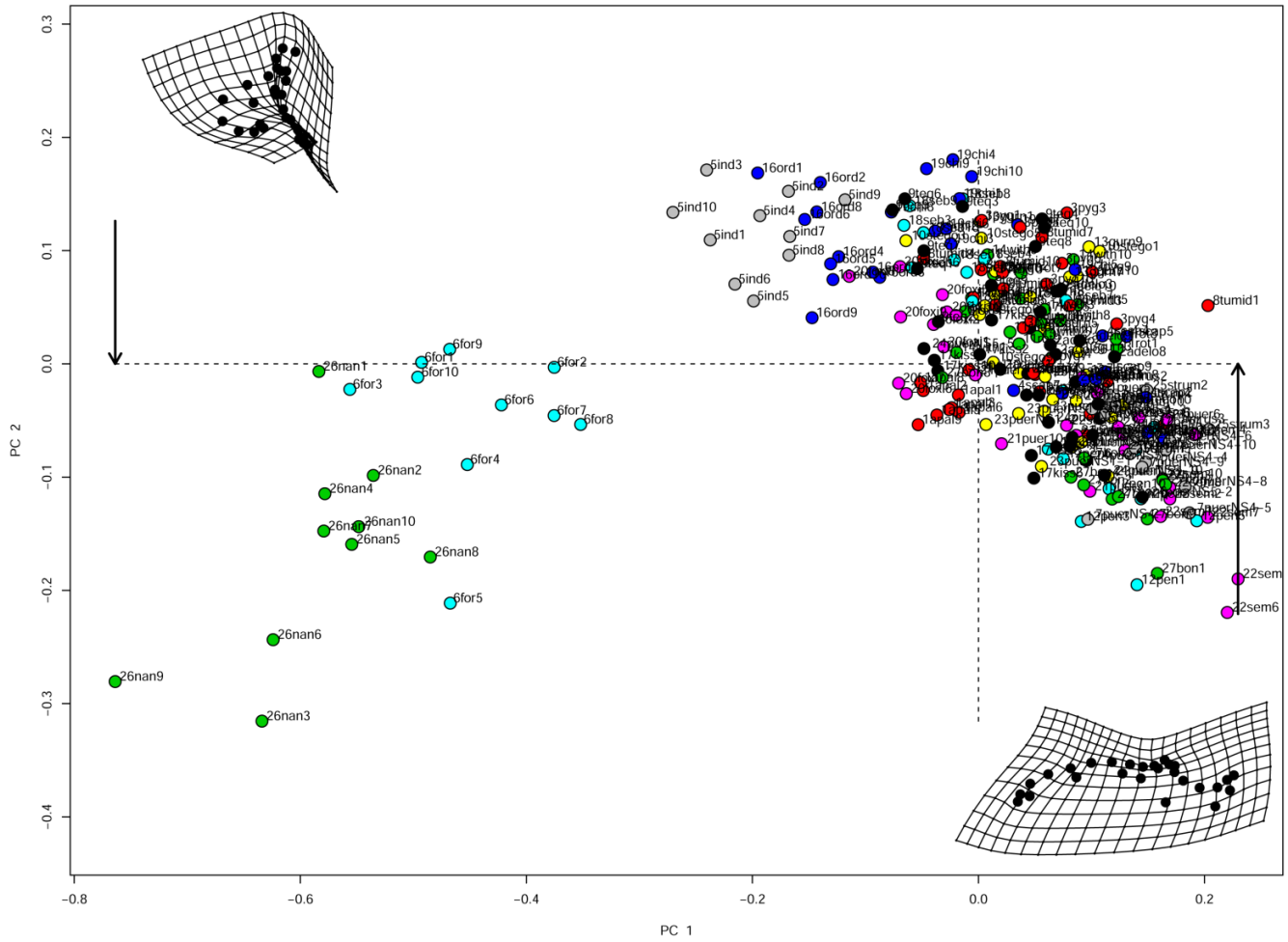

Figure 4-8. Individual specimen results from principal components analysis (PCA) for the ectophallus (PC1 vs. PC2). Species were randomly color-coded by the R package *geomorph* and the specimen names are codes used to identify each individual.

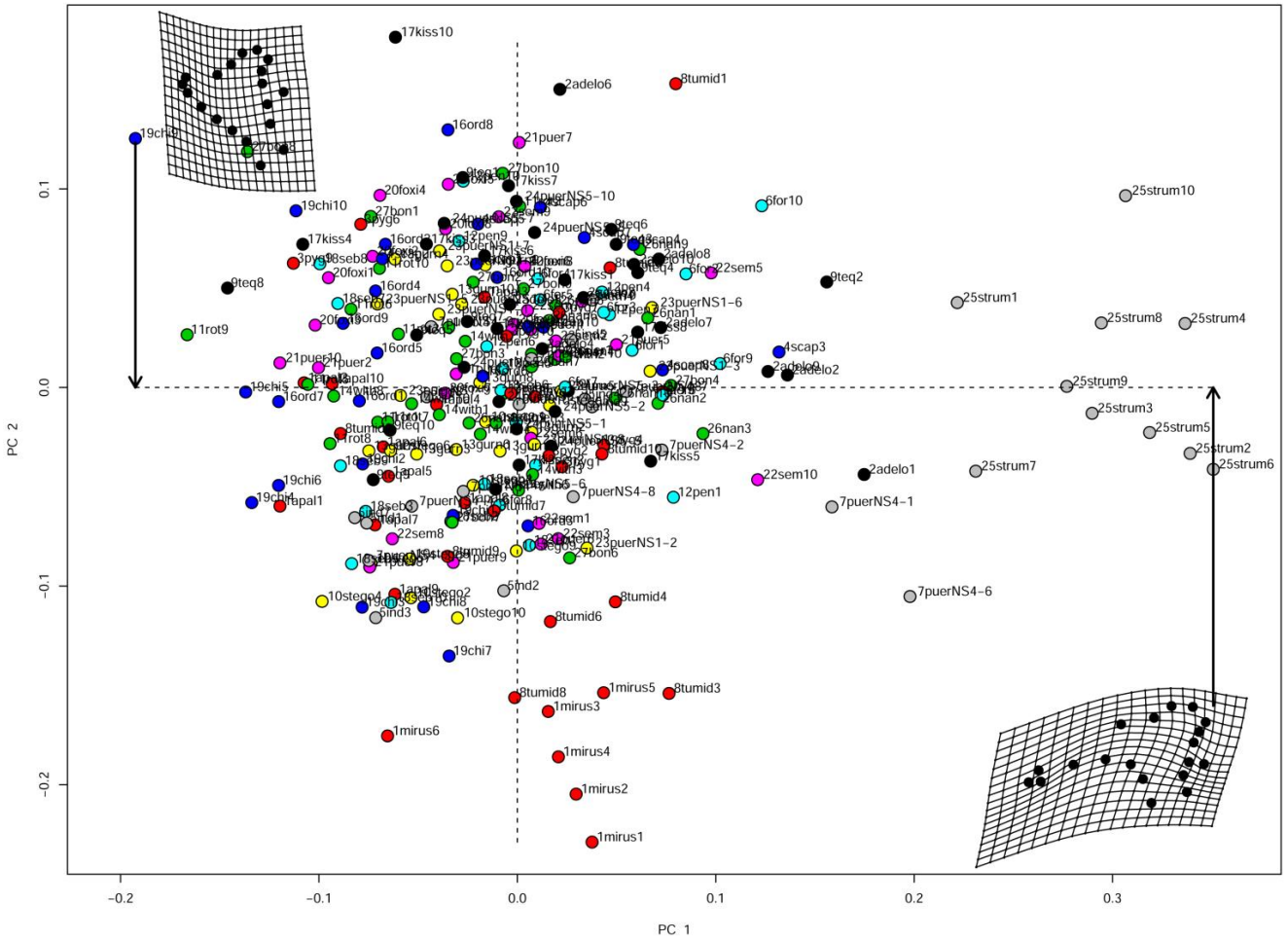

Figure 4-9. Individual specimen results from principal components analysis (PCA) for the epiphallus (PC1 vs. PC2). Species were randomly color-coded by the R package *geomorph* and the specimen names are codes used to identify each individual.

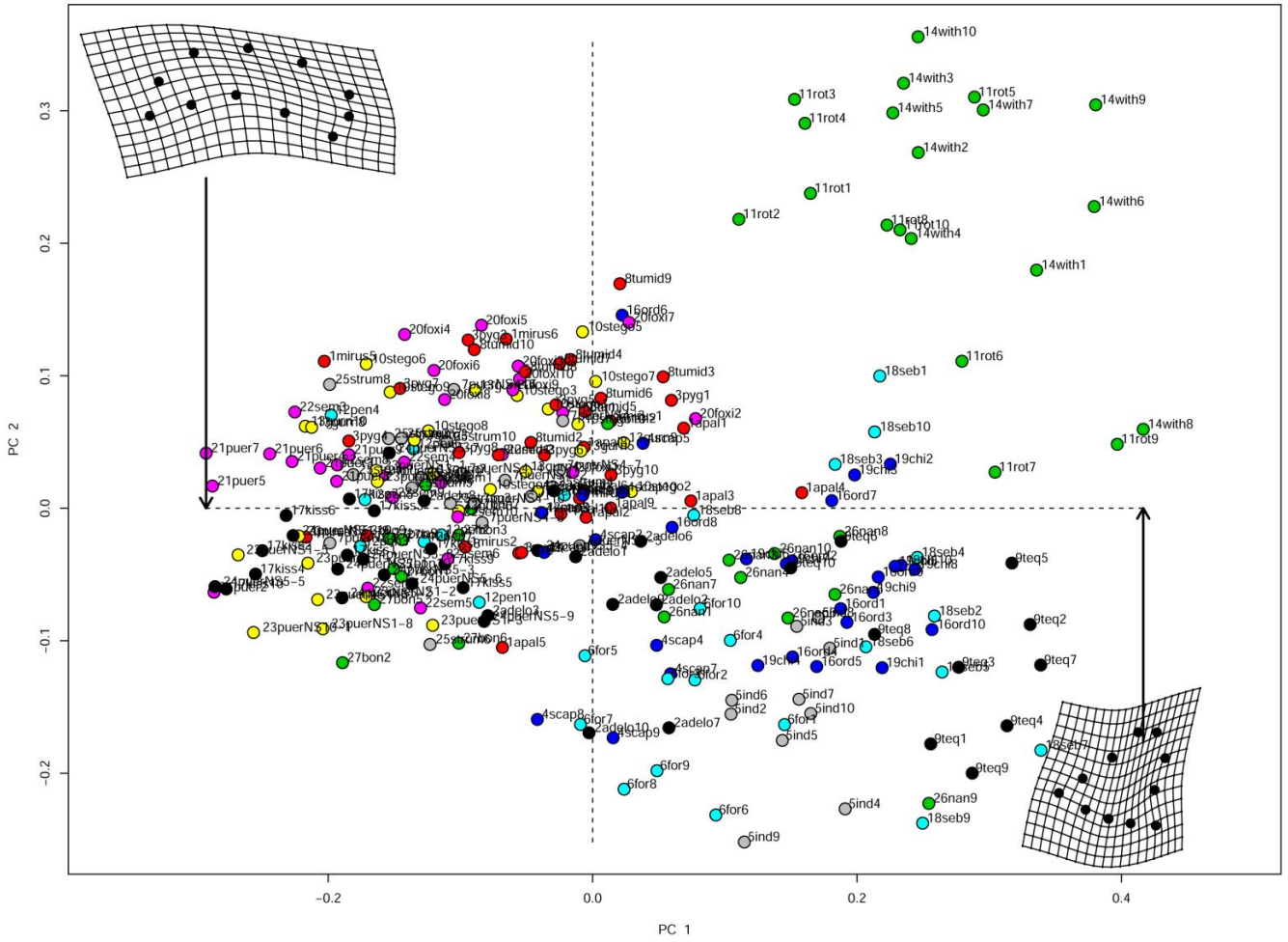

Figure 4-10. Individual specimen results from principal components analysis (PCA) for the lophus (PC1 vs. PC2). Species were randomly color-coded by the R package *geomorph* and the specimen names are codes used to identify each individual.

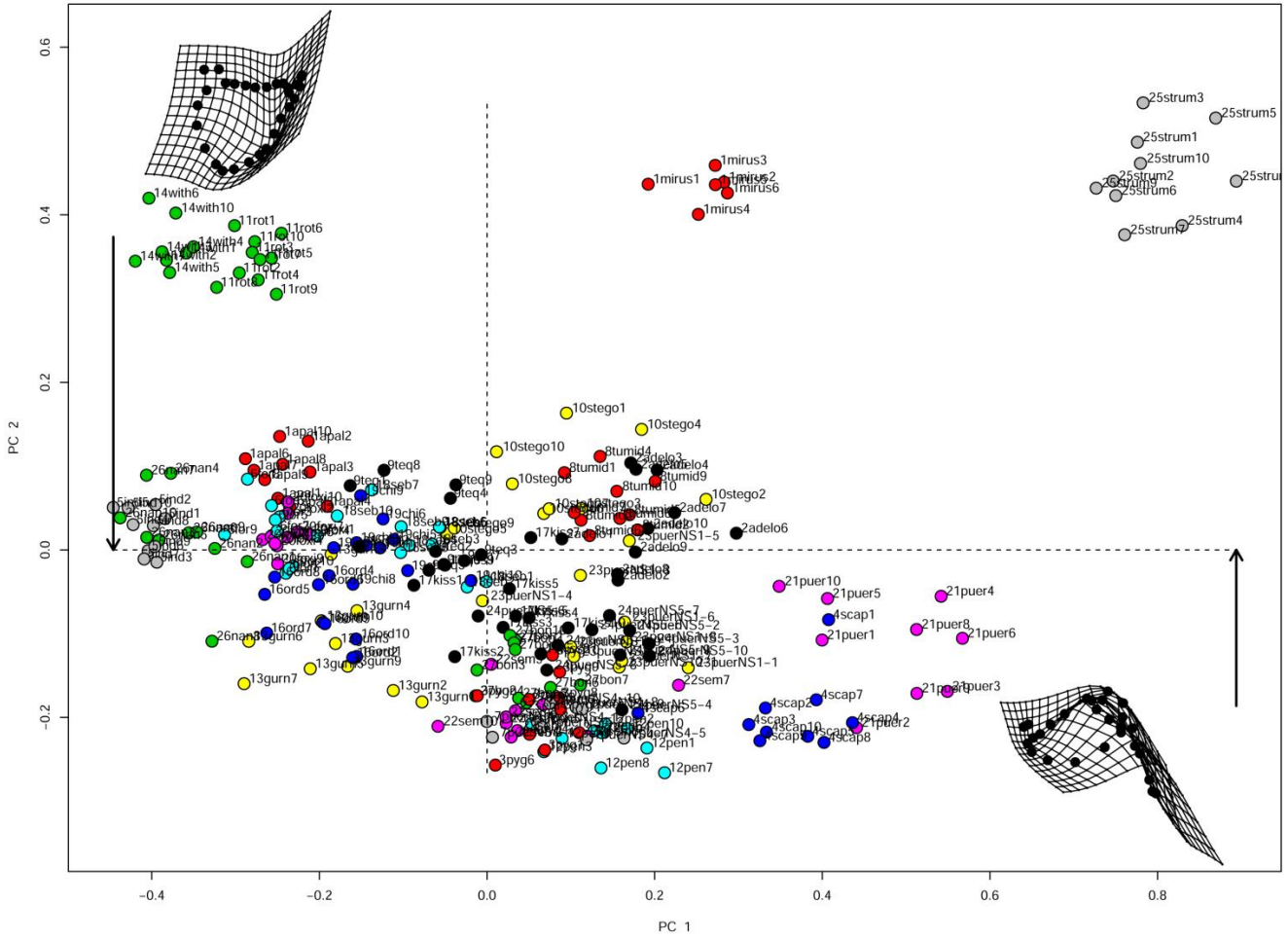

Figure 4-11. Individual specimen results from principal components analysis (PCA) for the aedeagal region (PC1 vs. PC2). Species were randomly color-coded by the R package *geomorph* and the specimen names are codes used to identify each individual.

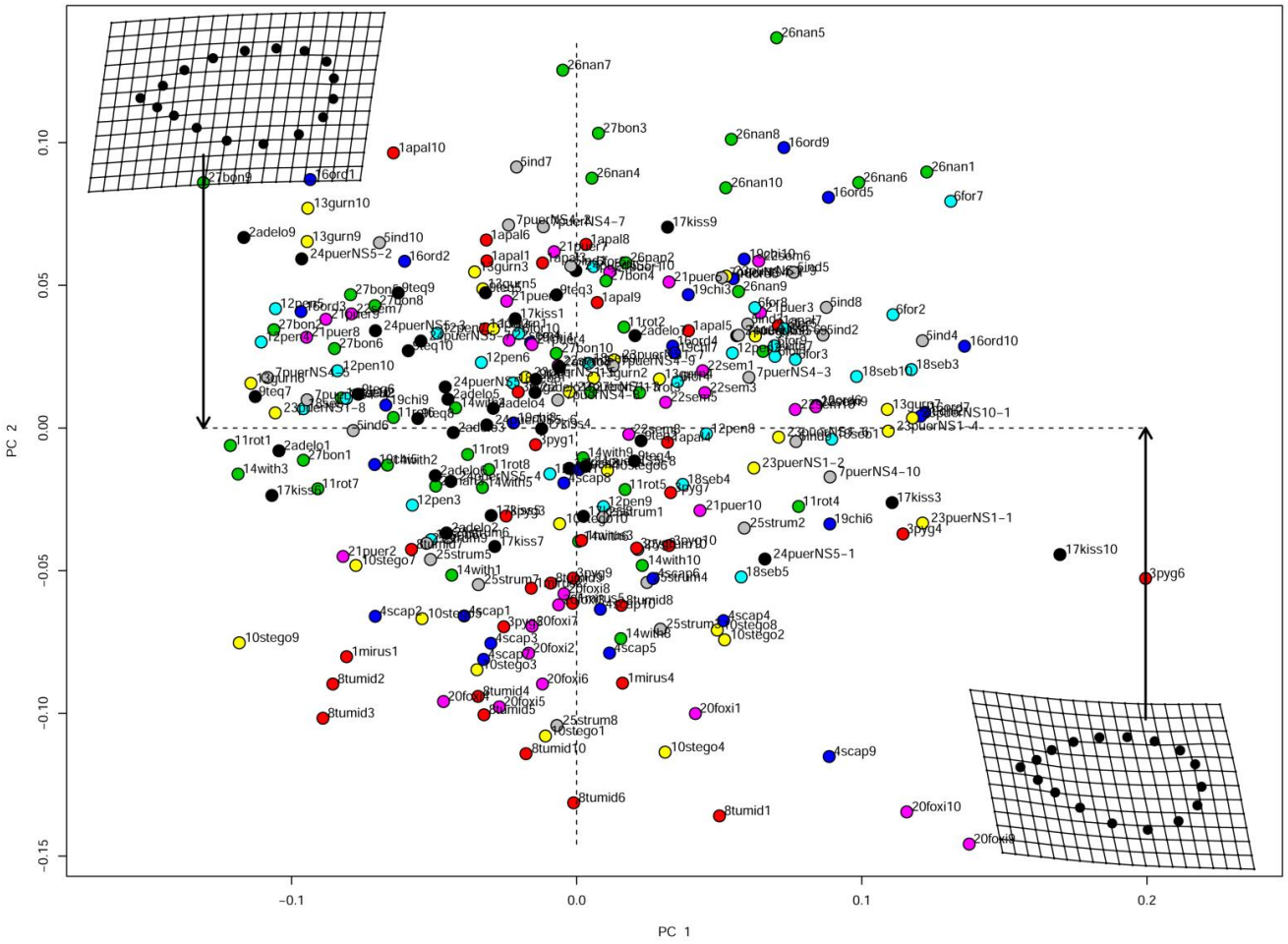

Figure 4-12. Individual specimen results from principal components analysis (PCA) for the tegmen (PC1 vs. PC2). Species were randomly color-coded by the R package *geomorph* and the specimen names are codes used to identify each individual.

Table 4-2. Principal components (PC) for all six shapes, with PC1 and 2 in bold because their associated Proportion of Variance values are displayed in Figs. 4-23 to 4-28: **A.** PC 1-17; **B.** PC 18-34; **C.** PC 35-51.

A

SHAPE		PC1	PC2	PC3	PC4	PC5	PC6	PC7	PC8	PC9	PC10	PC11	PC12	PC13	PC14	PC15	PC16	PC17
Cercus	Standard deviation	**0.1897**	**0.1166**	0.0919	0.0557	0.0505	0.0406	0.0340	0.0272	0.0234	0.0212	0.0175	0.0133	0.0121	0.0109	0.0101	0.0091	0.0076
	Proportion of Variance	**0.5179**	**0.1956**	0.1215	0.0446	0.0367	0.0238	0.0166	0.0106	0.0079	0.0065	0.0044	0.0025	0.0021	0.0017	0.0015	0.0012	0.0008
	Cumulative Proportion	**0.5179**	**0.7134**	0.8349	0.8796	0.9162	0.9400	0.9566	0.9672	0.9751	0.9816	0.9860	0.9885	0.9906	0.9923	0.9938	0.9950	0.9958
Ectophallus	Standard deviation	**0.1754**	**0.0901**	0.0571	0.0519	0.0398	0.0350	0.0289	0.0255	0.0225	0.0198	0.0179	0.0165	0.0142	0.0125	0.0120	0.0119	0.0112
	Proportion of Variance	**0.5917**	**0.1561**	0.0626	0.0519	0.0304	0.0235	0.0161	0.0125	0.0097	0.0075	0.0062	0.0052	0.0039	0.0030	0.0028	0.0027	0.0024
	Cumulative Proportion	**0.5917**	**0.7478**	0.8105	0.8623	0.8928	0.9163	0.9323	0.9449	0.9546	0.9621	0.9683	0.9735	0.9774	0.9804	0.9832	0.9859	0.9883
Epiphallus	Standard deviation	**0.0849**	**0.0661**	0.0470	0.0387	0.0351	0.0277	0.0228	0.0220	0.0201	0.0180	0.0172	0.0140	0.0135	0.0126	0.0117	0.0101	0.0093
	Proportion of Variance	**0.3507**	**0.2125**	0.1076	0.0729	0.0600	0.0373	0.0253	0.0236	0.0197	0.0158	0.0145	0.0095	0.0088	0.0077	0.0066	0.0050	0.0042
	Cumulative Proportion	**0.3507**	**0.5632**	0.6708	0.7437	0.8037	0.8410	0.8663	0.8900	0.9097	0.9255	0.9399	0.9494	0.9582	0.9659	0.9725	0.9775	0.9817
Lophus	Standard deviation	**0.1642**	**0.1058**	0.0571	0.0428	0.0361	0.0250	0.0207	0.0180	0.0166	0.0128	0.0103	0.0089	0.0072	0.0053	0.0038	0.0027	0.0024
	Proportion of Variance	**0.5777**	**0.2399**	0.0699	0.0392	0.0280	0.0134	0.0092	0.0069	0.0059	0.0035	0.0023	0.0017	0.0011	0.0006	0.0003	0.0002	0.0001
	Cumulative Proportion	**0.5777**	**0.8176**	0.8875	0.9267	0.9547	0.9681	0.9773	0.9842	0.9901	0.9936	0.9959	0.9976	0.9987	0.9993	0.9996	0.9998	0.9999
Aedeagal Region	Standard deviation	**0.2743**	**0.1837**	0.1592	0.1054	0.0961	0.0728	0.0694	0.0574	0.0520	0.0461	0.0407	0.0385	0.0305	0.0302	0.0263	0.0230	0.0197
	Proportion of Variance	**0.4144**	**0.1858**	0.1396	0.0612	0.0508	0.0292	0.0265	0.0181	0.0149	0.0117	0.0091	0.0081	0.0051	0.0050	0.0038	0.0029	0.0021
	Cumulative Proportion	**0.4144**	**0.6002**	0.7398	0.8010	0.8518	0.8809	0.9075	0.9256	0.9404	0.9521	0.9613	0.9694	0.9745	0.9796	0.9834	0.9863	0.9884
Tegmen	Standard deviation	**0.0636**	**0.0525**	0.0404	0.0180	0.0154	0.0105	0.0098	0.0084	0.0067	0.0063	0.0054	0.0046	0.0045	0.0034	0.0032	0.0030	0.0025
	Proportion of Variance	**0.4268**	**0.2910**	0.1721	0.0341	0.0248	0.0117	0.0101	0.0075	0.0048	0.0042	0.0031	0.0023	0.0021	0.0012	0.0011	0.0009	0.0007
	Cumulative Proportion	**0.4268**	**0.7178**	0.8899	0.9240	0.9488	0.9605	0.9706	0.9781	0.9829	0.9871	0.9902	0.9925	0.9946	0.9958	0.9968	0.9978	0.9985

B

SHAPE		PC18	PC19	PC20	PC21	PC22	PC23	PC24	PC25	PC26	PC27	PC28	PC29	PC30	PC31	PC32	PC33	PC34
Cercus	Standard deviation	0.0068	0.0060	0.0054	0.0051	0.0050	0.0048	0.0044	0.0037	0.0034	0.0031	0.0028	0.0027	0.0026	0.0023	0.0021	0.0020	0.0018
	Proportion of Variance	0.0007	0.0005	0.0004	0.0004	0.0004	0.0003	0.0003	0.0002	0.0002	0.0001	0.0001	0.0001	0.0001	0.0001	0.0001	0.0001	0.0001
	Cumulative Proportion	0.9965	0.9970	0.9974	0.9978	0.9982	0.9985	0.9988	0.9990	0.9992	0.9993	0.9994	0.9995	0.9996	0.9997	0.9997	0.9998	0.9998
Ectophallus	Standard deviation	0.0103	0.0092	0.0083	0.0078	0.0070	0.0063	0.0059	0.0053	0.0048	0.0040	0.0037	0.0037	0.0031	0.0029	0.0027	0.0026	0.0025
	Proportion of Variance	0.0021	0.0016	0.0013	0.0012	0.0009	0.0008	0.0007	0.0006	0.0004	0.0003	0.0003	0.0003	0.0002	0.0002	0.0001	0.0001	0.0001
	Cumulative Proportion	0.9904	0.9920	0.9933	0.9945	0.9954	0.9962	0.9968	0.9974	0.9978	0.9981	0.9984	0.9987	0.9989	0.9990	0.9992	0.9993	0.9994
Epiphallus	Standard deviation	0.0085	0.0082	0.0077	0.0068	0.0058	0.0054	0.0048	0.0037	0.0033	0.0028	0.0019	0.0017	0.0016	0.0012	0.0010	0.0007	N/A
	Proportion of Variance	0.0035	0.0033	0.0029	0.0022	0.0016	0.0014	0.0011	0.0007	0.0005	0.0004	0.0002	0.0001	0.0001	0.0001	0.0001	0.0000	N/A
	Cumulative Proportion	0.9852	0.9885	0.9914	0.9936	0.9953	0.9967	0.9978	0.9985	0.9990	0.9994	0.9996	0.9997	0.9998	0.9999	0.9999	1.0000	N/A
Lophus	Standard deviation	0.0015	N/A	N/A	N/A	N/A	N/A	N/A	N/A	N/A	N/A	N/A	N/A	N/A	N/A	N/A	N/A	N/A
	Proportion of Variance	0.0001	N/A	N/A	N/A	N/A	N/A	N/A	N/A	N/A	N/A	N/A	N/A	N/A	N/A	N/A	N/A	N/A
	Cumulative Proportion	1.0000	N/A	N/A	N/A	N/A	N/A	N/A	N/A	N/A	N/A	N/A	N/A	N/A	N/A	N/A	N/A	N/A
Aedeagal Region	Standard deviation	0.0184	0.0164	0.0154	0.0130	0.0122	0.0114	0.0097	0.0092	0.0091	0.0088	0.0080	0.0072	0.0066	0.0062	0.0061	0.0059	0.0051
	Proportion of Variance	0.0019	0.0015	0.0013	0.0009	0.0008	0.0007	0.0005	0.0005	0.0005	0.0004	0.0004	0.0003	0.0002	0.0002	0.0002	0.0002	0.0001
	Cumulative Proportion	0.9903	0.9917	0.9930	0.9940	0.9948	0.9955	0.9960	0.9965	0.9969	0.9974	0.9977	0.9980	0.9982	0.9985	0.9987	0.9989	0.9990
Tegmen	Standard deviation	0.0025	0.0019	0.0017	0.0009	0.0006	0.0005	0.0005	N/A	N/A	N/A	N/A	N/A	N/A	N/A	N/A	N/A	N/A
	Proportion of Variance	0.0007	0.0004	0.0003	0.0001	0.0000	0.0000	0.0000	N/A	N/A	N/A	N/A	N/A	N/A	N/A	N/A	N/A	N/A
	Cumulative Proportion	0.9991	0.9995	0.9998	0.9999	0.9999	0.9999	1.0000	N/A	N/A	N/A	N/A	N/A	N/A	N/A	N/A	N/A	N/A

C

SHAPE		PC35	PC36	PC37	PC38	PC39	PC40	PC41	PC42	PC43	PC44	PC45	PC46	PC47	PC48	PC49	PC50	PC51
Cercus	Standard deviation	0.0016	0.0014	0.0013	0.0012	N/A	N/A	N/A	N/A	N/A	N/A	N/A	N/A	N/A	N/A	N/A	N/A	N/A
	Proportion of Variance	0.0000	0.0000	0.0000	0.0000	N/A	N/A	N/A	N/A	N/A	N/A	N/A	N/A	N/A	N/A	N/A	N/A	N/A
	Cumulative Proportion	0.9999	0.9999	0.9999	1.0000	N/A	N/A	N/A	N/A	N/A	N/A	N/A	N/A	N/A	N/A	N/A	N/A	N/A
Ectophallus	Standard deviation	0.0022	0.0021	0.0019	0.0018	0.0016	0.0016	0.0013	0.0012	0.0011	0.0010	0.0009	0.0009	N/A	N/A	N/A	N/A	N/A
	Proportion of Variance	0.0001	0.0001	0.0001	0.0001	0.0001	0.0001	0.0000	0.0000	0.0000	0.0000	0.0000	0.0000	N/A	N/A	N/A	N/A	N/A
	Cumulative Proportion	0.9995	0.9996	0.9997	0.9997	0.9998	0.9998	0.9999	0.9999	0.9999	0.9999	0.9999	1.0000	N/A	N/A	N/A	N/A	N/A
Epiphallus	Standard deviation	N/A	N/A	N/A	N/A	N/A	N/A	N/A	N/A	N/A	N/A	N/A	N/A	N/A	N/A	N/A	N/A	N/A
	Proportion of Variance	N/A	N/A	N/A	N/A	N/A	N/A	N/A	N/A	N/A	N/A	N/A	N/A	N/A	N/A	N/A	N/A	N/A
	Cumulative Proportion	N/A	N/A	N/A	N/A	N/A	N/A	N/A	N/A	N/A	N/A	N/A	N/A	N/A	N/A	N/A	N/A	N/A
Lophus	Standard deviation	N/A	N/A	N/A	N/A	N/A	N/A	N/A	N/A	N/A	N/A	N/A	N/A	N/A	N/A	N/A	N/A	N/A
	Proportion of Variance	N/A	N/A	N/A	N/A	N/A	N/A	N/A	N/A	N/A	N/A	N/A	N/A	N/A	N/A	N/A	N/A	N/A
	Cumulative Proportion	N/A	N/A	N/A	N/A	N/A	N/A	N/A	N/A	N/A	N/A	N/A	N/A	N/A	N/A	N/A	N/A	N/A
Aedeagal Region	Standard deviation	0.0050	0.0043	0.0042	0.0041	0.0037	0.0036	0.0035	0.0032	0.0028	0.0026	0.0026	0.0024	0.0023	0.0022	0.0020	0.0020	0.0017
	Proportion of Variance	0.0001	0.0001	0.0001	0.0001	0.0001	0.0001	0.0001	0.0001	0.0000	0.0000	0.0000	0.0000	0.0000	0.0000	0.0000	0.0000	0.0000
	Cumulative Proportion	0.9991	0.9992	0.9993	0.9994	0.9995	0.9996	0.9996	0.9997	0.9997	0.9998	0.9998	0.9998	0.9999	0.9999	0.9999	0.9999	1.0000
Tegmen	Standard deviation	N/A	N/A	N/A	N/A	N/A	N/A	N/A	N/A	N/A	N/A	N/A	N/A	N/A	N/A	N/A	N/A	N/A
	Proportion of Variance	N/A	N/A	N/A	N/A	N/A	N/A	N/A	N/A	N/A	N/A	N/A	N/A	N/A	N/A	N/A	N/A	N/A
	Cumulative Proportion	N/A	N/A	N/A	N/A	N/A	N/A	N/A	N/A	N/A	N/A	N/A	N/A	N/A	N/A	N/A	N/A	N/A

This was followed by two types of evolutionary rate calculations, both of which incorporated the PG phylogeny and GPA means, operate under a Brownian motion model of evolution, and utilized 999 random permutations: **1)** multivariate evolutionary rate (function "compare.multi.evol.rates"), which returned a comparison of relative net evolutionary rates between all six shapes (Denton and Adams, 2015) (Fig. 4-19; Table 4-5), and **2)** comparative evolutionary rate (function "compare.evol.rates"), which returned a comparison of relative net evolutionary rate ratios between the PGss and the non-PGss for each shape set separately (Adams, 2014a) by assessing significance using the "permutation" approach as recommended by Adams and Collyer (2017) (Fig. 4-20; Table 4-6). Additionally, using GPA means and the PG phylogeny, phylogenetic signal (function "physignal") was calculated for all shape sets separately to estimate the degree of phylogenetic signal that was present in the data for each shape relative to what is expected under a Brownian motion model of evolution by using the multivariate version of Blomberg's K statistic (Adams, 2014b) (Fig. 4-21, Table 4-7. Finally, the phylogeny was combined with the shape data for each set and projected into six individual "phylomorphospaces" (by plotting a PCA based on the GPA means with the function "plotGMPhyloMorphoSpace") to visualize morphological and phylogenetic relationships (Figs 4-22 to 4-28).

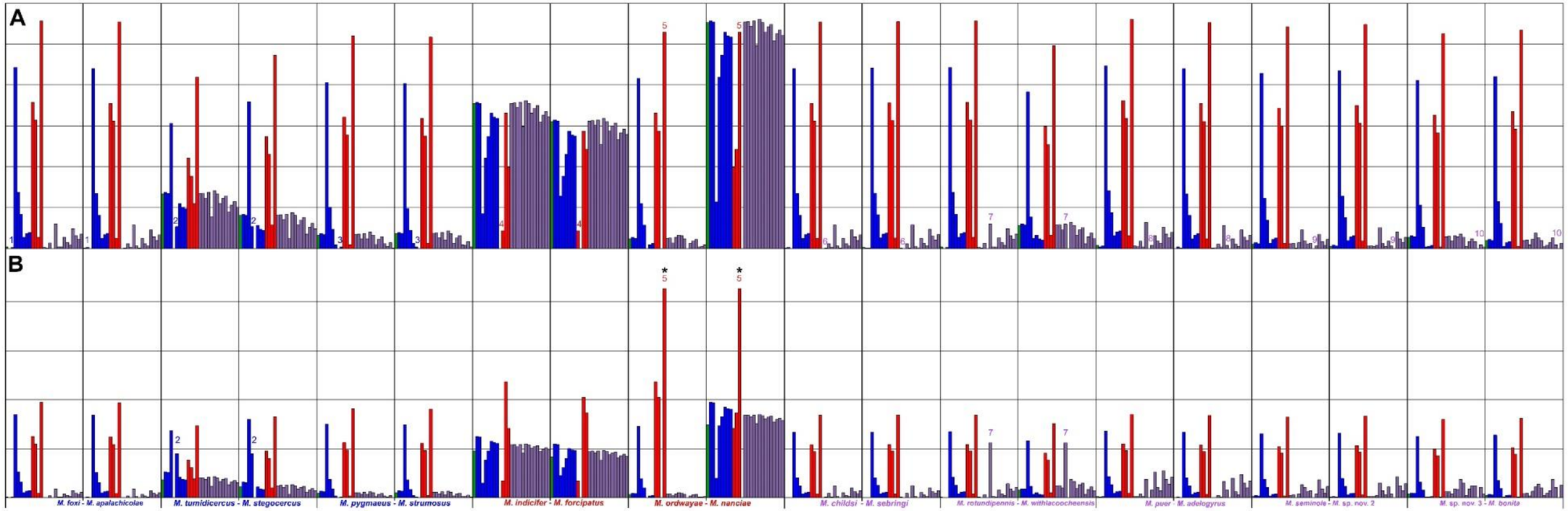

Figure 4-13. Results of the morphological disparity analysis for the cercus for all 10 pairs of PG sister species compared to all 27 species. Color-coding is by major lineage and species are organized, from left to right, in descending order of the phylogenetic tips (see Fig. 4-3). **A.** Without evolutionary time factored in and all sister species are identified with their corresponding pair of numbers. **B.** with evolutionary time factored in. The most (or nearly so) disparate pairs of sister species are identified by their corresponding pair of numbers (overall: Pair 5 and within lineages: Pairs 2, 5, 7) while astericeses indicate a statistically significant ($p < 0.05$) comparison before time was incorporated.

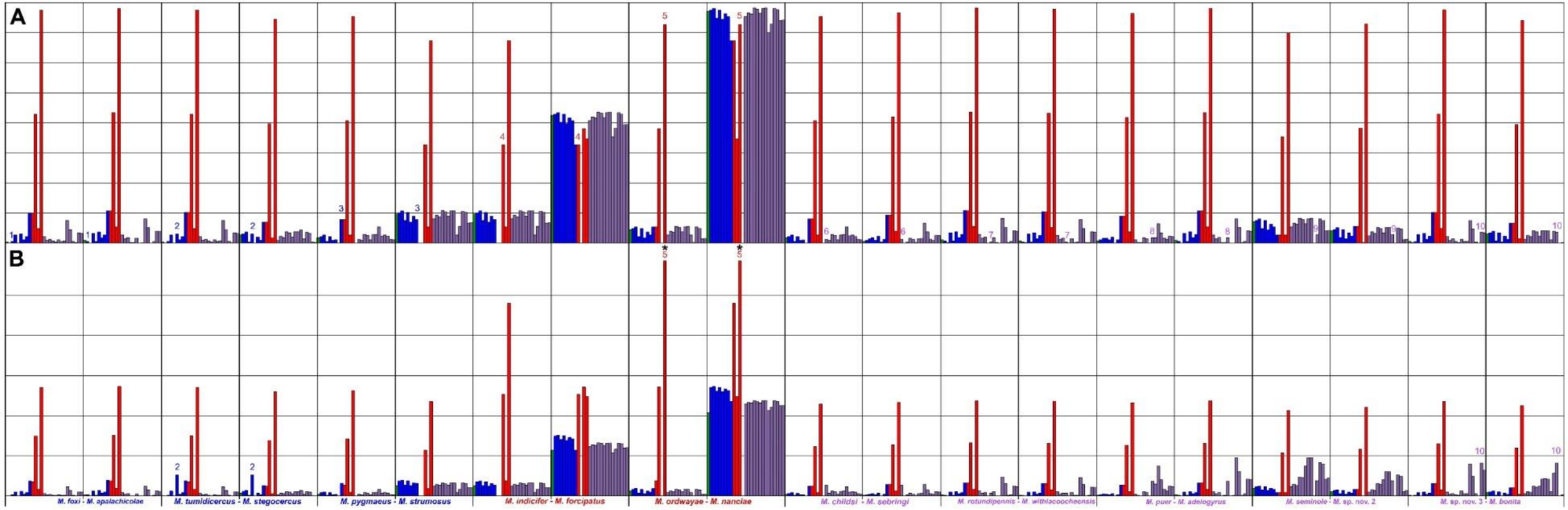

Figure 4-14. Results of the morphological disparity analysis for the ectophallus for all 10 pairs of PG sister species compared to all 27 species. Color-coding is by major lineage and species are organized, from left to right, in descending order of the phylogenetic tips (see Fig. 4-3). **A.** Without evolutionary time factored in and all sister species are identified with their corresponding pair of numbers. **B.** with evolutionary time factored in. The most (or nearly so) disparate pairs of sister species are identified by their corresponding pair of numbers (overall: Pair 5 and within lineages: Pairs 2, 5, 10) while asterices indicate a statistically significant ($p < 0.05$) comparison before time was incorporated.

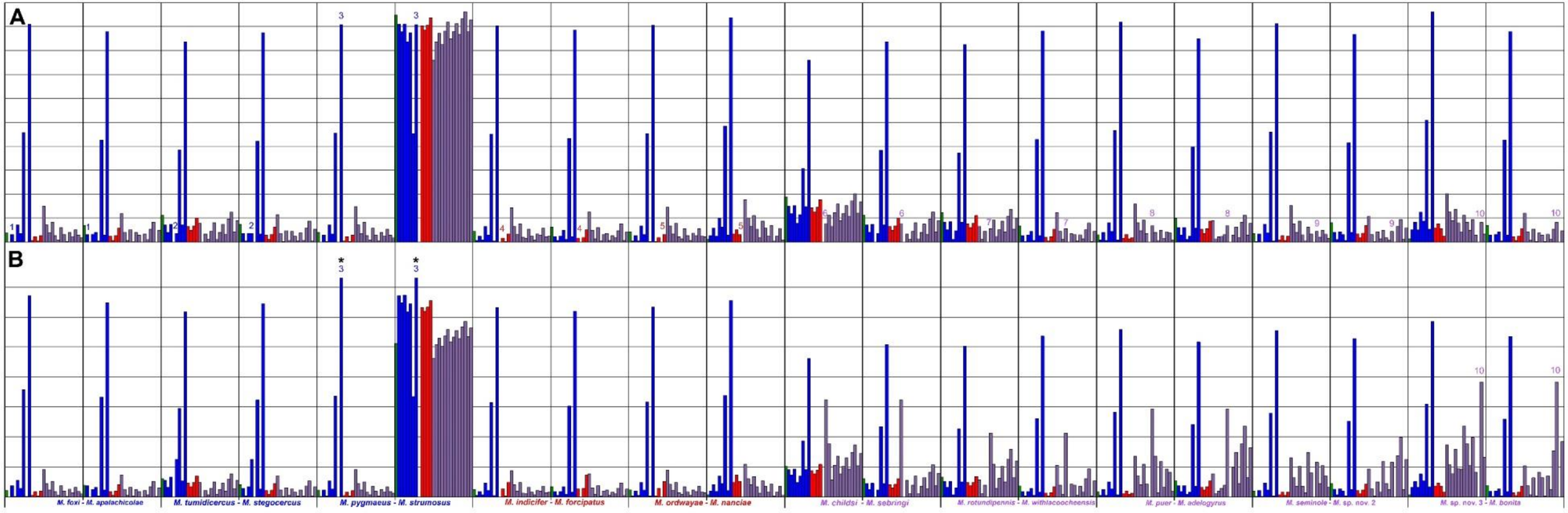

Figure 4-15. Results of the morphological disparity analysis for the epiphallus for all 10 pairs of PG sister species compared to all 27 species. Color-coding is by major lineage and species are organized, from left to right, in descending order of the phylogenetic tips (see Fig. 4-3). **A.** Without evolutionary time factored in and all sister species are identified with their corresponding pair of numbers. **B.** with evolutionary time factored in. The most (or nearly so) disparate pairs of sister species are identified by their corresponding pair of numbers (overall: Pair 3 and within lineages: Pairs 3, 10) while asterices indicate a statistically significant ($p < 0.05$) comparison before time was incorporated.

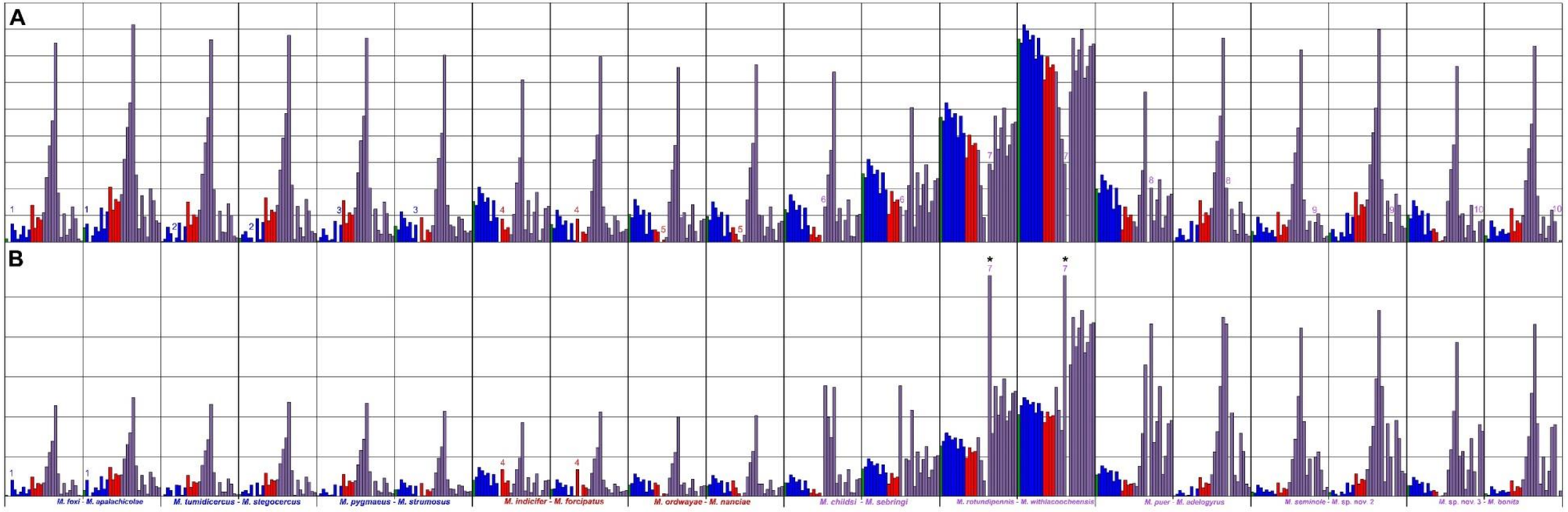

Figure 4-16. Results of the morphological disparity analysis for the lophus for all 10 pairs of PG sister species compared to all 27 species. Color-coding is by major lineage and species are organized, from left to right, in descending order of the phylogenetic tips (see Fig. 4-3). **A.** Without evolutionary time factored in and all sister species are identified with their corresponding pair of numbers. **B.** with evolutionary time factored in. The most (or nearly so) disparate pairs of sister species are identified by their corresponding pair of numbers (overall: Pair 7 and within lineages: Pairs 1, 4, 7) while asterices indicate a statistically significant ($p < 0.05$) comparison before time was incorporated.

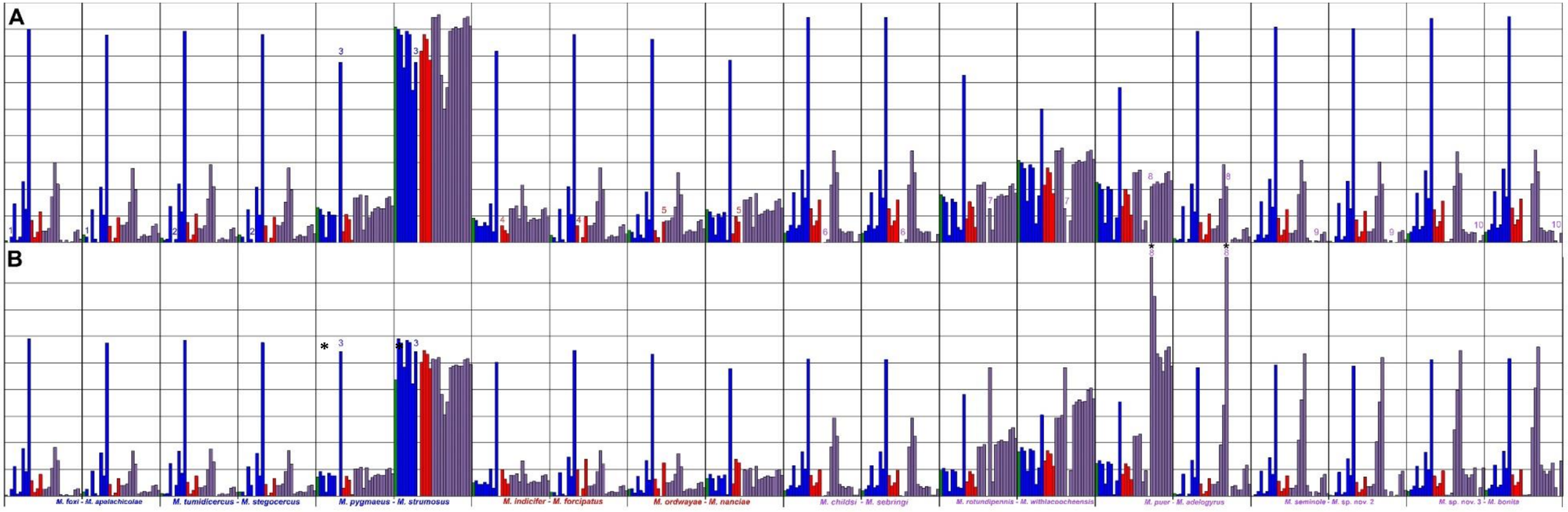

Figure 4-17. Results of the morphological disparity analysis for the aedeagal region for all 10 pairs of PG sister species compared to all 27 species. Color-coding is by major lineage and species are organized, from left to right, in descending order of the phylogenetic tips (see Fig. 4-3). **A.** Without evolutionary time factored in and all sister species are identified with their corresponding pair of numbers. **B.** with evolutionary time factored in. The most (or nearly so) disparate pairs of sister species are identified by their corresponding pair of numbers (overall: Pair 8 and within lineages: Pairs 3 and 8) while astericies indicate a statistically significant ($p < 0.05$) comparison before time was incorporated.

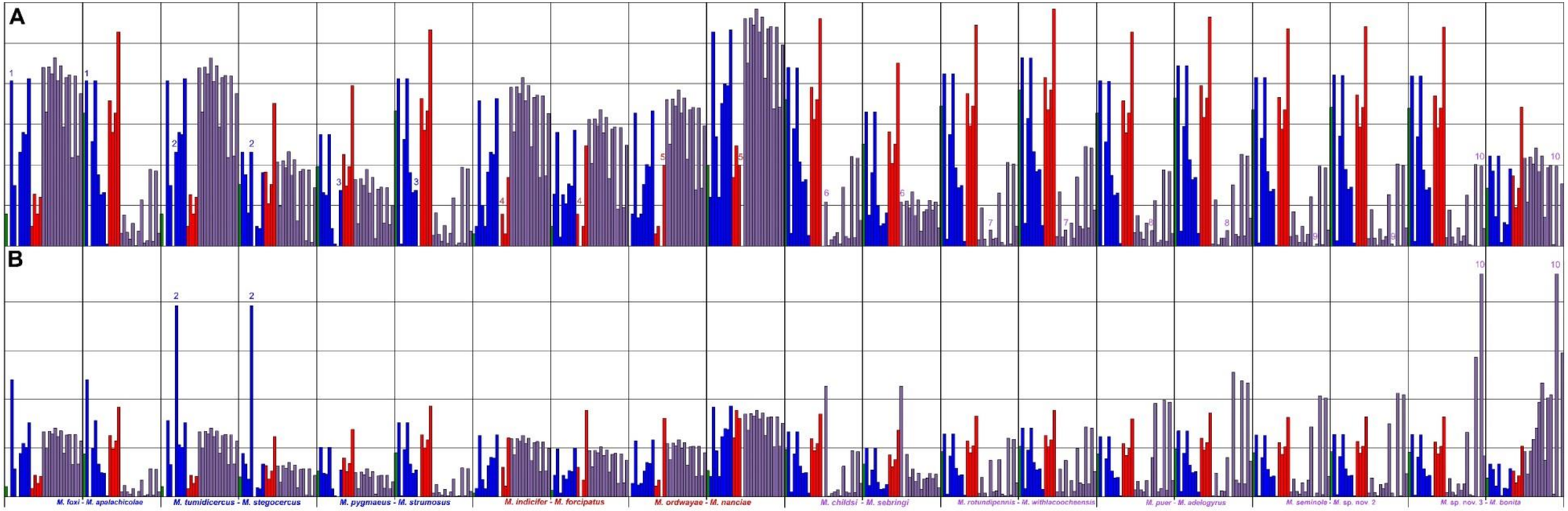

Figure 4-18. Results of the morphological disparity analysis for the tegmen for all 10 pairs of PG sister species compared to all 27 species. Color-coding is by major lineage and species are organized, from left to right, in descending order of the phylogenetic tips (see Fig. 4-3). **A.** Without evolutionary time factored in and all sister species are identified with their corresponding pair of numbers. **B.** with evolutionary time factored in. The most (or nearly so) disparate pairs of sister species are identified by their corresponding pair of numbers (within lineages: Pairs 2 and 10) while asterices indicate a statistically significant ($p < 0.05$) comparison before time was incorporated.

Table 4-3. For each of the six shapes, 351 total pairwise comparisons of morphological disparity were calculated between the 27 Puer Group species. SSD = Statistically Significant Disparities ($p < 0.05$). Shapes are ordered from highest to lowest value by # of SSD.

SHAPE	# of SSD	Relative % of SSD
Aedeagal Region	113	32.19%
Cercus	99	28.21%
Lophus	99	28.21%
Tegmen	83	23.65%
Epiphallus	53	15.10%
Ectophallus	51	14.53%

Results

Morphological Disparity Analysis

The visual results of the GPA (Fig. 4-6) and the morphological disparity analysis revealed that shape variation and relative percentage of statistically significant disparities based on 351 total pairwise comparisons are as follows, from highest to lowest (Table 4-3): aedeagal region (32.19%), cercus (28.21%), lophus (28.21%), tegmen (23.65%), epiphallus (15.10%), and ectophallus (14.53%). For almost every shape, a small number of species with highly divergent anatomical components tended to dominate in terms of the associated number of statistically significant disparities, resulting in high disparity values between many species pairs. The **1)** aedeagal region (Table 4-4M-O) had five dominant species: *M. mirus*, *M. strumosus*, *M. rotundipennis*, *M. withlacoocheensis*, and *M. puer*; **2)** cercus (Table 4-4A-C) had four: *M. scapularis*, *M. indicifer*, *M. forcipatus*, and *M. nanciae*; **3)** lophus (Table 4-4J-L) had four: *M. sebringi*, *M. tequestae*, *M. rotundipennis*, and *M. withlacoocheensis*; **4)** epiphallus

Table 4-4. Pairwise comparison of morphological disparity in each of the six shapes between all 27 Puer Group species. Species are grouped and their names colored in accordance with their major lineage, and organized in descending order of the phylogenetic tips (Fig. 4-3). The 10 sets of superscript numbers after most species names correspond with pairs of sister species (Fig. 4-3). **Bold** values indicate statistical significance ($p < 0.05$), with the colored ones highlighting significant disparity between sisters. **A-C** = Cercus, **D-F** = Ectophallus, **G-I** = Epiphallus, **J-L** = Lophus, **M-O** = Aedeagal Region, and **P-R** = Tegmen.

A. SHAPE: Cercus

SPECIES	*M. gurneyi*	*M. foxi* [1]	*M. apalachicolae* [1]	*M. scapularis*	*M. tumidicercus* [2]	*M. stegocercus* [2]	*M. mirus*	*M. pygmaeus* [3]	*M. strumosus* [3]
M. gurneyi		0.17%	0.05%	**21.96%**	6.68%	4.02%	1.18%	1.64%	1.80%
M. foxi [1]	0.17%		0.13%	**22.14%**	**6.85%**	4.20%	1.36%	1.82%	1.98%
M. apalachicolae [1]	0.05%	0.13%		**22.01%**	**6.73%**	4.07%	1.23%	1.69%	1.85%
M. scapularis	**21.96%**	**22.14%**	**22.01%**		**15.29%**	**17.94%**	**20.78%**	**20.32%**	**20.16%**
M. tumidicercus [2]	6.68%	**6.85%**	**6.73%**	**15.29%**		2.66%	5.49%	5.03%	4.87%
M. stegocercus [2]	4.02%	4.20%	4.07%	**17.94%**	2.66%		2.84%	2.38%	2.22%
M. mirus	1.18%	1.36%	1.23%	**20.78%**	5.49%	2.84%		0.46%	0.62%
M. pygmaeus [3]	1.64%	1.82%	1.69%	**20.32%**	5.03%	2.38%	0.46%		0.16%
M. strumosus [3]	1.80%	1.98%	1.85%	**20.16%**	4.87%	2.22%	0.62%	0.16%	
M. indicifer [4]	**17.71%**	**17.89%**	**17.76%**	4.25%	**11.04%**	**13.69%**	**16.53%**	**16.07%**	**15.91%**
M. forcipatus [4]	**15.53%**	**15.71%**	**15.58%**	6.43%	**8.86%**	**11.51%**	**14.35%**	**13.89%**	**13.73%**
M. ordwayae [5]	1.18%	1.35%	1.23%	**20.78%**	5.50%	2.84%	0.01%	0.47%	0.63%
M. nanciae [5]	**27.64%**	**27.81%**	**27.69%**	5.68%	**20.96%**	**23.62%**	**26.46%**	**26.00%**	**25.84%**
M. childsi [6]	0.05%	0.13%	0.00%	**22.01%**	6.73%	4.07%	1.23%	1.69%	1.85%
M. sebringi [6]	0.09%	0.08%	0.04%	**22.05%**	6.77%	4.11%	1.27%	1.73%	1.89%
M. tequestae	0.50%	0.68%	0.55%	**21.46%**	6.17%	3.52%	0.68%	1.14%	1.30%
M. rotundipennis [7]	0.16%	0.01%	0.11%	**22.12%**	**6.84%**	4.18%	1.35%	1.81%	1.97%
M. withlacoocheensis [7]	2.81%	2.99%	2.86%	**19.15%**	3.86%	1.21%	1.63%	1.17%	1.01%
M. puer [8]	0.38%	0.20%	0.33%	**22.34%**	**7.05%**	4.40%	1.56%	2.02%	2.18%
M. adelogyrus [8]	0.00%	0.17%	0.05%	**21.97%**	**6.68%**	4.03%	1.19%	1.65%	1.81%
M. kissimmee	1.16%	1.34%	1.21%	**20.80%**	5.51%	2.86%	0.02%	0.48%	0.64%
M. seminole [9]	0.53%	0.71%	0.58%	**21.43%**	6.14%	3.49%	0.65%	1.11%	1.27%
M. sp. nov. 2 [9]	0.24%	0.42%	0.29%	**21.72%**	6.44%	3.78%	0.94%	1.40%	1.56%
M. sp. nov. 1	2.26%	2.43%	2.31%	**19.71%**	4.42%	1.77%	1.07%	0.61%	0.45%
M. sp. nov. 3 [10]	1.39%	1.57%	1.44%	**20.57%**	5.28%	2.63%	0.21%	0.25%	0.41%
M. bonita [10]	0.94%	1.12%	0.99%	**21.02%**	5.73%	3.08%	0.24%	0.70%	0.86%
M. peninsularis	1.61%	1.79%	1.66%	**20.35%**	5.06%	2.41%	0.43%	0.03%	0.19%

Table 4-4 Continued.

B. SHAPE: Cercus

SPECIES	*M. indicifer* [4]	*M. forcipatus* [4]	*M. ordwayae* [5]	*M. nanciae* [5]	*M. childsi* [6]	*M. sebringi* [6]	*M. tequestae*	*M. rotundipennis* [7]	*M. withlacoocheensis* [7]
M. gurneyi	**17.71%**	**15.53%**	1.18%	**27.64%**	0.05%	0.09%	0.50%	0.16%	2.81%
M. foxi [1]	**17.89%**	**15.71%**	1.35%	**27.81%**	0.13%	0.08%	0.68%	0.01%	2.99%
M. apalachicolae [1]	**17.76%**	**15.58%**	1.23%	**27.69%**	0.00%	0.04%	0.55%	0.11%	2.86%
M. scapularis	4.25%	6.43%	**20.78%**	5.68%	**22.01%**	**22.05%**	**21.46%**	**22.12%**	**19.15%**
M. tumidicercus [2]	**11.04%**	**8.86%**	5.50%	**20.96%**	6.73%	6.77%	6.17%	**6.84%**	3.86%
M. stegocercus [2]	**13.69%**	**11.51%**	2.84%	**23.62%**	4.07%	4.11%	3.52%	4.18%	1.21%
M. mirus	**16.53%**	**14.35%**	0.01%	**26.46%**	1.23%	1.27%	0.68%	1.35%	1.63%
M. pygmaeus [3]	**16.07%**	**13.89%**	0.47%	**26.00%**	1.69%	1.73%	1.14%	1.81%	1.17%
M. strumosus [3]	**15.91%**	**13.73%**	0.63%	**25.84%**	1.85%	1.89%	1.30%	1.97%	1.01%
M. indicifer [4]		2.18%	**16.53%**	**9.93%**	**17.76%**	**17.80%**	**17.21%**	**17.87%**	**14.90%**
M. forcipatus [4]	2.18%		**14.35%**	**12.11%**	**15.58%**	**15.62%**	**15.03%**	**15.69%**	**12.72%**
M. ordwayae [5]	**16.53%**	**14.35%**		**26.46%**	1.23%	1.27%	0.68%	1.34%	1.64%
M. nanciae [5]	**9.93%**	**12.11%**	**26.46%**		**27.69%**	**27.73%**	**27.14%**	**27.80%**	**24.83%**
M. childsi [6]	**17.76%**	**15.58%**	1.23%	**27.69%**		0.04%	0.55%	0.11%	2.86%
M. sebringi [6]	**17.80%**	**15.62%**	1.27%	**27.73%**	0.04%		0.59%	0.07%	2.91%
M. tequestae	**17.21%**	**15.03%**	0.68%	**27.14%**	0.55%	0.59%		0.66%	2.31%
M. rotundipennis [7]	**17.87%**	**15.69%**	1.34%	**27.80%**	0.11%	0.07%	0.66%		2.98%
M. withlacoocheensis [7]	**14.90%**	**12.72%**	1.64%	**24.83%**	2.86%	2.91%	2.31%	2.98%	
M. puer [8]	**18.09%**	**15.91%**	1.55%	**28.02%**	0.33%	0.29%	0.88%	0.21%	3.19%
M. adelogyrus [8]	**17.72%**	**15.54%**	1.18%	**27.64%**	0.05%	0.09%	0.51%	0.16%	2.82%
M. kissimmee	**16.55%**	**14.37%**	0.01%	**26.48%**	1.21%	1.25%	0.66%	1.33%	1.65%
M. seminole [9]	**17.18%**	**15.00%**	0.65%	**27.11%**	0.58%	0.62%	0.03%	0.69%	2.28%
M. sp. nov. 2 [9]	**17.47%**	**15.29%**	0.94%	**27.40%**	0.29%	0.33%	0.26%	0.40%	2.57%
M. sp. nov. 1	**15.46%**	**13.28%**	1.08%	**25.38%**	2.31%	2.35%	1.75%	2.42%	0.56%
M. sp. nov. 3 [10]	**16.32%**	**14.14%**	0.22%	**26.24%**	1.44%	1.49%	0.89%	1.56%	1.42%
M. bonita [10]	**16.77%**	**14.59%**	0.23%	**26.70%**	0.99%	1.04%	0.44%	1.11%	1.87%
M. peninsularis	**16.10%**	**13.92%**	0.43%	**26.03%**	1.66%	1.70%	1.11%	1.78%	1.20%

Table 4-4 Continued.

C. SHAPE: Cercus

SPECIES	*M. puer* [8]	*M. adelogyrus* [8]	*M. kissimmee*	*M. seminole* [9]	*M.* sp. nov. 2 [9]	*M.* sp. nov. 1	*M.* sp. nov. 3 [10]	*M. bonita* [10]	*M. peninsularis*
M. gurneyi	0.38%	0.00%	1.16%	0.53%	0.24%	2.26%	1.39%	0.94%	1.61%
M. foxi [1]	0.20%	0.17%	1.34%	0.71%	0.42%	2.43%	1.57%	1.12%	1.79%
M. apalachicolae [1]	0.33%	0.05%	1.21%	0.58%	0.29%	2.31%	1.44%	0.99%	1.66%
M. scapularis	**22.34%**	**21.97%**	**20.80%**	**21.43%**	**21.72%**	**19.71%**	**20.57%**	**21.02%**	**20.35%**
M. tumidicercus [2]	**7.05%**	**6.68%**	5.51%	6.14%	6.44%	4.42%	5.28%	5.73%	5.06%
M. stegocercus [2]	4.40%	4.03%	2.86%	3.49%	3.78%	1.77%	2.63%	3.08%	2.41%
M. mirus	1.56%	1.19%	0.02%	0.65%	0.94%	1.07%	0.21%	0.24%	0.43%
M. pygmaeus [3]	2.02%	1.65%	0.48%	1.11%	1.40%	0.61%	0.25%	0.70%	0.03%
M. strumosus [3]	2.18%	1.81%	0.64%	1.27%	1.56%	0.45%	0.41%	0.86%	0.19%
M. indicifer [4]	**18.09%**	**17.72%**	**16.55%**	**17.18%**	**17.47%**	**15.46%**	**16.32%**	**16.77%**	**16.10%**
M. forcipatus [4]	**15.91%**	**15.54%**	**14.37%**	**15.00%**	**15.29%**	**13.28%**	**14.14%**	**14.59%**	**13.92%**
M. ordwayae [5]	1.55%	1.18%	0.01%	0.65%	0.94%	1.08%	0.22%	0.23%	0.43%
M. nanciae [5]	**28.02%**	**27.64%**	**26.48%**	**27.11%**	**27.40%**	**25.38%**	**26.24%**	**26.70%**	**26.03%**
M. childsi [6]	0.33%	0.05%	1.21%	0.58%	0.29%	2.31%	1.44%	0.99%	1.66%
M. sebringi [6]	0.29%	0.09%	1.25%	0.62%	0.33%	2.35%	1.49%	1.04%	1.70%
M. tequestae	0.88%	0.51%	0.66%	0.03%	0.26%	1.75%	0.89%	0.44%	1.11%
M. rotundipennis [7]	0.21%	0.16%	1.33%	0.69%	0.40%	2.42%	1.56%	1.11%	1.78%
M. withlacoocheensis [7]	3.19%	2.82%	1.65%	2.28%	2.57%	0.56%	1.42%	1.87%	1.20%
M. puer [8]		0.37%	1.54%	0.91%	0.62%	2.63%	1.77%	1.32%	1.99%
M. adelogyrus [8]	0.37%		1.17%	0.54%	0.25%	2.26%	1.40%	0.95%	1.62%
M. kissimmee	1.54%	1.17%		0.63%	0.92%	1.09%	0.23%	0.22%	0.45%
M. seminole [9]	0.91%	0.54%	0.63%		0.29%	1.72%	0.86%	0.41%	1.08%
M. sp. nov. 2 [9]	0.62%	0.25%	0.92%	0.29%		2.01%	1.15%	0.70%	1.37%
M. sp. nov. 1	2.63%	2.26%	1.09%	1.72%	2.01%		0.86%	1.31%	0.64%
M. sp. nov. 3 [10]	1.77%	1.40%	0.23%	0.86%	1.15%	0.86%		0.45%	0.22%
M. bonita [10]	1.32%	0.95%	0.22%	0.41%	0.70%	1.31%	0.45%		0.67%
M. peninsularis	1.99%	1.62%	0.45%	1.08%	1.37%	0.64%	0.22%	0.67%	

Table 4-4 Continued.

D. SHAPE: Ectophallus

SPECIES	*M. gurneyi*	*M. foxi* [1]	*M. apalachicolae* [1]	*M. scapularis*	*M. tumidicercus* [2]	*M. stegocercus* [2]	*M. mirus*	*M. pygmaeus* [3]	*M. strumosus* [3]
M. gurneyi		0.18%	0.47%	1.15%	0.19%	1.36%	0.38%	0.90%	4.86%
M. foxi [1]	0.18%		0.29%	1.33%	0.02%	1.54%	0.56%	1.08%	5.04%
M. apalachicolae [1]	0.47%	0.29%		1.62%	0.28%	1.83%	0.85%	1.37%	5.33%
M. scapularis	1.15%	1.33%	1.62%		1.34%	0.21%	0.77%	0.25%	3.71%
M. tumidicercus [2]	0.19%	0.02%	0.28%	1.34%		1.55%	0.58%	1.09%	5.05%
M. stegocercus [2]	1.36%	1.54%	1.83%	0.21%	1.55%		0.98%	0.46%	3.50%
M. mirus	0.38%	0.56%	0.85%	0.77%	0.58%	0.98%		0.52%	4.48%
M. pygmaeus [3]	0.90%	1.08%	1.37%	0.25%	1.09%	0.46%	0.52%		3.96%
M. strumosus [3]	4.86%	5.04%	5.33%	3.71%	5.05%	3.50%	4.48%	3.96%	
M. indicifer [4]	4.86%	5.04%	5.33%	3.71%	5.05%	3.50%	4.47%	3.96%	0.00%
M. forcipatus [4]	**21.21%**	**21.39%**	**21.68%**	**20.07%**	**21.41%**	**19.86%**	**20.83%**	**20.31%**	**16.35%**
M. ordwayae [5]	2.21%	2.39%	2.68%	1.06%	2.41%	0.85%	1.83%	1.31%	2.65%
M. nanciae [5]	**38.53%**	**38.71%**	**39.00%**	**37.38%**	**38.72%**	**37.17%**	**38.15%**	**37.63%**	**33.67%**
M. childsi [6]	0.88%	1.05%	1.35%	0.27%	1.07%	0.48%	0.49%	0.02%	3.99%
M. sebringi [6]	0.24%	0.41%	0.71%	0.91%	0.43%	1.12%	0.15%	0.66%	4.62%
M. tequestae	0.45%	0.63%	0.92%	0.70%	0.64%	0.91%	0.07%	0.45%	4.41%
M. rotundipennis [7]	0.54%	0.36%	0.07%	1.69%	0.35%	1.90%	0.93%	1.44%	5.40%
M. withlacoocheensis [7]	0.36%	0.18%	0.11%	1.51%	0.16%	1.72%	0.74%	1.26%	5.22%
M. puer [8]	0.37%	0.55%	0.84%	0.78%	0.56%	0.99%	0.01%	0.53%	4.49%
M. adelogyrus [8]	0.49%	0.31%	0.02%	1.64%	0.30%	1.85%	0.87%	1.39%	5.35%
M. kissimmee	0.52%	0.34%	0.05%	1.67%	0.33%	1.88%	0.90%	1.42%	5.38%
M. seminole [9]	3.55%	3.72%	4.02%	2.40%	3.74%	2.19%	3.16%	2.65%	1.31%
M. sp. nov. 2 [9]	2.08%	2.26%	2.55%	0.93%	2.27%	0.72%	1.70%	1.18%	2.78%
M. sp. nov. 1	0.43%	0.26%	0.04%	1.58%	0.24%	1.79%	0.82%	1.33%	5.30%
M. sp. nov. 3 [10]	0.24%	0.07%	0.23%	1.39%	0.05%	1.60%	0.63%	1.14%	5.10%
M. bonita [10]	1.53%	1.71%	2.00%	0.38%	1.72%	0.17%	1.15%	0.63%	3.33%
M. peninsularis	1.45%	1.63%	1.92%	0.30%	1.65%	0.09%	1.07%	0.55%	3.41%

Table 4-4 Continued.

E. SHAPE: Ectophallus

SPECIES	*M. indicifer* [4]	*M. forcipatus* [4]	*M. ordwayae* [5]	*M. nanciae* [5]	*M. childsi* [6]	*M. sebringi* [6]	*M. tequestae*	*M. rotundipennis* [7]	*M. withlacoocheensis* [7]
M. gurneyi	4.86%	**21.21%**	2.21%	**38.53%**	0.88%	0.24%	0.45%	0.54%	0.36%
M. foxi [1]	5.04%	**21.39%**	2.39%	**38.71%**	1.05%	0.41%	0.63%	0.36%	0.18%
M. apalachicolae [1]	5.33%	**21.68%**	2.68%	**39.00%**	1.35%	0.71%	0.92%	0.07%	0.11%
M. scapularis	3.71%	**20.07%**	1.06%	**37.38%**	0.27%	0.91%	0.70%	1.69%	1.51%
M. tumidicercus [2]	5.05%	**21.41%**	2.41%	**38.72%**	1.07%	0.43%	0.64%	0.35%	0.16%
M. stegocercus [2]	3.50%	**19.86%**	0.85%	**37.17%**	0.48%	1.12%	0.91%	1.90%	1.72%
M. mirus	4.47%	**20.83%**	1.83%	**38.15%**	0.49%	0.15%	0.07%	0.93%	0.74%
M. pygmaeus [3]	3.96%	**20.31%**	1.31%	**37.63%**	0.02%	0.66%	0.45%	1.44%	1.26%
M. strumosus [3]	0.00%	**16.35%**	2.65%	**33.67%**	3.99%	4.62%	4.41%	5.40%	5.22%
M. indicifer [4]		**16.36%**	2.64%	**33.67%**	3.98%	4.62%	4.41%	5.40%	5.21%
M. forcipatus [4]	**16.36%**		**19.00%**	**17.31%**	**20.34%**	**20.98%**	**20.76%**	**21.76%**	**21.57%**
M. ordwayae [5]	2.64%	**19.00%**		**36.32%**	1.34%	1.98%	1.76%	2.76%	2.57%
M. nanciae [5]	**33.67%**	**17.31%**	**36.32%**		**37.65%**	**38.29%**	**38.08%**	**39.07%**	**38.89%**
M. childsi [6]	3.98%	**20.34%**	1.34%	**37.65%**		0.64%	0.42%	1.42%	1.23%
M. sebringi [6]	4.62%	**20.98%**	1.98%	**38.29%**	0.64%		0.21%	0.78%	0.59%
M. tequestae	4.41%	**20.76%**	1.76%	**38.08%**	0.42%	0.21%		0.99%	0.81%
M. rotundipennis [7]	5.40%	**21.76%**	2.76%	**39.07%**	1.42%	0.78%	0.99%		0.19%
M. withlacoocheensis [7]	5.21%	**21.57%**	2.57%	**38.89%**	1.23%	0.59%	0.81%	0.19%	
M. puer [8]	4.49%	**20.84%**	1.84%	**38.16%**	0.50%	0.13%	0.08%	0.91%	0.73%
M. adelogyrus [8]	5.35%	**21.70%**	2.70%	**39.02%**	1.36%	0.73%	0.94%	0.05%	0.13%
M. kissimmee	5.38%	**21.73%**	2.73%	**39.05%**	1.40%	0.76%	0.97%	0.02%	0.16%
M. seminole [9]	1.31%	**17.67%**	1.33%	**34.98%**	2.67%	3.31%	3.10%	4.09%	3.90%
M. sp. nov. 2 [9]	2.78%	**19.13%**	0.13%	**36.45%**	1.20%	1.84%	1.63%	2.62%	2.44%
M. sp. nov. 1	5.29%	**21.65%**	2.65%	**38.96%**	1.31%	0.67%	0.88%	0.11%	0.08%
M. sp. nov. 3 [10]	5.10%	**21.46%**	2.46%	**38.77%**	1.12%	0.48%	0.69%	0.30%	0.11%
M. bonita [10]	3.33%	**19.68%**	0.68%	**37.00%**	0.66%	1.29%	1.08%	2.07%	1.89%
M. peninsularis	3.41%	**19.76%**	0.76%	**37.08%**	0.58%	1.22%	1.00%	2.00%	1.81%

Table 4-4 Continued.

F. SHAPE: Ectophallus

SPECIES	*M. puer* [8]	*M. adelogyrus* [8]	*M. kissimmee*	*M. seminole* [9]	*M.* sp. nov. 2 [9]	*M.* sp. nov. 1	*M.* sp. nov. 3 [10]	*M. bonita* [10]	*M. peninsularis*
M. gurneyi	0.37%	0.49%	0.52%	3.55%	2.08%	0.43%	0.24%	1.53%	1.45%
M. foxi [1]	0.55%	0.31%	0.34%	3.72%	2.26%	0.26%	0.07%	1.71%	1.63%
M. apalachicolae [1]	0.84%	0.02%	0.05%	4.02%	2.55%	0.04%	0.23%	2.00%	1.92%
M. scapularis	0.78%	1.64%	1.67%	2.40%	0.93%	1.58%	1.39%	0.38%	0.30%
M. tumidicercus [2]	0.56%	0.30%	0.33%	3.74%	2.27%	0.24%	0.05%	1.72%	1.65%
M. stegocercus [2]	0.99%	1.85%	1.88%	2.19%	0.72%	1.79%	1.60%	0.17%	0.09%
M. mirus	0.01%	0.87%	0.90%	3.16%	1.70%	0.82%	0.63%	1.15%	1.07%
M. pygmaeus [3]	0.53%	1.39%	1.42%	2.65%	1.18%	1.33%	1.14%	0.63%	0.55%
M. strumosus [3]	4.49%	5.35%	5.38%	1.31%	2.78%	5.30%	5.10%	3.33%	3.41%
M. indicifer [4]	4.49%	5.35%	5.38%	1.31%	2.78%	5.29%	5.10%	3.33%	3.41%
M. forcipatus [4]	**20.84%**	**21.70%**	**21.73%**	**17.67%**	**19.13%**	**21.65%**	**21.46%**	**19.68%**	**19.76%**
M. ordwayae [5]	1.84%	2.70%	2.73%	1.33%	0.13%	2.65%	2.46%	0.68%	0.76%
M. nanciae [5]	**38.16%**	**39.02%**	**39.05%**	**34.98%**	**36.45%**	**38.96%**	**38.77%**	**37.00%**	**37.08%**
M. childsi [6]	0.50%	1.36%	1.40%	2.67%	1.20%	1.31%	1.12%	0.66%	0.58%
M. sebringi [6]	0.13%	0.73%	0.76%	3.31%	1.84%	0.67%	0.48%	1.29%	1.22%
M. tequestae	0.08%	0.94%	0.97%	3.10%	1.63%	0.88%	0.69%	1.08%	1.00%
M. rotundipennis [7]	0.91%	0.05%	0.02%	4.09%	2.62%	0.11%	0.30%	2.07%	2.00%
M. withlacoocheensis [7]	0.73%	0.13%	0.16%	3.90%	2.44%	0.08%	0.11%	1.89%	1.81%
M. puer [8]		0.86%	0.89%	3.18%	1.71%	0.80%	0.61%	1.16%	1.08%
M. adelogyrus [8]	0.86%		0.03%	4.04%	2.57%	0.05%	0.25%	2.02%	1.94%
M. kissimmee	0.89%	0.03%		4.07%	2.60%	0.09%	0.28%	2.05%	1.97%
M. seminole [9]	3.18%	4.04%	4.07%		1.47%	3.98%	3.79%	2.02%	2.09%
M. sp. nov. 2 [9]	1.71%	2.57%	2.60%	1.47%		2.51%	2.32%	0.55%	0.63%
M. sp. nov. 1	0.80%	0.05%	0.09%	3.98%	2.51%		0.19%	1.96%	1.89%
M. sp. nov. 3 [10]	0.61%	0.25%	0.28%	3.79%	2.32%	0.19%		1.77%	1.70%
M. bonita [10]	1.16%	2.02%	2.05%	2.02%	0.55%	1.96%	1.77%		0.08%
M. peninsularis	1.08%	1.94%	1.97%	2.09%	0.63%	1.89%	1.70%	0.08%	

Table 4-4 Continued.

G. SHAPE: Epiphallus

SPECIES	*M. gurneyi*	*M. foxi* [1]	*M. apalachicolae* [1]	*M. scapularis*	*M. tumidicercus* [2]	*M. stegocercus* [2]	*M. mirus*	*M. pygmaeus* [3]	*M. strumosus* [3]
M. gurneyi		0.39%	0.70%	0.38%	1.11%	0.75%	**4.96%**	0.40%	**9.48%**
M. foxi [1]	0.39%		0.31%	0.02%	0.72%	0.36%	**4.57%**	0.01%	**9.09%**
M. apalachicolae [1]	0.70%	0.31%		0.33%	0.41%	0.04%	**4.26%**	0.30%	**8.78%**
M. scapularis	0.38%	0.02%	0.33%		0.74%	0.37%	**4.58%**	0.03%	**9.11%**
M. tumidicercus [2]	1.11%	0.72%	0.41%	0.74%		0.37%	3.85%	**0.71%**	8.37%
M. stegocercus [2]	0.75%	0.36%	0.04%	0.37%	0.37%		4.21%	**0.34%**	8.74%
M. mirus	**4.96%**	**4.57%**	**4.26%**	**4.58%**	**3.85%**	**4.21%**		**4.56%**	**4.52%**
M. pygmaeus [3]	0.40%	0.01%	0.30%	0.03%	0.71%	0.34%	**4.56%**		**9.08%**
M. strumosus [3]	**9.48%**	**9.09%**	**8.78%**	**9.11%**	**8.37%**	**8.74%**	**4.52%**	**9.08%**	
M. indicifer [4]	0.46%	0.07%	0.24%	0.08%	0.66%	0.29%	**4.50%**	0.05%	**9.03%**
M. forcipatus [4]	0.63%	0.24%	0.07%	0.25%	0.49%	0.12%	**4.33%**	0.22%	**8.86%**
M. ordwayae [5]	0.43%	0.04%	0.27%	0.06%	0.68%	0.31%	**4.53%**	0.03%	**9.05%**
M. nanciae [5]	0.12%	0.27%	0.58%	0.26%	1.00%	0.63%	**4.84%**	0.29%	**9.37%**
M. childsi [6]	**1.89%**	1.50%	1.19%	1.52%	0.78%	1.15%	**3.07%**	1.49%	**7.59%**
M. sebringi [6]	1.12%	0.73%	0.41%	0.74%	0.00%	0.37%	**3.84%**	0.71%	**8.37%**
M. tequestae	0.77%	0.38%	0.07%	0.40%	0.34%	0.03%	**4.19%**	0.37%	**8.71%**
M. rotundipennis [7]	1.23%	0.84%	0.53%	0.85%	0.11%	0.48%	**3.73%**	0.83%	**8.26%**
M. withlacoocheensis [7]	0.67%	0.28%	0.04%	0.29%	0.45%	0.08%	**4.29%**	0.26%	**8.82%**
M. puer [8]	0.30%	0.09%	0.40%	0.07%	0.81%	0.44%	**4.66%**	0.10%	**9.18%**
M. adelogyrus [8]	0.99%	0.60%	0.29%	0.62%	0.12%	0.24%	**3.97%**	0.59%	**8.49%**
M. kissimmee	0.70%	0.31%	0.00%	0.33%	0.41%	0.04%	**4.26%**	0.30%	**8.78%**
M. seminole [9]	0.36%	0.03%	0.34%	0.01%	0.75%	0.38%	**4.60%**	0.04%	**9.12%**
M. sp. nov. 2 [9]	0.81%	0.42%	0.10%	0.43%	0.31%	0.06%	**4.15%**	0.40%	**8.68%**
M. sp. nov. 1	0.15%	0.24%	0.55%	0.22%	0.96%	0.59%	**4.80%**	0.25%	**9.33%**
M. sp. nov. 3 [10]	0.13%	0.52%	0.83%	0.51%	1.25%	0.88%	**5.09%**	0.54%	**9.62%**
M. bonita [10]	0.69%	0.30%	0.01%	0.32%	0.42%	0.06%	**4.27%**	0.29%	**8.79%**
M. peninsularis	0.21%	0.18%	0.49%	0.17%	0.90%	0.54%	**4.75%**	0.19%	**9.27%**

Table 4-4 Continued.

H. SHAPE: Epiphallus

SPECIES	*M. indicifer* [4]	*M. forcipatus* [4]	*M. ordwayae* [5]	*M. nanciae* [5]	*M. childsi* [6]	*M. sebringi* [6]	*M. tequestae*	*M. rotundipennis* [7]	*M. withlacoocheensis* [7]
M. gurneyi	0.46%	0.63%	0.43%	0.12%	**1.89%**	1.12%	0.77%	1.23%	0.67%
M. foxi [1]	0.07%	0.24%	0.04%	0.27%	1.50%	0.73%	0.38%	0.84%	0.28%
M. apalachicolae [1]	0.24%	0.07%	0.27%	0.58%	1.19%	0.41%	0.07%	0.53%	0.04%
M. scapularis	0.08%	0.25%	0.06%	0.26%	1.52%	0.74%	0.40%	0.85%	0.29%
M. tumidicercus [2]	**0.66%**	0.49%	0.68%	1.00%	0.78%	0.00%	0.34%	0.11%	0.45%
M. stegocercus [2]	**0.29%**	0.12%	0.31%	0.63%	1.15%	0.37%	0.03%	0.48%	0.08%
M. mirus	**4.50%**	**4.33%**	**4.53%**	**4.84%**	**3.07%**	**3.84%**	**4.19%**	**3.73%**	**4.29%**
M. pygmaeus [3]	0.05%	0.22%	0.03%	0.29%	1.49%	0.71%	0.37%	0.83%	0.26%
M. strumosus [3]	**9.03%**	**8.86%**	**9.05%**	**9.37%**	**7.59%**	**8.37%**	**8.71%**	**8.26%**	**8.82%**
M. indicifer [4]		0.17%	0.02%	0.34%	1.43%	0.66%	0.31%	0.77%	0.21%
M. forcipatus [4]	0.17%		0.19%	0.51%	1.26%	0.49%	0.14%	0.60%	0.04%
M. ordwayae [5]	0.02%	0.19%		0.32%	1.46%	0.68%	0.34%	0.79%	0.23%
M. nanciae [5]	0.34%	0.51%	0.32%		1.77%	1.00%	0.65%	1.11%	0.55%
M. childsi [6]	1.43%	1.26%	1.46%	1.77%		0.77%	1.12%	0.66%	1.23%
M. sebringi [6]	0.66%	0.49%	0.68%	1.00%	0.77%		0.35%	0.11%	0.45%
M. tequestae	0.31%	0.14%	0.34%	0.65%	1.12%	0.35%		0.46%	0.11%
M. rotundipennis [7]	0.77%	0.60%	0.79%	1.11%	0.66%	0.11%	0.46%		0.56%
M. withlacoocheensis [7]	0.21%	0.04%	0.23%	0.55%	1.23%	0.45%	0.11%	0.56%	
M. puer [8]	0.15%	0.32%	0.13%	0.19%	1.59%	0.81%	0.47%	0.92%	0.36%
M. adelogyrus [8]	0.53%	0.36%	0.56%	0.87%	0.90%	0.13%	0.22%	0.24%	0.32%
M. kissimmee	0.25%	0.08%	0.27%	0.59%	1.19%	0.41%	0.07%	0.52%	0.04%
M. seminole [9]	0.10%	0.27%	0.07%	0.24%	1.53%	0.75%	0.41%	0.87%	0.30%
M. sp. nov. 2 [9]	0.35%	0.18%	0.37%	0.69%	1.09%	0.31%	0.03%	0.42%	0.14%
M. sp. nov. 1	0.30%	0.47%	0.28%	0.04%	1.74%	0.96%	0.62%	1.07%	0.51%
M. sp. nov. 3 [10]	0.59%	0.76%	0.57%	0.25%	**2.02%**	1.25%	0.90%	1.36%	0.80%
M. bonita [10]	0.23%	0.06%	0.26%	0.57%	1.20%	0.43%	0.08%	0.54%	0.02%
M. peninsularis	0.25%	0.42%	0.22%	0.09%	1.68%	0.91%	0.56%	1.02%	0.46%

Table 4-4 Continued.

I. SHAPE: Epiphallus

SPECIES	*M. puer* [8]	*M. adelogyrus* [8]	*M. kissimmee*	*M. seminole* [9]	*M.* sp. nov. 2 [9]	*M.* sp. nov. 1	*M.* sp. nov. 3 [10]	*M. bonita* [10]	*M. peninsularis*
M. gurneyi	0.30%	0.99%	0.70%	0.36%	0.81%	0.15%	0.13%	0.69%	0.21%
M. foxi [1]	0.09%	0.60%	0.31%	0.03%	0.42%	0.24%	0.52%	0.30%	0.18%
M. apalachicolae [1]	0.40%	0.29%	0.00%	0.34%	0.10%	0.55%	0.83%	0.01%	0.49%
M. scapularis	0.07%	0.62%	0.33%	0.01%	0.43%	0.22%	0.51%	0.32%	0.17%
M. tumidicercus [2]	0.81%	0.12%	0.41%	0.75%	0.31%	0.96%	1.25%	0.42%	0.90%
M. stegocercus [2]	0.44%	0.24%	0.04%	0.38%	0.06%	0.59%	0.88%	0.06%	0.54%
M. mirus	**4.66%**	**3.97%**	**4.26%**	**4.60%**	**4.15%**	**4.80%**	**5.09%**	**4.27%**	**4.75%**
M. pygmaeus [3]	0.10%	0.59%	0.30%	0.04%	0.40%	0.25%	0.54%	0.29%	0.19%
M. strumosus [3]	**9.18%**	**8.49%**	**8.78%**	**9.12%**	**8.68%**	**9.33%**	**9.62%**	**8.79%**	**9.27%**
M. indicifer [4]	0.15%	0.53%	0.25%	0.10%	0.35%	0.30%	0.59%	0.23%	0.25%
M. forcipatus [4]	0.32%	0.36%	0.08%	0.27%	0.18%	0.47%	0.76%	0.06%	0.42%
M. ordwayae [5]	0.13%	0.56%	0.27%	0.07%	0.37%	0.28%	0.57%	0.26%	0.22%
M. nanciae [5]	0.19%	0.87%	0.59%	0.24%	0.69%	0.04%	0.25%	0.57%	0.09%
M. childsi [6]	1.59%	0.90%	1.19%	1.53%	1.09%	1.74%	**2.02%**	1.20%	1.68%
M. sebringi [6]	0.81%	0.13%	0.41%	0.75%	0.31%	0.96%	1.25%	0.43%	0.91%
M. tequestae	0.47%	0.22%	0.07%	0.41%	0.03%	0.62%	0.90%	0.08%	0.56%
M. rotundipennis [7]	0.92%	0.24%	0.52%	0.87%	0.42%	1.07%	1.36%	0.54%	1.02%
M. withlacoocheensis [7]	0.36%	0.32%	0.04%	0.30%	0.14%	0.51%	0.80%	0.02%	0.46%
M. puer [8]		0.69%	0.40%	0.06%	0.50%	0.15%	0.44%	0.39%	0.09%
M. adelogyrus [8]	0.69%		0.29%	0.63%	0.18%	0.84%	1.12%	0.30%	0.78%
M. kissimmee	0.40%	0.29%		0.34%	0.10%	0.55%	0.84%	0.01%	0.49%
M. seminole [9]	0.06%	0.63%	0.34%		0.44%	0.21%	0.49%	0.33%	0.15%
M. sp. nov. 2 [9]	0.50%	0.18%	0.10%	0.44%		0.65%	0.94%	0.12%	0.60%
M. sp. nov. 1	0.15%	0.84%	0.55%	0.21%	0.65%		0.29%	0.54%	0.06%
M. sp. nov. 3 [10]	0.44%	1.12%	0.84%	0.49%	0.94%	0.29%		0.82%	0.34%
M. bonita [10]	0.39%	0.30%	0.01%	0.33%	0.12%	0.54%	0.82%		0.48%
M. peninsularis	0.09%	0.78%	0.49%	0.15%	0.60%	0.06%	0.34%	0.48%	

Table 4-4 Continued.

J. SHAPE: Lophus

SPECIES	*M. gurneyi*	*M. foxi* [1]	*M. apalachicolae* [1]	*M. scapularis*	*M. tumidicercus* [2]	*M. stegocercus* [2]	*M. mirus*	*M. pygmaeus* [3]	*M. strumosus* [3]
M. gurneyi		0.27%	1.10%	0.62%	0.04%	0.30%	1.49%	0.10%	1.20%
M. foxi [1]	0.27%		1.36%	0.89%	0.23%	0.57%	1.22%	0.36%	0.93%
M. apalachicolae [1]	1.10%	1.36%		0.47%	1.13%	0.80%	2.58%	1.00%	2.29%
M. scapularis	0.62%	0.89%	0.47%		0.66%	0.32%	2.11%	0.53%	1.82%
M. tumidicercus [2]	0.04%	0.23%	1.13%	0.66%		0.34%	1.45%	0.13%	1.16%
M. stegocercus [2]	0.30%	0.57%	0.80%	0.32%	0.34%		1.79%	0.20%	1.50%
M. mirus	1.49%	1.22%	2.58%	2.11%	1.45%	1.79%		1.58%	0.29%
M. pygmaeus [3]	0.10%	0.36%	1.00%	0.53%	0.13%	0.20%	1.58%		1.29%
M. strumosus [3]	1.20%	0.93%	2.29%	1.82%	1.16%	1.50%	0.29%	1.29%	
M. indicifer [4]	3.05%	2.78%	**4.15%**	3.67%	3.01%	3.35%	1.56%	3.15%	1.85%
M. forcipatus [4]	1.33%	1.06%	2.42%	1.95%	1.29%	1.62%	0.16%	1.42%	0.13%
M. ordwayae [5]	2.11%	1.84%	3.21%	2.73%	2.07%	2.41%	0.62%	2.21%	0.91%
M. nanciae [5]	1.94%	1.67%	3.04%	2.56%	1.90%	2.24%	0.45%	2.04%	0.74%
M. childsi [6]	2.47%	2.20%	**3.56%**	3.09%	2.43%	2.77%	0.98%	2.56%	1.27%
M. sebringi [6]	**5.14%**	**4.87%**	**6.23%**	**5.76%**	**5.10%**	**5.43%**	3.65%	**5.23%**	**3.94%**
M. tequestae	**7.52%**	**7.25%**	**8.62%**	**8.14%**	**7.48%**	**7.82%**	**6.03%**	**7.62%**	**6.32%**
M. rotundipennis [7]	**9.38%**	**9.11%**	**10.48%**	**10.00%**	**9.34%**	**9.68%**	**7.89%**	**9.48%**	**8.18%**
M. withlacoocheensis [7]	**15.26%**	**14.99%**	**16.35%**	**15.88%**	**15.22%**	**15.55%**	**13.77%**	**15.35%**	**14.06%**
M. puer [8]	**3.98%**	3.72%	**5.08%**	**4.61%**	3.95%	**4.28%**	2.50%	**4.08%**	2.79%
M. adelogyrus [8]	0.09%	0.36%	1.01%	0.53%	0.13%	0.21%	1.58%	0.01%	1.29%
M. kissimmee	2.39%	2.12%	**3.49%**	3.01%	2.35%	2.69%	0.90%	2.49%	1.19%
M. seminole [9]	0.80%	0.53%	1.89%	1.42%	0.76%	1.09%	0.69%	0.89%	0.40%
M. sp. nov. 2 [9]	0.71%	0.97%	0.39%	0.08%	0.74%	0.41%	2.19%	0.61%	1.90%
M. sp. nov. 1	2.92%	2.66%	**4.02%**	3.55%	2.89%	3.22%	1.44%	3.02%	1.73%
M. sp. nov. 3 [10]	2.06%	1.79%	3.16%	2.68%	2.02%	2.36%	0.57%	2.16%	0.86%
M. bonita [10]	0.51%	0.24%	1.60%	1.13%	0.47%	0.80%	0.98%	0.60%	0.69%
M. peninsularis	0.36%	0.09%	1.46%	0.98%	0.32%	0.66%	1.13%	0.46%	0.84%

Table 4-4 Continued.

K. SHAPE: Lophus

SPECIES	*M. indicifer* [4]	*M. forcipatus* [4]	*M. ordwayae* [5]	*M. nanciae* [5]	*M. childsi* [6]	*M. sebringi* [6]	*M. tequestae*	*M. rotundipennis* [7]	*M. withlacoocheensis* [7]
M. gurneyi	3.05%	1.33%	2.11%	1.94%	2.47%	**5.14%**	**7.52%**	**9.38%**	**15.26%**
M. foxi [1]	2.78%	1.06%	1.84%	1.67%	2.20%	**4.87%**	**7.25%**	**9.11%**	**14.99%**
M. apalachicolae [1]	**4.15%**	2.42%	3.21%	3.04%	**3.56%**	**6.23%**	**8.62%**	**10.48%**	**16.35%**
M. scapularis	3.67%	1.95%	2.73%	2.56%	3.09%	**5.76%**	**8.14%**	**10.00%**	**15.88%**
M. tumidicercus [2]	3.01%	1.29%	2.07%	1.90%	2.43%	**5.10%**	**7.48%**	**9.34%**	**15.22%**
M. stegocercus [2]	3.35%	1.62%	2.41%	2.24%	2.77%	**5.43%**	**7.82%**	**9.68%**	**15.55%**
M. mirus	1.56%	0.16%	0.62%	0.45%	0.98%	3.65%	**6.03%**	**7.89%**	**13.77%**
M. pygmaeus [3]	3.15%	1.42%	2.21%	2.04%	2.56%	**5.23%**	**7.62%**	**9.48%**	**15.35%**
M. strumosus [3]	1.85%	0.13%	0.91%	0.74%	1.27%	**3.94%**	**6.32%**	**8.18%**	**14.06%**
M. indicifer [4]		1.73%	0.94%	1.11%	0.58%	2.08%	**4.47%**	**6.33%**	**12.20%**
M. forcipatus [4]	1.73%		0.78%	0.61%	1.14%	**3.81%**	**6.19%**	**8.05%**	**13.93%**
M. ordwayae [5]	0.94%	0.78%		0.17%	0.36%	3.03%	**5.41%**	**7.27%**	**13.15%**
M. nanciae [5]	1.11%	0.61%	0.17%		0.53%	3.20%	**5.58%**	**7.44%**	**13.32%**
M. childsi [6]	0.58%	1.14%	0.36%	0.53%		2.67%	**5.05%**	**6.91%**	**12.79%**
M. sebringi [6]	2.08%	**3.81%**	3.03%	3.20%	2.67%		2.38%	**4.24%**	**10.12%**
M. tequestae	**4.47%**	**6.19%**	**5.41%**	**5.58%**	**5.05%**	2.38%		1.86%	**7.74%**
M. rotundipennis [7]	**6.33%**	**8.05%**	**7.27%**	**7.44%**	**6.91%**	**4.24%**	1.86%		**5.88%**
M. withlacoocheensis [7]	**12.20%**	**13.93%**	**13.15%**	**13.32%**	**12.79%**	**10.12%**	**7.74%**	**5.88%**	
M. puer [8]	0.93%	2.66%	1.87%	2.04%	1.52%	1.15%	3.54%	**5.40%**	**11.27%**
M. adelogyrus [8]	3.14%	1.41%	2.20%	2.03%	2.56%	**5.23%**	**7.61%**	**9.47%**	**15.34%**
M. kissimmee	0.66%	1.06%	0.28%	0.45%	0.08%	2.75%	**5.13%**	**6.99%**	**12.87%**
M. seminole [9]	2.25%	0.53%	1.31%	1.14%	1.67%	**4.34%**	**6.72%**	**8.58%**	**14.46%**
M. sp. nov. 2 [9]	**3.76%**	2.03%	2.82%	2.65%	3.17%	**5.84%**	**8.23%**	**10.09%**	**15.96%**
M. sp. nov. 1	0.13%	1.60%	0.81%	0.98%	0.46%	2.21%	**4.60%**	**6.46%**	**12.33%**
M. sp. nov. 3 [10]	0.99%	0.73%	0.05%	0.12%	0.41%	3.08%	**5.46%**	**7.32%**	**13.20%**
M. bonita [10]	2.54%	0.82%	1.60%	1.43%	1.96%	**4.63%**	**7.01%**	**8.87%**	**14.75%**
M. peninsularis	2.69%	0.96%	1.75%	1.58%	2.11%	**4.77%**	**7.16%**	**9.02%**	**14.89%**

Table 4-4 Continued.

L. SHAPE: Lophus

SPECIES	*M. puer* [8]	*M. adelogyrus* [8]	*M. kissimmee*	*M. seminole* [9]	*M.* sp. nov. 2 [9]	*M.* sp. nov. 1	*M.* sp. nov. 3 [10]	*M. bonita* [10]	*M. peninsularis*
M. gurneyi	**3.98%**	0.09%	2.39%	0.80%	0.71%	2.92%	2.06%	0.51%	0.36%
M. foxi [1]	3.72%	0.36%	2.12%	0.53%	0.97%	2.66%	1.79%	0.24%	0.09%
M. apalachicolae [1]	**5.08%**	1.01%	**3.49%**	1.89%	0.39%	**4.02%**	3.16%	1.60%	1.46%
M. scapularis	**4.61%**	0.53%	3.01%	1.42%	0.08%	3.55%	2.68%	1.13%	0.98%
M. tumidicercus [2]	3.95%	0.13%	2.35%	0.76%	0.74%	2.89%	2.02%	0.47%	0.32%
M. stegocercus [2]	**4.28%**	0.21%	2.69%	1.09%	0.41%	3.22%	2.36%	0.80%	0.66%
M. mirus	2.50%	1.58%	0.90%	0.69%	2.19%	1.44%	0.57%	0.98%	1.13%
M. pygmaeus [3]	**4.08%**	0.01%	2.49%	0.89%	0.61%	3.02%	2.16%	0.60%	0.46%
M. strumosus [3]	2.79%	1.29%	1.19%	0.40%	1.90%	1.73%	0.86%	0.69%	0.84%
M. indicifer [4]	0.93%	3.14%	0.66%	2.25%	**3.76%**	0.13%	0.99%	2.54%	2.69%
M. forcipatus [4]	2.66%	1.41%	1.06%	0.53%	2.03%	1.60%	0.73%	0.82%	0.96%
M. ordwayae [5]	1.87%	2.20%	0.28%	1.31%	2.82%	0.81%	0.05%	1.60%	1.75%
M. nanciae [5]	2.04%	2.03%	0.45%	1.14%	2.65%	0.98%	0.12%	1.43%	1.58%
M. childsi [6]	1.52%	2.56%	0.08%	1.67%	3.17%	0.46%	0.41%	1.96%	2.11%
M. sebringi [6]	1.15%	**5.23%**	2.75%	**4.34%**	**5.84%**	2.21%	3.08%	**4.63%**	**4.77%**
M. tequestae	3.54%	**7.61%**	**5.13%**	**6.72%**	**8.23%**	**4.60%**	**5.46%**	**7.01%**	**7.16%**
M. rotundipennis [7]	**5.40%**	**9.47%**	**6.99%**	**8.58%**	**10.09%**	**6.46%**	**7.32%**	**8.87%**	**9.02%**
M. withlacoocheensis [7]	**11.27%**	**15.34%**	**12.87%**	**14.46%**	**15.96%**	**12.33%**	**13.20%**	**14.75%**	**14.89%**
M. puer [8]		4.07%	1.59%	3.19%	**4.69%**	1.06%	1.92%	3.48%	3.62%
M. adelogyrus [8]	4.07%		2.48%	0.89%	0.62%	3.01%	2.15%	0.60%	0.45%
M. kissimmee	1.59%	2.48%		1.59%	3.09%	0.53%	0.33%	1.88%	2.03%
M. seminole [9]	3.19%	0.89%	1.59%		1.50%	2.13%	1.26%	0.29%	0.44%
M. sp. nov. 2 [9]	**4.69%**	0.62%	3.09%	1.50%		**3.63%**	2.76%	1.21%	1.07%
M. sp. nov. 1	1.06%	3.01%	0.53%	2.13%	**3.63%**		0.86%	2.42%	2.56%
M. sp. nov. 3 [10]	1.92%	2.15%	0.33%	1.26%	2.76%	0.86%		1.55%	1.70%
M. bonita [10]	3.48%	0.60%	1.88%	0.29%	1.21%	2.42%	1.55%		0.15%
M. peninsularis	3.62%	0.45%	2.03%	0.44%	1.07%	2.56%	1.70%	0.15%	

Table 4-4 Continued.

M. SHAPE: Aedeagal Region

SPECIES	*M. gurneyi*	*M. foxi* [1]	*M. apalachicolae* [1]	*M. scapularis*	*M. tumidicercus* [2]	*M. stegocercus* [2]	*M. mirus*	*M. pygmaeus* [3]	*M. strumosus* [3]
M. gurneyi		0.74%	2.92%	15.24%	1.63%	2.83%	**23.66%**	13.24%	**80.87%**
M. foxi [1]	0.74%		2.18%	14.50%	0.88%	2.09%	**22.91%**	12.50%	**80.13%**
M. apalachicolae [1]	2.92%	2.18%		12.32%	1.30%	0.09%	**20.73%**	10.32%	**77.95%**
M. scapularis	15.24%	14.50%	12.32%		13.61%	12.41%	8.41%	2.00%	**65.63%**
M. tumidicercus [2]	1.63%	0.88%	1.30%	13.61%		1.20%	**22.03%**	11.62%	**79.24%**
M. stegocercus [2]	2.83%	2.09%	0.09%	12.41%	1.20%		**20.83%**	10.41%	**78.04%**
M. mirus	**23.66%**	**22.91%**	**20.73%**	8.41%	**22.03%**	**20.83%**		10.41%	**57.22%**
M. pygmaeus [3]	13.24%	12.50%	10.32%	2.00%	11.62%	10.41%	10.41%		**67.63%**
M. strumosus [3]	**80.87%**	**80.13%**	**77.95%**	**65.63%**	**79.24%**	**78.04%**	**57.22%**	**67.63%**	
M. indicifer [4]	9.10%	8.35%	6.17%	6.15%	7.47%	6.27%	14.56%	4.15%	**71.78%**
M. forcipatus [4]	2.71%	1.97%	0.21%	12.53%	1.08%	0.12%	**20.94%**	10.53%	**78.16%**
M. ordwayae [5]	4.61%	3.87%	1.69%	10.63%	2.98%	1.78%	**19.05%**	8.63%	**76.26%**
M. nanciae [5]	12.37%	11.62%	9.44%	2.87%	10.74%	9.54%	11.29%	0.88%	**68.51%**
M. childsi [6]	3.61%	4.36%	6.54%	**18.86%**	5.24%	6.44%	**27.27%**	**16.86%**	**84.49%**
M. sebringi [6]	3.59%	4.33%	6.51%	**18.83%**	5.22%	6.42%	**27.24%**	**16.83%**	**84.46%**
M. tequestae	4.64%	5.39%	7.57%	**19.88%**	6.27%	7.47%	**28.30%**	**17.89%**	**85.51%**
M. rotundipennis [7]	**18.00%**	**17.26%**	15.08%	2.76%	**16.37%**	15.17%	5.65%	4.76%	**62.87%**
M. withlacoocheensis [7]	**30.79%**	**30.05%**	**27.87%**	15.55%	**29.16%**	**27.96%**	7.14%	**17.55%**	**50.08%**
M. puer [8]	**22.65%**	**21.91%**	**19.73%**	7.41%	**21.02%**	**19.82%**	1.00%	9.41%	**58.22%**
M. adelogyrus [8]	1.60%	0.86%	1.32%	13.64%	0.03%	1.23%	**22.06%**	11.64%	**79.27%**
M. kissimmee	0.56%	0.19%	2.37%	14.68%	1.07%	2.27%	**23.10%**	12.69%	**80.32%**
M. seminole [9]	0.08%	0.83%	3.01%	15.33%	1.71%	2.91%	**23.74%**	13.33%	**80.96%**
M. sp. nov. 2 [9]	0.56%	0.19%	2.37%	14.68%	1.07%	2.27%	**23.10%**	12.69%	**80.31%**
M. sp. nov. 1	0.43%	0.31%	2.49%	14.81%	1.20%	2.40%	**23.22%**	12.81%	**80.44%**
M. sp. nov. 3 [10]	3.27%	4.02%	6.20%	**18.51%**	4.90%	6.10%	**26.93%**	**16.51%**	**84.14%**
M. bonita [10]	3.94%	4.69%	6.87%	**19.18%**	5.57%	6.77%	**27.60%**	**17.19%**	**84.82%**
M. peninsularis	0.50%	1.24%	3.42%	**15.74%**	2.13%	3.33%	**24.16%**	13.74%	**81.37%**

Table 4-4 Continued.

N. SHAPE: Aedeagal Region

SPECIES	*M. indicifer* [4]	*M. forcipatus* [4]	*M. ordwayae* [5]	*M. nanciae* [5]	*M. childsi* [6]	*M. sebringi* [6]	*M. tequestae*	*M. rotundipennis* [7]	*M. withlacoocheensis* [7]
M. gurneyi	9.10%	2.71%	4.61%	12.37%	3.61%	3.59%	4.64%	**18.00%**	**30.79%**
M. foxi [1]	8.35%	1.97%	3.87%	11.62%	4.36%	4.33%	5.39%	**17.26%**	**30.05%**
M. apalachicolae [1]	6.17%	0.21%	1.69%	9.44%	6.54%	6.51%	7.57%	15.08%	**27.87%**
M. scapularis	6.15%	12.53%	10.63%	2.87%	**18.86%**	**18.83%**	**19.88%**	2.76%	15.55%
M. tumidicercus [2]	7.47%	1.08%	2.98%	10.74%	5.24%	5.22%	6.27%	**16.37%**	**29.16%**
M. stegocercus [2]	6.27%	0.12%	1.78%	9.54%	6.44%	6.42%	7.47%	15.17%	**27.96%**
M. mirus	14.56%	**20.94%**	**19.05%**	11.29%	**27.27%**	**27.24%**	**28.30%**	5.65%	7.14%
M. pygmaeus [3]	4.15%	10.53%	8.63%	0.88%	**16.86%**	**16.83%**	**17.89%**	4.76%	**17.55%**
M. strumosus [3]	**71.78%**	**78.16%**	**76.26%**	**68.51%**	**84.49%**	**84.46%**	**85.51%**	**62.87%**	**50.08%**
M. indicifer [4]		6.38%	4.49%	3.27%	12.71%	12.68%	13.74%	8.91%	**21.70%**
M. forcipatus [4]	6.38%		1.90%	9.66%	6.32%	6.30%	7.35%	**15.29%**	**28.08%**
M. ordwayae [5]	4.49%	1.90%		7.76%	8.22%	8.20%	9.25%	13.39%	**26.18%**
M. nanciae [5]	3.27%	9.66%	7.76%		**15.98%**	**15.95%**	**17.01%**	5.64%	**18.42%**
M. childsi [6]	12.71%	6.32%	8.22%	**15.98%**		0.03%	1.03%	**21.62%**	**34.41%**
M. sebringi [6]	12.68%	6.30%	8.20%	**15.95%**	0.03%		1.05%	**21.59%**	**34.38%**
M. tequestae	13.74%	7.35%	9.25%	**17.01%**	1.03%	1.05%		**22.64%**	**35.43%**
M. rotundipennis [7]	8.91%	**15.29%**	13.39%	5.64%	**21.62%**	**21.59%**	**22.64%**		12.79%
M. withlacoocheensis [7]	**21.70%**	**28.08%**	**26.18%**	**18.42%**	**34.41%**	**34.38%**	**35.43%**	12.79%	
M. puer [8]	13.56%	**19.94%**	**18.04%**	10.29%	**26.27%**	**26.24%**	**27.30%**	4.65%	8.14%
M. adelogyrus [8]	7.50%	1.11%	3.01%	10.77%	5.21%	5.19%	6.24%	16.40%	**29.19%**
M. kissimmee	8.54%	2.15%	4.05%	11.81%	4.17%	4.14%	5.20%	**17.45%**	**30.23%**
M. seminole [9]	9.18%	2.80%	4.69%	12.45%	3.53%	3.50%	4.56%	**18.09%**	**30.88%**
M. sp. nov. 2 [9]	8.54%	2.15%	4.05%	11.81%	4.17%	4.15%	5.20%	**17.44%**	**30.23%**
M. sp. nov. 1	8.66%	2.28%	4.18%	11.93%	4.05%	4.02%	5.08%	**17.57%**	**30.36%**
M. sp. nov. 3 [10]	12.37%	5.98%	7.88%	**15.64%**	0.34%	0.32%	1.37%	**21.27%**	**34.06%**
M. bonita [10]	13.04%	6.65%	8.55%	**16.31%**	0.33%	0.36%	0.70%	**21.95%**	**34.73%**
M. peninsularis	9.60%	3.21%	5.11%	12.87%	3.11%	3.09%	4.14%	**18.50%**	**31.29%**

Table 4-4 Continued.

O. SHAPE: Aedeagal Region

SPECIES	*M. puer* [8]	*M. adelogyrus* [8]	*M. kissimmee*	*M. seminole* [9]	*M.* sp. nov. 2 [9]	*M.* sp. nov. 1	*M.* sp. nov. 3 [10]	*M. bonita* [10]	*M. peninsularis*
M. gurneyi	**22.65%**	1.60%	0.56%	0.08%	0.56%	0.43%	3.27%	3.94%	0.50%
M. foxi [1]	**21.91%**	0.86%	0.19%	0.83%	0.19%	0.31%	4.02%	4.69%	1.24%
M. apalachicolae [1]	**19.73%**	1.32%	2.37%	3.01%	2.37%	2.49%	6.20%	6.87%	3.42%
M. scapularis	7.41%	13.64%	14.68%	15.33%	14.68%	14.81%	**18.51%**	**19.18%**	**15.74%**
M. tumidicercus [2]	**21.02%**	0.03%	1.07%	1.71%	1.07%	1.20%	4.90%	5.57%	2.13%
M. stegocercus [2]	**19.82%**	1.23%	2.27%	2.91%	2.27%	2.40%	6.10%	6.77%	3.33%
M. mirus	1.00%	**22.06%**	**23.10%**	**23.74%**	**23.10%**	**23.22%**	**26.93%**	**27.60%**	**24.16%**
M. pygmaeus [3]	9.41%	11.64%	12.69%	13.33%	12.69%	12.81%	**16.51%**	**17.19%**	13.74%
M. strumosus [3]	**58.22%**	**79.27%**	**80.32%**	**80.96%**	**80.31%**	**80.44%**	**84.14%**	**84.82%**	**81.37%**
M. indicifer [4]	13.56%	7.50%	8.54%	9.18%	8.54%	8.66%	12.37%	13.04%	9.60%
M. forcipatus [4]	**19.94%**	1.11%	2.15%	2.80%	2.15%	2.28%	5.98%	6.65%	3.21%
M. ordwayae [5]	**18.04%**	3.01%	4.05%	4.69%	4.05%	4.18%	7.88%	8.55%	5.11%
M. nanciae [5]	10.29%	10.77%	11.81%	12.45%	11.81%	11.93%	**15.64%**	**16.31%**	12.87%
M. childsi [6]	**26.27%**	5.21%	4.17%	3.53%	4.17%	4.05%	0.34%	0.33%	3.11%
M. sebringi [6]	**26.24%**	5.19%	4.14%	3.50%	4.15%	4.02%	0.32%	0.36%	3.09%
M. tequestae	**27.30%**	6.24%	5.20%	4.56%	5.20%	5.08%	1.37%	0.70%	4.14%
M. rotundipennis [7]	4.65%	16.40%	**17.45%**	**18.09%**	**17.44%**	**17.57%**	**21.27%**	**21.95%**	**18.50%**
M. withlacoocheensis [7]	8.14%	**29.19%**	**30.23%**	**30.88%**	**30.23%**	**30.36%**	**34.06%**	**34.73%**	**31.29%**
M. puer [8]		21.05%	**22.10%**	**22.74%**	**22.09%**	**22.22%**	**25.92%**	**26.60%**	**23.15%**
M. adelogyrus [8]	21.05%		1.04%	1.68%	1.04%	1.17%	4.87%	5.54%	2.10%
M. kissimmee	**22.10%**	1.04%		0.64%	0.00%	0.12%	3.83%	4.50%	1.06%
M. seminole [9]	**22.74%**	1.68%	0.64%		0.64%	0.52%	3.19%	3.86%	0.42%
M. sp. nov. 2 [9]	**22.09%**	1.04%	0.00%	0.64%		0.13%	3.83%	4.50%	1.06%
M. sp. nov. 1	**22.22%**	1.17%	0.12%	0.52%	0.13%		3.70%	4.38%	0.93%
M. sp. nov. 3 [10]	**25.92%**	4.87%	3.83%	3.19%	3.83%	3.70%		0.67%	2.77%
M. bonita [10]	**26.60%**	5.54%	4.50%	3.86%	4.50%	4.38%	0.67%		3.44%
M. peninsularis	**23.15%**	2.10%	1.06%	0.42%	1.06%	0.93%	2.77%	3.44%	

Table 4-4 Continued.

P. SHAPE: Tegmen

SPECIES	*M. gurneyi*	*M. foxi* [1]	*M. apalachicolae* [1]	*M. scapularis*	*M. tumidicercus* [2]	*M. stegocercus* [2]	*M. mirus*	*M. pygmaeus* [3]	*M. strumosus* [3]
M. gurneyi		0.16%	**0.66%**	0.14%	0.16%	0.30%	0.40%	0.39%	**0.67%**
M. foxi [1]	0.16%		**0.82%**	0.30%	0.00%	0.46%	0.56%	0.55%	**0.83%**
M. apalachicolae [1]	**0.66%**	**0.82%**		0.52%	**0.81%**	0.35%	0.25%	0.26%	0.01%
M. scapularis	0.14%	0.30%	0.52%		0.30%	0.16%	0.26%	0.25%	0.53%
M. tumidicercus [2]	0.16%	0.00%	**0.81%**	0.30%		0.46%	0.56%	0.55%	**0.82%**
M. stegocercus [2]	0.30%	0.46%	0.35%	0.16%	0.46%		0.10%	0.09%	0.36%
M. mirus	0.40%	0.56%	0.25%	0.26%	0.56%	0.10%		0.01%	0.26%
M. pygmaeus [3]	0.39%	0.55%	0.26%	0.25%	0.55%	0.09%	0.01%		0.27%
M. strumosus [3]	**0.67%**	**0.83%**	0.01%	0.53%	**0.82%**	0.36%	0.26%	0.27%	
M. indicifer [4]	0.06%	0.10%	**0.72%**	0.20%	0.10%	0.37%	0.46%	0.45%	**0.73%**
M. forcipatus [4]	0.10%	0.26%	0.56%	0.04%	0.25%	0.21%	0.31%	0.30%	0.57%
M. ordwayae [5]	0.00%	0.16%	**0.66%**	0.14%	0.16%	0.30%	0.40%	0.39%	**0.67%**
M. nanciae [5]	0.40%	0.24%	**1.06%**	0.54%	0.24%	**0.70%**	**0.80%**	**0.79%**	**1.07%**
M. childsi [6]	**0.72%**	**0.88%**	0.06%	0.58%	**0.88%**	0.42%	0.32%	0.33%	0.05%
M. sebringi [6]	0.50%	**0.66%**	0.15%	0.36%	**0.66%**	0.20%	0.10%	0.11%	0.16%
M. tequestae	**0.72%**	**0.88%**	0.07%	0.58%	**0.88%**	0.42%	0.32%	0.33%	0.06%
M. rotundipennis [7]	**0.69%**	**0.85%**	0.03%	0.55%	**0.85%**	0.39%	0.29%	0.30%	0.02%
M. withlacoocheensis [7]	**0.77%**	**0.93%**	0.11%	0.63%	**0.93%**	0.46%	0.37%	0.38%	0.10%
M. puer [8]	**0.65%**	**0.81%**	0.00%	0.51%	**0.81%**	0.35%	0.25%	0.26%	0.01%
M. adelogyrus [8]	**0.73%**	**0.89%**	0.07%	0.59%	**0.89%**	0.43%	0.33%	0.34%	0.06%
M. kissimmee	0.43%	0.59%	0.23%	0.29%	0.59%	0.12%	0.03%	0.04%	0.24%
M. seminole [9]	**0.67%**	**0.83%**	0.02%	0.53%	**0.83%**	0.37%	0.27%	0.28%	0.00%
M. sp. nov. 2 [9]	**0.68%**	**0.84%**	0.03%	0.54%	**0.84%**	0.38%	0.28%	0.29%	0.02%
M. sp. nov. 1	0.28%	0.44%	0.38%	0.14%	0.44%	0.03%	0.12%	0.11%	0.39%
M. sp. nov. 3 [10]	**0.68%**	**0.84%**	0.02%	0.54%	**0.84%**	0.37%	0.28%	0.29%	0.01%
M. bonita [10]	0.29%	0.44%	0.37%	0.15%	0.44%	0.02%	0.12%	0.11%	0.38%
M. peninsularis	0.59%	**0.75%**	0.06%	0.45%	**0.75%**	0.29%	0.19%	0.20%	0.07%

Table 4-4 Continued.

Q. SHAPE: Tegmen

SPECIES	*M. indicifer* [4]	*M. forcipatus* [4]	*M. ordwayae* [5]	*M. nanciae* [5]	*M. childsi* [6]	*M. sebringi* [6]	*M. tequestae*	*M. rotundipennis* [7]	*M. withlacoocheensis* [7]
M. gurneyi	0.06%	0.10%	0.00%	0.40%	**0.72%**	0.50%	**0.72%**	**0.69%**	**0.77%**
M. foxi [1]	0.10%	0.26%	0.16%	0.24%	**0.88%**	**0.66%**	**0.88%**	**0.85%**	**0.93%**
M. apalachicolae [1]	**0.72%**	0.56%	**0.66%**	**1.06%**	0.06%	0.15%	0.07%	0.03%	0.11%
M. scapularis	0.20%	0.04%	0.14%	0.54%	0.58%	0.36%	0.58%	0.55%	0.63%
M. tumidicercus [2]	0.10%	0.25%	0.16%	0.24%	**0.88%**	**0.66%**	**0.88%**	**0.85%**	**0.93%**
M. stegocercus [2]	0.37%	0.21%	0.30%	**0.70%**	0.42%	0.20%	0.42%	0.39%	0.46%
M. mirus	0.46%	0.31%	0.40%	**0.80%**	0.32%	0.10%	0.32%	0.29%	0.37%
M. pygmaeus [3]	0.45%	0.30%	0.39%	**0.79%**	0.33%	0.11%	0.33%	0.30%	0.38%
M. strumosus [3]	**0.73%**	0.57%	**0.67%**	**1.07%**	0.05%	0.16%	0.06%	0.02%	0.10%
M. indicifer [4]		0.16%	0.06%	0.34%	**0.78%**	0.56%	**0.78%**	**0.75%**	**0.83%**
M. forcipatus [4]	0.16%		0.10%	0.50%	**0.62%**	0.41%	**0.63%**	0.59%	**0.67%**
M. ordwayae [5]	0.06%	0.10%		0.40%	**0.72%**	0.50%	**0.72%**	**0.69%**	**0.77%**
M. nanciae [5]	0.34%	0.50%	0.40%		**1.12%**	**0.90%**	**1.12%**	**1.09%**	**1.17%**
M. childsi [6]	**0.78%**	**0.62%**	**0.72%**	**1.12%**		0.22%	0.00%	0.03%	0.05%
M. sebringi [6]	0.56%	0.41%	0.50%	**0.90%**	0.22%		0.22%	0.19%	0.27%
M. tequestae	**0.78%**	**0.63%**	**0.72%**	**1.12%**	0.00%	0.22%		0.03%	0.04%
M. rotundipennis [7]	**0.75%**	0.59%	**0.69%**	**1.09%**	0.03%	0.19%	0.03%		0.08%
M. withlacoocheensis [7]	**0.83%**	**0.67%**	**0.77%**	**1.17%**	0.05%	0.27%	0.04%	0.08%	
M. puer [8]	**0.72%**	0.56%	**0.65%**	**1.05%**	0.07%	0.15%	0.07%	0.04%	0.11%
M. adelogyrus [8]	**0.79%**	**0.63%**	**0.73%**	**1.13%**	0.01%	0.23%	0.01%	0.04%	0.04%
M. kissimmee	0.49%	0.33%	0.43%	**0.83%**	0.29%	0.07%	0.29%	0.26%	0.34%
M. seminole [9]	**0.73%**	0.58%	**0.67%**	**1.07%**	0.05%	0.17%	0.05%	0.02%	0.10%
M. sp. nov. 2 [9]	**0.74%**	0.59%	**0.68%**	**1.08%**	0.04%	0.18%	0.04%	0.01%	0.09%
M. sp. nov. 1	0.34%	0.18%	0.28%	**0.68%**	0.44%	0.22%	0.45%	0.41%	0.49%
M. sp. nov. 3 [10]	**0.74%**	0.58%	**0.68%**	**1.08%**	0.04%	0.18%	0.04%	0.01%	0.09%
M. bonita [10]	0.35%	0.19%	0.29%	**0.68%**	0.43%	0.22%	0.44%	0.40%	0.48%
M. peninsularis	**0.65%**	0.50%	0.59%	**0.99%**	0.13%	0.09%	0.13%	0.10%	0.18%

Table 4-4 Continued.

R. SHAPE: Tegmen

SPECIES	*M. puer* [8]	*M. adelogyrus* [8]	*M. kissimmee*	*M. seminole* [9]	*M.* sp. nov. 2 [9]	*M.* sp. nov. 1	*M.* sp. nov. 3 [10]	*M. bonita* [10]	*M. peninsularis*
M. gurneyi	**0.65%**	**0.73%**	0.43%	**0.67%**	**0.68%**	0.28%	**0.68%**	0.29%	0.59%
M. foxi [1]	**0.81%**	**0.89%**	0.59%	**0.83%**	**0.84%**	0.44%	**0.84%**	0.44%	**0.75%**
M. apalachicolae [1]	0.00%	0.07%	0.23%	0.02%	0.03%	0.38%	0.02%	0.37%	0.06%
M. scapularis	0.51%	0.59%	0.29%	0.53%	0.54%	0.14%	0.54%	0.15%	0.45%
M. tumidicercus [2]	**0.81%**	**0.89%**	0.59%	**0.83%**	**0.84%**	0.44%	**0.84%**	0.44%	**0.75%**
M. stegocercus [2]	0.35%	0.43%	0.12%	0.37%	0.38%	0.03%	0.37%	0.02%	0.29%
M. mirus	0.25%	0.33%	0.03%	0.27%	0.28%	0.12%	0.28%	0.12%	0.19%
M. pygmaeus [3]	0.26%	0.34%	0.04%	0.28%	0.29%	0.11%	0.29%	0.11%	0.20%
M. strumosus [3]	0.01%	0.06%	0.24%	0.00%	0.02%	0.39%	0.01%	0.38%	0.07%
M. indicifer [4]	**0.72%**	**0.79%**	0.49%	**0.73%**	**0.74%**	0.34%	**0.74%**	0.35%	**0.65%**
M. forcipatus [4]	0.56%	**0.63%**	0.33%	0.58%	0.59%	0.18%	0.58%	0.19%	0.50%
M. ordwayae [5]	**0.65%**	**0.73%**	0.43%	**0.67%**	**0.68%**	0.28%	**0.68%**	0.29%	0.59%
M. nanciae [5]	**1.05%**	**1.13%**	**0.83%**	**1.07%**	**1.08%**	**0.68%**	**1.08%**	**0.68%**	**0.99%**
M. childsi [6]	0.07%	0.01%	0.29%	0.05%	0.04%	0.44%	0.04%	0.43%	0.13%
M. sebringi [6]	0.15%	0.23%	0.07%	0.17%	0.18%	0.22%	0.18%	0.22%	0.09%
M. tequestae	0.07%	0.01%	0.29%	0.05%	0.04%	0.45%	0.04%	0.44%	0.13%
M. rotundipennis [7]	0.04%	0.04%	0.26%	0.02%	0.01%	0.41%	0.01%	0.40%	0.10%
M. withlacoocheensis [7]	0.11%	0.04%	0.34%	0.10%	0.09%	0.49%	0.09%	0.48%	0.18%
M. puer [8]		0.08%	0.23%	0.02%	0.03%	0.38%	0.02%	0.37%	0.06%
M. adelogyrus [8]	0.08%		0.30%	0.06%	0.05%	0.45%	0.05%	0.44%	0.14%
M. kissimmee	0.23%	0.30%		0.24%	0.25%	0.15%	0.25%	0.14%	0.16%
M. seminole [9]	0.02%	0.06%	0.24%		0.01%	0.39%	0.01%	0.39%	0.08%
M. sp. nov. 2 [9]	0.03%	0.05%	0.25%	0.01%		0.40%	0.00%	0.40%	0.09%
M. sp. nov. 1	0.38%	0.45%	0.15%	0.39%	0.40%		0.40%	0.01%	0.31%
M. sp. nov. 3 [10]	0.02%	0.05%	0.25%	0.01%	0.00%	0.40%		0.39%	0.09%
M. bonita [10]	0.37%	0.44%	0.14%	0.39%	0.40%	0.01%	0.39%		0.31%
M. peninsularis	0.06%	0.14%	0.16%	0.08%	0.09%	0.31%	0.09%	0.31%	

(Table 4-4G-I) had two: *M. mirus* and *M. strumosus*; and **5)** ectophallus (Table 4-4D-F) also had two, which were also the only species with any significant disparities: *M. forcipatus* and *M. nanciae*. The **6)** tegmen (Table 4-4P-R) lacked a dominant species.

Further examination of pairwise morphological disparity (Table 4-4A-R, Figs 4-13A to 4-18A) showed that, for each of the six shapes, the number of sister species sets (10 total pairs within lineages B-D only) that were statistically significant from each other (one to two pairs per shape) was never greater than for all other non-sister species and only twice within a lineage (*M. ordwaye-M. nanciae* (lineage C) for cercus and ectophallus). However, two sets of significantly disparate sister species were quite close to being the most disparate overall for two pairs: **1)** *M. nanciae-M. ordwayae* (lineage C) for cercus again and **2)** *M. pygmaeus-M. strumosus* (lineage B) for epiphallus.

When factoring in the estimated time between the earliest divergences between all pairwise species, the results shifted dramatically in that a pair of sister species then became the most disparate for all shapes (the tegmen was considered to have two) (Figs 4-13B to 4-18B). All of these sister pairs were also statistically significant before the inclusion of time except, curiously, for the two observed for the tegmen. Additionally, the patterns observed between the two sets of analyses were quite similar overall apart from the tegmen, which was quite variable. The most disparate pair for all shapes were as follows: **1)** cercus: *M. nanciae-M. ordwayae* (lineage C, diverged 1.24 million years ago (MYA)); **2)** ectophallus: *M. nanciae-M. ordwayae* (lineage C, 1.24 MYA); **3)** epiphallus: *M. pygmaeus-M. strumosus* (lineage B, 2.49 MYA); **4)** lophus: *M. rotundipennis-M. withlacoocheensis* (lineage D, 0.53 MYA); **5)** aedeagal region: *M.*

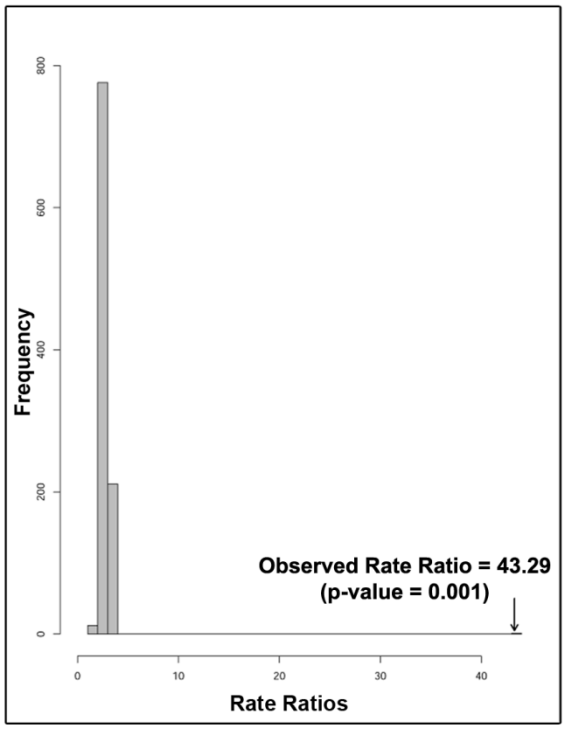

Fig. 4-19. Histogram representing the comparison of relative evolutionary rates for all six shapes ($p < 0.05$ = statistical significance).

puer-M. adelogyrus (lineage B, 0.47 MYA); and **6)** tegmen: *M.* sp. nov. 3-*M. bonita* (lineage D, 0.43 MYA) followed by *M. tumidicercus-M. stegocercus* (lineage B, 0.59 MYA). With the exception of the epiphallus pair, all others were far and away the most disparate relative to all other pairwise comparisons.

However, the other lineages for each shape were examined as well to determine if any contained sister species pairs that were also the most disparate (or close to it) compared to their lineage's additional species. This was found to be the case in several instances: **1)** cercus: *M. tumidicercus-M. stegocercus* (almost the highest ratio, lineage B, 0.59 MYA) and *M. rotundipennis-M. withlacoocheensis* (lineage D, 0.53 MYA); **2)**

ectophallus: *M. tumidicercus-M. stegocercus* (lineage B, 0.59 MYA) and *M.* sp. nov. 3-*M. bonita* (almost the highest ratio, lineage D, 0.43 MYA); **3)** epiphallus: *M.* sp. nov. 3-*M. bonita* (lineage D, 0.43 MYA); **4)** lophus: *M. foxi-M. apalachicolae* (almost the highest ratio, lineage B, 1.70 MYA) and *M. indicifer-M. forcipatus* (lineage C, 1.29 MYA); and **5)** aedeagal region: *M. pygmaeus-M. strumosus* (almost the highest ratio, lineage B, 1.24 MYA). Note, though, that, without time factored in, the final pair mentioned was the only one that was statistically significant.

Table 4-5. **A.** Comparison of relative evolutionary rates for all six shapes. **B.** Associated pairwise p-values. Shapes are ordered from highest to lowest rate ratio. **Bold** and * indicates statistical significance ($p < 0.05$).

A

	Observed Rate Ratio	**p-value**
Overall	42.44	**0.001***
SHAPE	**Shape Rate**	
Aedeagal Region	2.10	
Cercus	0.59	
Ectophallus	0.40	
Lophus	0.33	
Epiphallus	0.18	
Tegmen	0.049	

B

	Aedeagal Region	**Cercus**	**Ectophallus**	**Lophus**	**Epiphallus**	**Tegmen**
Aedeagal Region	**1**	**0.001***	**0.001***	**0.001***	**0.001***	**0.001***
Cercus	**0.001***	**1**	**0.016***	0.863	**0.001***	**0.001***
Ectophallus	**0.001***	**0.016***	**1**	1.00	**0.001***	**0.001***
Lophus	**0.001***	0.863	1.00	**1**	0.344	**0.001***
Epiphallus	**0.001***	**0.001***	**0.001***	0.344	**1**	**0.001***
Tegmen	**0.001***	**0.001***	**0.001***	**0.001***	**0.001***	**1**

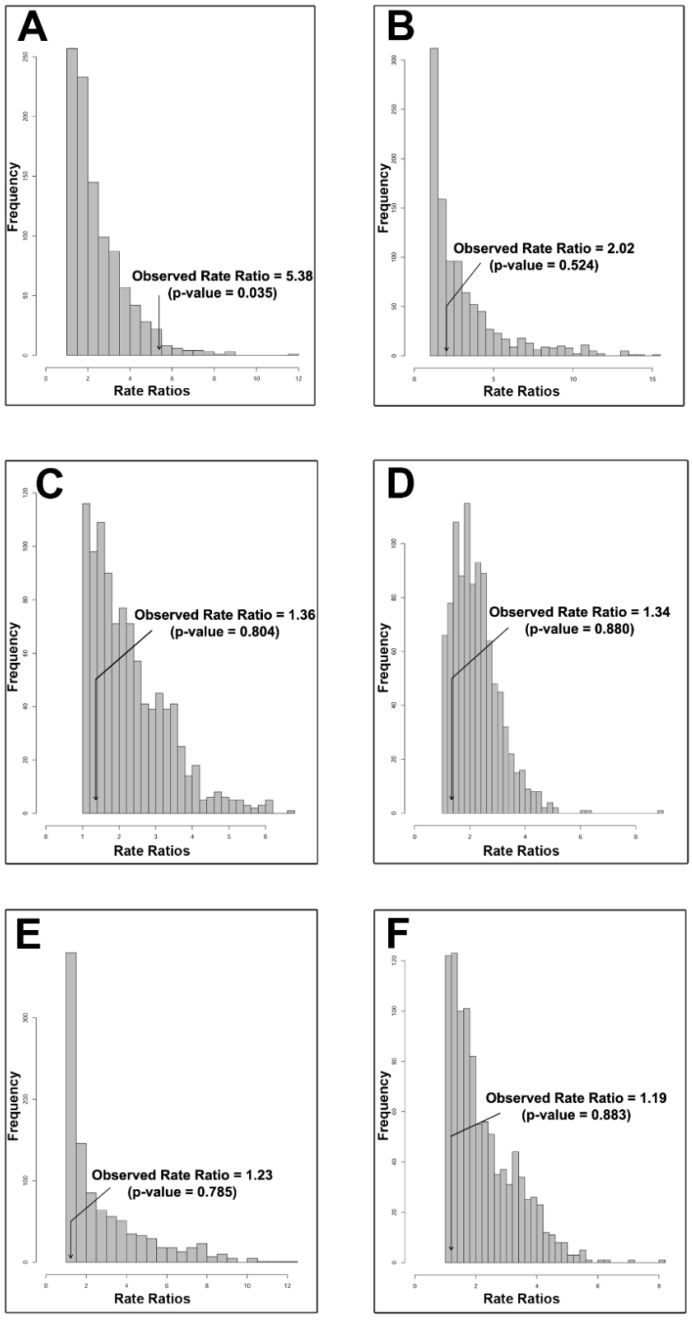

Fig. 4-20. Histograms representing the comparisons of the rate ratios for all six shapes between the relative evolutionary rate within the Puer Group *sensu stricto* (PGss) (9 species) and the non-PGss (18 species) ($p < 0.05$ = statistical significance). **A.** cercus, **B.** ectophallus, **C.** epiphallus, **D.** lophus, **E.** aedeagal region, and **F.** tegmen.

Table 4-6. Comparisons of the rate ratios for all six shapes between the relative evolutionary rate within the Puer Group *sensu stricto* (PGss) (9 species) and the non-PGss (18 species). Shapes are ordered from highest to lowest rate ratio. **Bold** and * indicates statistical significance ($p < 0.05$) while bold alone indicates that the PGss rate was higher.

SHAPE	Observed Rate Ratio	p-value	Rate of PGss	Rate of non-PGss
Cercus	5.38	**0.035***	0.00012	0.00062
Ectophallus	2.02	0.524	0.00016	0.00032
Lophus	1.36	0.804	**0.00064**	0.00047
Tegmen	1.34	0.880	**0.000058**	0.000043
Epiphallus	1.23	0.785	0.00013	0.00016
Aedeagal Region	1.19	0.883	**0.0014**	0.0011

Principal Components Analysis

PCA results showed that the first two axes (PC1 vs. PC2) described the majority of variation for all six shapes (Figs 4-7 to 4-12; Table 4-2). Each shape was fully described by at least 18 principal components (lophus possessed the least), but no more than 51 (aedeagal region). The percentage of cumulative variation for the first two axes for each shape, from highest to lowest, was: **1)** lophus: 81.76%, **2)** ectophallus: 74.78%, **3)** tegmen: 71.78%, **4)** cercus: 71.34%, **5)** aedeagal region: 60.02%, and **6)** epiphallus: 56.32%. Patterns of interest are intertwined with phylogeny and will be discussed in the subsequent section.

Incorporating Phylogeny

All six shapes had statistically significant phylogenetic signal as measured by Blomberg's K statistic (Fig. 4-21; Table 4-7). The PCA plots overlaid with the phylogeny (phylomorphospace – Figs 4-22 to 4-28) revealed a general pattern that

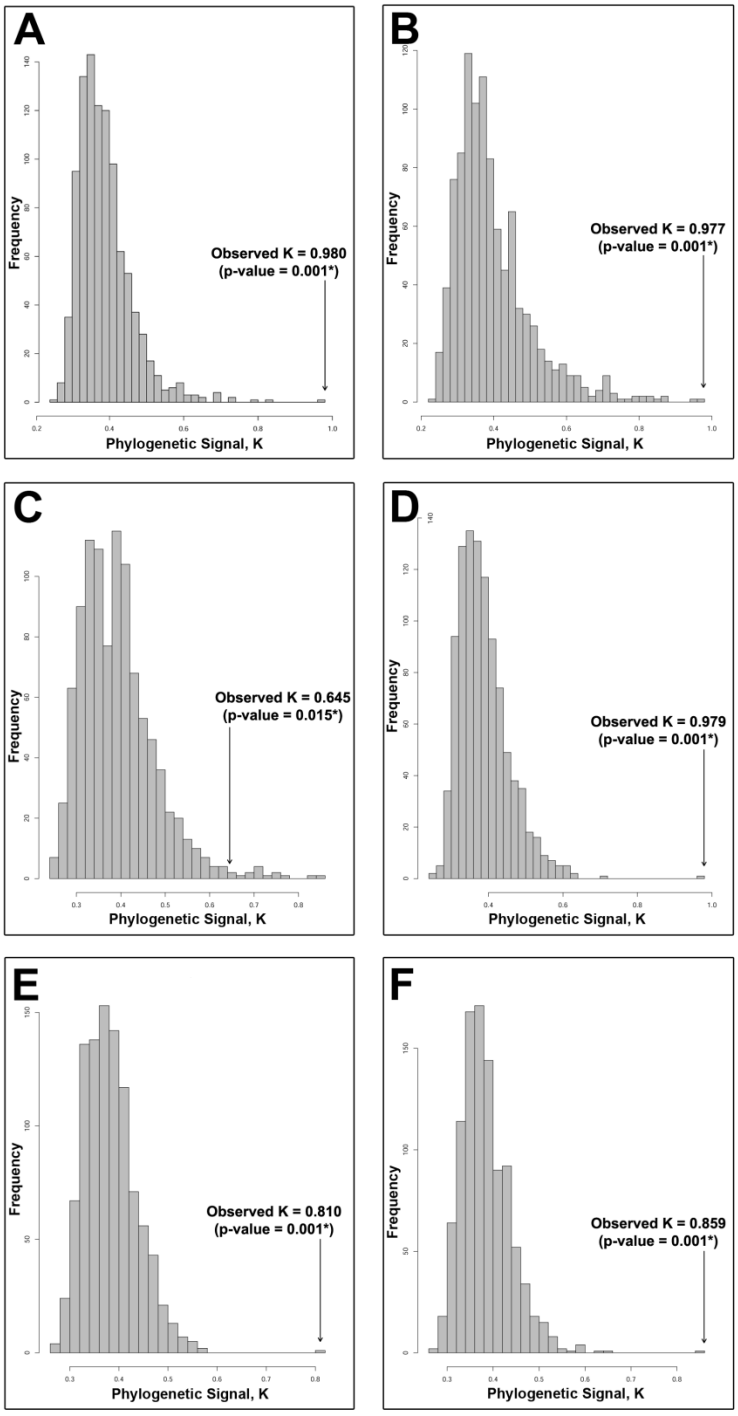

Figure 4.21. Phylogenetic signal (K) histograms for each of the six shapes ($p < 0.05$ = statistical significance): **A.** cercus, **B.** ectophallus, **C.** epiphallus, **D.** lophus, **E.** aedeagal region, and **F.** tegmen.

Table 4-7. Level of phylogenetic signal (K) found in each of the six shapes when taking into account the Puer Group phylogeny (Fig. 4-3). * indicates statistical significance ($p < 0.05$).

SHAPE	Observed K	p-value
Cercus	0.980	0.001*
Ectophallus	0.977	0.001*
Epiphallus	0.645	0.015*
Lophus	0.979	0.001*
Aedeagal Region	0.810	0.001*
Tegmen	0.859	0.001*

phylogenetically close species (and even the four major lineages) tended to cluster in shape space while less closely related species were more morphologically divergent. These clustering patterns also correspond well with the relative percentage of statistically significant morphological disparities. Plus, a relatively high amount of branch-crossing was present, which indicates shape convergence. Additionally, for most shapes (the exceptions being ectophallus (Fig. 4-24) and epiphallus (Fig. 4-25)), variation appeared to be quite great across most taxa, emanating from the first few relatively conserved, hypothesized ancestral shapes located towards the center of each phylomorphospace (Fig. 4-22). Furthermore, lineage C's four species stood out in the phylomorphospaces of four shapes (cercus (Fig. 4-23), ectophallus (Fig. 4-24), lophus (Fig. 4-26), and tegmen (Fig. 4-28)) because of their apparent wide divergence from other taxa and each other, and their occupation of unique regions of shape space (except for lophus). In contrast, across all shapes, the PGss (lineage D) tended to be conserved and clustered fairly closely in shape space except for two sister species: *M. puer* and *M. adelogyrus*, which were often fairly divergent from each other, other PGss species, and

even other taxa (e.g., see lophus (Fig. 4-26) and aedeagal region (Fig. 4-27)). An additional general pattern of interest was observed for the tegmen: lineage D was only statistically disparate from other PG species, most likely due to its current trajectory in phylomorphospace (Fig. 4-28), which is only shared by *M. gurneyi* (lineage A) and, partially, *M. apalachicolae* (lineage B).

A comparison of relative evolutionary rates across all six shapes revealed a high rate ratio (43.29) that was also statistically significant (Fig. 4-19 and Table 4-5). Based on relative rate, the intromittent genital component (aedeagal region) was demonstrated to be evolving the most rapidly at a rate (0.071) almost three and a half times greater than the next shape's rate (cercus: 0.021). These were followed by ectophallus (0.014), lophus (0.012), epiphallus (0.0058), and tegmen (0.0016). In terms of pairwise comparisons of rate between the shapes, all were found to be statistically significant except for lophus compared to cercus, ectophallus, and epiphallus.

A comparison of relative evolutionary rate ratios for the six individual shapes between the PGss and non-PGss (Fig. 4-20 and Table 4-6) showed that the cercus had the highest rate ratio overall at 5.44, along with a PGss rate that was the second lowest (behind the tegmen), and was the only ratio of statistical significance. Despite this, the PGss rate was still higher than the non-PGss rate in three cases: lophus, tegmen, and aedeagal region. Finally, for both groups, the aedeagal region possessed the highest rates of evolution and lowest rate ratio compared to all other shapes.

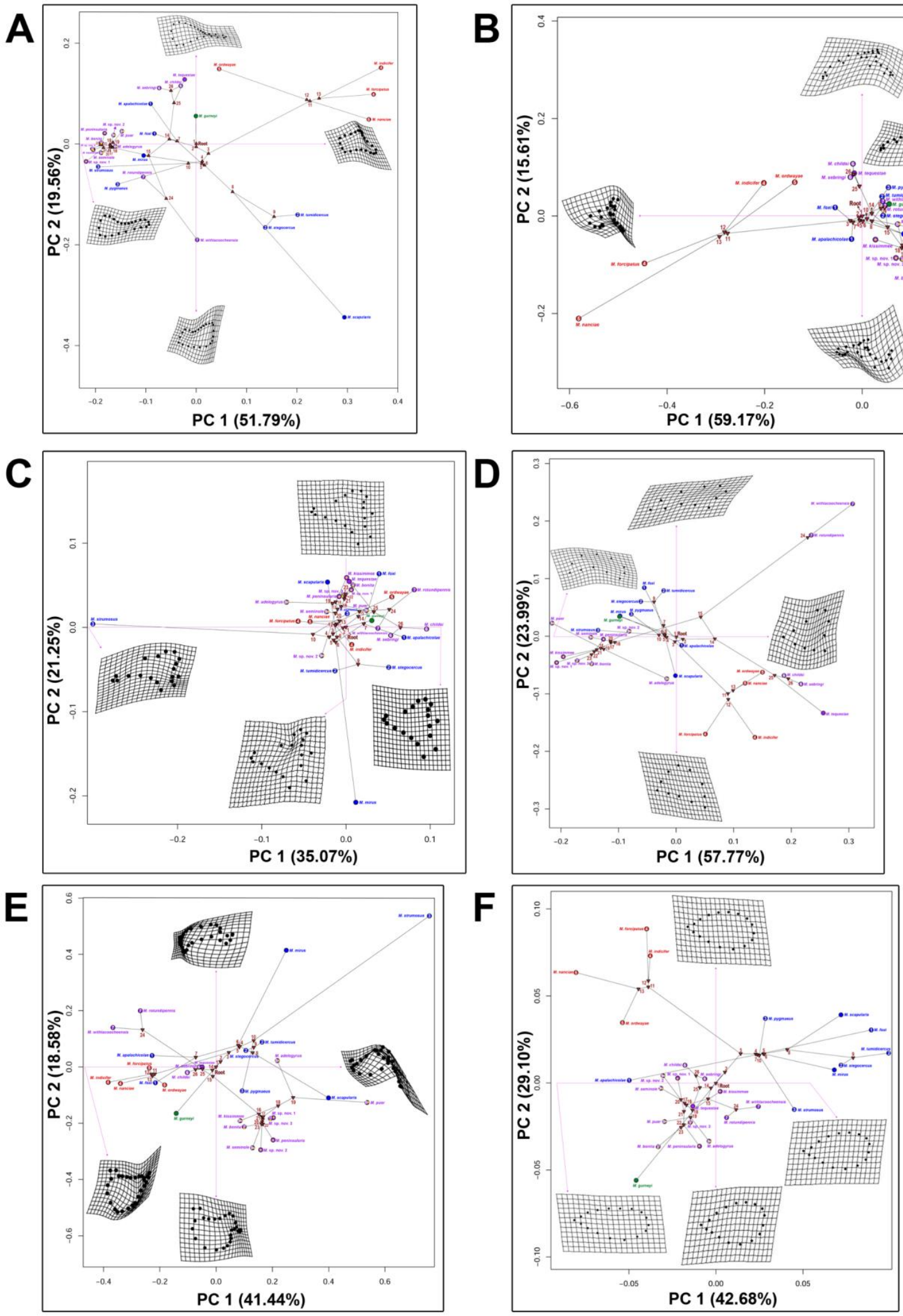

Figure 4-22. Comparison of phylomorphospaces (PC1 vs. PC2) for all six shapes with the most ancestral shape at the origin point. Species are colored by major lineage, sister species are identified by a paired set of numbers, and nodes are numbered, all according to the phylogeny (Fig. 4-3). Puer Group *sensu stricto* species are identified by the golden stars on their dots. The four landmarked shapes in each demonstrate the bending of that shape in relation to its morphospace trajectory. **A.** cercus, **B.** ectophallus, **C.** epiphallus, **D.** lophus, **E.** aedeagal region, and **F.** tegmen.*Note the relative scales on the axes of each phylomorphospace.

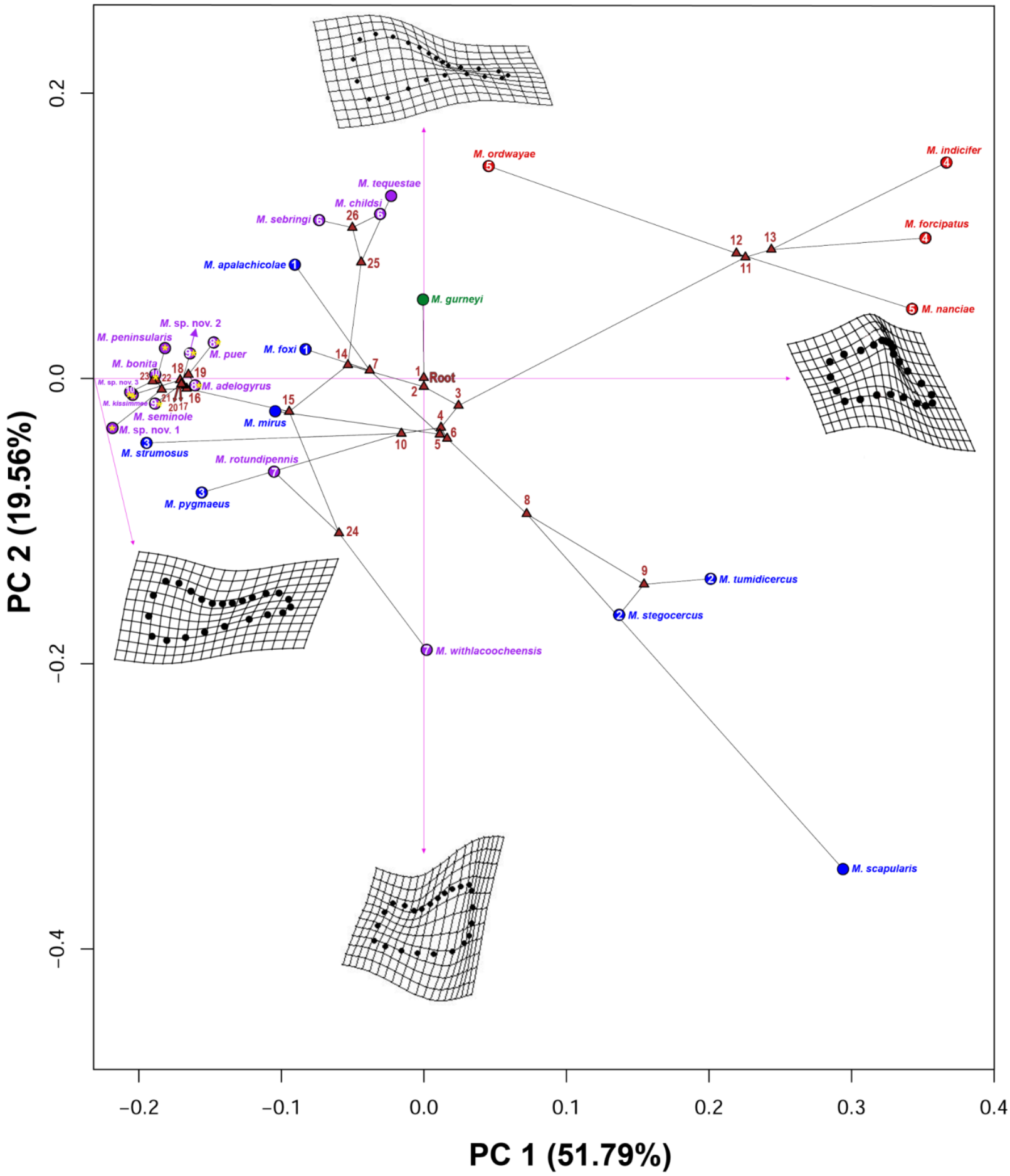

Figure 4-23. Phylomorphospace (PC1 vs. PC2) of cercus with the most ancestral shape at the origin point. Species are colored by major lineage, sister species are identified by a paired set of numbers, and nodes are numbered, all according to the phylogeny (Fig. 4-3). Puer Group *sensu stricto* species are identified by the golden stars on their dots. The four landmarked shapes demonstrate the bending of that shape in relation to its morphospace trajectory. *Note the scale on the axes in comparison to the phylomorphospaces of other shape.

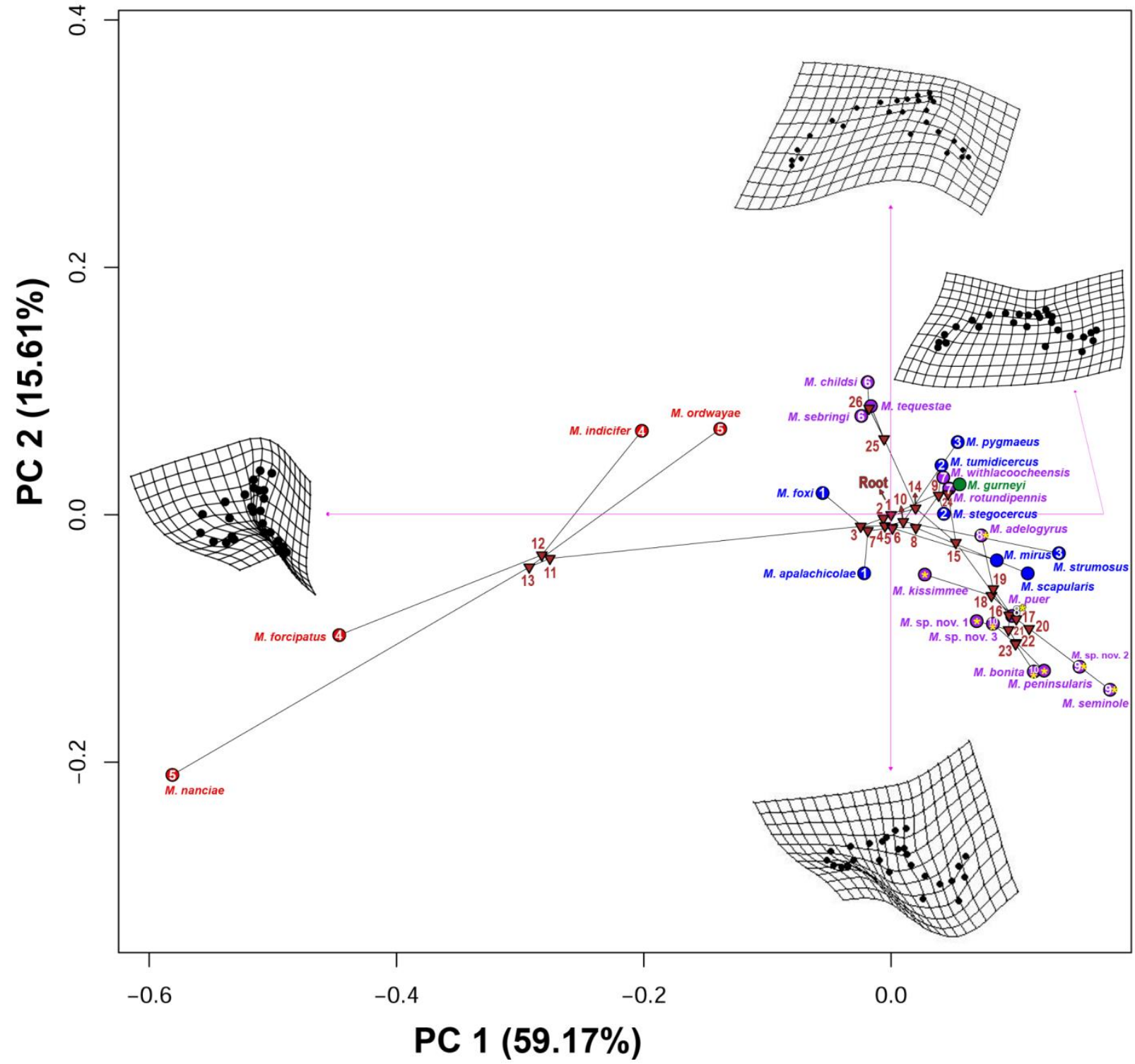

Figure 4-24. Phylomorphospace (PC1 vs. PC2) of the ectophallus with the most ancestral shape at the origin point. Species are colored by major lineage, sister species are identified by a paired set of numbers, and nodes are numbered, all according to the phylogeny (Fig. 4-3). Puer Group *sensu stricto* species are identified by the golden stars on their dots. The four landmarked shapes demonstrate the bending of that shape in relation to its morphospace trajectory. *Note the scale on the axes in comparison to the phylomorphospaces of other shapes.

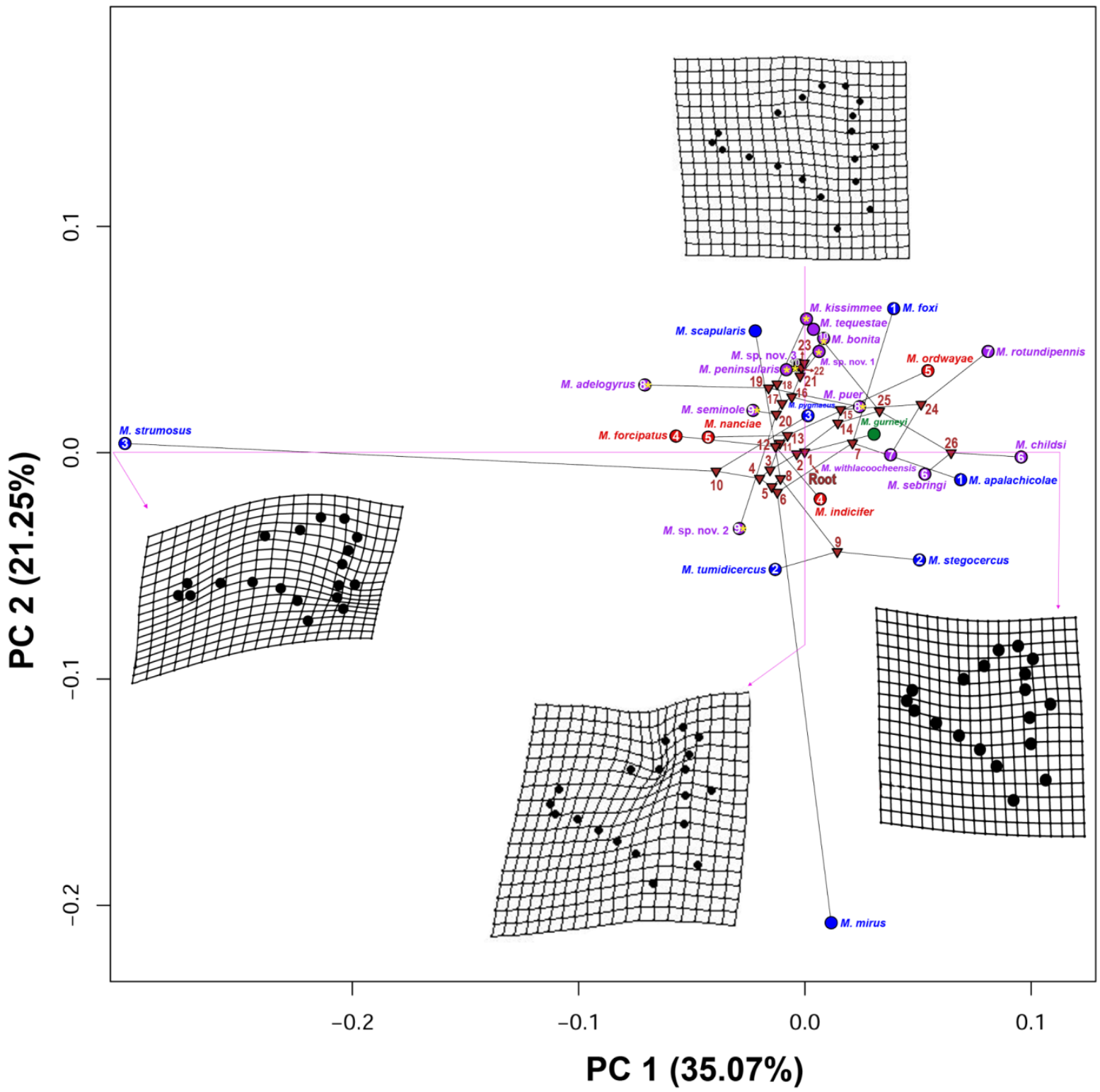

Figure 4-25. Phylomorphospace (PC1 vs. PC2) of the epiphallus with the most ancestral shape at the origin point. Species are colored by major lineage, sister species are identified by a paired set of numbers, and nodes are numbered, all according to the phylogeny (Fig. 4-3). Puer Group *sensu stricto* species are identified by the golden stars on their dots. The four landmarked shapes (rotated 90° clockwise) demonstrate the bending of that shape in relation to its morphospace trajectory. *Note the scale on the axes in comparison to the phylomorphospaces of other shape.

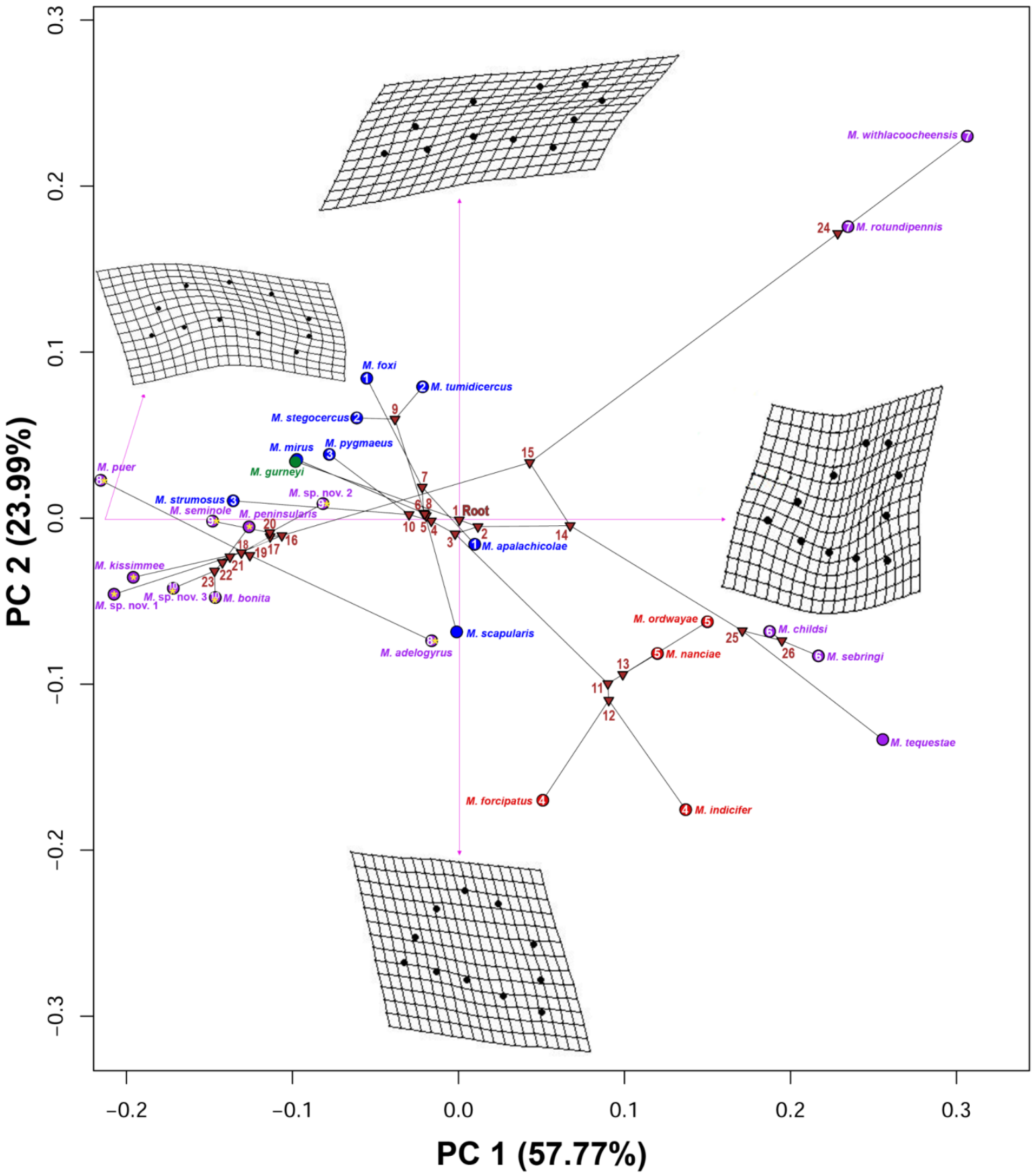

Figure 4-26. Phylomorphospace (PC1 vs. PC2) of the lophus with the most ancestral shape at the origin point. Species are colored by major lineage, sister species are identified by a paired set of numbers, and nodes are numbered, all according to the phylogeny (Fig. 4-3). Puer Group *sensu stricto* species are identified by the golden stars on their dots. The four landmarked shapes (rotated 90° clockwise) demonstrate the bending of that shape in relation to its morphospace trajectory. *Note the scale on the axes in comparison to the phylomorphospaces of other shapes

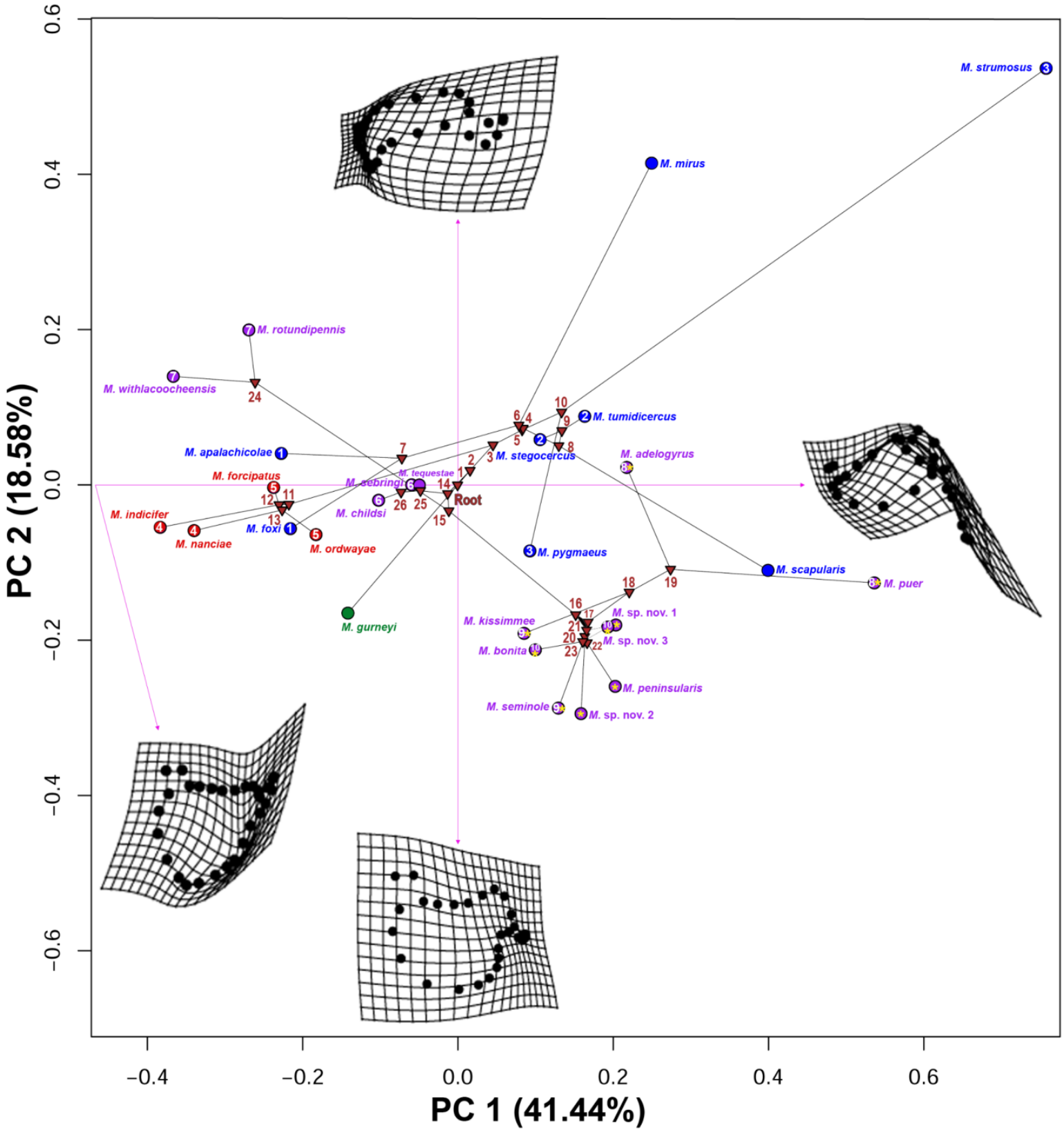

Figure 4-27. Phylomorphospace (PC1 vs. PC2) of the aedeagal region with the most ancestral shape at the origin point. Species are colored by major lineage, sister species are identified by a paired set of numbers, and nodes are numbered, all according to the phylogeny (Fig. 4-3). Puer Group *sensu stricto* species are identified by the golden stars on their dots. The four landmarked shapes demonstrate the bending of that shape in relation to its morphospace trajectory. *Note the scale on the axes in comparison to the phylomorphospaces of other shapes.

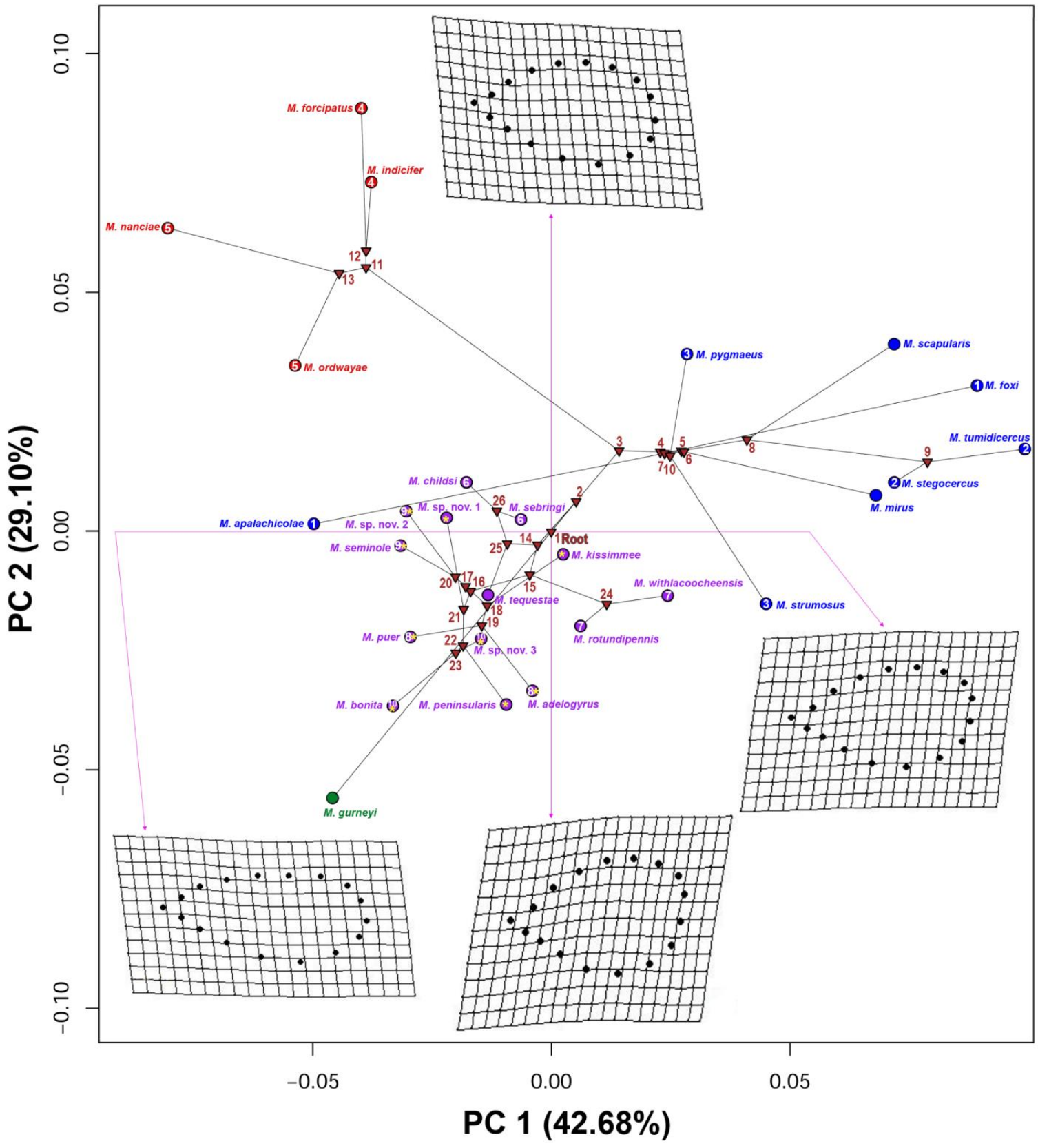

Figure 4-28. Phylomorphospace (PC1 vs. PC2) of the tegmen with the most ancestral shape at the origin point. Species are colored by major lineage, sister species are identified by a paired set of numbers, and nodes are numbered, all according to the phylogeny (Fig. 4-3). Puer Group *sensu stricto* species are identified by the golden stars on their dots. The four landmarked shapes demonstrate the bending of that shape in relation to its morphospace trajectory. *Note the scale on the axes in comparison to the phylomorphospaces of other shapes.

Discussion

Our investigations into the role of sexual selection in the evolution of the PG in the context of phylogeny have revealed much insight into relative divergence in shape and evolutionary rate of the six anatomical components analyzed. Male genitalia have long been considered to be rapid and divergent compared to non-genitalia (Eberhard, 1985; Eberhard, 1996; Hosken and Stockley, 2004; Eberhard, 2009; Eberhard, 2010a; Eberhard, 2010b; Song and Bucheli, 2010; Rowe and Arnqvist, 2011; Simmons, 2014) and we have demonstrated this with further strong evidence (e.g., Arnqvist, 1998; Mutanen and Kaitala, 2006; Marquez and Knowles, 2007; Rowe and Arnqvist, 2011). Perhaps even more striking is that we have shown this to be the case over the course of a geological time scale that can be considered quite short (3.71 MYO). This adds extra emphasis to the claim of rapidity in genital evolution, particularly in light of the wide divergence seen in most of the PG genital components included here (Figs 4-5, 4-6, and 4-22 to 4-28).

Evolutionary Rate of Anatomical Components

As expected, the highest rate of evolution was found to be associated with the aedeagal region, the collection of intromittent genital structures, at a rate that was almost three and a half times greater than the cercus, followed by the ectophallus, lophus, epiphallus, and tegmen (Fig. 4-19, Table 4-5). The rate ratio across these shapes was significant and quite high, demonstrating, probably not surprisingly, that the aedeagal region and tegmen are evolving at very different rates from each other with all other

components evolving at varying rates in-between. One surprise, though, was that the evolutionary rate for the lophus was not found to be statistically different from the rates of the cercus, ectophallus, and epiphallus. This is most likely due to the moderate amounts of variance observed in these four shapes (Figs 4-6A-D and 4-22) and possibly because the ectophallus and epiphallus were dominated by, respectively, the entirety of lineage C and two species from lineage B (Figs 4-24 and 4-25). This latter observation seems to also explain why the ectophallus and epiphallus had the least amount of significant morphological disparity (based on relative percentage: Table 4-3). Having established the presence of wide genital divergence and its relative rapidity evolutionarily speaking, our focus now turns towards elucidating the effect sexual selection has had on this complex biological system.

Sister Species and Runaway Selection

Regarding morphological disparity, sister species are expected to possess more divergent genitalia resulting from Fisherian runaway selection under the sexual selection hypothesis. We did not see this pattern, though, in the 10 sets of species pairs within the PG (lineages B-D only) in terms of statistical significance except for a single pair within lineage C for two shapes (cercus: Fig. 4-13A; Table 4-4A-C, and ectophallus: Fig. 4-14A; Table 4-4D-F). To be clear, numerous pairs of sister species were found to be significantly disparate, just not more-so than non-sisters. In line with our predictions, though, this pattern was completely reversed when evolutionary time was considered and cannot be considered to be a circular argument because morphological disparity was

calculated independently of phylogeny. By dividing pairwise morphological disparity by the estimated ancestral divergence time between any two species, we were able to calculate a ratio of disparity over time. Doing this revealed that a set of sister species pairs (that were statistically significant before the inclusion of time) dominated in terms of relative disparity for four of the anatomical components: cercus (Fig. 4-13B), ectophallus (Fig. 4-14B), lophus (Fig. 4-16B), and aedeagal region (Fig. 4-17B). The exceptions were the epiphallus (Fig. 4-15B), whose pair was only more moderately disparate than other species within lineage B, and the tegmen (Fig. 4-18B), which also had two pairs of sisters of moderate level, but neither were significantly disparate before the addition of time.

For all six components, the dominant sister species were some of the youngest in the PG and mostly belong to lineages C and D, the lineages with the youngest species (Fig. 4-3). The exceptions were the sisters for the epiphallus and one pair for the tegmen, both of which belong to lineage B, which contains most of the oldest PG species. The tegmen pair (*M. tumidicercus*-*M. stegocercus*), though, were estimated to be the youngest within the lineage by far, comparable to the estimated age of most sister pairs within lineage D. Of further interest, with evolutionary time still factored in, sister species from within lineages B-D almost always became the most disparate in terms of shape divergence, with at least one pair per component (Figs 4-14 to 4-18). The majority of these pairs were found within lineages C and D, especially those pairs possessing the highest disparity. Note, though, that, of these particular pairs, only *M. pygmaeus*-*M. strumosus* (lineage B, Figs 4-1 and 4-5), for the epiphallus, were disparate in terms of

statistical significance. As noted, this could be an artifact of their older estimated divergence time (2.49 MYA – Fig. 4-3) since all the other pairs displaying high disparity were relatively younger (at least 1.71 MYA).

Taken together, the results of synthesizing relative morphological disparity and evolutionary time are powerful evidence for our hypothesis that the male genitalia of the PG are undergoing runaway selection, but, obviously, only for some of the group's sister species. Initially, this may seem to run counter to our discovery that all six components possessed phylogenetic signal (Fig. 4-21; Table 4-7), implying that their evolution was largely shaped by phylogeny (descent with modification) as opposed to evolutionary processes, like selection (sexual or otherwise) (Song and Bucheli, 2010). Prior to this analysis it was uncertain if phylogenetic signal would even be present since the taxonomic identity of PG species has been historically and inexorably linked to the shape of multiple genital components, the aedeagus being the primary one (Hubbell, 1932; Strohecker, 1960; Deyrup, 1996; Squitier et al., 1998; Otte, 2012 ("2011")). Some of these components, such as the aedeagus (and, by association, the aedeagal region) and, to a lesser extent, the cerci, should be considered to be autapomorphic. In fact, due to this and other conflicting, non-genitalic characters, doubts had been cast about the monophyly of the PG as a whole and its historical subgroups (Rehn and Hebard, 1916; Blatchley, 1920; Hubbell, 1932; Lamb and Justice, 2005, Ch. II).

Some have suggested that rapid trait evolution is always expected to be independent of phylogeny because of the historical relationship between closely related species, meaning that genitalia divergence between sister species would have to

overcome phylogenetic inertia to be considered as rapidly evolving (Losos, 1999; Arnqvist and Rowe, 2002; Eberhard, 2004a; Simmons, 2014). Song and Bucheli (2010) contrarily argued that this idea is only correct based on the classification of the character in question. In other words, if the character is autapomorphic (species-specific), only then should phylogenetic signal be absent. Conversely, genital characters that can be classified as synapomorphic (but are still relatively divergent to each other and to non-genital characters between species in accordance with the sexual selection hypothesis (Eberhard, 1985)) and have phylogenetic signal can still be classified as rapidly evolving. This explains well why Song and Bucheli (2010) found statistically similar levels of signal across data sets comprised of genital and non-genital characters. Based on the latter's conclusions, Simmons (2014) oddly interpreted them to mean that the speed of genital divergence was not particularly rapid, which appears to be a misinterpretation of the basic tenets of sexual selection (Eberhard, 1985). Obviously, though, based on the PG evidence before us, we have found ourselves at a conflicting crossroads of knowledge because we found phylogenetic signal in two wildly-divergent, mostly-autapomorphic structures (cercus: Figs 4-1, 4-6A, 4-7, 4-13, and 4-23 and aedegal region: Figs 4-5, 4-6E, 4-11, 4-17, and 4-27) that have evolved rapidly over evolutionary time, both compared to each other and relative to a non-genital character (tegmen) (Fig. 4-19; Table 4-5).

This "signal vs. rate" debate was modeled by Revell et al. (2008) using many numerical simulations and it was discovered, based on the simplest model for the evolution of quantitative traits, that the two measures were not related. This was also

noted earlier by Blomberg and Garland (2002) who reviewed the concept of phylogenetic inertia to demonstrate how much it has changed since its first modern use in 1944. They then explained how this had resulted in the erroneous assumption that assessments of phylogenetic signal, which are simply measures of pattern recognition, are correlated with underlying evolutionary processes. However, Revell et al., (2008) did find that a link was possible in a number of special circumstances, the most relevant one being the concept of fluctuating selection. Also known as evolutionary tempo, this appears to be the most probable reason to explain our situation of dueling conceptual dichotomies in the PG.

Tempo is here defined as an acceleration or deceleration in the rate of evolution (Blomberg et al., 2003), which would definitely account for the unusual pattern we see in the PG given its relatively young age. That is, its evolutionary tempo may be in a phase of acceleration, at least for species of the youngest lineages, C and D, which are also associated with the geologically youngest region of the southeast: peninsular Florida. We have found particular support for this in that almost all of the greatest morphological disparity observed (significant or otherwise) across all lineages and within lineages, when time is factored in, has been in lineages C and D (Figs 4-13 to 4-18; Table 4-4). Furthermore, the estimated speciation rate for these two clades, and the three major clades within lineage D, have been shown to be fairly high (especially within D) (at least 0.87 species per million years), and all were higher than the speciation rate of lineage B (0.78 species per million years) (Ch. II). Accelerating tempo in light of the relatively short time period that the PG has existed would also serve to explain why only

some of the 10 pairs of PG sister species (compared to non-sisters) were the most disparate overall at this point in time. This would also clarify why most of the sister pairs within lineages displaying the greatest disparity were also not significantly disparate in a statistical sense: such divergence is in progress.

The PGss: A Case Study for Accelerating Evolutionary Tempo

Lineage D has three major clades (Fig. 4-3) and, although the PGss clade was only estimated to be the third youngest, it also has the highest species richness in the entire PG (at nine species), contains three of the 10 pairs of sisters species in the PG, and two of these pairs were found to be the youngest overall. Additionally, its estimated speciation rate of 2.31 species per million years (CH. II) may possibly be one of the highest known for an insect clade, let alone one not residing on a traditional oceanic island, suggesting recent, explosive speciation. Based on these things and what is known about the copulation process for the PG (Woller and Song, 2017), we suspected that sexual selection by cryptic female choice (Eberhard, 1985; Eberhard, 1996; Arnqvist, 1997; Edvardsson and Arnqvist, 2000; Miller, 2003; Eberhard, 2004a; Bergsten and Miller, 2008; Briceno and Eberhard, 2009; Eberhard, 2009; Eberhard, 2010a; Eberhard, 2010b; Ah-King, 2014; Simmons, 2014) has been the primary driver of speciation for the PGss. If so, we expected to find that the shape of the genitalia of its species would be the most divergent from each other compared to other PG species in terms of evolutionary time, plus PGss genitalia would also be the most rapidly evolving overall.

Unfortunately, the revealed patterns were not so clear and what we found instead requires some explanation.

First, only with the addition of estimated divergence time was morphological disparity highest (and statistically significant) for any of the PGss sister species (*M. puer-M. adelogyrus* - Fig. 4-1), but only for one component: aedeagal region (Figs 4-5 and 4-17B; Table 4-4M-O), the most rapidly evolving of all six examined shapes (Fig. 4-19; Table 4-5). At the level of lineage alone, the youngest sisters (*M.* sp. nov. 3-*M. bonita*, estimated at 0.43 MYO – Figs 4-1, 4-3, and 4-5) also displayed high disparity over time (but not (yet) of statistical significance) for two components: ectophallus (Figs 4-14B; Table 4-4D-F) and epiphallus (highest overall: Figs 4-15B; Table 4-4G-I). This indicates that PGss genitalia were only the most divergent from each other (compared to non-PGss species) a small fraction of the time, but the fact that one of the PGss sister pairs was revealed to be the most disparate by far for the most rapidly evolving component is intriguing because it indicates there is more to this story. An examination of the phylomorphospaces of the PGss (Fig. 4-22) also advocates for this idea. Although the subgroup's species are typically clustered, an ample amount of divergence (statistically significant or not) can be seen within the subgroup, especially between sister species (and especially *M. puer-M. adelogyrus*).

Perhaps the most compelling evolutionary tale within the PGss involves the namesake of the entire PG, *M. puer*, which was found to possess one of the most significantly divergent aedeagal regions compared to all other PGss species and several other PG species (Fig. 4-2; Table 4-4M-O). Another interesting thing about *M. puer* is

that it is also one of the most widely distributed PGss species (Fig. 4-2) and seems to be one of the few that has dispersed northwards. Such a widespread species might not be expected to also have the most unusually-shaped aedeagal region and yet it does, adding further support for an accelerated evolutionary tempo in at least the PGss. Factoring in what is known about the geographical distribution between *M. puer* and its sister, *M. adelogyrus*, may also be illuminating as they were estimated to have only diverged 0.47 MYA, the second-youngest split in the entire PG. The two species have two very distinct, non-overlapping ranges, because, as astutely noted by Hubbell (1932), they are separated by the St. Johns River, the longest in Florida. Unfortunately, our previous biogeographical analyses of the PG using BioGeoBEARS (Ch. II, Matzke, 2013, 2014) returned mixed results regarding the estimated processes that would explain the modern-day distribution of these sisters and included sympatry (dominant), dispersal, and founder-events. Since allopatry at finer scales can resemble sympatry in BioGeoBEARS analyses (Ch. II), vicariance as a result of the river may explain the ancestral split of these two species.

Conceptually, the presence of this physiographic barrier may seem to suggest that the evolutionary tempo of sexual selection should have decelerated once *M. puer* and *M. adelogyrus* were reproductively isolated because there was less selective pressure being placed on the system. We suggest, though, that the opposite scenario is probably more likely based on our shape analysis evidence and the fact that sexual selection has been found to operate intraspecifically (Arnqvist, 1997; Mutanen and Kaitala, 2006; Rowe and Arnqvist, 2011). Adding fuel to this argument is the fairly high degree of

observable intraspecific variation in the aedeagal region of the ten specimens included in our shape analysis (Fig. 4-11), which well-encompass the range in variation (Hubbell, 1932; DAW, personal observations). However, from a taxonomic perspective and based on the species concept of the PG, this variation does not yet suggest the splitting of *M. puer* into multiple species because the appearance of the aedeagal region (and other genitalia) are still more similar intraspecifically than interspecifically. Still, it would seem that this PGss species in particular may be further along the speciation continuum (Powell et al., 2013) than the others and, given more time, may undergo speciation on its path to overcoming phylogenetic inertia (Blomberg and Garland (2002). Other PGss species may be experiencing similar situations, but the effect of sexual selection is not yet as pronounced.

Secondly, we compared the relative evolutionary rates of the six analyzed components for the PGss against those of the rest of the PG in order to determine which group had genitalia that were evolving the most rapidly (Fig. 4-20; Table 4-6). Once again, the pattern we found was mixed, with the difference in the evolutionary rate of the cercus the only statistically significant rate ratio. This particular finding can be explained by knowing something about the cerci within the PGss; they are collectively the most basic in shape in the PG and are extraordinarily similar compared to the great variation seen in other PG species (Fig. 4-13, Table 4-4A-C). Thus, the rate ratio is so high because the rate of evolution for the cercus in the PGss is comparatively low. Despite the lack of additional significant rate ratios, there is more to the story because the evolutionary rates within the PGss were greater than the same rates for the non-PGss for

three components (from highest to lowest in terms of difference compared to non-PGss species): lophus, tegmen, and aedeagal region. These results make the compelling argument that, despite the lack of statistical significance, at least two of the genital components in the PGss are actually evolving more rapidly than outside of the PGss. Even more telling is that the lophus and aedeagal region seem to be the most strongly associated with females due to their direct contact and function during copulation (Woller and Song, 2017). The rapid evolution of these components seems to be best-explained currently by the cryptic female choice hypothesis of sexual selection.

Relating Shape Evolution to Function

A number of previous studies have suggested that since genital components have differing functions they will evolve at dissimilar rates because they may be under different selective pressures (Marquez and Knowles, 2007; Song and Wenzel, 2008; Song and Bucheli, 2010; Rowe and Arnqvist, 2011; Simmons, 2014). Woller and Song (2017) found possible evidence for these ideas within the PG's male genitalia because of the varied tasks that these components engage in during copulation. Moreover, our findings here, especially for the PGss, seem to strongly suggest that evolutionary tempo of sexual selection is acting at different speeds on different genital components. What follows will be a synopsis of some of the more interesting connections between the probable roles of the components during the mating process and the results of our shape analyses centered on the evolutionary rate comparisons of the five examined genital structures in the context of evolutionary tempo.

First and foremost, the aedeagal region consistently displayed the highest level of variation in shape divergence across all analyses that included the entirety of the PG and across all lineages (Figs 4-6E, 4-17, and 4-27; Tables 4-3, 4-4M-O, and 4-5). This was consistent with our expectations for an autapomorphic character such as this, particularly one around which the morphological species concept of the PG has largely been constructed (Hubbell, 1932; Strohecker, 1960; Deyrup, 1996; Squitier et al., 1998; Otte, 2012 ("2011")). If sexual selection by cryptic female choice is the primary driver of the genital divergence of males in the PG (and, by association, speciation), then we would definitely expect the pattern we see here: that the primary intromittent genital component was found to be the most divergent in shape and possessed the highest rate of comparative evolution.

At the opposite end of the rate spectrum for the PG was the epiphallus, which was found to be evolving over 12 times slower than the aedeagal region (Table 4-5) and also had one of the lowest levels of statistically significant disparity (based on relative percentage: Table 4-3), over two times less than the aedeagal region. Two possible reasons may explain this pattern: **1)** the epiphalli of *M. mirus* and *M. strumosus* (lineage B, Figs 4-1 and 4-4C) were dominant in terms of shape divergence (Figs 4-15A and 4-25; Table 4-4G-I) and overwhelmed the statistical analysis. Looking at the morphological disparity results and phylomorphospace, it can clearly be seen that moderate variation exists in this component, but obviously not yet enough to be statistically relevant. **2)** In terms of function, the two primary tasks of the epiphallus during copulation seem to be supporting the male's phallic complex as an attachment

site for muscles and allowing a male to gain access to a female's internal genitalia (Woller and Song, 2017). This second task can be split into two subtasks, each of which involves a unique, exposed (not covered by muscle tissue) subcomponent: **i)** the ancorae, which allow a male to hook onto (with pressure alone – imagine the claw end of a hammer pulling down on an mostly flat object) and pull down the female's external subgenital plate and **ii)** the lophi, which a male pushes into the female's lophi receptacles on the interior of her subgenital plate in order to hold open her subgenital plate during mating (Woller and Song, 2017). The ancorae were not included in this study because their shape appears to be essentially the same across species, they have not been particularly useful historically as taxonomic characters (in at least *Melanoplus*), and the job they perform seems so basic that there is either a lack of selective pressure on the ancorae or stabilizing selection is so high that these components have converged on a shared shape. As it stands, either one of these ideas might explain the low evolutionary rate that we observed.

As for why such great variation exists in the shape of the epiphallus for *M. mirus* and *M. strumosus* (sister species to *M. pygmaeus* - Fig. 4-1), they belong to lineage B and the common ancestor of its species has been estimated to be older than those of lineages C and D (Fig. 4-3). This suggests that these species have been on their evolutionary trajectory for a longer period, so an accumulation of greater differences in morphology (in general) might be expected. Perhaps, even, due to drift caused by long periods of isolation when taking into account their relative geographic distributions (Fig. 4-2). *M. mirus* is the furthest northeast species in the PG and has been relatively isolated

from other species in one of the older regions of the southeast while *M. strumosus* is the most far-flung species and is also relatively isolated in some populations. On the other hand, the proposed biogeographical history of *M. strumosus* (Ch. II) estimated that this species evolved in Florida's panhandle with *M. pygmaeus*, but while the latter dispersed west, the former dispersed north and then west. In light of this, sexual selection is the more likely agent of divergence of the epiphallus shape in at least *M. strumosus*, but probably also in the rest of the PG by associated default, but weakly so (seemingly). Combining all of these thoughts for this anatomical component, the evolutionary tempo of sexual selection might be increasing or decreasing, but it currently depends on perspective in the absence of more compelling evidence for one over the other. However, if the tasks of the epiphallus as a whole cannot be considered to be specialized, then it stands to reason that diversifying selective pressure from sexual selection would be relatively low.

As mentioned, the lophus can be considered to be the most-specialized subcomponent of the epiphallus and, unlike the ancorae, it is often used as a taxonomic character to differentiate many species of Acrididae because of its fairly unique shape across species (e.g., Otte, 2012 ("2011"); Hill, 2015) In terms of evolutionary rate, the lophus was revealed to be above epiphallus, but at a rate that was twice as high. Interestingly, its levels of statistically significant disparity (based on relative percentage: Table 4-3) were the second-highest, just after the aedeagal region (and tied with cercus). This suggests a fairly high level of variation and this can be seen somewhat in the GPA results (Fig. 4-6D) and much more easily in its phylomorphospace (Fig. 4-26), which

had some of the most unusual patterns for the species in the non-PGss clades of lineage D.

The aforementioned use of the lophus in pinning down a female's subgenital plate during copulation seems like a basic function as with the ancorae. However, it seems, at least in many cases across Acrididae (Randell, 1963), that there is some correlation in size and shape of the female's interior lophus receptacles and the lophi of the male, which probably explains their unique shapes. A cursory examination of females of PG species did not reveal any major observable differences (DAW, personal observations), but they could be subtle. The differences (in at least the PG) could also be sensory-related because Woller and Song (2017) discovered that the lophi of *M. rotundipennis* were covered in scales. At the time, our working hypothesis was that they acted as friction anchors to hold a female's subgenital plate in place, but in light of this new evidence it would seem that there is more going on with this component from an evolutionary point of view. Thus, we propose that the lophus is in the midst of accelerating evolutionary tempo in the PG, particularly given the unique phylomorphospace trajectories of many of the group's species (Fig. 4-26), many of which belong to the lineages containing the species estimated to be the youngest: C and D. Note that lineage B's species, which are almost all estimated to be some of the oldest in the PG are quite conserved in comparison, further evidence of increasing tempo with relative age.

In many respects, the evolutionary scenario we have proposed for the epiphallus appears to be similar for that of the ectophallus. Its levels of statistically significant

disparity (based on relative percentage: Table 4-3) are even similar as its probable primary function during copulation in that it serves as a much-larger attachment site for muscles. Plus, the shape of the ectophallus is dominated by the four species (two pairs of sister species) comprising lineage C (Figs 4-1, 4-6B, and 4-24), which are far more divergent from the rest of the PG compared to the two extreme species for the epiphallus (note the relative scales on Figs 4-24 and 4-25). These similarities are seemingly shattered, though, when taking into account the evolutionary rate of the ectophallus, which is the third-highest and almost two and a half times faster than that of the ectophallus (Table 4-5). The possible reason for such a high rate probably lies, once again, with the relatively younger age of lineage C's species (Fig. 4-3) and, possibly, the fact that the ectophallus serves as a "morphological bridge" between the aedeagal region (connected to its posterior end) and the epiphallus/lophus (connected along its dorsal edge). The ectophallus also possesses several subcomponents of variable taxonomic importance that have been noted to play unique roles during copulation (in at least the PG – Woller and Song, 2017).

Our collected evidence and ideas point to the ectophallus being under sexual selection, but, unusually, perhaps the tempo is accelerating in lineage C, but appears to be decelerating (or is just much slower) in lineages A, B, and D. If so, the reason for this pattern is murky at this time, but may have its roots in the disjointed modern-day distribution of lineage C's species (Fig. 4-2). Our previous biogeographical history for this lineage suggested that founder-events and/or vicariance played the largest roles in at least initial speciation (Ch. II). The relative geographical isolation, in particular, of the

two youngest (barely so) sister species in lineage C, *M. ordwaye-M. nanciae* (Figs 4-1 and 4-5) might explain well the high amount of shape divergence they essentially display across all six shapes (Fig. 4-22). For instance, they are the most disparate pair, when time is included, for ectophallus (Fig. 4-14B) and cercus (Fig. 4-13B). Based on these observations, this lineage could be considered a classic example of runaway selection.

The cercus (one of the few external genital structures and the only one included) was revealed to have the second-highest rate of evolution, but still almost three and a half times slower than the aedeagal region. Additionally, its levels of statistically significant disparity (based on relative percentage: Table 4-3) were also the second-highest (but tied with lophus) and this fairly high level of variation is easily observable in all lineages except, as noted earlier, the PGss clade of lineage B (Figs 4-6A and 4-23). As with the aedeagal region, the cercus can be considered to be an autapomorphic character or mostly so since the interspecific differences are not as great as in the aedeagal region and homology is easier to assign (plus the PGss' highly similar shape confounds the species-identifiable nature of this character by human observers). Even though most species in the PG are readily able to be identified taxonomically by their cercus shape, its function during copulation is still unclear.

Previously, we proposed a number of possible functions for the cerci, the primary one being that they acted as general supports for the subgenital plate of the female (Woller and Song, 2017). Along these lines, it seemed as if the tips of the cerci of *M. rotundipennis* in our study were being pushed into a mild invagination towards the posterior end of the female's abdomen and we suggested that follow-up studies were

needed. Unfortunately, we have not yet done this, but since cerci have been observed to be sensory structures (Snodgrass, 1935; Uvarov, 1966; Snodgrass, 1993; Gordh and Headrick, 2001; Chapman, 2012), it stands to reason that they may be acting as such during copulation for some still-unknown purpose. However, based on the evidence before us, the most obvious purpose would be to act as conspecific identification tools. This makes sense from an evolutionary perspective in light of the typical *Melanoplus* mating system of coerciveness (Otte, 1970; Bland 1987; Woller and Song, 2017) because it would just make sense for a female to have a way to identify appropriate males in a seemingly touch-based system before expending energy on what amounts to useless copulation. Many other insects do have such systems in place (e.g., Eberhard, 1985; McPeek et al., 2008, 2010), so it seems reasonable that it would exist here as well, but there are no known grasshopper studies yet on this topic.

If, though, the function of the cerci in the PG is for females to judge potential mate identity, then the expectation is that the relative evolutionary rate for the cerci should be slow. This is because mate-identifying traits should be under stabilizing selection and only demonstrate punctuated shifts in shape divergence during speciation events or, otherwise, the opposite sexes of conspecifics might no longer be able to reproduce successfully in the absence of clarity regarding initial identification (Templeton, 1979; Paterson, 1993; McPeek et al., 2008, 2010). McPeek et al. (2008, 2010) tested this hypothesis using shape analysis on damselfly cerci and found the expected pattern, from which they drew the conlusion that intraspecific sexual selection was either very low or not acting on damselfly cerci at all. Their findings seem to run

quite contrary to our own results, which could mean one of two things for the PG: **1)** that cerci are not used as conspecific identifiers after all, or only partially so, indicating that something else is used as the (primary) method (pheromones are a possibility, but this idea has also not been investigated for *Melanoplus* yet). This would also mean that the function of the cerci during copulation is still up for debate. **2)** The high levels of divergence observed in the cercus occurred during speciation events, as suggested by McPeek et al. (2008, 2010), which would suggest that the shape divergence pattern we see now is an evolutionary remnant of decreasing tempo.

We are not sure which of these hypotheses fits better at this juncture because of the conflicting patterns we have observed in the cerci of the two youngest lineages. The cercus shape of Lineage C's species were found to be almost entirely significantly divergent from one another and from almost all other species, especially when factoring in time (Figs 4-13 to 4-18; Table 4-4A-C). Lineage C also boasts a species (*M. nanciae* – shaped like a crab claw – Figs 4-1 and 4-4A) with the most unique cercus shape in the PG while the cercus of its sister species (*M. ordwayae* – Fig. 4-1) is quite basic. The cercus shape of lineage D's *M. rotundipennis-M. withlacoocheensis* possesses a pattern reminiscent of lineage C, mostly when including time. Lineage D's other two clades, though, can be characterized as having the opposite pattern in that their cercus shapes are are also very similar and none are statistically significant from each other or within their respective clades (Fig. 4-13A to 4-18A, Table 4-4A-C), even with the inclusion of time (Fig. 4-13B to 4-18B). The dilemma is thus this: if the cercus shape in one young lineage is highly divergent, then why is this pattern not found across the other lineages of similar

age, especially if the components are used as intraspecific identifiers? This latter hypothesis is especially confounded by the cercus shape of the PGss. In the absence of further evidence, we think that a combination of the two proposed hypotheses makes the most sense, that cercus shape is mostly not being used as a conspecific identifying tool and that the high evolutionary rate for the cercus we see is actually on the decline as evolutionary tempo decelerates from past speciation events, a situation predicted by Kraaijeveld et al. (2011). Of course, we are still in the dark as to why the cercus shape in lineage C and part of D diverged wildly in the first place, although it may just be that selection pressure was stronger in these lineages for whatever reason. Deeper investigations into the functions of this component may bring meaning and possibly even reveal how the sexes of PG species (and other *Melanoplus* species) are identifying each other before commencing copulation.

The Curious Evolutionary Case of Puer Group Tegmina

The tegmen was chosen in particular to be the baseline, non-genital component to which all five others would be compared because it is an obvious character and easy to remove from the body. Plus, from simple observations, it does not appear to be functional (DAW, personal observations) other than to possibly cover the tympanum (which also do not appear to be functional either - DAW, personal observations) or to be under any sort of selection given its highly similar shape across all PG species. In fact, it seems that the tegmen and tympanum may be examples of plesiomorphic characters in at least the PG's species, if not other brachypterous *Melanoplus*. This apparent absence of

selective pressure may very well explain the low variability observed in the shape of the tegmen overall (Fig. 4-6F) and the patterns of relatively high variability seen across lineages and their species in the results of several of our analyses (Figs 4-18 and 4-26; Tables 4-3 and 4-4P-R).

Further supporting this idea is that the tegmen had the lowest rate of evolution compared to the genital components (Table 4-5). Interestingly, one of the few clear patterns to emerge for this component was that all of the species within lineages C and D were only significantly disparate from species from other lineages (Fig. 4-18A; Table4-4P-R). This was also observed in the interesting clustering patterns for all four lineages in the corresponding phylomorphospace (Fig. 4-28), which indicate that almost every lineage has essentially evolved fairly unique tegmina shapes (A and D have evolved similarly). This suggests that, contrary to lineage B, the tegmina of lineages C and D have not evolved too far beyond the reconstruction of the ancestral consensus shape (at the origin point in Fig. 4-28), which most likely explains the displayed disparity pattern. Based on phylomorphospace alone, it could further be suggested that, between lineages C and D, D is more similar in shape overall to the ancestral PG species. At first glance, it might seem that *M. gurneyi* (lineage A) and, at least partially, *M. apalachicolae* (lineage B) have converged on the shape of lineage D. On the other hand, given what we suspect about the biogeographical history of lineage D (specifically, how it probably evolved due to a combination of sympatry and dispersal into the mid-peninsular zone of Florida, see Ch. II), it is actually more likely that lineage D has simply not had enough time to diverge from the ancestral shape present when lineage A split from D (1.37 MYA). As

M. gurneyi has had a longer amount of estimated time (3.71 MYO) to evolve its shape, this would explain why the trajectory of *M gurneyi's* shape has extended into phylomorphospace beyond lineage D.

Furthermore, evolution of the tegmen may not be as devoid of selection as it first seems for at least the PGss because its relative evolutionary rate, while not a significantly high ratio, was found to be fairly high in comparison to all non-PGss species (but still the lowest rate out of all six shapes). Furthermore, the PGss sister species *M.* sp. nov. 3-*M. bonita* were found to be only one of two pairs that were highly disparate (but not statistically significant) in the shape of their tegmina when taking into account their estimated time of divergence (Fig. 4-18B) at 0.43 MYA. Not only is this the youngest divergence age estimate in the PGss (Fig. 4-3), but these two species also reside in one of the southeast's youngest areas (Fig. 4-2). This divergence may simply be due to the stochastic effect of drift or mutation, but the disparity level and short geologic time span involved seems to indicate something more and bears further investigation.

With time incorporated, the only other high disparity level of note (but also not statistically significant) observed for the tegmen was in lineage B's sister species *M. tumidicercus-M. stegocercus*, which is noted only because, at 0.59 MYO, this, too, is one of the youngest species pairs, albeit within the second oldest lineage. This second finding of a similar pattern seems to echo, if not further call for, the suggestions just made for *M.* sp. nov. 3-*M. bonita*. As noted previously, the lack of significant levels of disparity for both sister pairs may just be due to their fairly young age if they are currently in the midst of evolving in unique directions in phylomorphospace (Fig. 4-28).

The point is that even in anatomical components considered to be evolving relatively slowly or, perhaps, in the absence of selective pressure, further investigation is warranted in light of the concept of evolutionary tempo. The tempo for the PG may simply be very low to non-existent for this component, but could potentially be increasing for parts of the group, especially if selection of some sort is at work. Alternately, if the wings are just evolving in conjunction with the body's shape, in general, then further genetic studies in search of gene linkage may be the key to unlocking this mystery.

Conclusions

We have answered the call of Simmons (2014) and Bond et al. (2003) for further studies that would provide additional quantitative support for the continued claim that sexual selection leads to rapid and divergent genitalia by examining ample amounts of evidence, including biogeographical analyses (Ch. II), estimated speciation rate (Ch. II), relative evolutionary rates, and phylogenetic comparisons of genital morphology. Our results suggest a number of interesting things regarding the evolution of shape. Key among these is that the primary intromittent genital component (aedeagal region) was revealed to be (as predicted), far and away, the most rapidly evolving (and most variable) of all analyzed shapes, especially compared to a non-genital character. This result, in particular, combined with the fact that a pair of sister species was found to be undergoing Fisherian runaway selection for each genital component in the context of evolutionary time, provides strong evidence for the idea that sexual selection has been

the primary driver of speciation in the PG, at least for the more recent portion of its history. Our previous biogeographical results (Ch. II) do suggest that other factors have been at work as well, such as dispersal, sympatric speciation, and founder-events, but have most likely been larger factors in the past give the relatively young age of lineages C and D, which, overall, displayed the most divergence in terms of shape.

Furthermore, our combined shape analysis evidence only seemed to partially confirm our hypothesis that the genitalia of lineage D's PGss clade would be the most divergent within compared to other species and that the evolutionary rate of said genitalia would be the highest overall. Even so, the combination of this evidence in the context of evolutionary time, biogeographical analyses (Ch. II), and estimated speciation rate (Ch. II) of the PGss strongly indicates that the primary driver of genital divergence in the PGss, and thus speciation, is indeed sexual selection and that evolutionary tempo appears to be accelerating for several of the genital components. In terms of overall evolutionary tempo of the PG's components, several differing trends in speed were suggested across all shapes based on multiples lines of evidence. The presence of phylogenetic signal across all six components seems to be more of an historical artifact since evolutionary tempo appears to be accelerating in general in at least lineages C and D. This suggests that some of the components may eventually overcome phylogenetic inertia (Blomberg and Garland, 2002; Revell et al., 2008).

All of this simply reinforces the fact that no single evolutionary force has shaped the evolution of the components we examined. In fact, some of these structures may be experiencing, or have experienced, multiple selection pressures of varying degrees

simultaneously (Arnqvist 1997; Hosken and Stockley 2003; McPeek et al., 2008). Case in point, while we have continually invoked the cryptic female choice hypothesis of sexual selection for the PG based on the evidence before us, we have now also realized that the same evidence has some cracks in it that may suggest that the sexually antagonistic coevolution hypothesis has been involved as an additional driver of shape divergence (Parker, 1979; Arnqvist, 1997; Arnqvist et al., 2000; Arnqvist and Rowe, 2002; Chapman et al., 2003; Eberhard, 2004a; Eberhard, 2004b; Arnqvist and Rowe, 2005; Eberhard, 2009; Eberhard, 2010a; Eberhard, 2010b; Rowe and Arnqvist, 2011; Ah-King, 2014; Gavrilets, 2014; Simmons, 2014). Some of the analyzed male genital components may actually be entangled in an arms race with female components, the two prominent possibilities being, respectively, the lophus and the lophus receptacle, and the cercus and possibly some portion of the female's abdomen. Historically, there has been a bias towards only studying the morphology of males for a variety of reasons (Eberhard, 1985; Arnqvist, 1997; Ah-King et al., 2014; Woller et al., 2017), but, clearly, female anatomy of PG species should be examined more carefully, especially in a copulation framework as in Woller and Song (2017). Finally, it has been suggested that cryptic female choice may actually be a subset of sexually antagonistic coevolution (Hosten and Stockley, 2004; Arnqvist and Rowe, 2005; Rowe and Arnqvist, 2011; Simmons, 2014) and while our results cannot add evidence to this debate it does seem rational to merge these hypotheses in order to gain a greater, more cohesive, understanding of how sexual selection is driving the evolution of a given group.

CHAPTER V

CONCLUSIONS

Reflecting on the completion of this study, there can be little doubt that the 27 flightless grasshopper species of the Puer Group (PG) (Orthoptera: Acrididae: Melanoplinae: *Melanoplus*) (*Rehn and Hebard*, 1916; Hubbell, 1932; Strohecker, 1960; Deyrup, 1996; Squitier et al., 1998; Otte, 2012 ("2011")) comprise a fascinating and complex biological system heavily influenced by the fluctuations in sea level during the Pliocene and Pleistocene, especially during the latter (Hubbell, 1932; Hubbell, 1961; Deyrup, 1989; Webb, 1990; Lane, 1994; Hine, 2009; Swaby et al., 2016). These sea level shifts resulted in an oceanic island system that is now a landlocked archipelago, but still reflects the speciation and dispersal patterns of its ancestral roots (*Hubbell, 1932; Hubbell, 1961;* MacArthur and Wilson, 1967; *White, 1970;* Hubbell, 1985; *Webb, 1990*; Deyrup, 1990, Myers, 1990; *Lane, 1994;* Turner et al., 2006; Gillespie and Baldwin, 2012).

Furthermore, beyond general sea level changes, our collective evidence indicates, as predicted, that the biogeographical and speciation history of this biological system was largely shaped by allopatry (in the form of oceanic islands) in its past and sympatry (via sexual selection by cryptic female choice Eberhard, 1985; Eberhard, 1996) more recently. This is particularly the case for those PG species found almost exclusively in peninsular Florida, which also represent the majority of the group's species. We have also further confirmed (e.g., Arnqvist, 1998; Mutanen and Kaitala, 2006; Marquez and

Knowles, 2007; Rowe and Arnqvist, 2011), with ample amounts of quantitative evidence (Simmons, 2014; Bond et al., 2003), that the evolution of genitalia can be both rapid and divergent under sexual selection (Eberhard, 1985; Eberhard, 1996; Hosken and Stockley, 2004; Eberhard, 2009; Eberhard, 2010a; Eberhard, 2010b; Song and Bucheli, 2010; Rowe and Arnqvist, 2011; Simmons, 2014), particularly so when evolutionary time is taken into account. Additionally, based on our assessments of the probable function of genital components (some of which are new to science) during copulation (using one PG species as a proxy) and our shape analyses of five of those male genital components (for all PG species) in the context of evolutionary time, we hypothesized that the evolutionary tempo (Blomberg and Garland, 2002; Revell et al., 2008) of sexual selection is accelerating and/or decelerating depending on the component and its associated function(s). Of further importance was our discovery that one of the youngest PG clades has speciated at a rate that may be the highest yet found in an insect clade (Mendelson and Shaw, 2005; Lapoint et al., 2011; Wessel et al., 2013), a finding made even more incredible by the fact that similar rates have previously been relegated to current oceanic islands.

Our investigation of this system has added much-needed resolution to the biological black box that is speciation and even some resolution to the geological history of Florida, which is complicated as a result of its relatively young age (peninsular Florida, in particular). Despite these breakthroughs, there is clearly much more to investigate and elucidate, which is exciting. The species of the PG obviously make for a wonderfully unique study system of speciation and we advocate here for the group's

continued use as such, and sooner than later because the group's associated xeric habitats (especially scrub) are under continued threat of destruction and fragmentation (Deyrup, 1990; Turner et al., 2006; Weekley et al., 2008). The synergy of our evidence tells us a rich, deep story about evolutionary patterns and processes, the surface of which we have only begun to scratch. As a result, I anticipate being involved in the study of this system, both in an evolutionary and taxonomic context, for many years to come.

REFERENCES

Adams DC. 2014a. Quantifying and comparing phylogenetic evolutionary rates for shape and other high-dimensional phenotypic data. Systematic Biology 63(2):166-177.

Adams DC. 2014b. A generalized K statistic for estimating phylogenetic signal from shape and other high-dimensional multivariate data. Systematic Biology 63(5):685-697.

Adams DC, Collyer ML. 2017. Multivariate phylogenetic comparative methods: Evaluations, comparisons, and recommendations. Systematic Biology 0(0):1-18.

Adams DC, Collyer ML, Kaliontzopoulou A, Sherratt E. 2017. Geomorph: Software for geometric morphometric analyses. R package version 3.0.5. https://cran.r-project.org/package=geomorph

Adams DC, Rohlf FJ, Slice DE. 2013. A field comes of age: geometric morphometrics in the 21st century. Hystrix, the Italian Journal of Mammalogy 24(1):7-14.

Ah-King M, Barron AB, Herberstein ME. 2014. Genital evolution: why are females still understudied? PLOS Biology 12(5):1-7.

Ahmed I, Gillott C. 1982. The spermatheca of *Melanoplus sanguinipes* (Fabr.). I. Morphology, histology, and histochemistry. International Journal of Invertebrate Reproduction 4:281-295.

Allen GM, Main MB. 2005. Florida's Geologic History. Wildlife Ecology and Conservation Department, Florida Cooperative Extension Service. Gainesville, FL: University of Florida. Document #WEC189: 3 p.

Amédégnato C. 1976. Structure et évolution des genitalia chez les Acrididae et familles apparentées. Acrida 5:1-15.

Ander K. 1970. Orthoptera Saltatoria. In: Tuxen SL, editor. Taxonomist's Glossary of Genitalia In Insects. 2nd ed. Copenhagen, Denmark: J. Jørgenson & Co. p 61-71.

Arnqvist G. 1998. The evolution of animal genitalia: distinguishing between hypotheses by single species studies. Biological Journal of the Linnean Society 60:365-379.

Arnqvist G, Edvardsson M, Friberg U, Nilsson T. 2000. Sexual conflict promotes speciation in insects. Proceedings of the National Academy of Sciences, USA 97(19):10460-10464.

Arnqvist G, Rowe L. 2002. Correlated Evolution of male and female morphologies in water striders. Evolution 56(5):936-947.

Arnqvist G, Rowe L. 2005. Sexual conflict. Princeton, NJ: Princeton University Press.

Bennik RM, Buckley TR, Hoare RJB, Holwell GI. 2016. Molecular phylogeny reveals the repeated evolution of complex male genital traits in the New Zealand moth genus *Izatha* (Lepidoptera: Xyloryctidae). Systematic Entomology 41:309-322.

Bergsten J, Miller KB. Phylogeny of diving beetles reveals a coevolutionary arms race between the sexes. PLOS ONE 2(6):e522.

Bernt M. 2013. MITOS: Improved de novo metazoan mitochondrial genome annotation. Molecular Phylogenetic Evolution 69:313-319.

Beutel RG, Friedrich F, Ge S-Q, Yang X-K. 2014. Insect Morphology and Phylogeny. Berlin, Germany & Boston, U.S.A.: Walter de Gruyter GmbH. 516 p.

Bland RG. 1987. Mating behavior of the grasshopper *Melanoplus tequestae* (Orthoptera:

Acrididae). Florida Entomologist 70(4):483-487.

Blatchley WS. 1920. The Orthoptera of Northeastern America with especial reference to the Fauna of Indiana and Florida. Indianapolis, IN: Nature Publishing Co.

Blomberg SP, Garland, Jr. T. 2002. Tempo and mode in evolution: phylogenetic inertia, adaptation and comparative methods. Journal of Evolutionary Biology 15:899-910.

Blomberg SP, Garland, Jr. T., Ives, AR. 2003. Testing for phylogenetic signal in comparative data: Behavioral traits are more labile. Evolution 57(4):717-745.

Boldyrev BT. 1929. Spermatophore fertilization in the Migratory Locust (*Locusta migratoria* L.). Izvestija po prikladnoj Entomologii (Reports on applied Entomology) 4(1):189-218.

Bond JE, Beamer DA, Hedin MC, Sierwald P. 2003. Gradual evolution of male genitalia in a sibling species complex of millipedes (Diplopoda: Spirobolida: Rhinocricidae: *Anadenobolus*). Invertebrate Systematics 17:711-717.

Bouckaert RR, Heled J, Kuehnert D, Vaughan TG, Wu C-H, Xie D, Suchard MA, Rambaut A, Drummond AJ. 2014. BEAST 2: A software platform for Bayesian evolutionary analysi. PLOS Computational Biology 10(4):e1003537.

Breeschoten T, Clark DR, Schilthuizen M. 2013. Evolutionary patterns of asymmetric genitalia in the beetle tribe Cyclocephalini (Coleoptera: Scarabaeidae: Dynastinae). Contributions to Zoology 82(2):95-106.

Briceño RD, Eberhard WG. 2009. Experimental demonstration of possible cryptic female choice on male tsetse fly genitalia. Journal of Insect Physiology 55:989-

996.

Briceño RD, Eberhard WG, Chinea-Cano E, Wegrzynek D, dos Santos Rolo T. 2016. Species-specific differences in the behavior of male tsetse fly genitalia hidden in the female during copulation. Ethology Ecology & Evolution 28(1):53-76.

Burdette KE, Rink WJ, Mallinson DJ, Means GH, Parham PR. 2013. Electron spin resonance optical dating of marine, estuarine, and aeolian sediments in Florida, USA. Quaternary Research 79:66-74.

Cameron SL. 2014. How to sequence and annotate insect mitochondrial genomes for systematic and comparative genomics research. Systematic Entomology 39:400-411.

Caplan J, Niethammer M, Taylor II RM, Czymmek KJ. 2011. The power of correlative microscopy: multi-modal, multi-scale, multi-dimensional. Current Opinion in Structural Biology 21(5):686-693.

Carstens BC, Knowles LL. 2006. Variable nuclear markers for *Melanoplus oregonensis* identified from the screening of a genomic library. Molecular Ecology Notes 6:683-685.

Chapman RF. 2012. The Insects: Structure and Function. 5th ed. New York, U.S.A.: Cambridge University Press. p 959.

Chapman T, Arnqvist G, Bangham J, Rowe L. 2003. Sexual conflict. Trends in Ecology & Evolution 18(1):41-47.

Cigliano MM, Braun H, Eades DC, Otte D. Orthoptera Species File. Version 5.0/5.0. [11-5-2016]. Available at: http://Orthoptera.SpeciesFile.org

Darwin C. 1872. On the origin of species, 6th Ed. Cambridge, England: Cambridge University Press. 568 p.

Denton JSS, Adams DC. 2015. A new phylogenetic test for comparing multiple high-dimensional evolutionary rates suggests interplay of evolutionary rates and modularity in lanternfishes (Myctophiformes; Myctophidae). Evolution 69(9):2425-2440.

Deyrup M. 1989. Arthropods endemic to Florida scrub. Florida Scientist 52:254-270.

Deyrup M. 1990. Arthropod footprints in the sands of time. Florida Entomologist 73:529-538.

Deyrup M. 1996. Two new grasshoppers from relict uplands of Florida (Orthoptera: Acrididae). Transactions of the American Entomological Society 122:199-211.

Deyrup M, Carrel J. 2012. Lake Wales Ridge Scrub Arthropods. Archbold Biological Station, FL. Florida's Wildlife Legacy Initiative and the U.S. Fish and Wildlife Service State Wildlife Grant T-15-D: Conservation Status and Management of Lake Wales Ridge Arthropods Restricted to Scrub Habitat.

Dirsh VM. 1956. The phallic complex in Acridoidea (Orthoptera) in relation to taxonomy. Transactions of the Royal Entomological Society of London 108(7):223-270.

Dirsh VM. 1965. The African Genera of Acridoidea. New York, U.S.A.: Cambridge University Press. 594 p.

Dirsh VM. 1973. Genital organs in Acridomorphoidea (Insecta) as taxonomic character. Journal of Zoological Systematics and Evolutionary Research 11(1):133-154.

Dougherty LR, Rahman IA, Burdfield-Steel ER, Greenway EVG, Shuker DM. 2015. Experimental reduction of intromittent organ length reduces male reproductive success in a bug. Proceedings of the Royal Society of London, Series B: Biological Sciences 282:1-8.

Drummond A, Rambaut A. 2007. BEAST: Bayesian evolutionary analysis by sampling trees. BMC Evolutionary Biology 7(1):214.

Drummond A, Suchard MA, Xie D, Rambaut A. 2012. Bayesian phylogenetics with BEAUti and the BEAST 1.7. Molecular Biology and Evolution 29(8):1969-1973.

Eades DC. 1961. The terminology of phallic structures in the Cyrtacanthacridinae (Orthoptera, Acrididae). Entomological News 72:141-149.

Eades DC. 2000. Evolutionary relationships of phallic structures of Acridomorpha (Orthoptera). Journal of Orthoptera Research 9:181-210.

Eberhard WG. 1985. Sexual Selection and Animal Genitalia. Massachusetts, U.S.A.: Harvard University Press. 256 p.

Eberhard WG. 1996. Female control: Sexual selection by cryptic female choice. Princeton, NJ: Princeton University Press.

Eberhard WG. 2004a. Male–female conflict and genitalia: failure to confirm predictions in insects and spiders. Biological Reviews 79:121-186.

Eberhard WG. 2004b. Rapid divergent evolution of sexual morphology: Comparative tests of antagonistic coevolution and traditional female choice. Evolution 58(9):1947-1970.

Eberhard WG. 2009. Postcopulatory sexual selection: Darwin's omission and its

consequences. Proceedings of the National Academy of Sciences 106:10025-10032.

Eberhard WG. 2010a. Evolution of genitalia: theories, evidence, and new directions. Genetica 138:5-18.

Eberhard WG. 2010b. Rapid divergent evolution of genitalia: Theory and data updated. In: Leonard J, Cordoba-Aguilar A, editors. The evolution of primary sexual characters in animals. Oxford, U.K.: Oxford University Press. p 40-78.

Eberhard WG, Ramirez N. 2004. Functional morphology of the male genitalia of four species of *Drosophila*: failure to confirm both lock and key and male-female conflict predictions. Annals of the Entomological Society of America 97(5):1007-1017.

Edgar RC. 2004. MUSCLE: multiple sequence alignment with high accuracy and high throughput. Nucleic Acids Research 33:511-518.

Edvardsson M, Arnqvist G. 2000. Copulatory courtship and cryptic female choice in red our beetles *Tribolium castaneum*. Proceedings of the Royal Society of London, Series B: Biological Sciences 267:559-563.

Eisner T, Shepherd J, Happ GM. 1966. Tanning of grasshopper eggs by an exocrine secretion. Science 152(3718):95-97.

Faulwetter S, Vasileiadou A, Kouratoras M, Dailianis T, Arvanitidis C. 2013. Micro-computed tomography: introducing new dimensions to taxonomy. ZooKeys 263:1-45.

Federov SM. 1927. Studies in the copulation and oviposition of *Anacridium aegyptium*,

L. (Orthoptera, Acrididae). Transactions of the Entomological Society of London 75(1):53-61.

Firman RC, Gasparini C, Manier MK, Pizzari T. 2017. Postmating female control: 20 years of cryptic female choice. Trends in Ecology & Evolution 32(5):368-382.

Frazee SR, Masly JP. 2015. Multiple sexual selection pressures drive the rapid evolution of complex morphology in a male secondary genital structure. Ecology and Evolution 5(19):4437-4450.

Gavrilets S. 2014. Is Sexual Conflict an "Engine of Speciation"? Cold Spring Harb Perspectives in Biology 6:a017723.

Gillespie RG, Baldwin BG. 2009. Island biogeography of remote archipelagos: Interplay between ecological and evolutionary processes. In: Losos JB, Ricklefs R, editors. The theory of island biogeography revisited. Princeton, NJ: Princeton University Press. p 358-387.

Gordh G, Headrick D. 2001. A Dictionary of Entomology. Wallingford, U.K. & New York, U.S.A.: CABI Publishing. p 1-1032.

Gosálvez J, Kjelland ME, López-Fernández C. 2010. Sperm DNA in grasshoppers: structural features and fertility implications. Journal of Orthoptera Research 19(2):1-10.

Greco M, Bell D, Woolnough L, Laycock S, Corps N, Mortimore D, Hudson D. 2014. 3-D visualisation, printing, and volume determination oF the tracheal respiratory system in the adult desert locust, *Schistocerca gregaria*. Entomologia Experimentalis et Applicata 152:42-51.

Gregory GE. 1965. The formation and fate of the spermatophore in the African migratory locust, *Locusta migratoria migratorioides* Reiche and Fairmaire. Transactions of the Royal Entomological Society of London 117(2):33-66.

Grieshop K, Polak M. 2012. The precopulatory function of male genital spines in *Drosophila ananassae* [Doleschall] (Diptera: Drosophilidae) revealed by laser surgery. Evolution 66(8):2637-2645.

Gunz P, Mitteroecker P. 2012. Semilandmarks: a method for quantifying curves and surfaces. Hystrix, the Italian Journal of Mammalogy 24(1):103-109.

Hahn C, Bachmann L, Chevreux B. 2013. Reconstructing mitochondrial genomes directly from genomic next-generation sequencing reads—a baiting and iterative mapping approach. Nucleic Acids Research 41:e129.

Hartmann R. 1970. Experimental and histological studies on the spermatophore formation of the grasshopper *Gomphocerus rufus* L. (Orthoptera, Acrididae). Zeitschrift für Morphologie der Tiere 68(2):140-176.

Heled J, Drummond A. 2010. Bayesian inference of species trees from multilocus data. Molecular Biology and Evolution 27(3):570-580.

Hill JG. 2015. Revision and biogeography of the *Melanoplus scudderi* species group (Orthoptera: Acrididae: Melanoplinae) with a description of 21 new species and establishment of the *Carnegiei* and *Davisi* species groups. Transactions of the American Entomological Society 141:252-350.

Hine AC. 2009. Geology of Florida. Canada: Brooks/Cole. 32 p.

Ho SYW, Tong KJ, Foster CSP, Ritchie AM, Lo N, Crisp MD. 2015. Biogeographic

calibrations for the molecular clock. Biology Letters 11:20150194.

Holwell GI, Kazakova O, Evans F, O'Hanlon JC, Barry KL. 2015. The functional significance of chiral genitalia: patterns of asymmetry, functional morphology and mating success in the praying mantis *Ciulfina baldersoni*. PLOS ONE 10(6):1-14.

Hörnschemeyer T, Beutel RG, Pasop F. 2002. Head Structures of *Priacma serrata* Leconte (Coleptera, Archostemata) Inferred From X-ray Tomography. Journal of Morphology 252:298-314.

Hosken DJ, Stockley P. 2004. Sexual selection and genitalia evolution. Trends in Ecology & Evolution 19:87-93.

Hotzy C, Polak M, Ro JL, Arnqvist G. 2012. Phenotypic engineering unveils the function of genital morphology. Current Biology 22:2258-2261.

Hubbell TH. 1932. A revision of the Puer group of the North American genus *Melanoplus*, with remarks on the taxonomic value of the concealed male genitalia in the Cyrtacanthacridinae (Orthoptera, Acrididae). Miscellaneous Publications of the Museum of Zoology, University of Michigan 23:1-64.

Hubbell TH. 1961. Endemism and speciation in relation to Pleistocene changes in Florida and the southeastern coastal plain. 11th International Congress of Entomology, 1960. Vienna, Austria. p 466-469.

Hubbell TH. 1985. Unfinished business and beckoning problems. Florida Entomologist 68(1):1-15.

Jongerius SR, Lentink D. 2010. Structural analysis of a dragonfly wing. Experimental

Mechanics 50:1323–1334.

Katoh K, Kuma K, Toh H, Miyata T. 2005. MAFFT version 5: improvement in accuracy of multiple sequence alignment. Nucleic Acids Research 33:511-518.

Kelly DA, Moore BC. 2016. The morphological diversity of intromittent organs. Integrative and Comparative Biology 56(4):630-634.

Key KHL. 1989. Revision of the genus *Praxibulus* (Orthoptera: Acrididae). Invertebrate Taxonomy 3(1):1-121.

Kirkpatrick M. 1982. Sexual selection and the evolution of female choice. Evolution 36(1):1-12.

Klingenberg CP. 2013. Visualizations in geometric morphometrics: how to read and how to make graphs showing shape changes. Hystrix, the Italian Journal of Mammalogy 24(1):15-24.

Kraaijeveld K, Kraaijeveld-Smit FJL, Maan ME. 2011. Sexual selection and speciation: the comparative evidence revisited. Biological Review 86:367-377.

Kyl G. 1938. A study of copulation and the formation of spermatophores in *Melanoplus differentialis*. Proceedings of the Iowa Academy of Science 45:299-308.

Lamb T, Justice TC. 2005. Comparative phylogeography of Florida scrub insects: implications for systematics, biogeography, and conservation. Final Report for Project NG01-002. Tallahassee, FL: Florida Fish and Wildlife Conservation Commission.

Lamichhaney S, Berglund J, Almen MS, Maqbool K, Grabherr M, Martinez-Barrio A, Promerova M, Rubin C-J, Wang C, Zamani N, Grant BR, Grant PR, Webster

MT, Andersson L. 2015. Evolution of Darwin's finches and their beaks revealed by genome sequencing. Nature 518:371-377.

Lane E (Ed.). 1994. Florida's geological history and geological resources. Tallahassee, FL: Florida Geological Survey. 35:64 p.

Lanfear R, Calcott B, Ho SYW, Guindon S. 2012. PartitionFinder: combined selection of partitioning schemes and substitution models for phylogenetic analyses. Molecular Biology and Evolution 29(6):1695-1701.

Lapoint RT, Gidaya A, O'Grady PM. 2011. Phylogenetic relationships in the spoon tarsus subgroup of Hawaiian *drosophila*: Conflict and concordance between gene trees. Molecular Phylogenetics and Evolution 58:492-501.

Lawry JV. 2006. The incredible shrinking bee: insects as models for microelectromechanical devices. London: Imperial College Press.

Lay M, Zissler D, Hartmann R. 1999. Ultrastructural and functional aspects of the spermatheca of the African Migratory Locust *Locusta migratoria migratorioides* (Reiche and Fairmaire) (Orthoptera: Acrididae). International Journal of Insect Morphology and Embryology 28:349-361.

Losos JB. 1999. Uncertainty in the reconstruction of ancestral character states and limitations on the use of phylogenetic comparative methods. Animal Behaviour 58:1319-1324.

Losos JB, Schluter D. 2000. Analysis of an evolutionary species-area relationship. Nature 408:847-850.

Lowe TM, Eddy SR. 1997. tRNAscan-SE: A program for improved detection of transfer

RNA genes in genomic sequence. Nucleic Acids Research 25:955-964.

MacArthur RH, Wilson EO. 1967. The theory of island biogeography. Princeton, NJ: Princeton University Press. 23 p.

Márquez EJ, Knowles LL. 2007. Correlated evolution of multivariate traits: detecting co-divergence across multiple dimensions. European Society for Evolutionary Biology 20:2334-2348.

Maruska KP, Ung US, Fernald RD. 2012. The African cichlid fish *Astatotilapia burtoni* uses acoustic communication for reproduction: sound production, hearing, and behavioral significance. PLOS ONE 7(5):e37612.

Mattei AL, Riccio ML, Avila FW, Wolfner MF. 2015. Integrated 3D view of postmating responses by the *Drosophila melanogaster* female reproductive tract, obtained by micro-computed tomography scanning. Proceedings of the National Academy of Sciences, USA 112(27):8475-8480.

Matzke NJ. 2013. BioGeoBEARS: BioGeography with Bayesian (and likelihood) evolutionary analysis in R Scripts: R package, v. 0.2.

Matzke NJ. 2014. Model selection in historical biogeography reveals that founder-event speciation is a crucial process in island clades. Systematic Biology 63(6):951-970.

McCune AR. 1997. How fast is speciation? Molecular, geological, and phylogenetic evidence from adaptive radiations of fishes. In: Givnish TJ, Sytsma KJ, editors. Molecular Evolution and Adaptive Radiation. New York, USA: Cambridge University Press. p 585-610.

McPeek MA, Shen L, Torrey JZ, Farid H. 2008. The tempo and mode of three-dimensional morphological evolution in male reproductive structures. The American Naturalist 171(5):E158-178.

McPeek MA, Symes LB, Zong DM, McPeek CL. 2010. Species recognition and patterns of population variation in the reproductive structures of a damselfly genus. Evolution 65(2):419-428.

Mendelson TC, Shaw KL. 2005. Rapid speciation in an arthropod. Nature 433:375-376.

Michalik P, Piacentini L, Lipke E, Ramírez MJ. 2013. The enigmatic Otway odd-clawed spider (*Progradungula otwayensis* Milledge, 1997, Gradungulidae, Araneae): Natural history, first description of the female and micro-computed tomography of the male palpal organ. ZooKeys 335:101-112.

Miller KB. 2003. The phylogeny of diving beetles (Coleoptera: Dytiscidae) and the evolution of sexual conflict. Biological Journal of the Linnean Society 79:359-388.

Miller MA, et al. 2011. The CIPRES Portals: http://www.phylo.org/sub_sections/portal

Muhs DR, Wehmiller JF, Simmons KR, York LL. 2003. Quaternary sea-level history of the United States. Development in Quaternary Sciences 1:147-183.

Mushinsky HR, McCoy ED. 1995. Vertebrate species composition of selected scrub islands on the Lake Wales Ridge of central Florida. Nongame Wildlife Program Project report no. GFC-87-149. Tallahassee, Florida: Florida Game and Fresh Water Fish Commission.

Mutanen M, Kaitala A. Genital variation in a dimorphic moth *Selenia tetralunaria*

(Lepidoptera, Geometridae). Biological Journal of the Linnean Society 87:297-307.

Myers RL. 1990. Scrub and high pine. In: Myers RL, Ewel JJ, editors. Ecosystems of Florida. Orlando, FL: University of Central Florida Press. p 150-193.

O'Leary MA, Kaufman SG. 2012. MorphoBank 3.0: Web application for morphological phylogenetics and taxonomy. http://www.morphobank.org.

Olvido AE, Fernandes PR, Mousseau TA. 2010. Relative effects of juvenile and adult environmental factors on mate attraction and recognition in the cricket, *Allonemobius socius*. Journal of Insect Science 10(90):1-17.

Otte D. 1970. A comparative study of communicative behavior in grasshoppers. Miscellaneous Publications of the Museum of Zoology, University of Michigan 141:1-169.

Otte D. 2012 ("2011"). Eighty New *Melanoplus* Species from the United States (Acrididae: Melanoplinae). Transactions of the American Entomological Society 138(1, 2):73-167.

Parker GA. 1979. Sexual selection and sexual conflict. In: Blum MS, Blum NA, editors. Sexual selection and reproductive competition in insects. New York, USA: Academic Press. p 123-166.

Parks DH, Mankowski T, Zangooei S, Porter MS, Armanini DG, Baird DJ, Langille MGI, Beiko RG. 2013. GenGIS 2: geospatial analysis of traditional and genetic biodiversity, with new gradient algorithms and an extensible plugin framework. PLOS ONE 8(7):e69885.

Pickford R, Gillott C. 1971. Insemination in the migratory grasshopper, *Melanoplus sanguinipes* (Fabr.). Canadian Journal of Zoology/Revue Canadienne de Zoologie 49:1583-1588.

Polly PD, Lawing AM, Fabre A-C, Goswami A. 2013. Phylogenetic principal components analysis and geometric morphometrics. Hystrix, the Italian Journal of Mammalogy 2013(24):1.

Rambaut A, Drummond AJ. 2009. FigTree v1.3.1.

Randell RL. 1963. On the presence of concealed genitalic structures in female Caelifera (Insecta; Orthoptera). Transactions of the American Entomological Society 88(4):247-260.

Ree RH, Smith SA. 2008. Maximum likelihood inference of geographic range evolution by dispersal, local extinction, and cladogenesis. Systematic Biology 57(1):4-14.

Rehn JAG, Hebard M. 1916. Studies in the Dermaptera and Orthoptera of the Coastal Plain and Piedmont Region of the Southeastern United States. Proceedings of the Academy of Natural Sciences of Philadelphia 68:87-314.

Revell LJ, Harmon LJ, Collar DC. 2008. Phylogenetic signal, evolutionary process, and rate. Society of Systematic Biologists 57(4):591-601.

Rhebergen FT, Courtier-Orgogozo V, Dumont J, Schilthuizen M, Lang M. 2016. *Drosophila pachea* asymmetric lobes are part of a grasping device and stabilize onesided mating. BMC Evolutionary Biology 16(176):1-24.

Richmond MP, Johnson S, Markow TA. 2012. Evolution of reproductive morphology among recently diverged taxa in the *Drosophila mojavensis* species cluster.

Ecology and Evolution 2(2):397-408.

Ritchie MG. 2007. Sexual selection and speciation. Annual Review of Ecology, Evolution and Systematics 38:79-102.

Roberts HR. 1941. A comparative study of the subfamilies of the Acrididae (Orthoptera) primarily on the basis of their phallic structures. Proceedings of the Academy of Natural Sciences of Philadelphia 93:201-246.

Rohlf FJ. 2017. TPS Suite. SUNY Stony Brook. http://life.bio.sunysb.edu/morph/

Ronn J, Katvala M, Arnqvist G. 2007. Coevolution between harmful male genitalia and female resistance in seed beetles. Proceedings of the National Academy of Sciences 104(26):10921-10925.

Ronquist F. 2012. MrBayes 3.2: efficient Bayesian phylogenetic inference and model choice across a large model space. Systematic Biology 61:539-542.

Rowe L, Arnqvist G. 2011. Sexual selection and the evolution of genital shape and complexity in water striders. Evolution 66(1):40-54.

Sanabria-Urbán S, Song H, Oyama K, González-Rodríguez A, Serrano-Meneses MA, Castillo RCd. 2016. Body size adaptations to altitudinal climatic variation in neotropical grasshoppers of the genus sphenarium (Orthoptera: Pyrgomorphidae). PLOS ONE:1-24.

Schluter D. 2001. Ecology and the origin of species. Trends in Ecology & Evolution 16(7):372-380.

Schmitt M, Uhl G. 2015. Functional morphology of the copulatory organs of a reed beetle and a shining leaf beetle (Coleoptera: Chrysomelidae: Donaciinae,

Criocerinae) using X-ray micro-computed tomography. In: Jolivet P., Santiago-Blay J., Schmitt M. (Eds) Research on Chrysomelidae 5. ZooKeys 547:193-203.

Schoville SD, Stuckey M, Roderick GK. 2011. Pleistocene origin and population history of a neoendemic alpine butterfly. Molecular Ecology 20:1233-1247.

Scott TM, Campbell KM, Rupert FR, Arthur JD, Green RC, Means GH, Missimer TM, Lloyd J, M., Yon JW, Duncan JG. 2001. Geologic map of the state of Florida. Tallahassee, FL: Florida Geological Survey. 80: 32 p.

Seehausen O, van Alphen JJM. 1999. Can sympatric speciation by disruptive sexual selection explain rapid evolution of cichlid diversity in Lake Victoria? Ecology Letters 2:262-271.

Simmons LW. 2014. Sexual selection and genitalia evolution. Australian Journal of Entomology 53(1):1-17.

Simonsen TJ, Kitching IJ. 2014. Virtual dissections through micro-CT scanning: a method for non-destructive genitalia 'dissections' of valuable Lepidoptera material. Systematic Entomology 39:606-618.

Slifer EH, King RL. 1936. An internal structure in the Cyrtacanthacrinæ (Orthoptera, Acrididæ) of possible taxonomic value. Journal of the New York Entomological Society 44(4):345-348.

Slifer EH. 1939. The internal genitalia of female Acridinae, Oedipodinae and Pauliniinae (Orthoptera, Acrididae). Journal of Morphology 65(3):437-469.

Slifer EH. 1940a. The internal genitalia of female Thrinchinae, Batrachotetriginae, Pamphaginae and Pyrgomorphinae (Orthoptera, Acrididae). Journal of

Morphology 66(1):175-195.

Slifer EH. 1940b. The internal genitalia of female Ommexechinae and Cyrthacanthacridinae (Orthoptera: Acrididae). Journal of Morphology 67(2):199-239.

Slifer EH. 1943. The internal genitalia of some previously unstudied species of female Acrididae (Orthoptera). Journal of Morphology 72(2):225-237.

Snodgrass RE. 1935. The abdominal mechanisms of a grasshopper. Smithsonian Miscellaneous Collections 94(6):1-89.

Snodgrass RE. 1993. Principles of Insect Morphology. New York, U.S.A.: Cornell University Press. 667 p.

Song H. 2004. Post-adult emergence development of genitalic structures in *Schistocerca* Stål and *Locusta* L. (Orthoptera: Acrididae). Proceedings of the Entomological Society of Washington 106(1):181-191.

Song H, Bucheli SR. 2010. Comparison of phylogenetic signal between male genitalia and non-genital characters in insect systematics. Cladistics 26:23-35.

Song H, Mariño-Pérez R. 2013. Re-evaluation of taxonomic utility of male phallic complex in higher-level classification of Acridomorpha (Orthoptera: Caelifera). Insect Systematics & Evolution 44:241-260.

Song H, Wenzel JW. 2008. Mosaic pattern of genital divergence in three populations of *Schistocerca lineata* Scudder, 1899 (Orthoptera: Acrididae: Cyrtacanthacridinae). Biological Journal of the Linnean Society 94:289-301.

Squitier JM, Deyrup M, Capinera JL. 1998. A new species of *Melanoplus* (Orthoptera:

Acrididae) from an isolated upland in Peninsular Florida. Florida Entomologist 81(3):451-460.

Stamatakis A, Hoover P, Rougemont J. 2008. A Rapid Bootstrap Algorithm for the RAxML Web-Servers. Systematic Biology 75:758-771.

Stauffer TW, Whitman DW. 1997. Grasshopper Oviposition. In: Gangwere SK, Muralirangan MC, Muralirangan M, editors. The Bionomics of Grasshoppers, Katydids, and Their Kin. Wallingford, U.K. & New York, U.S.A.: CAB International. p 231-280.

Strohecker HF. 1960. Several new species of North American Orthoptera. Pan-Pacific Entomologist 36:31-35.

Swaby AN, Lucas MD, Ross RM (Eds.). 2016. The teacher-friendly guide to the earth science of the southeastern US, 2nd Ed., New York, U.S.A: Paleontological Research Institution. 472 p.

R Core Team. 2013. R: A language and environment for statistical computing. Vienna, Austria: R Foundation for Statistical Computing: http://www.R-project.org/

Tracer. 2003-2009. MCMC Trace Analysis Tool.

Turner WR, Wilcove DS, Swain HM. 2006. Assessing the effectiveness of reserve acquisition programs in protecting rare and threatened species. Conservation Biology 20:1657-1669.

Uvarov B. 1966. Grasshoppers and Locusts, Vol. 1. Cambridge, U.K.: The Syndics of the Cambridge University Press. 481 p.

Vaidya G, Lohman DJ, Meier R. 2011. SequenceMatrix: concatenation software for the

fast assembly of multi-gene datasets with character set and codon information. Cladistics 27:171-180.

Van Dam MH, Matzke NJ. 2016. Evaluating the influence of connectivity and distance on biogeographical patterns in the south-western deserts of North America. Journal of Biogeography 43:1514-1532.

Webb SD. 1990. Historical biogeography. In: Myers RL, Ewel JJ, editors. Ecosystems of Florida. Orlando, FL: University of Central Florida Press. p 70-102.

Webster M, Sheets HD. 2010. A practical introduction to landmark-based geometric morphometrics. Quantitative Methods in Paleobiology 16:163-188.

Weekley CW, Menges ES, Pickert RL. 2008. An ecological map of Florida's Lake Wales Ridge: a new boundary delioneation and an assessment of post-Columbian habitat loss. Florida Scientist 71(1):45-64.

Wessel A, Hoch H, Asche M, Rintelen Tv, Stelbrink B, Heck V, Stone FD, Howarth FIG. 2013. Founder effects initiated rapid species radiation in Hawaiian cave planthoppers. Proceedings of the National Academy of Sciences 110(23):9391-9396.

West-Eberhard MJ. 1983. Sexual selection, social competition, and speciation. The Quarterly Review of Biology 58(2):155-183.

White WA. 1970. The geomorphology of the Florida peninsula. Tallahassee, FL: Bureau of Geology, Division of Interior Resoruces, Florida Department of Natural Resources. Geological Bulletin No. 51: 198 p.

Whitman DW, Loher W. 1984. Morphology of male sex organs and insemination in the

grasshopper *Taeniopoda eques* (Burmeister). Journal of Morphology 179:1-12.

Wipfler B, Machida R, Müller B, Beutel RG. 2011. On the head morphology of Grylloblattodea (Insecta) and the systematic position of the order, with a new nomenclature for the head muscles of Dicondylia. Systematic Entomology 36(2):241-266.

Wojcieszek JM, Austin P, Harvey MS, Simmons LW. 2012. Micro-CT scanning provides insight into the functional morphology of millipede genitalia. Journal of Zoology 287:91-95.

Wojcieszek JM, Simmons LW. 2011. Evidence for stabilizing selection and slow divergent evolution of male genitalia in a millipede (*Antichiropus variabilis*). Evolution 66(4):1138-1153.

Woller, D.A. and Song, H. 2017. Investigating the functional morphology of genitalia during copulation in the grasshopper *Melanoplus rotundipennis* (Scudder, 1878) via correlative microscopy. Journal of Morphology. 278(3):334–359. doi: 10.1002/jmor.20642

Wulff NC, Lehmann AW, Hipsley CA, Lehmann GUC. 2015. Copulatory courtship by bushcricket genital titillators revealed by functional morphology, μCT scanning for 3D reconstruction and female sense structures. Arthropod Structure and Development 44:388-397.

APPENDIX

R script (R Core Team, 2014) used to perform the geometric morphometric analyses for Chapter IV using the package *geomorph* (Adams et al., 2017)

```
#HYPOTHESES 1-3


#check working drectory and set if need be

getwd()

#result: "C:/users/DAW/Documents"

setwd("C:/users/DAW/Documents/Hypo1-3")

getwd() #check

#result: "C:/users/DAW/Documents/Hypo1-3"


#change Console's ability to show more lines of data

options(max.print=1000000)


#load geomorph library

library(geomorph)


############################################################

############################################################

#HYPOTHESIS 1
```

```
#AEDEAGAL REGION

#give data set a name and bring it in
aedeagal_region <- readland.tps("aedeagal_region2.tps", specID = "imageID")
aedeagal_region #check

#assign classification levels and make a group out of Species
aedeagal_regionclass <- read.csv("aedeagal_region2.csv", header=TRUE)
aedeagal_regionclass #check
aedeagal_regiongroup <- factor(paste(aedeagal_regionclass$Species))
levels(aedeagal_regiongroup)

#assign species level for PCA means analysis
aedeagal_regionclass2 <- read.csv("species.csv", header=TRUE)
aedeagal_regionclass2 #check

#bring in previously-created sliders file
aedeagal_regioncurves <- as.matrix(read.csv("aedeagal_region_curveslide.csv",
header=T))
aedeagal_regioncurves #check

#perform GPA
```

```
aedeagal_regiongpa <- gpagen(aedeagal_region, curves=aedeagal_regioncurves,
ProcD=FALSE, print.progress = TRUE)
aedeagal_regiongpa #check
plot(aedeagal_regiongpa) #check via plot view

#calculate means of GPA landmark data for PCA means analysis
aedeagal_regiongpameans <- (aggregate(two.d.array(aedeagal_regiongpa$coords) ~
aedeagal_regiongroup, FUN=mean))[,-1]
aedeagal_regiongpameans #check
rownames(aedeagal_regiongpameans) <- levels(aedeagal_regiongroup)
rownames(aedeagal_regiongpameans)
aedeagal_regiongpameans #check new names are in place
aedeagal_regiongpameans <- arrayspecs(aedeagal_regiongpameans, 29,2)
aedeagal_regiongpameans #Table check new arrangement is correct

#send GPA landmark coordinates data to Excel
library(xlsx)
#1) GPA landmark coordinates - all specimens
write.xlsx(aedeagal_regiongpa$coords, "c:/Users/DAW/Documents/Hypo1-
3/aedeagal_region_GPA1.xlsx")
#2) GPA centroid size
```

```
write.xlsx(aedeagal_regiongpa$Csize, "c:/Users/DAW/Documents/Hypo1-
3/aedeagal_region_GPA2.xlsx")
#3) GPA consensus shape
write.xlsx(aedeagal_regiongpa$consensus, "c:/Users/DAW/Documents/Hypo1-
3/aedeagal_region_GPA3.xlsx")

#send GPA means landmark coordinates data to Excel
library(xlsx)
#GPA landmark coordinates - means
write.xlsx(aedeagal_regiongpameans, "c:/Users/DAW/Documents/Hypo1-
3/aedeagal_region_GPA-means.xlsx")

#create GDF from GPA data for morphological disparity analysis
aedeagal_regiongdf <- geomorph.data.frame(coords = aedeagal_regiongpa$coords,
species = aedeagal_regionclass$Species)
aedeagal_regiongdf #check

#perform morphological disparity (MD) without covariates, using Overall Mean
(consensus) - using 1 as a dummy variable for this
aedeagal_regionmd <- morphol.disparity(f1 = coords ~ 1, groups =~ species, data =
aedeagal_regiongdf, iter=999, print.progress = TRUE)
aedeagal_regionmd #calls results
```

```
#send MD results to Excel
library(xlsx)
#1) Observed Procrustes variances for defined groups (species) compared to Overall
Mean (consensus)
write.xlsx(aedeagal_regionmd$Procrustes.var, "c:/Users/DAW/Documents/Hypo1-
3/aedeagal_region_morpho-disp1B.xlsx")
#2) Observed pairwise absolute differences (distances) between groups (species) in
Procrustes variances
write.xlsx(aedeagal_regionmd$PV.dist, "c:/Users/DAW/Documents/Hypo1-
3/aedeagal_region_morpho-disp2B.xlsx")
#3) P-Values
write.xlsx(aedeagal_regionmd$PV.dist.Pval, "c:/Users/DAW/Documents/Hypo1-
3/aedeagal_region_morpho-disp3B.xlsx")

#run PCA analysis on all specimens from GPA data
#plots with number codes for specimens (cleaner)
aedeagal_regionpca <- plotTangentSpace(aedeagal_regiongpa$coords, axis1 = 1, axis2 =
2, label = TRUE, groups = aedeagal_regiongroup)
#plots with ID's for specimens (messier)
aedeagal_regionpca <- plotTangentSpace(aedeagal_regiongpa$coords, axis1 = 1, axis2 =
2, label = aedeagal_regionclass$ID, groups = aedeagal_regiongroup)
```

```
#run PCA analysis on means of all specimens from GPA data
aedeagal_regionpcameans <- plotTangentSpace(aedeagal_regiongpameans, axis1 = 1,
axis2 = 2, label = aedeagal_regionclass2$Species, groups = aedeagal_regiongroup)

#send PCA results on all specimens to Excel
library(xlsx)
#1) PCA scores summary
write.xlsx(aedeagal_regionpca$pc.summary$importance,
"c:/Users/DAW/Documents/Hypo1-3/aedeagal_region_pca1.xlsx")
#2) PCA scores for all specimens
write.xlsx(aedeagal_regionpca$pc.scores, "c:/Users/DAW/Documents/Hypo1-
3/aedeagal_region_pca2.xlsx")
#3) PCA shape coordinates of extreme ends of all PC axes
write.xlsx(aedeagal_regionpca$pc.shapes, "c:/Users/DAW/Documents/Hypo1-
3/aedeagal_region_pca3.xlsx")

#send PCA results on means of all specimens to Excel
library(xlsx)
#1) PCA scores summary
write.xlsx(aedeagal_regionpcameans$pc.summary$importance,
"c:/Users/DAW/Documents/Hypo1-3/aedeagal_region_pca-means1.xlsx")
```

```
#2) PCA scores for all specimens
write.xlsx(aedeagal_regionpcameans$pc.scores, "c:/Users/DAW/Documents/Hypo1-3/aedeagal_region_pca-means2.xlsx")
#3) PCA shape coordinates of extreme ends of all PC axes
write.xlsx(aedeagal_regionpcameans$pc.shapes, "c:/Users/DAW/Documents/Hypo1-3/aedeagal_region_pca-means3.xlsx")

############################################################

#CERCUS

#give data set a name and bring it in
cercus <- readland.tps("cercus2.tps", specID = "imageID")
cercus #check

#assign classification levels and make a group out of Species
cercusclass <- read.csv("cercus2.csv", header=TRUE)
cercusclass #check
cercusgroup <- factor(paste(cercusclass$Species))
levels(cercusgroup)

#assign species level for PCA means analysis
```

```
cercusclass2 <- read.csv("species.csv", header=TRUE)
cercusclass2 #check

#bring in previously-created sliders file
cercuscurves <- as.matrix(read.csv("cercus_curveslide.csv", header=T))
cercuscurves #check

#perform GPA
cercusgpa <- gpagen(cercus, curves=cercuscurves, ProcD=FALSE, print.progress =
TRUE)
cercusgpa #check
plot(cercusgpa) #check via plot view

#calculate means of GPA landmark data for PCA means analysis
cercusgpameans <- (aggregate(two.d.array(cercusgpa$coords) ~ cercusgroup,
FUN=mean))[,-1]
cercusgpameans #check
rownames(cercusgpameans) <- levels(cercusgroup)
rownames(cercusgpameans)
cercusgpameans #check new names are in place
cercusgpameans <- arrayspecs(cercusgpameans, 23,2)
cercusgpameans #Table check new arrangement is correct
```

```
#send GPA landmark coordinates data to Excel
library(xlsx)
#1) GPA landmark coordinates - all specimens
write.xlsx(cercusgpa$coords, "c:/Users/DAW/Documents/Hypo1-3/cercus_GPA1.xlsx")
#2) GPA centroid size
write.xlsx(cercusgpa$Csize, "c:/Users/DAW/Documents/Hypo1-3/cercus_GPA2.xlsx")
#3) GPA consensus shape
write.xlsx(cercusgpa$consensus, "c:/Users/DAW/Documents/Hypo1-
3/cercus_GPA3.xlsx")

#send GPA means landmark coordinates data to Excel
library(xlsx)
#GPA landmark coordinates - means
write.xlsx(cercusgpameans, "c:/Users/DAW/Documents/Hypo1-3/cercus_GPA-
means.xlsx")

#create GDF from GPA data for morphological disparity analysis
cercusgdf <- geomorph.data.frame(coords =cercusgpa$coords, species =
cercusclass$Species)
cercusgdf #check
```

```
#perform morphological disparity (MD) without covariates, using Overall Mean
(consensus) - using 1 as a dummy variable for this
cercusmd <- morphol.disparity(f1 = coords ~ 1, groups =~ species, data = cercusgdf,
iter=999, print.progress = TRUE)
cercusmd #calls results

#send MD results to Excel
library(xlsx)
#1) Observed Procrustes variances for defined groups (species) compared to Overall
Mean (consensus)
write.xlsx(cercusmd$Procrustes.var, "c:/Users/DAW/Documents/Hypo1-
3/cercus_morpho-disp1B.xlsx")
#2) Observed pairwise absolute differences (distances) between groups (species) in
Procrustes variances
write.xlsx(cercusmd$PV.dist, "c:/Users/DAW/Documents/Hypo1-3/cercus_morpho-
disp2B.xlsx")
#3) P-Values
write.xlsx(cercusmd$PV.dist.Pval, "c:/Users/DAW/Documents/Hypo1-
3/cercus_morpho-disp3B.xlsx")

#run PCA analysis on all specimens from GPA data
#plots with number codes for specimens (cleaner)
```

```
cercuspca <- plotTangentSpace(cercusgpa$coords, axis1 = 1, axis2 = 2, label = TRUE,
groups = cercusgroup)
#plots with ID's for specimens (messier)
cercuspca <- plotTangentSpace(cercusgpa$coords, axis1 = 1, axis2 = 2, label =
cercusclass$ID, groups = cercusgroup)

#run PCA analysis on means all specimens from GPA data
cercuspcameans <- plotTangentSpace(cercusgpameans, axis1 = 1, axis2 = 2, label =
cercusclass2$Species, groups = cercusgroup)

#send PCA results on all specimens to Excel
library(xlsx)
#1) PCA scores summary
write.xlsx(cercuspca$pc.summary$importance, "c:/Users/DAW/Documents/Hypo1-
3/cercus_pca1.xlsx")
#2) PCA scores for all specimens
write.xlsx(cercuspca$pc.scores, "c:/Users/DAW/Documents/Hypo1-
3/cercus_pca2.xlsx")
#3) PCA shape coordinates of extreme ends of all PC axes
write.xlsx(cercuspca$pc.shapes, "c:/Users/DAW/Documents/Hypo1-
3/cercus_pca3.xlsx")
```

```
#send PCA results on means of all specimens to Excel
library(xlsx)
#1) PCA scores summary
write.xlsx(cercuspcameans$pc.summary$importance,
"c:/Users/DAW/Documents/Hypo1-3/cercus_pca-means1.xlsx")
#2) PCA scores for all specimens
write.xlsx(cercuspcameans$pc.scores, "c:/Users/DAW/Documents/Hypo1-3/cercus_pca-
means2.xlsx")
#3) PCA shape coordinates of extreme ends of all PC axes
write.xlsx(cercuspcameans$pc.shapes, "c:/Users/DAW/Documents/Hypo1-
3/cercus_pca-means3.xlsx")

##########################################################

#ECTOPHALLUS

#give data set a name and bring it in
ectophallus <- readland.tps("ectophallus2.tps", specID = "imageID")
ectophallus #check

#assign classification levels and make a group out of Species
ectophallusclass <- read.csv("ectophallus2.csv", header=TRUE)
```

```
ectophallusclass #check
ectophallusgroup <- factor(paste(ectophallusclass$Species))
levels(ectophallusgroup)

#assign species level for PCA means analysis
ectophallusclass2 <- read.csv("species.csv", header=TRUE)
ectophallusclass2 #check

#bring in previously-created sliders file
ectophalluscurves <- as.matrix(read.csv("ectophallus_curveslide.csv", header=T))
ectophalluscurves #check

#perform GPA
ectophallusgpa <- gpagen(ectophallus, curves=ectophalluscurves, ProcD=FALSE,
print.progress = TRUE)
ectophallusgpa #check
plot(ectophallusgpa) #check via plot view

#calculate means of GPA landmark data for PCA means analysis
ectophallusgpameans <- (aggregate(two.d.array(ectophallusgpa$coords) ~
ectophallusgroup, FUN=mean))[,-1]
ectophallusgpameans #check
```

```
rownames(ectophallusgpameans) <- levels(ectophallusgroup)
rownames(ectophallusgpameans)
ectophallusgpameans #check new names are in place
ectophallusgpameans <- arrayspecs(ectophallusgpameans, 27,2)
ectophallusgpameans #Table check new arrangement is correct

#send GPA landmark coordinates data to Excel
library(xlsx)
#1) GPA landmark coordinates - all specimens
write.xlsx(ectophallusgpa$coords, "c:/Users/DAW/Documents/Hypo1-
3/ectophallus_GPA1.xlsx")
#2) GPA centroid size
write.xlsx(ectophallusgpa$Csize, "c:/Users/DAW/Documents/Hypo1-
3/ectophallus_GPA2.xlsx")
#3) GPA consensus shape
write.xlsx(ectophallusgpa$consensus, "c:/Users/DAW/Documents/Hypo1-
3/ectophallus_GPA3.xlsx")

#send GPA means landmark coordinates data to Excel
library(xlsx)
#GPA landmark coordinates - means
```

```
write.xlsx(ectophallusgpameans, "c:/Users/DAW/Documents/Hypo1-
3/ectophallus_GPA-means.xlsx")

#create GDF from GPA data for morphological disparity analysis
ectophallusgdf <- geomorph.data.frame(coords =ectophallusgpa$coords, species =
ectophallusclass$Species)
ectophallusgdf #check

#perform morphological disparity (MD) without covariates, using Overall Mean
(consensus) - using 1 as a dummy variable for this
ectophallusmd <- morphol.disparity(f1 = coords ~ 1, groups =~ species, data =
ectophallusgdf, iter=999, print.progress = TRUE)
ectophallusmd #calls results

#send MD results to Excel
library(xlsx)
#1) Observed Procrustes variances for defined groups (species) compared to Overall
Mean (consensus)
write.xlsx(ectophallusmd$Procrustes.var, "c:/Users/DAW/Documents/Hypo1-
3/ectophallus_morpho-disp1B.xlsx")
#2) Observed pairwise absolute differences (distances) between groups (species) in
Procrustes variances
```

```
write.xlsx(ectophallusmd$PV.dist, "c:/Users/DAW/Documents/Hypo1-
3/ectophallus_morpho-disp2B.xlsx")
#3) P-Values
write.xlsx(ectophallusmd$PV.dist.Pval, "c:/Users/DAW/Documents/Hypo1-
3/ectophallus_morpho-disp3B.xlsx")

#run PCA analysis on all specimens from GPA data
#plots with number codes for specimens (cleaner)
ectophalluspca <- plotTangentSpace(ectophallusgpa$coords, axis1 = 1, axis2 = 2, label =
TRUE, groups = ectophallusgroup)
#plots with ID's for specimens (messier)
ectophalluspca <- plotTangentSpace(ectophallusgpa$coords, axis1 = 1, axis2 = 2, label =
ectophallusclass$ID, groups = ectophallusgroup)

#run PCA analysis on means all specimens from GPA data
ectophalluspcameans <- plotTangentSpace(ectophallusgpameans, axis1 = 1, axis2 = 2,
label = ectophallusclass2$Species, groups = ectophallusgroup)

#send PCA results on all specimens to Excel
library(xlsx)
#1) PCA scores summary
```

```
write.xlsx(ectophalluspca$pc.summary$importance, "c:/Users/DAW/Documents/Hypo1-3/ectophallus_pca1.xlsx")
#2) PCA scores for all specimens
write.xlsx(ectophalluspca$pc.scores, "c:/Users/DAW/Documents/Hypo1-3/ectophallus_pca2.xlsx")
#3) PCA shape coordinates of extreme ends of all PC axes
write.xlsx(ectophalluspca$pc.shapes, "c:/Users/DAW/Documents/Hypo1-3/ectophallus_pca3.xlsx")

#send PCA results on means of all specimens to Excel
library(xlsx)
#1) PCA scores summary
write.xlsx(ectophalluspcameans$pc.summary$importance, "c:/Users/DAW/Documents/Hypo1-3/ectophallus_pca-means1.xlsx")
#2) PCA scores for all specimens
write.xlsx(ectophalluspcameans$pc.scores, "c:/Users/DAW/Documents/Hypo1-3/ectophallus_pca-means2.xlsx")
#3) PCA shape coordinates of extreme ends of all PC axes
write.xlsx(ectophalluspcameans$pc.shapes, "c:/Users/DAW/Documents/Hypo1-3/ectophallus_pca-means3.xlsx")

##########################################################
```

```
#EPIPHALLUS

#give data set a name and bring it in
epiphallus <- readland.tps("epiphallus2.tps", specID = "imageID")
epiphallus #check

#assign classification levels and make a group out of Species
epiphallusclass <- read.csv("epiphallus2.csv", header=TRUE)
epiphallusclass #check
epiphallusgroup <- factor(paste(epiphallusclass$Species))
levels(epiphallusgroup)

#assign species level for PCA means analysis
epiphallusclass2 <- read.csv("species.csv", header=TRUE)
epiphallusclass2 #check

#bring in previously-created sliders file
epiphalluscurves <- as.matrix(read.csv("epiphallus_curveslide.csv", header=T))
epiphalluscurves #check

#perform GPA
```

```
epiphallusgpa <- gpagen(epiphallus, curves=epiphalluscurves, ProcD=FALSE,
print.progress = TRUE)
epiphallusgpa #check
plot(epiphallusgpa) #check via plot view

#calculate means of GPA landmark data for PCA means analysis
epiphallusgpameans <- (aggregate(two.d.array(epiphallusgpa$coords) ~
epiphallusgroup, FUN=mean))[,-1]
epiphallusgpameans #check
rownames(epiphallusgpameans) <- levels(epiphallusgroup)
rownames(epiphallusgpameans)
epiphallusgpameans #check new names are in place
epiphallusgpameans <- arrayspecs(epiphallusgpameans, 19,2)
epiphallusgpameans #Table check new arrangement is correct

#send GPA landmark coordinates data to Excel
library(xlsx)
#1) GPA landmark coordinates - all specimens
write.xlsx(epiphallusgpa$coords, "c:/Users/DAW/Documents/Hypo1-
3/epiphallus_GPA1.xlsx")
#2) GPA centroid size
```

```
write.xlsx(epiphallusgpa$Csize, "c:/Users/DAW/Documents/Hypo1-
3/epiphallus_GPA2.xlsx")
#3) GPA consensus shape
write.xlsx(epiphallusgpa$consensus, "c:/Users/DAW/Documents/Hypo1-
3/epiphallus_GPA3.xlsx")

#send GPA means landmark coordinates data to Excel
library(xlsx)
#GPA landmark coordinates - means
write.xlsx(epiphallusgpameans, "c:/Users/DAW/Documents/Hypo1-3/epiphallus_GPA-
means.xlsx")

#create GDF from GPA data for morphological disparity analysis
epiphallusgdf <- geomorph.data.frame(coords =epiphallusgpa$coords, species =
epiphallusclass$Species)
epiphallusgdf #check

#perform morphological disparity (MD) without covariates, using Overall Mean
(consensus) - using 1 as a dummy variable for this
epiphallusmd <- morphol.disparity(f1 = coords ~ 1, groups =~ species, data =
epiphallusgdf, iter=999, print.progress = TRUE)
epiphallusmd #calls results
```

```
#send MD results to Excel
library(xlsx)
#1) Observed Procrustes variances for defined groups (species) compared to Overall
Mean (consensus)
write.xlsx(epiphallusmd$Procrustes.var, "c:/Users/DAW/Documents/Hypo1-
3/epiphallus_morpho-disp1B.xlsx")
#2) Observed pairwise absolute differences (distances) between groups (species) in
Procrustes variances
write.xlsx(epiphallusmd$PV.dist, "c:/Users/DAW/Documents/Hypo1-
3/epiphallus_morpho-disp2B.xlsx")
#3) P-Values
write.xlsx(epiphallusmd$PV.dist.Pval, "c:/Users/DAW/Documents/Hypo1-
3/epiphallus_morpho-disp3B.xlsx")

#run PCA analysis on all specimens from GPA data
#plots with number codes for specimens (cleaner)
epiphalluspca <- plotTangentSpace(epiphallusgpa$coords, axis1 = 1, axis2 = 2, label =
TRUE, groups = epiphallusgroup)
#plots with ID's for specimens (messier)
epiphalluspca <- plotTangentSpace(epiphallusgpa$coords, axis1 = 1, axis2 = 2, label =
epiphallusclass$ID, groups = epiphallusgroup)
```

```
#run PCA analysis on means all specimens from GPA data
epiphalluspcameans <- plotTangentSpace(epiphallusgpameans, axis1 = 1, axis2 = 2,
label = epiphallusclass2$Species, groups = epiphallusgroup)
#¡Te amo, mi bonita!
#send PCA results on all specimens to Excel
library(xlsx)
#1) PCA scores summary
write.xlsx(epiphalluspca$pc.summary$importance, "c:/Users/DAW/Documents/Hypo1-
3/epiphallus_pca1.xlsx")
#2) PCA scores for all specimens
write.xlsx(epiphalluspca$pc.scores, "c:/Users/DAW/Documents/Hypo1-
3/epiphallus_pca2.xlsx")
#3) PCA shape coordinates of extreme ends of all PC axes
write.xlsx(epiphalluspca$pc.shapes, "c:/Users/DAW/Documents/Hypo1-
3/epiphallus_pca3.xlsx")

#send PCA results on means of all specimens to Excel
library(xlsx)
#1) PCA scores summary
write.xlsx(epiphalluspcameans$pc.summary$importance,
"c:/Users/DAW/Documents/Hypo1-3/epiphallus_pca-means1.xlsx")
```

```
#2) PCA scores for all specimens
write.xlsx(epiphalluspcameans$pc.scores, "c:/Users/DAW/Documents/Hypo1-
3/epiphallus_pca-means2.xlsx")
#3) PCA shape coordinates of extreme ends of all PC axes
write.xlsx(epiphalluspcameans$pc.shapes, "c:/Users/DAW/Documents/Hypo1-
3/epiphallus_pca-means3.xlsx")

############################################################

#LOPHUS

#give data set a name and bring it in
lophus <- readland.tps("lophus2.tps", specID = "imageID")
lophus #check

#assign classification levels and make a group out of Species
lophusclass <- read.csv("lophus2.csv", header=TRUE)
lophusclass #check
lophusgroup <- factor(paste(lophusclass$Species))
levels(lophusgroup)

#assign Species level for PCA means analysis
```

```
lophusclass2 <- read.csv("Species.csv", header=TRUE)
lophusclass2 #check

#bring in previously-created sliders file
lophuscurves <- as.matrix(read.csv("lophus_curveslide.csv", header=T))
lophuscurves #check

#perform GPA
lophusgpa <- gpagen(lophus, curves=lophuscurves, ProcD=FALSE, print.progress =
TRUE)
lophusgpa #check
plot(lophusgpa) #check via plot view

#calculate means of GPA landmark data for PCA means analysis
lophusgpameans <- (aggregate(two.d.array(lophusgpa$coords) ~ lophusgroup,
FUN=mean))[,-1]
lophusgpameans #check
rownames(lophusgpameans) <- levels(lophusgroup)
rownames(lophusgpameans)
lophusgpameans #check new names are in place
lophusgpameans <- arrayspecs(lophusgpameans, 11,2)
lophusgpameans #Table check new arrangement is correct
```

```
#send GPA landmark coordinates data to Excel
library(xlsx)
#1) GPA landmark coordinates - all specimens
write.xlsx(lophusgpa$coords, "c:/Users/DAW/Documents/Hypo1-
3/lophus_GPA1.xlsx")
#2) GPA centroid size
write.xlsx(lophusgpa$Csize, "c:/Users/DAW/Documents/Hypo1-3/lophus_GPA2.xlsx")
#3) GPA consensus shape
write.xlsx(lophusgpa$consensus, "c:/Users/DAW/Documents/Hypo1-
3/lophus_GPA3.xlsx")

#send GPA means landmark coordinates data to Excel
library(xlsx)
#GPA landmark coordinates - means
write.xlsx(lophusgpameans, "c:/Users/DAW/Documents/Hypo1-3/lophus_GPA-
means.xlsx")

#create GDF from GPA data for morphological disparity analysis
lophusgdf <- geomorph.data.frame(coords =lophusgpa$coords, species =
lophusclass$Species)
lophusgdf #check
```

```
#perform morphological disparity (MD) without covariates, using Overall Mean
(consensus) - using 1 as a dummy variable for this
lophusmd <- morphol.disparity(f1 = coords ~ 1, groups =~ species, data = lophusgdf,
iter=999, print.progress = TRUE)
lophusmd #calls results

#send MD results to Excel
library(xlsx)
#1) Observed Procrustes variances for defined groups (species) compared to Overall
Mean (consensus)
write.xlsx(lophusmd$Procrustes.var, "c:/Users/DAW/Documents/Hypo1-
3/lophus_morpho-disp1B.xlsx")
#2) Observed pairwise absolute differences (distances) between groups (species) in
Procrustes variances
write.xlsx(lophusmd$PV.dist, "c:/Users/DAW/Documents/Hypo1-3/lophus_morpho-
disp2B.xlsx")
#3) P-Values
write.xlsx(lophusmd$PV.dist.Pval, "c:/Users/DAW/Documents/Hypo1-
3/lophus_morpho-disp3B.xlsx")

#run PCA analysis on all specimens from GPA data
```

```
#plots with number codes for specimens (cleaner)
lophuspca <- plotTangentSpace(lophusgpa$coords, axis1 = 1, axis2 = 2, label = TRUE,
groups = lophusgroup)
#plots with ID's for specimens (messier)
lophuspca <- plotTangentSpace(lophusgpa$coords, axis1 = 1, axis2 = 2, label =
lophusclass$ID, groups = lophusgroup)

#run PCA analysis on means all specimens from GPA data
lophuspcameans <- plotTangentSpace(lophusgpameans, axis1 = 1, axis2 = 2, label =
lophusclass2$Species, groups = lophusgroup)

#send PCA results on all specimens to Excel
library(xlsx)
#1) PCA scores summary
write.xlsx(lophuspca$pc.summary$importance, "c:/Users/DAW/Documents/Hypo1-
3/lophus_pca1.xlsx")
#2) PCA scores for all specimens
write.xlsx(lophuspca$pc.scores, "c:/Users/DAW/Documents/Hypo1-
3/lophus_pca2.xlsx")
#3) PCA shape coordinates of extreme ends of all PC axes
write.xlsx(lophuspca$pc.shapes, "c:/Users/DAW/Documents/Hypo1-
3/lophus_pca3.xlsx")
```

```
#send PCA results on means of all specimens to Excel
library(xlsx)
#1) PCA scores summary
write.xlsx(lophuspcameans$pc.summary$importance,
"c:/Users/DAW/Documents/Hypo1-3/lophus_pca-means1.xlsx")
#2) PCA scores for all specimens
write.xlsx(lophuspcameans$pc.scores, "c:/Users/DAW/Documents/Hypo1-
3/lophus_pca-means2.xlsx")
#3) PCA shape coordinates of extreme ends of all PC axes
write.xlsx(lophuspcameans$pc.shapes, "c:/Users/DAW/Documents/Hypo1-
3/lophus_pca-means3.xlsx")

##########################################################

#WING
#give data set a name and bring it in
wing <- readland.tps("wing2.tps", specID = "imageID")
wing #check

#assign classification levels and make a group out of Species
wingclass <- read.csv("wing2.csv", header=TRUE)
```

```
wingclass #check
winggroup <- factor(paste(wingclass$Species))
levels(winggroup)

#assign species level for PCA means analysis
wingclass2 <- read.csv("species.csv", header=TRUE)
wingclass2 #check

#bring in previously-created sliders file
wingcurves <- as.matrix(read.csv("wing_curveslide.csv", header=T))
wingcurves #check

#perform GPA
winggpa <- gpagen(wing, curves=wingcurves, ProcD=FALSE, print.progress = TRUE)
winggpa #check
plot(winggpa) #check via plot view

#calculate means of GPA landmark data for PCA means analysis
winggpameans <- (aggregate(two.d.array(winggpa$coords) ~ winggroup,
FUN=mean))[,-1]
winggpameans #check
rownames(winggpameans) <- levels(winggroup)
```

```
rownames(winggpameans)
winggpameans #check new names are in place
winggpameans <- arrayspecs(winggpameans, 17,2)
winggpameans #Table check new arrangement is correct

#send GPA landmark coordinates data to Excel
library(xlsx)
#1) GPA landmark coordinates - all specimens
write.xlsx(winggpa$coords, "c:/Users/DAW/Documents/Hypo1-3/wing_GPA1.xlsx")
#2) GPA centroid size
write.xlsx(winggpa$Csize, "c:/Users/DAW/Documents/Hypo1-3/wing_GPA2.xlsx")
#3) GPA consensus shape
write.xlsx(winggpa$consensus, "c:/Users/DAW/Documents/Hypo1-
3/wing_GPA3.xlsx")

#send GPA means landmark coordinates data to Excel
library(xlsx)
#GPA landmark coordinates - means
write.xlsx(winggpameans, "c:/Users/DAW/Documents/Hypo1-3/wing_GPA-
means.xlsx")

#create GDF from GPA data for morphological disparity analysis
```

```
winggdf <- geomorph.data.frame(coords =winggpa$coords, species =
wingclass$Species)
winggdf #check

#perform morphological disparity (MD) without covariates, using Overall Mean
(consensus) - using 1 as a dummy variable for this
wingmd <- morphol.disparity(f1 = coords ~ 1, groups =~ species, data = winggdf,
iter=999, print.progress = TRUE)
wingmd #calls results

#send MD results to Excel
library(xlsx)
#1) Observed Procrustes variances for defined groups (species) compared to Overall
Mean (consensus)
write.xlsx(wingmd$Procrustes.var, "c:/Users/DAW/Documents/Hypo1-3/wing_morpho-
disp1B.xlsx")
#2) Observed pairwise absolute differences (distances) between groups (species) in
Procrustes variances
write.xlsx(wingmd$PV.dist, "c:/Users/DAW/Documents/Hypo1-3/wing_morpho-
disp2B.xlsx")
#3) P-Values
```

```
write.xlsx(wingmd$PV.dist.Pval, "c:/Users/DAW/Documents/Hypo1-3/wing_morpho-disp3B.xlsx")

#run PCA analysis on all specimens from GPA data
#plots with number codes for specimens (cleaner)
wingpca <- plotTangentSpace(winggpa$coords, axis1 = 1, axis2 = 2, label = TRUE, groups = winggroup)
#plots with ID's for specimens (messier)
wingpca <- plotTangentSpace(winggpa$coords, axis1 = 1, axis2 = 2, label = wingclass$ID, groups = winggroup)

#run PCA analysis on means all specimens from GPA data
wingpcameans <- plotTangentSpace(winggpameans, axis1 = 1, axis2 = 2, label = wingclass2$Species, groups = winggroup)

#send PCA results on all specimens to Excel
library(xlsx)
#1) PCA scores summary
write.xlsx(wingpca$pc.summary$importance, "c:/Users/DAW/Documents/Hypo1-3/wing_pca1.xlsx")
#2) PCA scores for all specimens
write.xlsx(wingpca$pc.scores, "c:/Users/DAW/Documents/Hypo1-3/wing_pca2.xlsx")
```

```
#3) PCA shape coordinates of extreme ends of all PC axes
write.xlsx(wingpca$pc.shapes, "c:/Users/DAW/Documents/Hypo1-3/wing_pca3.xlsx")

#send PCA results on means of all specimens to Excel
#1) PCA scores summary
write.xlsx(wingpcameans$pc.summary$importance, "c:/Users/DAW/Documents/Hypo1-3/wing_pca-means1.xlsx")
#2) PCA scores for all specimens
write.xlsx(wingpcameans$pc.scores, "c:/Users/DAW/Documents/Hypo1-3/wing_pca-means2.xlsx")
#3) PCA shape coordinates of extreme ends of all PC axes
write.xlsx(wingpcameans$pc.shapes, "c:/Users/DAW/Documents/Hypo1-3/wing_pca-means3.xlsx")
########################################
########################################
#HYPOTHESIS 2

#bring in the PG time tree
pgtimetree<-read.tree (file = "PGtimetree.tre", text = NULL, tree.names = NULL) #give the tree a name
pgtimetree #check that file is input correctly
plot(pgtimetree) #look at tree
```

```
#begin process of combining GPA means data for all 6 shapes
#convert each 3D array with GPA means data into a 2D array for combination procedure
aedeagal_region_means2D <- two.d.array(aedeagal_regiongpameans)
aedeagal_region_means2D #check
cercus_means2D <- two.d.array(cercusgpameans)
cercus_means2D #check
ectophallus_means2D <- two.d.array(ectophallusgpameans)
ectophallus_means2D #check
epiphallus_means2D <- two.d.array(epiphallusgpameans)
epiphallus_means2D #check
lophus_means2D <- two.d.array(lophusgpameans)
lophus_means2D #check
wing_means2D <- two.d.array(winggpameans)
wing_means2D #check

pgmeanscombo2D<-
cbind(aedeagal_region_means2D,cercus_means2D,ectophallus_means2D,epiphallus_me
ans2D,lophus_means2D,wing_means2D) #combines all 6 sets of 2D matrices
pgmeanscombo2D #check

#total landmarks and (3D array series that correspond)
```

#aedeagal_region (A) = 29 (#1-29)

#cercus (B) = 23 (30-52)

#ectophallus (C) = 27 (#53-79)

#epiphallus (D) = 19 (#80-98)

#lophus (E) = 11 (#99-109)

#wing (F) = 17 (#110-126)

pgmeanscombo3D <- arrayspecs(pgmeanscombo2D, 126, 2) #converts combo 2D array into a 3D array where 126 = the total landmark number of all shapes and 2 = 2 dimensions

pgmeanscombo3D #check

#prepare data for comparison of multivariate evolutionary rates (MER)

pgland_gp<-
c("A","A","A","A","A","A","A","A","A","A","A","A","A","A","A","A","A","A","A","A","A","A","A","A","A","A","A","A","A","B","B","B","B","B","B","B","B","B","B","B","B","B","B","B","B","B","B","B","B","B","B","B","C","C","C","C","C","C","C","C","C","C","C","C","C","C","C","C","C","C","C","C","C","C","C","C","C","C","C","D","D","D","D","D","D","D","D","D","D","D","D","D","D","D","D","D","D","D","E","E","E","E","E","E","E","E","E","E","E","F","F","F","F","F","F","F","F","F","F","F","F","F","F","F","F","F") #defines the groups for MER comparison where "A" = landmarks for shape #1, "B" = 2nd set, etc.

pgland_gp #check

```
#run MER with time tree
pgMER2<-compare.multi.evol.rates(A=pgmeanscombo3D,gp=pgland_gp,
Subset=FALSE, phy=pgtimetree, iter=999, print.progress = TRUE)
pgMER2 #shows results
pgMER2$pairwise.pvalue #displays all pairwise p-values
plot(pgMER2)

########################################
#calculate phylogenetic signal for each shape using time tree

aedeagal_regionPS2 <- physignal(A=aedeagal_regiongpameans,phy=pgtimetree,
iter=999, print.progress = TRUE)
plot(aedeagal_regionPS2) #visual summary

cercusPS2 <- physignal(A=cercusgpameans,phy=pgtimetree, iter=999, print.progress =
TRUE)
plot(cercusPS2) #visual summary

ectophallusPS2 <- physignal(A=ectophallusgpameans,phy=pgtimetree, iter=999,
print.progress = TRUE)
plot(ectophallusPS2) #visual summary
```

```
epiphallusPS2 <- physignal(A=epiphallusgpameans,phy=pgtimetree, iter=999,
print.progress = TRUE)
plot(epiphallusPS2) #visual summary

lophusPS2 <- physignal(A=lophusgpameans,phy=pgtimetree, iter=999, print.progress =
TRUE)
plot(lophusPS2) #visual summary

wingPS2 <- physignal(A=winggpameans,phy=pgtimetree, iter=999, print.progress =
TRUE)
plot(wingPS2) #visual summary
########################################
########################################
#HYPOTHESIS 3

#constructing phylomorphospaces using time tree

#to acquire word and number version
aedeagal_regionPMS2_1 <-
plotGMPhyloMorphoSpace(pgtimetree,aedeagal_regiongpameans, xaxis = 1, yaxis = 2,
```

```
zaxis = NULL, ancStates=TRUE,tip.labels=TRUE,node.labels=TRUE,
plot.param=list(t.bg="purple",l.col="black",lwd=3,txt.cex=0.3,txt.col="blue"))
#send ancestral state results to Excel
library(xlsx)
write.xlsx(aedeagal_regionPMS2_1, "c:/Users/DAW/Documents/Hypo1-
3/aedeagal_region-ancestral_states2.xlsx")
#to acquire clean version
aedeagal_regionPMS2_2 <-
plotGMPhyloMorphoSpace(pgtimetree,aedeagal_regiongpameans,tip.labels=FALSE,no
de.labels=FALSE,plot.param=list(t.bg="purple",t.cex=1.2,n.bg="brown",n.pch=25,n.cex
=0.75,l.col="black",lwd=0.5))

#to acquire word and number version
cercusPMS2_1 <- plotGMPhyloMorphoSpace(pgtimetree,cercusgpameans, xaxis = 1,
yaxis = 2, zaxis = NULL, ancStates=TRUE,tip.labels=TRUE,node.labels=TRUE,
plot.param=list(t.bg="purple",l.col="black",lwd=3,txt.cex=0.3,txt.col="blue"))
#send ancestral state results to Excel
library(xlsx)
write.xlsx(cercusPMS2_1, "c:/Users/DAW/Documents/Hypo1-3/cercus-
ancestral_states2.xlsx")
#to acquire clean version
```

```
cercusPMS2_2 <-
plotGMPhyloMorphoSpace(pgtimetree,cercusgpameans,tip.labels=FALSE,node.labels=
FALSE,plot.param=list(t.bg="purple",t.cex=1.2,n.bg="brown",n.pch=25,n.cex=0.75,l.co
l="black",lwd=0.5))

#to acquire word and number version
ectophallusPMS2_1 <- plotGMPhyloMorphoSpace(pgtimetree,ectophallusgpameans,
xaxis = 1, yaxis = 2, zaxis = NULL,
ancStates=TRUE,tip.labels=TRUE,node.labels=TRUE,
plot.param=list(t.bg="purple",l.col="black",lwd=3,txt.cex=0.3,txt.col="blue"))
#send ancestral state results to Excel
library(xlsx)
write.xlsx(ectophallusPMS2_1, "c:/Users/DAW/Documents/Hypo1-3/ectophallus-
ancestral_states2.xlsx")
#to acquire clean version
ectophallusPMS2_2 <-
plotGMPhyloMorphoSpace(pgtimetree,ectophallusgpameans,tip.labels=FALSE,node.lab
els=FALSE,plot.param=list(t.bg="purple",t.cex=1.2,n.bg="brown",n.pch=25,n.cex=0.75
,l.col="black",lwd=0.5))

#to acquire word and number version
```

```
epiphallusPMS2_1 <- plotGMPhyloMorphoSpace(pgtimetree,epiphallusgpameans, xaxis
= 1, yaxis = 2, zaxis = NULL, ancStates=TRUE,tip.labels=TRUE,node.labels=TRUE,
plot.param=list(t.bg="purple",l.col="black",lwd=3,txt.cex=0.3,txt.col="blue"))
#send ancestral state results to Excel
library(xlsx)
write.xlsx(epiphallusPMS2_1, "c:/Users/DAW/Documents/Hypo1-3/epiphallus-
ancestral_states2.xlsx")
#to acquire clean version
epiphallusPMS2_2 <-
plotGMPhyloMorphoSpace(pgtimetree,epiphallusgpameans,tip.labels=FALSE,node.labe
ls=FALSE,plot.param=list(t.bg="purple",t.cex=1.2,n.bg="brown",n.pch=25,n.cex=0.75,l
.col="black",lwd=0.5))

#to acquire word and number version
lophusPMS2_1 <- plotGMPhyloMorphoSpace(pgtimetree,lophusgpameans, xaxis = 1,
yaxis = 2, zaxis = NULL, ancStates=TRUE,tip.labels=TRUE,node.labels=TRUE,
plot.param=list(t.bg="purple",l.col="black",lwd=3,txt.cex=0.3,txt.col="blue"))
#send ancestral state results to Excel
library(xlsx)
write.xlsx(lophusPMS2_1, "c:/Users/DAW/Documents/Hypo1-3/lophus-
ancestral_states2.xlsx")
#to acquire clean version
```

```
lophusPMS2_2 <-
plotGMPhyloMorphoSpace(pgtimetree,lophusgpameans,tip.labels=FALSE,node.labels=
FALSE,plot.param=list(t.bg="purple",t.cex=1.2,n.bg="brown",n.pch=25,n.cex=0.75,l.co
l="black",lwd=0.5))
#If you're reading this, drop me a line and let me know: asilid at gmail.com
#to acquire word and number version
wingPMS2_1 <- plotGMPhyloMorphoSpace(pgtimetree,winggpameans, xaxis = 1, yaxis
= 2, zaxis = NULL, ancStates=TRUE,tip.labels=TRUE,node.labels=TRUE,
plot.param=list(t.bg="purple",l.col="black",lwd=3,txt.cex=0.3,txt.col="blue"))#send
ancestral state results to Excel
library(xlsx)
write.xlsx(wingPMS2_1, "c:/Users/DAW/Documents/Hypo1-3/wing-
ancestral_states2.xlsx")
#to acquire clean version
wingPMS2_2 <-
plotGMPhyloMorphoSpace(pgtimetree,winggpameans,tip.labels=FALSE,node.labels=F
ALSE,plot.param=list(t.bg="purple",t.cex=1.2,n.bg="brown",n.pch=25,n.cex=0.75,l.col
="black",lwd=0.5))

##########################################
#comparative evolutionary rate (ER) analyses for the shapes using time tree
```

```
#Set 1 - all 4 lineages compared to each other for each shape


#Lineage 1 = 0 (1 species) (Green)
#Lineage 2 = 1 (8 species) (Blue)
#Lineage 3 = 2 (4 species) (Red)
#Lineage 4 = 3 (14 species) (Purple)
#So long and thanks for all the fish!
pgspecies_gp1_2 <- factor(c(1,1,1,1,1,1,1,1,2,2,2,2,3,3,3,3,3,3,3,3,3,3,3,3,3,3,3,3,0))
#assigns groups to the species - to be used for each shape using the tree's tip labels
(pgtimetree$tip.label)
pgspecies_gp1_2 #check
names(pgspecies_gp1_2) <- pgtimetree$tip.label #assigns species names to the groups
above
names(pgspecies_gp1_2) #check


aedeagal_regionpgER1_2 <- compare.evol.rates(A=aedeagal_regiongpameans,
phy=pgtimetree, method="permutation", pgspecies_gp1_2, iter=999, print.progress =
TRUE)
aedeagal_regionpgER1_2 #summarizes results
aedeagal_regionpgER1_2$pairwise.pvalue #returns pairwise p-values
plot(aedeagal_regionpgER1_2) #plots results
```

```
cercuspgER1_2 <- compare.evol.rates(A=cercusgpameans, phy=pgtimetree,
method="permutation", pgspecies_gp1_2, iter=999, print.progress = TRUE)
cercuspgER1_2 #summarizes results
cercuspgER1_2$pairwise.pvalue #returns pairwise p-values
plot(cercuspgER1_2)

ectophalluspgER1_2 <- compare.evol.rates(A=ectophallusgpameans, phy=pgtimetree,
method="permutation", pgspecies_gp1_2, iter=999, print.progress = TRUE)
ectophalluspgER1_2 #summarizes results
ectophalluspgER1_2$pairwise.pvalue #returns pairwise p-values
plot(ectophalluspgER1_2)

epiphalluspgER1_2 <- compare.evol.rates(A=epiphallusgpameans, phy=pgtimetree,
method="permutation", pgspecies_gp1_2, iter=999, print.progress = TRUE)
epiphalluspgER1_2 #summarizes results
epiphalluspgER1_2$pairwise.pvalue #returns pairwise p-values
plot(epiphalluspgER1_2)

lophuspgER1_2 <- compare.evol.rates(A=lophusgpameans, phy=pgtimetree,
method="permutation", pgspecies_gp1_2, iter=999, print.progress = TRUE)
lophuspgER1_2 #summarizes results
lophuspgER1_2$pairwise.pvalue #returns pairwise p-values
```

```
plot(lophuspgER1_2)

wingpgER1_2 <- compare.evol.rates(A=winggpameans, phy=pgtimetree,
method="permutation", pgspecies_gp1_2, iter=999, print.progress = TRUE)
wingpgER1_2 #summarizes results
wingpgER1_2$pairwise.pvalue #returns pairwise p-values
plot(wingpgER1_2)

##########################################################

#Set 2 - PGss vs. non-PG using time tree

#PGss = 0 (9 species)
#non-PGss = 1 (18 species)

pgspecies_gp2_2 <- factor(c(1,1,1,1,1,1,1,1,1,1,1,1,0,0,0,0,0,0,0,0,0,1,1,1,1,1,1))
#assigns groups to the species - to be used for each shape using the tree's tip labels
(pgtimetree$tip.label)
pgspecies_gp2_2 #check
names(pgspecies_gp2_2) <- pgtimetree$tip.label #assigns species names to the groups
above
names(pgspecies_gp2_2) #check
```

```
aedeagal_regionpgER2_2 <- compare.evol.rates(A=aedeagal_regiongpameans,
phy=pgtimetree, pgspecies_gp2_2, method="permutation", iter=999, print.progress =
TRUE)
aedeagal_regionpgER2_2 #summarizes results
plot(aedeagal_regionpgER2_2)

cercuspgER2_2 <- compare.evol.rates(A=cercusgpameans, phy=pgtimetree,
pgspecies_gp2_2, method="permutation", iter=999, print.progress = TRUE)
cercuspgER2_2 #summarizes results
plot(cercuspgER2_2)

ectophalluspgER2_2 <- compare.evol.rates(A=ectophallusgpameans, phy=pgtimetree,
pgspecies_gp2_2, method="permutation", iter=999, print.progress = TRUE)
ectophalluspgER2_2 #summarizes results
plot(ectophalluspgER2_2)

epiphalluspgER2_2 <- compare.evol.rates(A=epiphallusgpameans, phy=pgtimetree,
pgspecies_gp2_2, method="permutation", iter=999, print.progress = TRUE)
epiphalluspgER2_2 #summarizes results
plot(epiphalluspgER2_2)
```

```
lophuspgER2_2 <- compare.evol.rates(A=lophusgpameans, phy=pgtimetree,
pgspecies_gp2_2, method="permutation", iter=999, print.progress = TRUE)
lophuspgER2_2 #summarizes results
plot(lophuspgER2_2)

wingpgER2_2 <- compare.evol.rates(A=winggpameans, phy=pgtimetree,
pgspecies_gp2_2, method="permutation", iter=999, print.progress = TRUE)
wingpgER2_2 #summarizes results
plot(wingpgER2_2)

##########################################################

#Set 3 - Lineage C vs. non-C using time tree

#C = 0 (4 species)
#non-C = 1 (23 species)

pgspecies_gp3_2 <- factor(c(1,1,1,1,1,1,1,1,1,0,0,0,0,1,1,1,1,1,1,1,1,1,1,1,1,1,1))
#assigns groups to the species - to be used for each shape using the tree's tip labels
(pgtimetree$tip.label)
pgspecies_gp3_2 #check
```

```
names(pgspecies_gp3_2) <- pgtimetree$tip.label #assigns species names to the groups above
names(pgspecies_gp3_2) #check

aedeagal_regionpgER3_2 <- compare.evol.rates(A=aedeagal_regiongpameans, phy=pgtimetree, pgspecies_gp3_2, method="permutation", iter=999, print.progress = TRUE)
aedeagal_regionpgER3_2 #summarizes results
plot(aedeagal_regionpgER3_2)

cercuspgER3_2 <- compare.evol.rates(A=cercusgpameans, phy=pgtimetree, pgspecies_gp3_2, method="permutation", iter=999, print.progress = TRUE)
cercuspgER3_2 #summarizes results
plot(cercuspgER3_2)

ectophalluspgER3_2 <- compare.evol.rates(A=ectophallusgpameans, phy=pgtimetree, pgspecies_gp3_2, method="permutation", iter=999, print.progress = TRUE)
ectophalluspgER3_2 #summarizes results
plot(ectophalluspgER3_2)

epiphalluspgER3_2 <- compare.evol.rates(A=epiphallusgpameans, phy=pgtimetree, pgspecies_gp3_2, method="permutation", iter=999, print.progress = TRUE)
```

```
epiphalluspgER3_2 #summarizes results
plot(epiphalluspgER3_2)

lophuspgER3_2 <- compare.evol.rates(A=lophusgpameans, phy=pgtimetree,
pgspecies_gp3_2, method="permutation", iter=999, print.progress = TRUE)
lophuspgER3_2 #summarizes results
plot(lophuspgER3_2)

wingpgER3_2 <- compare.evol.rates(A=winggpameans, phy=pgtimetree,
pgspecies_gp3_2, method="permutation", iter=999, print.progress = TRUE)
wingpgER3_2 #summarizes results
plot(wingpgER3_2)
```